# The Mesenchymal Niche in Leukemia Predisposition Syndromes

# De mesenchymale niche in leukemie predispositie syndromen

**Si Chen**

Erasmus MC
University Medical Center Rotterdam

**ISBN**: 978-94-6332-183-9
**Layout:** E.C.M.M. Simons
**Cover:** E.C.M.M. Simons
**Printing**: GVO drukkers & vormgevers B.V.


The work described in this thesis was performed at the Department of Hematology of the Erasmus Medical Center, Rotterdam, the Netherlands. The work presented in this thesis was financially supported by the Dutch Cancer Society (KWF Kankerbestrijding), Amsterdam, The Netherlands; the Netherlands Organization of Scientific Research (NWO) and the Netherlands Genomics Initiative (Zenith). Printing of this thesis was financially supported by Erasmus University Rotterdam; Intermicon B.V.; family and friends: Bowen, Vicky & Jay, Zhoukai, Nikki & Mat, MJ, John & Xiaoli, Nora, Rene, Razia, Matilda, Clay, Bob, Neda, Fenna, Zhenni, Willem & Ruth, Saskia & Lamine, Clara, Ronnie

# The Mesenchymal Niche in Leukemia Predisposition Syndromes

# De mesenchymale niche in leukemie predispositie syndromen

**Doctoral dissertation**

to obtain the degree of Doctor from the
Erasmus University Rotterdam
by command of the
rector magnificus

Prof.dr. H.A.P. Pols

and in accordance with the decision of the Doctorate Board.
The public defence shall be held on

Tuesday, 13 June 2017 at 11.30 hrs

by

**Si Chen**

born in Chenzhou, China

**Erasmus University Rotterdam**

## DOCTORAL COMMITTEE

**Promotor:** Prof.dr. I.P. Touw

**Other members:** Prof.dr. H.R. Delwel
Prof.dr. J.N.J. Philipsen
Prof.dr. J.H. Jansen

**Co-promotor:** Dr. H.G.P. Raaijmakers

## CONTENTS

# 1

# GENERAL INTRODUCTION

## 1. NORMAL AND MALIGNANT HEMATOPOIESIS

### Normal hematopoiesis and hematopoietic stem cells

In the mammalian blood system, there are more than ten different types of mature blood cells, including red blood cells (RBCs), megakaryocytes, myeloid cells (monocyte/macrophage and neutrophil), and lymphocytes.[1,2] Most mature blood cells have a short life span, so hematopoietic stem cells (HSCs) are required to continuously replenish the blood system in adult life (**Figure 1**). During mammalian development, HSCs emerge from multiple hematopoietic sites sequentially, including the yolk sac, the aorta-gonad mesonephros (AGM) region, placenta, fetal liver, and eventually the bone marrow. Interestingly, the HSCs from different sites have distinct characteristics, reflecting the diversity in the supporting niche and in the intrinsic properties of HSCs at each developmental stage. For example, it is well known that HSCs in the fetal liver stage are actively in cycle and in the adult bone marrow, they reside as rare cells that are mostly quiescent. During development, multiple waves of hematopoiesis have been defined including the primitive and definitive wave. The primitive wave of hematopoiesis is transient and takes place in the yolk sac, which is quickly replaced by the definitive wave, adult-type hematopoiesis in the AGM region followed by other hematopoietic sites.[1]

The two defining features of HSCs are self-renewal and multi-potency (**Figure 1**), a state usually referred to as pluripotency. It is critical for the HSCs to keep these two processes in a delicate balance: a sufficient pool of quiescent HSCs must be maintained throughout the life time of an organism; meanwhile HSCs must continuously differentiate to replenish the short lived progenitor and mature blood cells. Any imbalance in these two processes would cause severe diseases. For instance, if differentiation of HSCs is not complemented with a usual loss of self-renewal capacity, or incomplete differentiation into mature blood cells occurs, pre-leukemic progression might be the end result.[3,4] Tremendous efforts have been dedicated to isolate and define the differentiation potential of subsets of developing hematopoietic cells, so to have a better understanding of how HSCs keep these two processes in check. In particular, immunophenotypic cell surface markers have been frequently applied, in combination with sensitive *in vitro* (e.g. colony-forming assays) and *in vivo* (transplantation) functional assays.[2] These studies have shown that HSC differentiation follows a hierarchical structure in which the multipotent capacity of these cells is progressively limited (**Figure 1**).

Firstly, sitting atop of the hematopoietic tree, HSCs can be subdivided into long-term and short-term HSCs (LT-HSCs and ST-HSCs), which can give rise to the multipotent progenitors (MPPs). MPPs no longer contain self-renewal ability, but still have the full-lineage differentiation potential.[5,6] Going down the hierarchy, MPPs differentiate into the oligopotent progenitors: the common lymphoid progenitors (CLPs)[7,8] and the common myeloid progenitors (CMPs).[9] Together, the oligopotent CLPs and CMPs give rise to all the lineage-committed mature blood cells in the hematopoietic system. For example, CLPs

produce different lymphoid cells that comprise the immune system, including nature killer (NK) cells, B and T lymphocytes; whereas CMPs differentiate into megakaryocytes/erythrocyte progenitors (MEPs) or granulocytes/macrophage progenitors (GMPs). MEPs can further give rise to RBCs or megakaryocytes, whereas GMPs differentiate into monocytes/macrophages and granulocytes.

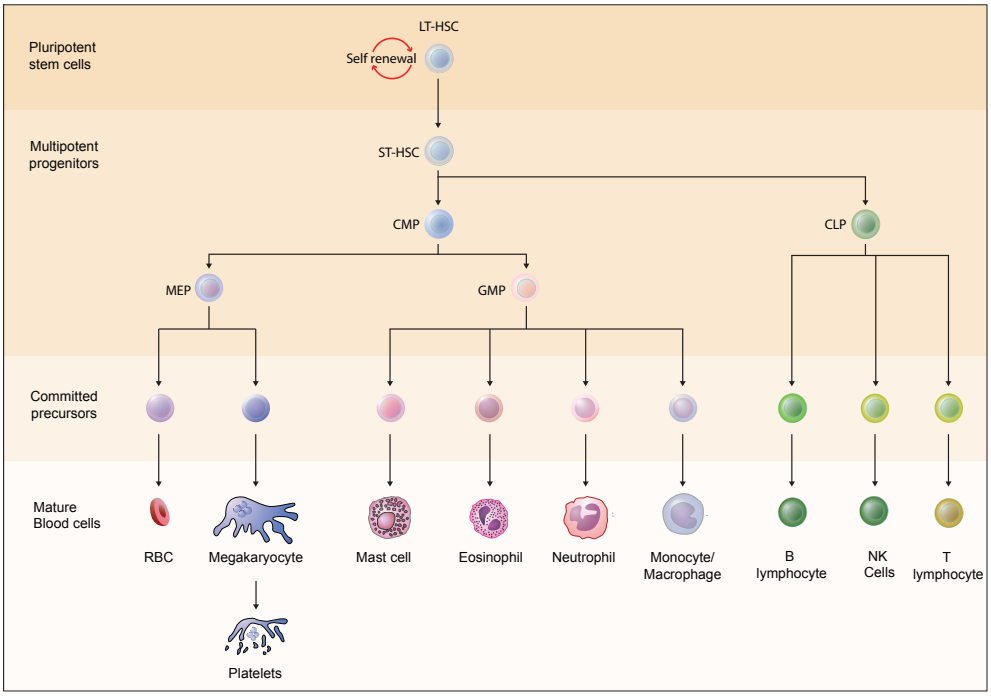


**Figure 1. Scheme of the hematopoietic tree**[1] (adapted from Orkin et al, 2008) A LT-HSC can undergo either self-renewal or differentiation. The production of mature blood cells of different lineages depends on the differentiation of the LT-HSCs and ST-HSCs. As the lineage development takes place, the multipotency of these stem/progenitor cells becomes progressively limited. Eventually fully committed mature blood cells are produced, continuously replenishing the blood system in adult life.

## The conventional view of the architecture of hematopoiesis is challenged

Recent discoveries using different HSC labelling techniques such as endogenous fluorescent tagging[10] and inducible genetic labelling[11] in combination with transplantation data, gene expression analysis and epigenetic profiling, have challenged the traditional view of the architecture of hematopoiesis as discussed above. These data suggest that under homeostatic and/or stress conditions, hematopoiesis is comprised of heterogeneous clones of HSCs with pre-defined functional features challenging the dogma that a single HSC continuously differentiates to replenish the blood system. Rather than a single pluripotent HSC balancing between self-renewal and differentiation, the new findings suggest that the

heterogeneous clones of HSCs have different cell kinetics, balancing multipotent clones that are transient with clones that provide long-term cell output. A latest study[10] suggests HSCs have a clone-specific stereotyped behavior that is epigenetically instructed, where the "epigenetic memory" is persistent and guides their function under different exogenous conditions, supporting a notion of cell autonomy. This notion seems to contradict the general thoughts of stem/progenitors being plastic cells capable of responding variably to the specific environment, arguing at least partially against the niche hypothesis (discussed in section 2 of this chapter) that the self-renewal or differentiation features of HSCs are dependent on HSC niche cues. These new findings challenge the traditional concepts of stem cell plasticity, hematopoietic hierarchy and stem cell niche to be refined. Bearing these evolving data in mind, the rest of this introduction relates to the conventional view of hematopoiesis and the work in this thesis builds on the current knowledge about the stem cell niche.

### Malignant transformation of HSCs

Following the conventional view of hematopoiesis, to ensure the homeostasis of the hematopoietic system, the normal HSCs must sustain self-renewal and multi-lineage differentiation in balance. Dysregulation in any of the two mechanisms may lead to the multi-step malignant transformation of HSCs to cancer/leukemia stem cells (CSCs/LSCs), hence the development of leukemia. Disruptions in many signaling pathways regulating self-renewal of the normal HSCs have been shown to result in tumorigenesis/leukemogenesis, among which are the well-studied Wnt, Sonic hedgehog (Shh), Notch, JAK/STAT and RAS/MAPK pathways.[12] Genetic changes that lead to leukemia development must occur either in the LT-HSCs or in progenies that first acquire the self-renewal capacity. For example, LT-HSCs can undergo a series of independent genetic and/or epigenetic changes that enable them to evade apoptosis and protective immune surveillance, transforming the HSCs to become leukemic-like. Alternatively, self-renewal genes or genes that block differentiation can be activated at the progenitor level (e.g. GMPs), giving rise to LSCs with the ability of deregulated self-renewal.[3] On the other hand, transcriptional factors (TFs) regulating the lineage-restricted differentiation must be tightly regulated, any disturbance in these TFs would lead to leukemia development as well.[1] More than twenty transcriptional factors have been described in hematopoietic malignances.[1] Among others, somatic mutations in *GATA-1*, *PU.1* and *C/EBPa*, *Pax5* and *E2A* have been respectively identified in Down Syndrome-associated megakaryocytic leukemia, myeloid leukemias and B-lymphoid leukemia.[13-16]

## 2. THE BONE MARROW MICROENVIRONMENT AND THE HSC NICHE

### Composition of the bone marrow niche and its function

The diverse functions of HSCs (incl. self-renewal, differentiation, and proliferation) must be tightly regulated and maintained in a finely tuned balance, which depends on factors derived from cell intrinsic and extrinsic sources. Extrinsic factors can be secreted from an assorted cellular types, among which components of the bone marrow microenvironment (BMME) have been regularly implicated as one of the many sources. Architecture of the BMME is rather complex and a dynamic range of components have been identified. This thesis focuses on one of them: the "HSC niche", an essential element of the BMME. The concept of the HSC niche has not been fully appreciated until half a century ago, we finally began to understand the crucial role of the HSC niche in hematopoietic homeostasis. Following the first experimental definition of a stem cell,[17,18] Michael Dexter, Brian Lord, Raymond Schofield and their colleagues in Manchester developed *in vitro* assays of mesenchymal "stromal" cultures that could maintain primitive hematopoietic cells;[19] in addition, they provided *in vivo* evidence showing that the stem and progenitor cells localize in specific regions within the bone marrow, suggesting the role of the bone in regulating hematopoiesis.[20] Shortly thereafter, the "niche hypothesis" was formulated, introducing the stem cell niche as a specific regulatory unit in maintaining the stem cell function and protecting them from external insults.[21]

Structural appreciation of the BMME is continuously evolving and distinct niches have been anatomically and physiologically defined within the BM. Among the different niches identified, this thesis focuses on the HSC niche, an important constituents of the BMME. Though the cellular complexity and functional heterogeneity of the HSC niche remain incompletely understood, this chapter (**Chapter 1**) reviews some aspects of the current understanding of the BM HSC and progenitor (HSPC) niche. Building on these discoveries, we performed a series of experiments described in this thesis, hoping to bring new insights into the contribution of the BM HSC niche to normal and malignant hematopoiesis.

A niche is defined by its anatomy and function,[22] a local microenvironment that directly maintains and regulates a stem or progenitor cell.[23] Throughout development, the HSCs reside in dynamic niches of different tissues defining the specific HSC developmental state. The first HSC niche is probably in the AGM region and yolk sac, allowing the HSCs to proliferate and expand; then the HSCs localize to the placenta and fetal liver, before migrating to the bone marrow where they are mostly quiescent to protect their integrity and functions.[24] It is of considerable interest to better understand the cellular composition and function of the HSC niche, especially the BM HSC niche, which is key to the maintenance of postnatal hematopoietic homeostasis. In the recent years, the discovery of cell surface

markers that could robustly identify HSCs *in vivo*[25] has critically contributed to the effort in defining the HSC niche. The fact that a simple combination of a few surface markers can accurately identify HSCs with high purity, allowed us to localize HSCs in tissue sections, providing important clues about the relevant localizations of the bone marrow HSC niche. In addition, a combination of experiments using *in vitro* (co-)culture assays and genetic mouse models have generated crucial insights into the functional relevance of a specific HSC niche component (**Figure 2**).

### Osteoblasts and the endosteal niche

Osteoblasts lining along the endosteal surface (**Figure 2**) were the first niche component described to regulate hematopoiesis. In the 1990s, Taichman et al established *in vitro* co-culture systems showing that osteoblasts could maintain primitive hematopoietic cells via the production of granulocyte colony-stimulating factor (G-CSF).[26,27] Later *in vivo* experiments using the Col2.3ΔTK conditional mouse model have revealed that specific ablation of osteoblast lineage cells resulted in bone loss and reduced HSCs numbers, accompanied by decreased level of hematopoietic progenitors.[28,29] Other *in vivo* studies uncovered the potential mechanism, showing the loss of HSPCs upon osteoblastic perturbation is mediated via Notch signaling and N-cadherin (*Cdh2*)-mediated adhesion.[30,31]

Since then, researchers have questioned the exact/direct role of these mature bone-lining cells in HSC regulation. For instance, absence of osteoblasts in *biglycan*-deficient mice showed no effects on HSC number or function[32]; whereas, increasing the number of osteoblasts by treating the mice with the chemical element strontium did not alter HSC activity[33] either. In addition, *in vivo* imaging studies of mice under homeostatic condition indicated few HSCs were in direct contact with osteoblasts and also few HSCs could be detected within 5 μm range of the endosteum.[25,34] Surprisingly, conditional deletion of *Cdh2* in hematopoietic and stromal cells or osteolineage cells had no effects on the number and function of HSCs, questioning the involvement of N-cadherin in osteoblasts-HSCs interaction.[32,35,36]

In fact, more recent work has suggested an indirect effect of mature osteoblasts in HSC maintenance. For example, through activation of parathyroid hormone receptor (PTHR), osteoblasts secrete cytokines, chemokines, growth factors (e.g. IL-6, RANKL and Jagged1) and extracellular matrix proteins (MMPs) that can influence other bone marrow cells including the vasculature, which could indirectly contribute to HSC regulation.[30,37] Though these data seem to suggest that the mature osteoblasts do not directly contribute to HSC maintenance, bone-forming progenitors around the endosteum are crucial for hematopoiesis. Conditional postnatal deletion of *Sp7* (osterix) (marks osteoprogenitors) severely impaired hematopoiesis in the metaphysis region[38] and bone-forming osteoprogenitors can promote the formation of HSCs niche (e.g. by recruiting vasculature) in the bone marrow.[39,40] Moreover, during BM

tissue injury, such as in a transplantation setting, HSCs have been found to preferentially home to the endosteal region in irradiated mice; but in mice under normal condition, HSCs seem to distribute randomly across the marrow.[41] Altogether, these findings indicate that the endosteal niche is essential for hematopoiesis and the mature osteoblasts probably have an indirect role in modulating HSCs by influencing other bone marrow cells and the vasculature via secreted factors (**Figure 2**).

## The perivascular niche

As earlier mentioned, the complexity and heterogeneity of the cellular components of the HSPC niche have been gradually appreciated, thanks to technical advancements. The first milestone was the introduction of SLAM family receptors, allowing identification of LT-HSCs ($CD48^-CD150^+Lin^-c\text{-}Kit^+Sca\text{-}1^+$)[25] to an accuracy where one in two isolated cells is able to reconstitute the whole BM of a transplant mouse. In parallel, optical clearing techniques enabling deep imaging through tissue sections, have granted much better assessments of the spatial relationship between HSCs and the relevant niche components. Combination of cell surface markers and the recent *in situ* imaging studies have revealed interesting findings. In homeostatic conditions, around 85% of HSCs are in close contact with sinusoidal blood vessels; meanwhile, both dividing and non-dividing HSCs (defined by Ki-67 staining) are shown to be distant from the endosteal surface.[34] These data suggest that HSCs are likely nurtured in a perivascular niche composed of perivascular stromal cells and endothelial cells, which secrete factors that are essential to HSCs maintenance and regulation (**Figure 2**). The exact relationship among these perivascular niche cells expressing different markers remain to be defined. Researchers just begin to deconstruct the complexity in relating each niche component to HSC function by experiments using a reductionist approach: systematically depleting essential niche factors from different cellular sources and examining the effect of such depletion on HSC biology.

## Key HSC supporting factors & the perivascular mesenchyme

The identity and function of niche components and key factors relevant for HSPC regulation have been much better defined in mice than in human. CXC chemokine ligand 12 (CXCL12), also known as stromal cell-derived factor (SDF)-1 has long been described to be a key HSC niche factor. Together with its primary binding receptor CXCR4, CXCL12-CXCR4 signaling plays a crucial role in the retention[42-45], quiescence[46,47] and repopulating[47] of HSCs in the bone marrow. It is worth noting that recent findings have indicated the cellular sources of CXCL12 are critical to HSC or progenitor activity; depending on the source, CXCL12 could differentially affect the stem cells or progenitors. For instance, loss of *Cxcl12* or *Cxcr4* expression from several perivascular mesenchymal stem/progenitor cells (MSCs/MPCs), including CXCL12-abundant reticular (CAR) cells[48], *Nestin*-GFP cells[49], $Lepr^+$ cells[50], and $Prx\text{-}1^+$ cells[51], resulted in reduced number of HSCs accompanied by an elevated mobilization.

Findings from these mouse models are congruent with several imaging studies showing that most HSCs juxtapose sinusoidal blood vessels, which are closely associated with the perivascular mesenchymal cells expressing high levels of CXCL12 (**Figure 2**).[25,32,34] On the other hand, instead of the HSCs, depletion of *Cxcl12* from osterix$^{+}$ (*Sp7*-Cre) osteoprogenitors and osteoblasts (*Col2.3*-cre) affected the progenitors, where the hematopoietic progenitor cells (HPCs) are mobilized. Furthermore, diminution of osteoblast-expressing CXCL12 specifically depleted the lymphoid progenitors.[50,51] Interestingly, conditional deletion of *Cxcl12* from *Nestin*-Cre-expressing stromal cells or *Vav1*-Cre hematopoietic cells had little or no effects on HSCs, nor on the more restricted HPCs.[50] These studies provided a more refined insight into the heterogeneity of CXCL12-producing cells in the perivascular niche and their distinct relations with the activities of HSCs and HPCs (**Figure 2**), suggesting the existence of distinct cellular niches in the bone marrow for stem and progenitor cells.

In addition to CXCL12, stem cell factor (SCF; also known as KITL) is another essential HSC-maintenance factor. SCF is primarily expressed perivascularly, as revealed by studies in a Scf$^{GFP}$ knock-in model.[52] Similar to CXCL12, the cellular source of SCF is relevant to the different effects on stem or progenitor cells and this relevance has been interrogated using mouse models of conditional *Scf* deletion from distinct stromal population(s). Deletion of *Scf* from *Lepr*-expressing perivascular stromal cells depleted HSCs; whereas loss of *Scf* from hematopoietic cells (*Vav1*-cre), osteoblasts (*Col2.3*-cre) and *Nestin*-Cre or *Nestin*-CreER-expressing cells did not affect HSC frequency.[52] Besides CXCL12 and SCF, other factors such as angiopoietin-1 (Ang-1) and thrombopoietin (TPO) have also been indicated important to HSC maintenance. Ang-1 signaling promotes the quiescent state of HSCs in the bone marrow niche and protects the stem cells from myelosuppression.[53] Together with its receptor MPL (expressed on HSCs), Ang1-MPL signaling is required for maintaining the quiescence of LT-HSCs by regulating cell-cycle related genes.[54] However, the important cellular source(s) of Ang-1 and TPO for HSC maintenance remain to be defined and conditional deletion experiments will be required to address this.

### Perivascular endothelial cells

Staining of bone marrow tissue section using SLAM-HSCs and endothelial markers demonstrated that endothelial cells also contribute to the perivascular niche.[25] VEGFR2 and E-selectin are specific markers for BM endothelial cells. Conditional deletion of VEGFR2 signalling blocked the recovery of sinusoidal endothelial cells (SECs) and prevented the engraftment and reconstitution of HSPCs in irradiated mice;[55] whereas deletion of E-selectin improved HSCs survival and accelerated hematopoietic recovery after chemotherapy or irradiation in mice, suggesting E-selectin promotes HSC proliferation.[56] In addition, loss of *Cxcl12* or *Scf* from *Tie2*-Cre endothelial cells specifically reduced the frequency of LT-HSCs and donor cells from the mutant mice showed significantly lower reconstitution capacity

during transplantation.[50,52] Taken together, these data demonstrated that endothelial cells are a crucial component of the perivascular niche and BM endothelial cells derived niche factors are physiologically important to HSPCs biology.

### Other components in the perivascular niche

It is important to note that endothelial cells and mesenchymal stromal cells are not the only cellular components of the perivascular niche (**Figure 2**). The sympathetic nervous system (SNS),[57,58] macrophages,[59,60] non-myelinating Schwann cells[61] among others have all been implicated in regulating HSCs retention, mobilization and circulation via CXCL12 expression, interaction with other (e.g. *Nestin*$^{+}$) mesenchymal cells, circadian oscillation or TGF-ß activation. Interestingly, mature hematopoietic cells such as macrophages or megakaryocytes can also regulate HSC activity by interacting with other niche elements or on their own. For example, in normal condition, megakaryocytes can act as a gatekeeper for HSC quiescence through secretion of CXCL4 and TGFß-1; while after chemotherapeutic challenge, megakaryocytes can promote HSC expansion via FGF1 secretion.[62,63] In a nutshell, experiments derived from these mouse models have highlighted the complexity of the HSPC niche. Our understanding of the identity, function and the lineage relationship among the many different niche cell types remains incomplete. Besides, still little is known about the human equivalence of the identified niche populations in mice.

In the few studies that investigated the cellular component of the HSC niche in human, nerve growth factor receptor (CD271) and melanoma cell adhesion molecule (CD146) have been the most widely studied markers. Human bone marrow CD271$^{+}$ cells has been shown to support hematopoiesis and are enriched for CFU-Fs with tri-lineage differentiation potential *in vitro. In situ* histology staining showed that marker CD271 stains for bone-lining cells in the trabecular region as well as perivascular cells in the marrow, both in proximity to human CD34$^{+}$ HSPCs.[64,65] CD146 defines subsets of bone marrow CD271 population to be either endosteal (CD146$^{-}$) or perivascular (CD146$^{+}$), labelling adventitial reticular cells that are enriched for CFU-F and express SCF and CXCL12.[40,64] Other markers such as PDGFRα (CD140α) and integrin αV (CD51) have also been demonstrated to label clonogenic cells in the human bone marrow that support hematopoiesis and form mesenspheres *in vitro*.[66] To date, very little is known about how the different niche populations described in mice are reflected in humans. Hence, the spatial and functional relationship between the different mesenchymal cells and HSPCs in humans remains to be defined.

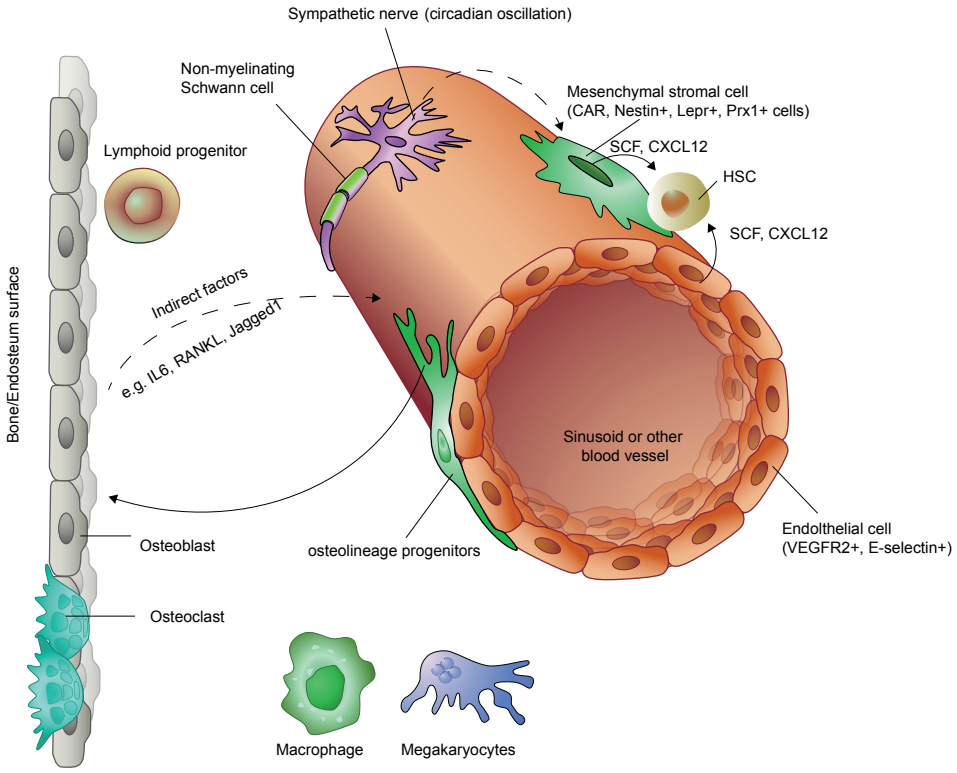


**Figure 2. the HSPC niche composition** (adapted from Morrison et al, 2014).[23] The HSCs and HPCs occupy distinct bone marrow niche, which is typically divided into the endosteal niche and the perivascular niche. Majority of HSCs are found to localize adjacent to sinusoids or other blood vessels, where endothelial cells (typically marked by VEGFR2 and E-selectin) and mesenchymal stromal cells (expressing CAR, nestin, lepr, and prx1) regulate HSC activity via the secretion of HSC-supporting factors, such as CXCL12 and SCF. Other factors might also be involved. Osteoprogenitors (osterix expressing) are important bone forming cells that play a key role in HSC regulation as well. The bone-lining osteoblasts and osteoclasts seem to be more directly involved in the maintenance and differentiation of the early lymphoid progenitors, while they are more likely to play an indirect role in HSC regulation. Other cellular types also contribute to the complex architecture of the HSPC niche, including sympathetic nerves, non-myelinating Schwann cells, macrophages and megakaryocytes.

The cellular composition of the HSPC niche is complex and heterogeneous. This thesis covered the role of several key HSPC niche components in mouse models and human patients. Specifically, in **Chapter 3**, we extensively investigated osterix$^{+}$ mesenchymal progenitor cells (MPCs) using mouse models. In **Chapter 2, 3 and 4**, we studied CD271$^{+}$ mesenchymal cells in human patients.

## 3. HUMAN PRE-LEUKEMIC CONDITIONS

### 3.1 Bone marrow failure syndromes: ribosomopathies

Bone marrow failure (BMF) syndromes can be either inherited or acquired. The inherited form is characterized by ineffective hematopoiesis, frequent physical anomalies and predisposition to cancer with distinct clinical presentations specific to each disease. Inherited BMF syndromes include Fanconi Anemia (FA), Dyskeratosis Congenita (DC), Shwachman-Diamond Syndrome (SDS), Diamond-Blackfan Anemia (DBA), congenital amegakaryocytic thrombocytopenia (CAMT) and severe congenital neutropenia (SCN).[67] In the past decades, tremendous efforts have been dedicated to a better understanding of the genetics associated with inherited BMF syndromes. Alongside, we have also gained considerable insights in normal hematopoiesis and how this is disrupted in BMF patients. Importantly, these studies have advanced our knowledge in fundamental biological pathways, such as ribosome biogenesis. A group of inherited BMF syndromes including DBA, SDS and DC is associated with defective ribosome biogenesis. These syndromes, together with 5q- syndrome, a subtype of adult myelodysplastic syndrome (MDS) where the ribosomal gene RPS14 is mutated, are collectively known as ribosomopathies.

Ribosome biogenesis is a highly-regulated and complex process that plays a key role in the regulation of protein translation.[68] Eukaryotic ribosomes consist of the small 40S and the large 60S subunits, which join together to form the translationally active 80S ribosome. Ribosome assembly is a complex process using large amount of cellular biosynthetic energy. This process requires many important components including 4 structural ribosomal RNAs (rRNAs), around 80 core ribosomal proteins, more than 150 associated proteins and around 70 small nucleolar RNAs (snoRNAs).[69] The 40S subunit contains 18S rRNA and the 60S subunit contains 28S, 5.8S, and 5S rRNAs. The 5.8S, 18S and 28S rRNAs are transcribed by RNA polymerase I whereas 5S rRNA is transcribed by RNA polymerase III. In the nucleolus, ribosomal proteins, nonribosomal assembly/processing factors and snoRNAs bind to the precursor rRNA transcripts to facilitate a series of cleavage and modification events, including methylation and pseudouridylation to produce pre-60S and pre-40S preribosomal/precursor particles. These preribosomal/precursor particles are then transported to the cytoplasm for the final steps of producing actively translating mature ribosomes.[70] Mutations in distinct ribosomal proteins have been linked to defects at the specific steps in pre-rRNA processing, resulting in incomplete/dysfunctional ribosome biogenesis and ultimately defects in protein translation machinery, which give rise to specific ribosomal abnormalities that present diverse clinical phenotypes (**Figure 3**).

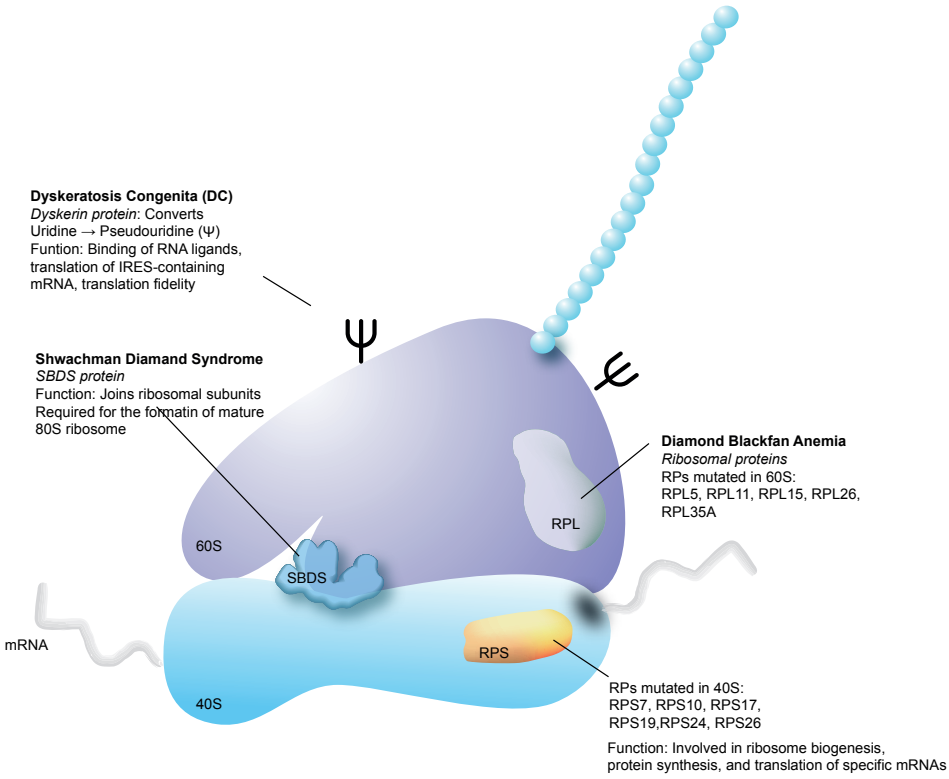


**Figure 3. Key ribosome components and mutations associated with ribosomopathies** (adapted from Ruggero et al, 2014).[68] The dyskerin protein, an rRNA pseudouridine synthase is encoded by *DKC1* gene, that is frequently mutated in X-DC. SDS is caused by mutations in *Sbds* gene that is important for joining the two ribosomal subunits. In DBA, RP genes encoding ribosomal proteins that are associated with small and large ribosomal subunits are often mutated.

## Diamond-Blackfan Anemia

In 1999, recurrent mutations in a ribosomal protein gene *RPS19* were reported in patients with DBA.[71] Thereafter, heterozygous mutations resulting in haploinsufficiency in 11 additional ribosomal genes have been identified (**Table 1**). DBA is probably the congenital BMF syndrome with the highest degree of genetic heterogeneity. On average, 60%-70% of DBA cases are due to mutations in ribosomal genes, which leave the rest of the patients genetically unidentified.[68] In some cases of DBA, X-linked mutations in the transcription factor *GATA1*, which is critical for erythropoiesis have been reported.[72] Typically, DBA patients have normochromic anemia that is macrocytic with reticulocytopenia. Bone marrow of these patients is usually normocellular with defective or absence of erythroid precursors. Approximately 40%-62% of DBA patients have physical anomalies including craniofacial (e.g. lip or palate cleft) or thumb abnormalities, cardiac defects and short stature.[73] Other noted characteristics that have been integrated into the diagnosis of DBA include elevated level of

adenosine deaminase in RBCs and the presence of fetal membrane antigen "i" (**Table 1**).[74,75] Currently, the only curative treatment is bone marrow transplantation. Typical supportive care for DBA patients aims to improve erythropoiesis by applying steroids and chronic RBCs transfusions.[76]

Generally in DBA, as a result of heterozygous mutations leading to haploinsufficiency or reduced expression in different ribosomal proteins, the level of 40S or 60S ribosomal subunits is significantly lower, so as the amount of mature 80S ribosomes.[77-80] Though an overall decrease in the number of mature ribosomes, DBA patients carrying mutations in the 11 different ribosomal genes present distinct clinical features; yet the effect of decreased ribosomal protein activity *in vivo* and in a tissue-specific manner remain to be revealed.

## 5q⁻ Syndrome

*5q⁻* syndrome was first described in 1974. It is an acquired MDS characterized by a *5q⁻* cytogenetic clonal abnormality. Interestingly, *5q⁻* patients shares many clinical features with DBA patients.[81] According to the World Health Organization (WHO) criteria, *5q⁻* syndrome is clinically characterized by severe macrocytic anemia, thrombocytosis with hypolobulated micromegakaryocytes, and a lower rate of progression to acute myeloid leukemia (AML) compared to other MDS subtypes (**Table 1**).[82] Ribosomal gene *RPS14* resides in the common deleted region of *5q*. The link between this ribosomal gene and the disease dates back to the experiment where a small interfering RNA screen was performed. Each gene within the *5q⁻* syndrome common deleted region was knocked down, only knock-down of *RPS14* showed defects specifically in erythropoiesis, while the other lineages were relatively preserved. Notably, introduction of the *RPS14* gene back into the samples from *5q⁻* patients rescued erythroid differentiation.[83] *RPS14* haploinsufficiency results in significantly lower level of the 40S small ribosomal subunit, most likely due to defective pre-18S rRNA processing.[83] Thus, the molecular pathophysiology of *5q⁻* MDS appears to overlap with that of DBA.[84] In addition to *RPS14*, other genes and microRNAs present within the *5q* locus have been shown to contribute to other aspects of the disease phenotype.[85]

## Shwachman-Diamond Syndrome

SDS was first reported in 1964 in a group of 5 children.[86] It is a rare (around 1 in 50,000 births) autosomal recessive disease[69], characterized by ineffective hematopoiesis(mostly neutropenia), exocrine pancreatic dysfunction, and an increased risk for the development of clonal cytogenetic abnormalities, MDS and AML (**Table 1**). Patients typically present steatorrhea and serious infection due to neutropenia, but often show signs of anemia, thrombocytopenia, short stature and skeletal defects as well.[68] Bone marrow transplantation is the only definitive therapy and SDS patients are mostly treated with supportive cares including pancreatic enzymes, antibiotics, RBCs or platelets transfusions, and G-CSF.[87]

Approximately 90% of SDS patients are caused by biallelic mutations in the *SBDS* gene located on chromosome 7q11, among which 75% of these mutations are due to a gene conversion with an adjacent highly homologous pseudogene, *SBDSP*, which contains mutations that disrupt protein production.[88] The *SBDS* gene is revolutionarily conserved with orthologs in archaea, plants and vertebrates, and it is ubiquitously expressed across a broad range of tissues. Though the exact structure and function of *SBDS* remain to be revealed, accumulating evidence indicates the important role it plays in ribosome biogenesis and RNA processing.[89] A number of experiments conducted earlier in yeast, followed by findings in mouse models, suggest that SBDS promotes the release of eukaryotic initiating factor (EIF6) from the pre-60S ribosome by catalyzing the GTPase activity of elongation factor-like 1 (EFL1).[90,91] The GTP coupled EFL1 undergoes a structural conformation change that induces the release of ELF6, which then allows the full maturation of the large 60S subunit and its binding to the 40S.[90,91] This ribosome joining step is crucial to the subsequent formation of the mature 80S functional ribosome. Deletion of *Sbds* in animal models resulted in polysome profiles with halfmers, a pattern that is observed when the 40S subunit failed to join the 60S subunit.[91] In addition, reduced ribosomal subunit joining has been observed in SDS patients, further indicating that the ELF6 releasing function of SBDS is impaired due to mutations in the *SBDS* gene.[92,93] Interestingly, besides the suggested role of SBDS in ribosome biogenesis, recent evidence has uncovered its non-ribosomal activities, ranging from stabilizing the mitotic spindle,[94,95] to the metabolism of cytoskeleton in neutrophils,[96] to improving cellular survival in the context of cellular stress.[97] These non-ribosomal activities may also play an important role in the clinical phenotypes of SDS patients.

| Disease | Gene Defect | Clinical Features | Cancer Risk | Diagnosis |
|---|---|---|---|---|
| **Diamond Blackfan Anemia (DBA)** | RPS: 7, 10, 17, 19, 24, 26<br>RPL: 5, 11, 15, 26, 35A | Macrocytic anemia; short stature; cranifocial defects; thumb abnormalities | ?osteosarcoma; ?MDS | RPS19/RPS24 sequencing; elevated ADA; elevated Hgb F levels |
| **5q-syndrome** | RPS14 | Macrocytic anemia; hypolobulated micromegakaryocytes | 10% progression to ALM | bone marrow aspiration/biopsy with karyotype |
| **Swachman-Diamond syndrome (SDS)** | SBDS | neutroponie/infections; pancreatic insufficiency; short stature | MDS and AML | SBDS gene testing |

**Table 1. Summary of the clinical features, cancer risks and diagnostics for ribosomopathies: DBA, 5q- syndrome and SDS.**[69]
ADA: adenosine deaminase; Hgb F: fetal hemoglobin

Of the abovementioned ribosomopathies, **Chapter 3** in this thesis studied the rare congenital BMF disease SDS. In this chapter, we modelled SDS by specifically deleting the gene *Sbds* in the osterix-expressing MPCs and investigated the contribution of the niche to disease pathogenesis.

### 3.2 (Low-risk) Myelodysplastic Syndromes (LRMDS)

Myelodysplastic syndromes (MDS) probably represent the most common group of acquired bone marrow failures syndrome in adults, specifically in the elderly.[98] So far, MDS have been considered to be clonal disorders of the hematopoietic compartment characterized by ineffective hematopoiesis, dysplastic cell morphology, cytopenia in the peripheral blood, and a high propensity for clonal evolution to AML. Typically, MDS may be classified as indolent (low-risk) or aggressive (high-risk) MDS, depending on the survival and risk for leukemic progression. The clinical presentation of MDS patients is heterogeneously grouped to many different subtypes, likely due to the great variety of genetic lesions contributing to disease pathogenesis. It is the principal hematological pre-malignancy, with >30,000 patients diagnosed per year in the United states.[99] At the moment, MDS is diagnosed through a combination of assessments on both morphologic abnormalities and histological architecture using bone marrow aspirate and biopsy. When these assessments are coupled with conventional karyotyping (abnormal in ~50% of *de novo* MDS patients) and mutation analysis, we can in most cases confirm disease clonality.[98] In the past decades, the classical prognostication scoring systems of MDS have undergone continuous revisions, trying to address the limitations of each version. The International Prognostic Scoring System (IPSS) was first introduced in 1997,[100] and revised in 2012 (IPSS-R).[101] Though IPSS-R is the most widely used tool for predicting the disease risk, complementary risk models including the WHO classification-based prognostic scoring system (WPSS), the MD Anderson Comprehensive Scoring system, and the MDS Anderson Lower Risk MDS Model have been developed.[102-104]

#### Model of disease pathogenesis

In order for a MDS clone to result in clinical manifestations, the balance of self-renewal and differentiation must be deregulated as discussed in section 1.2 of this introduction, usually via a multi-step transformation. The steps associated with MDS disease pathogenesis (**Figure 4**)[105] include 1) enhanced self-renewal in the MDS disease-initiating HSPCs;[106] 2) increased proliferative capacity accompanied by the acquisition of anti-apoptotic mechanisms in the disease-sustaining clone; 3) impaired differentiation; 4) (epi)genetic instability; 5) circumvention of the immune system; and (6) suppressed normal hematopoiesis. The clinical manifestation of the disease, including the types/degrees of cytopenia present and whether the disease is indolent or aggressive, could be perhaps due to the degree at which each step is affected.

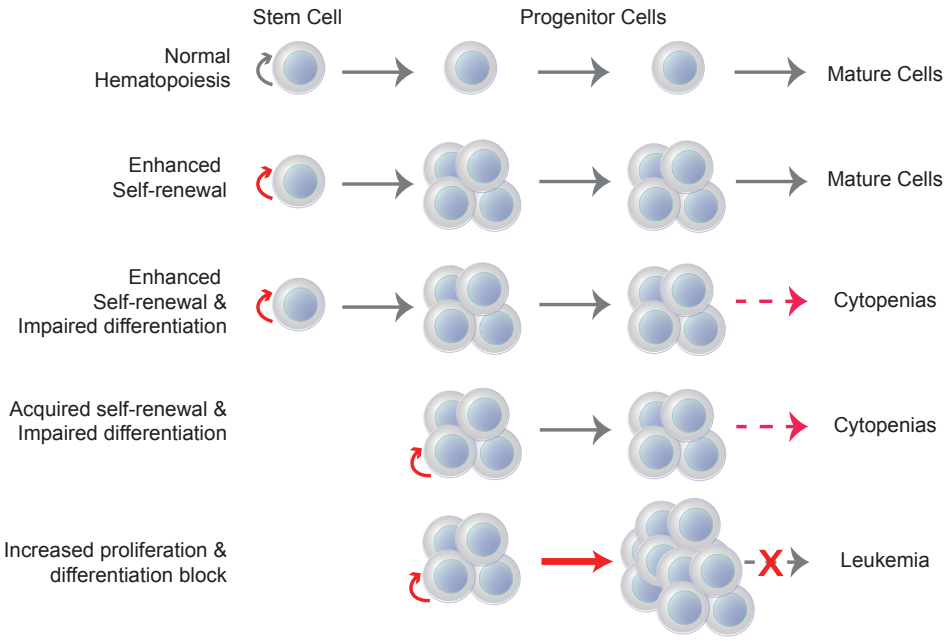


**Figure 4. Different pathways to transformation in MDS** (adapted from Bejar R et al, 2011).[105] The key feature of MDS is clonal expansion and ineffective hematopoiesis, which often result in cytopenias. The observed clinical phenotypes are likely due to the combination of different genetic and epigenetic abnormalities, driving cellular events that give clonal advantage of certain lesions. Individual lesions, such as enhanced self-renewal or altered apoptosis may cause one single transformation step, where in itself is clinically silent. However, when several abnormalities (e,g, acquired self-renewal and impaired differentiation) co-occur, such cooperation between two or more lesions is likely required for the full disease manifestation.

## Molecular genetics of MDS

Recent advancements in high-resolution genome-wide techniques, e.g. single nucleotide polymorphism (SNP) genotyping arrays, comparative genome hybridization, and targeted sequencing have allowed us to discover additional (recurrently) mutated genes, and (occult) chromosomal abnormalities, which have improved our understanding of the genetic basis associated with MDS development.[98]

## Chromosomal abnormalities

Knowing the chromosomal abnormalities of a patient is useful both diagnostically and prognostically. For example, deletion of Chromosome 5q (5q-) is the most common cytogenetic abnormality in MDS patient, with an incidence of roughly 15%. These patients typically have a relatively favorable prognosis with particularly good response to lenalidomide treatment.[101,107] Careful analysis of the genes associated with commonly deleted regions (CDRs) in 5q- patients have implicated the importance of several genes in the pathogenesis of this MDS subtype. Haploinsufficiency of the ribosomal gene *RPS14* was identified to be

critical for the severe dyserythropoiesis, of which the mechanism was detailed in section 3.1. Haploinsufficiencies of the two microRNAs, *miR-145* and *miR-146* are found to cause elevated platelet counts and may provide a selective advantage to the 5q- clone.[108] Another two groups of MDS patients with 20q- (2-5%) and –Y (2-4%) abnormalities are also considered to be in the favorable prognosis group as are patients with a normal karyotype.[105] The loss of Y chromosome seems to be unrelated to the disease pathogenesis of –Y patients.[109] Unlike 5q- subtype, analysis of the CDR of 20q identified 19 genes localized in this region; yet none of these genes have been conclusively associated with MDS pathogenesis.[110,111]

Unlike the good-risk cytogenetic abnormalities mentioned above, patients with 7q deletion, also known as monosomy 7 (~10%) are associated with relatively poor prognosis.[105] So far, at least three CDRs on 7q have been identified; unfortunately, the underlying molecular lesions that drive the disease phenotypes are not well understood.[112-114] As the only recurrent chromosomal amplification, trisomy 8 is indicated in around 8% of MDS patients and belongs to the group of intermediate-risk cytogenetic abnormality with less than half the median expected survival of patients with a normal karyotype (22.0 vs 53.4 months).[115] Nevertheless, trisomy 8 patients respond to immunosuppressive therapy quite well.[105]

### Common genetic and epigenetic abnormalities

Numerous sequencing studies have identified a number of frequently mutated genes in MDS and many of them directly contribute to disease pathogenesis and leukemia development. To date, *TET2* is one of the most frequently mutated genes in MDS patients with an incidence of nearly 20%; *TET2* mutations have also been identified in several other myeloid neoplasms, including MPN (10%), CML (30%-50%) and AML (25%).[116,117] *TET2* is a member of the TET family, which encodes methylcytosine oxidases, involved in regulating DNA methylation.[118,119] In addition, mutations in *ASXL1* and *EZH2* have been identified to affect histone modifications with an incidence of 10% and 6% respectively in MDS patients.[120-122] In line with these reports, mutations in the DNA methyltransferase gene *DNMT3A* have been identified in ~12% of MDS patients.[98,123] Collectively, these findings indicate the important role of epigenetic dysregulation and altered gene expression in driving the pathogenesis of MDS.

Interestingly, in 2009, the first whole-genome sequencing of an AML sample discovered recurrent mutations in the isocitrate dehydrogenase genes *IDH1* and *IDH2*, which were first described in glioblastoma and thought to be tissue-specific oncogenes.[124] Later work has focused on targeted sequencing of these two genes in AML and MDS. These work demonstrated that *IDH* mutations altered the function of these metabolic enzymes catalyzing the conversion of α-ketoglutarate (αKG) to 2-hydroxyglutarate (2HG), which resulted in the accumulation of the 2HG oncometabolite.[125,126] Mutations in IDH1 and IDH2 have been

identified in rare cases of MDS (~5%) and are often associated with more advanced disease and progression to AML.[127,128]

Subsequently, whole genome sequencing has identified a novel class of mutated genes in MDS patients, encoding mRNA splicing factors. The first gene identified in this group was *SF3B1*. It is particularly frequently mutated (>70%) in a subgroup of MDS patients with refractory anemia with ring sideroblasts (RARS).[129] Soon after, mutations in other splicing factors such as *SRSF2*, *U2AF1* and *ZRSR2* were identified.[130,131] Together as a group, splicing factor mutations became the most frequently mutated class of genes in MDS, which were identified in >50% of MDS patients (**Figure 5**). Nonetheless, the association between these splicing factor mutations and MDS disease pathogenesis is yet to be understood.

In the earlier genetic studies conducted between 1987 and 2005, the first genetic mutations identified in MDS patients were *TP53*, *NRAS/KRAS* and *RUNX1* among many others.[132-135] *TP53* is a classical tumor suppressor gene, which is often mutated in tumor cells, associated with genomic instability. Mutation of *TP53* is found in 5%-15% of MDS patients, associated with poor prognosis and treatment resistance.[136,137] In some cases of MDS, patients are characterized by activating mutations of the downstream *RAS* genes such as *NRAS* (10%-15%) and *KRAS* (1%-2%), often associated with poor prognosis and progression to AML.[135] *RUNX1* belongs to the member of the transcriptional core-binding factor gene family and is the second most commonly mutated gene in MDS with a frequency of 7%-15%; the incidence is higher in therapy-related diseases.[138] In both MDS and AML, the presence of RUNX1 mutations indicate poor prognosis.[139]

Taken altogether, developments in whole genome sequencing techniques have provided us with a much better understanding of the mutational landscape of MDS and valuable insights into the clonal architecture of different neoplasms. However, these discoveries have not yet had major impact on treatment. Until today, the available drugs are not curative and allogeneic hematopoietic stem cell transplantation (HSCT) remains to be the only curative therapy.

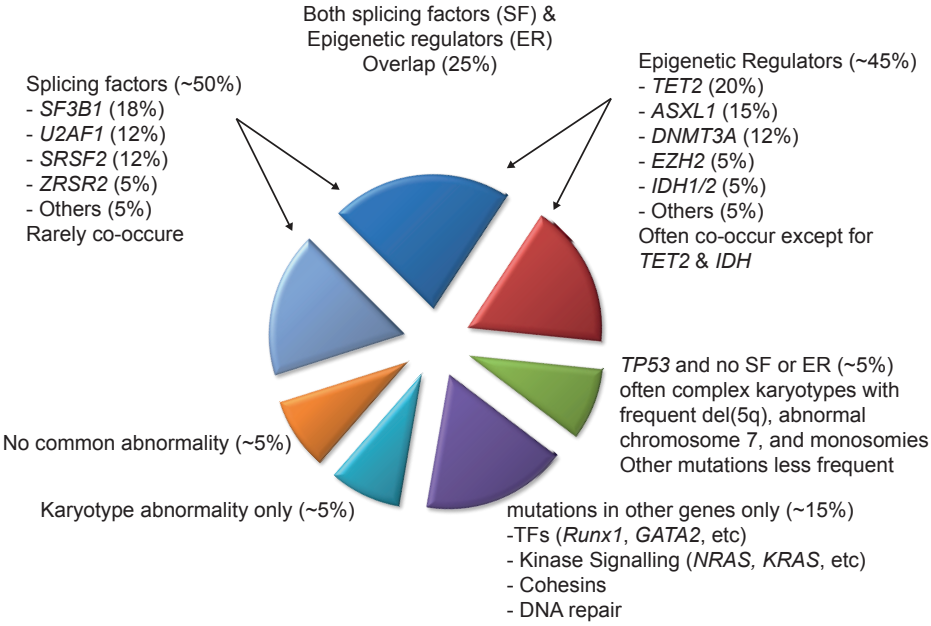


**Figure 5. Distribution of chromosomal abnormalities and (recurrent) genetic mutations in MDS** (adapted from Bejar R et al, 2014).[98] The most frequent mutations seen in MDS patients are mutations in splicing factors (SF) (~50%) or epigenetic regulators (ER) (~45%); around 25% of patients have mutations in both groups. Mutations in *TP53* gene often co-occur with other complex chromosomal abnormalities. Mutations in other genes can co-occur with or in the absence of SF or ER lesions in ~15% of patients; where only 10% of patients do not carry the commonly recurrent mutations.

MDS - the principal human pre-leukemic disorder is extensively studied in this thesis. **Chapter 2** and **Chapter 4**, for the first time in the field, characterized the molecular landscape of highly purified mesenchymal population in LRMDS. In **Chapter 3**, to investigate the broader relevance of the findings in SDS mouse model to human patients, we looked into the purified mesenchymal cells from 45 MDS patients. Chapter 5 explored the stromal compartment in a mouse model of MDS.

## 4. ROLE OF THE HSPC NICHE IN HEMATOPOIETIC DISORDERS

As mentioned earlier, the HSPC niche plays a critical role in regulating stem cell quiescence and number, particularly, in ensuring HSPC homeostasis. It is therefore reasonable to hypothesize that perturbation of the HSPC niche may contribute to the disease pathogenesis of hematological (pre)malignancies. Increasing evidence has challenged the traditional view that pre-leukemic and leukemic disorders are hematopoietic cell-autonomous diseases, but rather that the microenvironmental context can initiate and/or modify hematopoietic neoplasia.[140] The hypothesis was first (indirectly) supported by the description of donor derived leukemia (DDL), a rare event following allogeneic hematopoietic cell transplantation (HCT), likely due to an altered microenvironment in the transplant recipients, leading to oncogenic transformation of the normal donor hematopoietic cells.[141]

### Model of niche-induced leukemogenesis

Summarizing findings in the past decades defining the contribution of the bone marrow niche to leukemogenesis, two different but not mutually exclusive models have been proposed: niche-induced and niche-facilitated leukemogenesis (**Figure 6**). The first studies demonstrating microenvironment-induced disruption in hematopoiesis are associated with myeloproliferative neoplasm/disease (MPN/MPD). In 2005, Rupec et al. showed that mice with ubiquitous deletion of IκBα developed MPN-like phenotypes. But conditional deletion of IκBα in myeloid lineage and in fetal liver cells did not result in disease development, suggesting the observed MPN is likely initiated by non-hematopoietic cells with inactive IκBα.[142] Soon after, in a retinoic acid receptor (RAR) $\gamma^{-/-}$ MPN mouse model, myeloproliferation was not intrinsic to hematopoietic cells, but due to alterations in the microenvironment as only transplantation of wild-type cells into RAR$\gamma^{-/-}$ recipients resulted in disease development, not vice versa.[143] A parallel study demonstrated that similar MPN phenotypes were only observed when deletion of retinoblastoma protein (Rb) took place in both hematopoietic cells and their BMME, as deletion in either one cellular source alone was not sufficient to induce any phenotype.[144] Likewise, similar transplantation experiments in the mind bomb 1 (Mib1$^{-/-}$) mouse model revealed a BMME-dependent development of MPD due to defective Notch activation in the non-hematopoietic cells.[145] Together, these examples indicated that the hyper-proliferation phenotype of MPN is induced by alterations in the BMME; however, these findings did not specify the disease-causing niche component and hematopoietic cell transformation was not observed.

Disruption of *Dicer1*, an endonuclease essential for microRNA biogenesis, in an osterix-expressing osteoprogenitor cell induced MDS-like phenotype and secondary leukemia with novel cytogenetic abnormalities. This study provided the first evidence demonstrating that primary alterations in a specific cellular component of the HSPC niche can initiate

malignancy in a distinct, parenchymal cell; thus, introducing the concept of "niche-induced oncogenesis" in the hematopoietic system.[146] Deletion of *Dicer1* in osterix$^+$ osteoprogenitors led to the downregulation of *Sbds*, the disease-causing gene of human SDS.[146] Interestingly, the mouse model of conditional *Sbds* deletion in osterix$^+$ osteoprogenitors faithfully recapitulated the MDS-like hematopoietic phenotypes in human SDS.[146] The concept of niche-induced oncogenesis is further supported by another study indicating that disease-relevant mutation in PTPN11, a gene often mutated in Noonan syndrome, specifically in mesenchymal progenitor cells (including osterix$^+$ cells) indirectly disrupted the function of HSPCs and induced the development of MPN in mice.[147] In line with these findings, another study has reported that activating mutations in ß–catenin in osteoblasts associated with increased Notch signaling, resulted in the development of AML in mice.[148] Taken together, these data suggest that primary dysfunction in a specific component of the HSPC niche, in particular the mesenchymal progenitor cells, can initiate hematological malignancies.

### Model of niche-facilitated leukemogenesis

In parallel, several other studies have supported the model of "niche-facilitated leukemogenesis" (**Figure 6**). In this proposed model, the malignant hematopoietic cells can shape the HSPC niche into a self-reinforcing leukemic niche, which impairs normal hematopoiesis, favors the function of LSCs, and therefore contributes to disease pathogenesis. In contrast to the previously mentioned "niche-induced" model, an altered osteoblastic niche is a result of cell-cell interactions with leukemic cells. In a mouse model of chronic myeloid leukemia (CML), severe osteoblastic defects in cell number and function were observed, leading to a major bone loss associated with high level of CCL3 in mice and human patients.[149] In line with this report, data obtained from a transgenic model of BCR-ABL1$^+$ CML showed that the HSPC niche was remodeled into a leukemic niche with expansion of functionally impaired osteoblasts. Notch, TGF-ß and inflammatory signaling were found to be involved in the remodeling process. In addition, CCL3, TPO and direct cell-cell contact resulted in the osteoblastic expansion. Exposure of either normal HSCs or LSCs to the leukemic osteoblastic niche led to a reduced reconstitution capacity of the normal cells, but the function of LSCs remained intact, congruent with the decreased level of key HSCs-supporting factors.[150] These findings suggest that inhibition of the "remodeling" effect of the leukemic cells, which likely shapes the niche in a way most beneficial to LSCs, but detrimental to normal HSCs, might have a negative impact on leukemic progression. However, further research into this direction is required.

Another study demonstrating the importance of cooperation between the niche and aberrant hematopoietic cells was performed in a xenotransplantation model of MDS. Only co-transplantation of MDS-initiating Lin$^-$CD34$^+$CD38$^-$ stem cells with patient-derived mesenchymal stem/progenitor cells (MSPCs), isolated based on plastic adherence, resulted

in the development of MDS-like phenotypes in murine recipients. These patient-derived MSPCs presented altered differentiation pattern and distinct global transcriptome profile compared to the normal counterparts, probably due to factors such as N-cadherin, ILGFBP2, VEGFA and LIF as a result of interacting with the hematopoietic MDS cells.[151]

In the meantime, parallel studies have provided us with a better understanding of the mechanism underlying how LSCs alter the HSPC niche, specifically the perivascular niche. As previously mentioned, the arterioles in the bone marrow are highly innervated by the SNS, which plays an essential role in regulating HSCs activity. In a murine (JAK2 V617F$^+$) MPN model, the malignant HSCs resulted in neuropathy (loss of neural fibers) and depletion of nestin$^+$ mesenchymal cells via the secretion of IL-1ß. The loss of neural fibers and mesenchymal elements severely accelerated MPN development. Treatment with sympathomimetic agent (ß3-adrenergic agonist) restored the loss of nestin$^+$ mesenchymal cells and blocked the development of disease, indirectly via the reduction of MPN cells.[152] These findings were supported by another study reporting leukemia-induced neuropathy of the SNS promotes leukemic bone marrow infiltration in a murine AML model of MLL-AF9 AML. AML development impaired the quiescence of nestin$^+$ cells, promoting the differentiation of MSPCs towards osteoblasts, while not favoring the peri-arteriolar niche cells with HSC-supporting capacity. Interestingly, leukemogenesis was promoted by the ß2-adrenergic receptor expressed on the stromal cells of the leukemic bone marrow, suggesting that the malignant cells might be able to “hijack” the SNS to integrate the BMME, to foster and advance the neoplasm.[153]

Taken together, we have gained a more comprehensive understanding of the architecture of the BMME at a cellular resolution, which allowed us to interrogate the contribution of specific HSPC niche component to disease pathogenesis using different (conditional) genetic mouse models. While these experimental tools have advanced our knowledge, these experimental conditions are unlikely to be met in human investigations, so the human relevance of these findings is yet to be established.

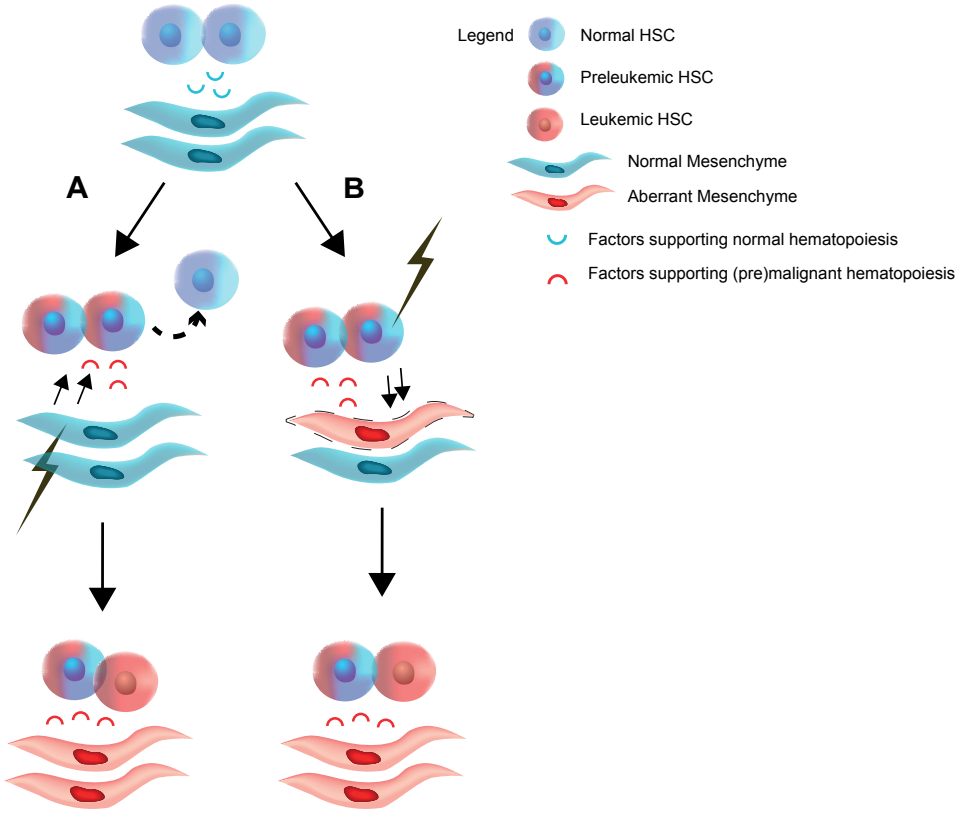


**Figure 6. The role of the niche in leukemogenesis.** (A) Model of "niche-induced leukemogenesis": primary alteration in the cellular component of the HSPC niche can disrupt normal hematopoiesis, induce transformation of normal HSCs to become aberrant pre-leukemic HSCs, and further promote the development of leukemia. (B) Model of "niche-facilitated leukemogenesis": acquisition of genetic abnormalities in normal HSCs transform these normal cells to become pre-leukemic. These pre-leukemic HSCs remodel their niche into an aberrant niche that contribute to the transformation of the pre-leukemic cells into leukemic HSCs.

## Role of the HSPC niche in Human MDS

Alterations in the bone marrow environment have long been documented in MDS and other myeloid malignancies. The "topography" (localization) of the hematopoietic elements within the marrow is often disrupted.[154-156] Elevated levels of VEGF and numerous inflammatory cytokines (e.g. IL-6, IL-8, TNFα, TGFß etc.) are often observed in the bone marrow of MDS patients, which were thought to be the result of the interplay among the aberrant hematopoietic cells, activated immune system and the stroma.[157,158] Though many immunodeficient mouse models have been developed for investigating human hematopoietic malignancies via xenograft transplantation, application of this approach has proven to be difficult in MDS. In MDS, transplantation studies have consistently shown poor engraftment of myelodysplastic cells in immunodeficient mice, and failure to recapitulate hematopoietic phenotypes of human MDS.[159-162] These observations suggest that MDS is a disease of the tissue, that disruption of hematopoiesis goes beyond changes in the hematopoietic cells alone.

So far, our knowledge about the role of the MDS stroma is derived from *ex vivo* expanded stromal cells based on their plastic adherence property – also known as bone marrow derived stromal cells (BMDSC). Though the data is highly controversial, BMDSC isolated from MDS and AML patients have been identified to carry genetic abnormalities.[163,164] Other data defining the transcriptional changes of these BMDSC from MDS patients have revealed the following: reduced expression of adhesion molecules[165] and transcriptional factors[166], activation of p38MAPK signalling[167] and TNF- modulating genes[168], and increased expression of a range of cytokines.[151] However, how these adherent stromal cells in a dish reflect the complex bone marrow architecture of human patients remains largely unknown.

## 5. SCOPE AND OUTLINE OF THE THESIS

Accumulating evidence in the past years has revealed that hematopoietic disorders are diseases of the tissue, where the niche cells, immune cells, among other elements, in addition to aberrancies in the hematopoietic compartment contribute to disease pathogenesis. As mentioned earlier, insights into the biology of the bone marrow niche elements in hematopoietic aberrancies have been limited to studies investigating *ex vivo* expanded stromal cells where the relevance to their *in situ* counterparts remains largely unknown. The first goal of this thesis as described in **chapter 2**, is to characterize the global transcriptome of prospectively isolated, directly purified mesenchymal elements from a cohort of low-risk MDS (LR-MDS) patients. Our previous work in mouse modeling has supported the concept of "niche-induced leukemogenesis" by showing ribosomal stress in osteoprogenitors can induce MDS-like hematopoietic abnormalities, recapitulating key phenotypes in SDS patients. In **chapter 3**, we interrogated the molecular mechanism(s) behind this concept as well as its relevance to human disease by combining mouse modelling of *Sbds* deletion in osterix$^{+}$ MPCs and investigating human-equivalent mesenchymal cells in SDS and MDS patients. Extending our findings from chapter 2 and chapter 3, in **chapter 4**, we revealed activation of Nuclear Factor-κB (NF-κB) pathway as a biological commonality in LR-MDS mesenchyme, supported by *ex vivo* genetic study demonstrating the inhibitory effect of mesenchymal NF-κB signaling in normal hematopoiesis. In **chapter 5**, we were interested in the other side of the coin by using a hematopoietic cell-autonomous model of MDS - the *Vav-Nup98-Hoxd13* (NHD13) model to investigate the effect of altered HSPCs (NHD13+ MDS cells) on their niche and how this niche may affect normal hematopoiesis and contribute to bone marrow failure. In the end, the findings in this thesis are summarized in **chapter 6**, along with discussions concerning the relevance of our findings to the field of hematopoietic (pre)malignancies, broader relevance to cancer and potential future perspectives.

## REFERENCES OF INTRODUCTION

1. Orkin SH, Zon LI. Hematopoiesis: An evolving paradigm for stem cell biology. *Cell*. 2008;132(4):631-644.
2. Seita J, Weissman IL. Hematopoietic stem cell: self-renewal versus differentiation. *Wiley Interdiscip Rev Syst Biol Med*. 2010;2(6):640-653.
3. Weissman I. Stem cell research: paths to cancer therapies and regenerative medicine. *JAMA*. 2005;294(11):1359-1366.
4. Reya T, Morrison SJ, Clarke MF, Weissman IL. Stem cells, cancer, and cancer stem cells. *Nature*. 2001;414(6859):105-111.
5. Morrison SJ, Weissman IL. The long-term repopulating subset of hematopoietic stem cells is deterministic and isolatable by phenotype. *Immunity*. 1994;1(8):661-673.
6. Christensen JL, Weissman IL. Flk-2 is a marker in hematopoietic stem cell differentiation: a simple method to isolate long-term stem cells. *Proc Natl Acad Sci U S A*. 2001;98(25):14541-14546.
7. Serwold T, Ehrlich LI, Weissman IL. Reductive isolation from bone marrow and blood implicates common lymphoid progenitors as the major source of thymopoiesis. *Blood*. 2009;113(4):807-815.
8. Kondo M, Weissman IL, Akashi K. Identification of clonogenic common lymphoid progenitors in mouse bone marrow. *Cell*. 1997;91(5):661-672.
9. Akashi K, Traver D, Miyamoto T, Weissman IL. A clonogenic common myeloid progenitor that gives rise to all myeloid lineages. *Nature*. 2000;404(6774):193-197.
10. Yu VW, Yusuf RZ, Oki T, et al. Epigenetic Memory Underlies Cell-Autonomous Heterogeneous Behavior of Hematopoietic Stem Cells. *Cell*. 2016;167(5):1310-1322 e1317.
11. Busch K, Klapproth K, Barile M, et al. Fundamental properties of unperturbed haematopoiesis from stem cells in vivo. *Nature*. 2015;518(7540):542-546.
12. Taipale J, Beachy PA. The Hedgehog and Wnt signalling pathways in cancer. *Nature*. 2001;411(6835):349-354.
13. Wechsler J, Greene M, McDevitt MA, et al. Acquired mutations in GATA1 in the megakaryoblastic leukemia of Down syndrome. *Nat Genet*. 2002;32(1):148-152.
14. Mueller BU, Pabst T, Osato M, et al. Heterozygous PU.1 mutations are associated with acute myeloid leukemia. *Blood*. 2002;100(3):998-1007.
15. Pabst T, Mueller BU, Zhang P, et al. Dominant-negative mutations of CEBPA, encoding CCAAT/enhancer binding protein-alpha (C/EBPalpha), in acute myeloid leukemia. *Nat Genet*. 2001;27(3):263-270.
16. Mullighan CG, Goorha S, Radtke I, et al. Genome-wide analysis of genetic alterations in acute lymphoblastic leukaemia. *Nature*. 2007;446(7137):758-764.
17. Till JE, Mc CE. A direct measurement of the radiation sensitivity of normal mouse bone marrow cells. *Radiat Res*. 1961;14:213-222.
18. Becker AJ, Mc CE, Till JE. Cytological demonstration of the clonal nature of spleen colonies derived from transplanted mouse marrow cells. *Nature*. 1963;197:452-454.
19. Dexter TM, Allen TD, Lajtha LG. Conditions controlling the proliferation of haemopoietic stem cells in vitro. *J Cell Physiol*. 1977;91(3):335-344.
20. Lord BI, Testa NG, Hendry JH. The relative spatial distributions of CFUs and CFUc in the normal mouse femur. *Blood*. 1975;46(1):65-72.

21. Schofield R. The relationship between the spleen colony-forming cell and the haematopoietic stem cell. . *Blood Cells*. 1978;4((1-2)):7-45.

22. Scadden DT. The stem-cell niche as an entity of action. *Nature*. 2006;441(7097):1075-1079.

23. Morrison SJ, Scadden DT. The bone marrow niche for haematopoietic stem cells. *Nature*. 2014;505(7483):327-334.

24. Boulais PE, Frenette PS. Making sense of hematopoietic stem cell niches. *Blood*. 2015;125(17):2621-2629.

25. Kiel MJ, Yilmaz OH, Iwashita T, Yilmaz OH, Terhorst C, Morrison SJ. SLAM family receptors distinguish hematopoietic stem and progenitor cells and reveal endothelial niches for stem cells. *Cell*. 2005;121(7):1109-1121.

26. Taichman RS, Emerson SG. Human osteoblasts support hematopoiesis through the production of granulocyte colony-stimulating factor. *J Exp Med*. 1994;179(5):1677-1682.

27. Taichman RS, Reilly MJ, Emerson SG. Human osteoblasts support human hematopoietic progenitor cells in vitro bone marrow cultures. *Blood*. 1996;87(2):518-524.

28. Visnjic D, Kalajzic Z, Rowe DW, Katavic V, Lorenzo J, Aguila HL. Hematopoiesis is severely altered in mice with an induced osteoblast deficiency. *Blood*. 2004;103(9):3258-3264.

29. Zhu J, Garrett R, Jung Y, et al. Osteoblasts support B-lymphocyte commitment and differentiation from hematopoietic stem cells. *Blood*. 2007;109(9):3706-3712.

30. Calvi LM, Adams GB, Weibrecht KW, et al. Osteoblastic cells regulate the haematopoietic stem cell niche. *Nature*. 2003;425(6960):841-846.

31. Zhang J, Niu C, Ye L, et al. Identification of the haematopoietic stem cell niche and control of the niche size. *Nature*. 2003;425(6960):836-841.

32. Kiel MJ, Radice GL, Morrison SJ. Lack of evidence that hematopoietic stem cells depend on N-cadherin-mediated adhesion to osteoblasts for their maintenance. *Cell Stem Cell*. 2007;1(2):204-217.

33. Lymperi S, Horwood N, Marley S, Gordon MY, Cope AP, Dazzi F. Strontium can increase some osteoblasts without increasing hematopoietic stem cells. *Blood*. 2008;111(3):1173-1181.

34. Acar M, Kocherlakota KS, Murphy MM, et al. Deep imaging of bone marrow shows non-dividing stem cells are mainly perisinusoidal. *Nature*. 2015;526(7571):126-130.

35. Greenbaum AM, Revollo LD, Woloszynek JR, Civitelli R, Link DC. N-cadherin in osteolineage cells is not required for maintenance of hematopoietic stem cells. *Blood*. 2012;120(2):295-302.

36. Bromberg O, Frisch BJ, Weber JM, Porter RL, Civitelli R, Calvi LM. Osteoblastic N-cadherin is not required for microenvironmental support and regulation of hematopoietic stem and progenitor cells. *Blood*. 2012;120(2):303-313.

37. Dai JC, He P, Chen X, Greenfield EM. TNFalpha and PTH utilize distinct mechanisms to induce IL-6 and RANKL expression with markedly different kinetics. *Bone*. 2006;38(4):509-520.

38. Zhou X, Zhang Z, Feng JQ, et al. Multiple functions of Osterix are required for bone growth and homeostasis in postnatal mice. *Proc Natl Acad Sci U S A*. 2010;107(29):12919-12924.

39. Chan CK, Chen CC, Luppen CA, et al. Endochondral ossification is required for haematopoietic stem-cell niche formation. *Nature*. 2009;457(7228):490-494.

40. Sacchetti B, Funari A, Michienzi S, et al. Self-renewing osteoprogenitors in bone marrow sinusoids can organize a hematopoietic microenvironment. *Cell*. 2007;131(2):324-336.

41. Lo Celso C, Fleming HE, Wu JW, et al. Live-animal tracking of individual haematopoietic stem/progenitor cells in their niche. *Nature*. 2009;457(7225):92-96.

42. Peled A, Petit I, Kollet O, et al. Dependence of human stem cell engraftment and repopulation of NOD/SCID mice on CXCR4. *Science*. 1999;283(5403):845-848.

43. Ara T, Itoi M, Kawabata K, et al. A role of CXC chemokine ligand 12/stromal cell-derived factor-1/pre-B cell growth stimulating factor and its receptor CXCR4 in fetal and adult T cell development in vivo. *J Immunol*. 2003;170(9):4649-4655.

44. Bonig H, Priestley GV, Nilsson LM, Jiang Y, Papayannopoulou T. PTX-sensitive signals in bone marrow homing of fetal and adult hematopoietic progenitor cells. *Blood*. 2004;104(8):2299-2306.

45. Kawabata K, Ujikawa M, Egawa T, et al. A cell-autonomous requirement for CXCR4 in long-term lymphoid and myeloid reconstitution. *Proc Natl Acad Sci U S A*. 1999;96(10):5663-5667.

46. Nie Y, Han YC, Zou YR. CXCR4 is required for the quiescence of primitive hematopoietic cells. *J Exp Med*. 2008;205(4):777-783.

47. Tzeng YS, Li H, Kang YL, Chen WC, Cheng WC, Lai DM. Loss of Cxcl12/Sdf-1 in adult mice decreases the quiescent state of hematopoietic stem/progenitor cells and alters the pattern of hematopoietic regeneration after myelosuppression. *Blood*. 2011;117(2):429-439.

48. Sugiyama T, Kohara H, Noda M, Nagasawa T. Maintenance of the hematopoietic stem cell pool by CXCL12-CXCR4 chemokine signaling in bone marrow stromal cell niches. *Immunity*. 2006;25(6):977-988.

49. Mendez-Ferrer S, Michurina TV, Ferraro F, et al. Mesenchymal and haematopoietic stem cells form a unique bone marrow niche. *Nature*. 2010;466(7308):829-834.

50. Ding L, Morrison SJ. Haematopoietic stem cells and early lymphoid progenitors occupy distinct bone marrow niches. *Nature*. 2013;495(7440):231-235.

51. Greenbaum A, Hsu YM, Day RB, et al. CXCL12 in early mesenchymal progenitors is required for haematopoietic stem-cell maintenance. *Nature*. 2013;495(7440):227-230.

52. Ding L, Saunders TL, Enikolopov G, Morrison SJ. Endothelial and perivascular cells maintain haematopoietic stem cells. *Nature*. 2012;481(7382):457-462.

53. Arai F, Hirao A, Ohmura M, et al. Tie2/angiopoietin-1 signaling regulates hematopoietic stem cell quiescence in the bone marrow niche. *Cell*. 2004;118(2):149-161.

54. Yoshihara H, Arai F, Hosokawa K, et al. Thrombopoietin/MPL signaling regulates hematopoietic stem cell quiescence and interaction with the osteoblastic niche. *Cell Stem Cell*. 2007;1(6):685-697.

55. Hooper AT, Butler JM, Nolan DJ, et al. Engraftment and reconstitution of hematopoiesis is dependent on VEGFR2-mediated regeneration of sinusoidal endothelial cells. *Cell Stem Cell*. 2009;4(3):263-274.

56. Winkler IG, Barbier V, Nowlan B, et al. Vascular niche E-selectin regulates hematopoietic stem cell dormancy, self renewal and chemoresistance. *Nat Med*. 2012;18(11):1651-1657.

57. Katayama Y, Battista M, Kao WM, et al. Signals from the sympathetic nervous system regulate hematopoietic stem cell egress from bone marrow. *Cell*. 2006;124(2):407-421.

58. Mendez-Ferrer S, Lucas D, Battista M, Frenette PS. Haematopoietic stem cell release is regulated by circadian oscillations. *Nature*. 2008;452(7186):442-447.

59. Chow A, Lucas D, Hidalgo A, et al. Bone marrow CD169+ macrophages promote the retention of hematopoietic stem and progenitor cells in the mesenchymal stem cell niche. *J Exp Med*. 2011;208(2):261-271.

60. Winkler IG, Sims NA, Pettit AR, et al. Bone marrow macrophages maintain hematopoietic stem cell (HSC) niches and their depletion mobilizes HSCs. *Blood*. 2010;116(23):4815-4828.

61. Yamazaki S, Ema H, Karlsson G, et al. Nonmyelinating Schwann cells maintain hematopoietic stem cell hibernation in the bone marrow niche. *Cell*. 2011;147(5):1146-1158.

62. Bruns I, Lucas D, Pinho S, et al. Megakaryocytes regulate hematopoietic stem cell quiescence through CXCL4 secretion. *Nat Med*. 2014;20(11):1315-1320.

63. Zhao M, Perry JM, Marshall H, et al. Megakaryocytes maintain homeostatic quiescence and promote post-injury regeneration of hematopoietic stem cells. *Nat Med*. 2014;20(11):1321-1326.

64. Tormin A, Li O, Brune JC, et al. CD146 expression on primary nonhematopoietic bone marrow stem cells is correlated with in situ localization. *Blood*. 2011;117(19):5067-5077.

65. Chen S, Zambetti NA, Bindels EM, et al. Massive parallel RNA sequencing of highly purified mesenchymal elements in low-risk MDS reveals tissue-context-dependent activation of inflammatory programs. *Leukemia*. 2016;30(9):1938-1942.

66. Pinho S, Lacombe J, Hanoun M, et al. PDGFRalpha and CD51 mark human nestin+ sphere-forming mesenchymal stem cells capable of hematopoietic progenitor cell expansion. *J Exp Med*. 2013;210(7):1351-1367.

67. Dokal I, Vulliamy T. Inherited bone marrow failure syndromes. *Haematologica*. 2010;95(8):1236-1240.

68. Ruggero D, Shimamura A. Marrow failure: a window into ribosome biology. *Blood*. 2014;124(18):2784-2792.

69. Narla A, Ebert BL. Ribosomopathies: human disorders of ribosome dysfunction. *Blood*. 2010;115(16):3196-3205.

70. Henras AK, Soudet J, Gerus M, et al. The post-transcriptional steps of eukaryotic ribosome biogenesis. *Cell Mol Life Sci*. 2008;65(15):2334-2359.

71. Draptchinskaia N, Gustavsson P, Andersson B, et al. The gene encoding ribosomal protein S19 is mutated in Diamond-Blackfan anaemia. *Nat Genet*. 1999;21(2):169-175.

72. Sankaran VG, Ghazvinian R, Do R, et al. Exome sequencing identifies GATA1 mutations resulting in Diamond-Blackfan anemia. *J Clin Invest*. 2012;122(7):2439-2443.

73. Lipton JM, Ellis SR. Diamond-Blackfan anemia: diagnosis, treatment, and molecular pathogenesis. *Hematol Oncol Clin North Am*. 2009;23(2):261-282.

74. Glader BE, Backer K, Diamond LK. Elevated erythrocyte adenosine deaminase activity in congenital hypoplastic anemia. *N Engl J Med*. 1983;309(24):1486-1490.

75. Fargo JH, Kratz CP, Giri N, et al. Erythrocyte adenosine deaminase: diagnostic value for Diamond-Blackfan anaemia. *Br J Haematol*. 2013;160(4):547-554.

76. Vlachos A, Federman N, Reyes-Haley C, Abramson J, Lipton JM. Hematopoietic stem cell transplantation for Diamond Blackfan anemia: a report from the Diamond Blackfan Anemia Registry. *Bone Marrow Transplant*. 2001;27(4):381-386.

77. Choesmel V, Bacqueville D, Rouquette J, et al. Impaired ribosome biogenesis in Diamond-Blackfan anemia. *Blood*. 2007;109(3):1275-1283.

78. Choesmel V, Fribourg S, Aguissa-Toure AH, et al. Mutation of ribosomal protein RPS24 in Diamond-Blackfan anemia results in a ribosome biogenesis disorder. *Hum Mol Genet*. 2008;17(9):1253-1263.

79. Flygare J, Aspesi A, Bailey JC, et al. Human RPS19, the gene mutated in Diamond-Blackfan anemia, encodes a ribosomal protein required for the maturation of 40S ribosomal subunits. *Blood*. 2007;109(3):980-986.

80. Idol RA, Robledo S, Du HY, et al. Cells depleted for RPS19, a protein associated with Diamond Blackfan Anemia, show defects in 18S ribosomal RNA synthesis and small ribosomal subunit production. *Blood Cells Mol Dis*. 2007;39(1):35-43.

81. Van den Berghe H, Cassiman JJ, David G, Fryns JP, Michaux JL, Sokal G. Distinct haematological disorder with deletion of long arm of no. 5 chromosome. *Nature*. 1974;251(5474):437-438.

82. Vardiman JW, Harris NL, Brunning RD. The World Health Organization (WHO) classification of the myeloid neoplasms. *Blood*. 2002;100(7):2292-2302.

83. Ebert BL, Pretz J, Bosco J, et al. Identification of RPS14 as a 5q- syndrome gene by RNA interference screen. *Nature*. 2008;451(7176):335-339.

84. Ebert BL, Lee MM, Pretz JL, et al. An RNA interference model of RPS19 deficiency in Diamond-Blackfan anemia recapitulates defective hematopoiesis and rescue by dexamethasone: identification of dexamethasone-responsive genes by microarray. *Blood*. 2005;105(12):4620-4626.

85. Ebert BL. Deletion 5q in myelodysplastic syndrome: a paradigm for the study of hemizygous deletions in cancer. *Leukemia*. 2009;23(7):1252-1256.

86. Schwachman H DL, Oski FA, Khaw KT. The syndrome of pancreatic insufficiency and bone marrow dysfunction. *J Pediatr*. 1964;65:645-663.

87. Burroughs L, Woolfrey A, Shimamura A. Shwachman-Diamond syndrome: a review of the clinical presentation, molecular pathogenesis, diagnosis, and treatment. *Hematol Oncol Clin North Am*. 2009;23(2):233-248.

88. Boocock GR, Morrison JA, Popovic M, et al. Mutations in SBDS are associated with Shwachman-Diamond syndrome. *Nat Genet*. 2003;33(1):97-101.

89. Ganapathi KA, Austin KM, Lee CS, et al. The human Shwachman-Diamond syndrome protein, SBDS, associates with ribosomal RNA. *Blood*. 2007;110(5):1458-1465.

90. Menne TF, Goyenechea B, Sanchez-Puig N, et al. The Shwachman-Bodian-Diamond syndrome protein mediates translational activation of ribosomes in yeast. *Nat Genet*. 2007;39(4):486-495.

91. Finch AJ, Hilcenko C, Basse N, et al. Uncoupling of GTP hydrolysis from eIF6 release on the ribosome causes Shwachman-Diamond syndrome. *Genes Dev*. 2011;25(9):917-929.

92. Wong CC, Traynor D, Basse N, Kay RR, Warren AJ. Defective ribosome assembly in Shwachman-Diamond syndrome. *Blood*. 2011;118(16):4305-4312.

93. Burwick N, Coats SA, Nakamura T, Shimamura A. Impaired ribosomal subunit association in Shwachman-Diamond syndrome. *Blood*. 2012;120(26):5143-5152.

94. Austin KM, Gupta ML, Jr., Coats SA, et al. Mitotic spindle destabilization and genomic instability in Shwachman-Diamond syndrome. *J Clin Invest*. 2008;118(4):1511-1518.

95. Orelio C, Verkuijlen P, Geissler J, van den Berg TK, Kuijpers TW. SBDS expression and localization at the mitotic spindle in human myeloid progenitors. *PLoS One*. 2009;4(9):e7084.

96. Orelio C, Kuijpers TW. Shwachman-Diamond syndrome neutrophils have altered chemoattractant-induced F-actin polymerization and polarization characteristics. *Haematologica*. 2009;94(3):409-413.

97. Ball HL, Zhang B, Riches JJ, et al. Shwachman-Bodian Diamond syndrome is a multi-functional protein implicated in cellular stress responses. *Hum Mol Genet*. 2009;18(19):3684-3695.

98. Bejar R, Steensma DP. Recent developments in myelodysplastic syndromes. *Blood*. 2014;124(18):2793-2803.

99. Goldberg SL, Chen E, Corral M, et al. Incidence and clinical complications of myelodysplastic syndromes among United States Medicare beneficiaries. *J Clin Oncol*. 2010;28(17):2847-2852.

100. Greenberg P, Cox C, LeBeau MM, et al. International scoring system for evaluating prognosis in myelodysplastic syndromes. *Blood*. 1997;89(6):2079-2088.

101. Greenberg PL, Tuechler H, Schanz J, et al. Revised international prognostic scoring system for myelodysplastic syndromes. *Blood*. 2012;120(12):2454-2465.

102. Malcovati L, Della Porta MG, Strupp C, et al. Impact of the degree of anemia on the outcome of patients with myelodysplastic syndrome and its integration into the WHO classification-based Prognostic Scoring System (WPSS). *Haematologica*. 2011;96(10):1433-1440.

103. Kantarjian H, O'Brien S, Ravandi F, et al. Proposal for a new risk model in myelodysplastic syndrome that accounts for events not considered in the original International Prognostic Scoring System. *Cancer*. 2008;113(6):1351-1361.

104. Garcia-Manero G, Shan J, Faderl S, et al. A prognostic score for patients with lower risk myelodysplastic syndrome. *Leukemia*. 2008;22(3):538-543.

105. Bejar R, Levine R, Ebert BL. Unraveling the molecular pathophysiology of myelodysplastic syndromes. *J Clin Oncol*. 2011;29(5):504-515.

106. Nimer SD. MDS: a stem cell disorder--but what exactly is wrong with the primitive hematopoietic cells in this disease? *Hematology Am Soc Hematol Educ Program*. 2008:43-51.

107. List A, Dewald G, Bennett J, et al. Lenalidomide in the myelodysplastic syndrome with chromosome 5q deletion. *N Engl J Med*. 2006;355(14):1456-1465.

108. Starczynowski DT, Kuchenbauer F, Argiropoulos B, et al. Identification of miR-145 and miR-146a as mediators of the 5q- syndrome phenotype. *Nat Med*. 2010;16(1):49-58.

109. Wiktor A, Rybicki BA, Piao ZS, et al. Clinical significance of Y chromosome loss in hematologic disease. *Genes Chromosomes Cancer*. 2000;27(1):11-16.

110. Bench AJ, Nacheva EP, Hood TL, et al. Chromosome 20 deletions in myeloid malignancies: reduction of the common deleted region, generation of a PAC/BAC contig and identification of candidate genes. UK Cancer Cytogenetics Group (UKCCG). *Oncogene*. 2000;19(34):3902-3913.

111. Wang PW, Eisenbart JD, Espinosa R, 3rd, Davis EM, Larson RA, Le Beau MM. Refinement of the smallest commonly deleted segment of chromosome 20 in malignant myeloid diseases and development of a PAC-based physical and transcription map. *Genomics*. 2000;67(1):28-39.

112. Le Beau MM, Espinosa R, 3rd, Davis EM, Eisenbart JD, Larson RA, Green ED. Cytogenetic and molecular delineation of a region of chromosome 7 commonly deleted in malignant myeloid diseases. *Blood*. 1996;88(6):1930-1935.

113. Dohner K, Brown J, Hehmann U, et al. Molecular cytogenetic characterization of a critical region in bands 7q35-q36 commonly deleted in malignant myeloid disorders. *Blood*. 1998;92(11):4031-4035.

114. Asou H, Matsui H, Ozaki Y, et al. Identification of a common microdeletion cluster in 7q21.3 subband among patients with myeloid leukemia and myelodysplastic syndrome. *Biochem Biophys Res Commun*. 2009;383(2):245-251.

115. Haase D, Germing U, Schanz J, et al. New insights into the prognostic impact of the karyotype in MDS and correlation with subtypes: evidence from a core dataset of 2124 patients. *Blood*. 2007;110(13):4385-4395.

116. Delhommeau F, Dupont S, Della Valle V, et al. Mutation in TET2 in myeloid cancers. *N Engl J Med*. 2009;360(22):2289-2301.

117. Mullighan CG. TET2 mutations in myelodysplasia and myeloid malignancies. *Nat Genet*. 2009;41(7):766-767.

118. Ko M, Huang Y, Jankowska AM, et al. Impaired hydroxylation of 5-methylcytosine in myeloid cancers with mutant TET2. *Nature*. 2010;468(7325):839-843.

119. Tahiliani M, Koh KP, Shen Y, et al. Conversion of 5-methylcytosine to 5-hydroxymethylcytosine in mammalian DNA by MLL partner TET1. *Science*. 2009;324(5929):930-935.

120. Gelsi-Boyer V, Trouplin V, Adelaide J, et al. Mutations of polycomb-associated gene ASXL1 in myelodysplastic syndromes and chronic myelomonocytic leukaemia. *Br J Haematol*. 2009;145(6):788-800.

121. Ernst T, Chase AJ, Score J, et al. Inactivating mutations of the histone methyltransferase gene EZH2 in myeloid disorders. *Nat Genet*. 2010;42(8):722-726.

122. Nikoloski G, Langemeijer SM, Kuiper RP, et al. Somatic mutations of the histone methyltransferase gene EZH2 in myelodysplastic syndromes. *Nat Genet*. 2010;42(8):665-667.

123. Ley TJ, Ding L, Walter MJ, et al. DNMT3A mutations in acute myeloid leukemia. *N Engl J Med*. 2010;363(25):2424-2433.

124. Mardis ER, Ding L, Dooling DJ, et al. Recurring mutations found by sequencing an acute myeloid leukemia genome. *N Engl J Med*. 2009;361(11):1058-1066.

125. Dang L, White DW, Gross S, et al. Cancer-associated IDH1 mutations produce 2-hydroxyglutarate. *Nature*. 2009;462(7274):739-744.

126. Ward PS, Patel J, Wise DR, et al. The common feature of leukemia-associated IDH1 and IDH2 mutations is a neomorphic enzyme activity converting alpha-ketoglutarate to 2-hydroxyglutarate. *Cancer Cell*. 2010;17(3):225-234.

127. Thol F, Weissinger EM, Krauter J, et al. IDH1 mutations in patients with myelodysplastic syndromes are associated with an unfavorable prognosis. *Haematologica*. 2010;95(10):1668-1674.

128. Kosmider O, Gelsi-Boyer V, Slama L, et al. Mutations of IDH1 and IDH2 genes in early and accelerated phases of myelodysplastic syndromes and MDS/myeloproliferative neoplasms. *Leukemia*. 2010;24(5):1094-1096.

129. Papaemmanuil E, Cazzola M, Boultwood J, et al. Somatic SF3B1 mutation in myelodysplasia with ring sideroblasts. *N Engl J Med*. 2011;365(15):1384-1395.

130. Yoshida K, Sanada M, Shiraishi Y, et al. Frequent pathway mutations of splicing machinery in myelodysplasia. *Nature*. 2011;478(7367):64-69.

131. Graubert TA, Shen D, Ding L, et al. Recurrent mutations in the U2AF1 splicing factor in myelodysplastic syndromes. *Nat Genet*. 2011;44(1):53-57.

132. Pedersen-Bjergaard J, Andersen MK, Christiansen DH, Nerlov C. Genetic pathways in therapy-related myelodysplasia and acute myeloid leukemia. *Blood*. 2002;99(6):1909-1912.

133. Pedersen-Bjergaard J, Christiansen DH, Andersen MK, Skovby F. Causality of myelodysplasia and acute myeloid leukemia and their genetic abnormalities. *Leukemia*. 2002;16(11):2177-2184.

134. Kaneko H, Misawa S, Horiike S, Nakai H, Kashima K. TP53 mutations emerge at early phase of myelodysplastic syndrome and are associated with complex chromosomal abnormalities. *Blood*. 1995;85(8):2189-2193.

135. Christiansen DH, Andersen MK, Desta F, Pedersen-Bjergaard J. Mutations of genes in the receptor tyrosine kinase (RTK)/RAS-BRAF signal transduction pathway in therapy-related myelodysplasia and acute myeloid leukemia. *Leukemia*. 2005;19(12):2232-2240.

136. Horiike S, Kita-Sasai Y, Nakao M, Taniwaki M. Configuration of the TP53 gene as an independent prognostic parameter of myelodysplastic syndrome. *Leuk Lymphoma*. 2003;44(6):915-922.

137. Kita-Sasai Y, Horiike S, Misawa S, et al. International prognostic scoring system and TP53 mutations are independent prognostic indicators for patients with myelodysplastic syndrome. *Br J Haematol*. 2001;115(2):309-312.

138. Christiansen DH, Andersen MK, Pedersen-Bjergaard J. Mutations of AML1 are common in therapy-related myelodysplasia following therapy with alkylating agents and are significantly associated with deletion or loss of chromosome arm 7q and with subsequent leukemic transformation. *Blood*. 2004;104(5):1474-1481.

139. Chen CY, Lin LI, Tang JL, et al. RUNX1 gene mutation in primary myelodysplastic syndrome--the mutation can be detected early at diagnosis or acquired during disease progression and is associated with poor outcome. *Br J Haematol*. 2007;139(3):405-414.

140. Scadden DT. Nice neighborhood: emerging concepts of the stem cell niche. *Cell*. 2014;157(1):41-50.

141. Flynn CM, Kaufman DS. Donor cell leukemia: insight into cancer stem cells and the stem cell niche. *Blood*. 2007;109(7):2688-2692.

142. Rupec RA, Jundt F, Rebholz B, et al. Stroma-mediated dysregulation of myelopolesis in mice lackingk l kappa B alpha. *Immunity*. 2005;22(4):479-491.

143. Walkley CR, Olsen GH, Dworkin S, et al. A microenvironment-induced myeloproliferative syndrome caused by retinoic acid receptor gamma deficiency. *Cell*. 2007;129(6):1097-1110.

144. Walkley CR, Shea JM, Sims NA, Purton LE, Orkin SH. Rb regulates interactions between hematopoietic stem cells and their bone marrow microenvironment. *Cell*. 2007;129(6):1081-1095.

145. Kim YW, Koo BK, Jeong HW, et al. Defective Notch activation in microenvironment leads to myeloproliferative disease. *Blood*. 2008;112(12):4628-4638.

146. Raaijmakers MH, Mukherjee S, Guo S, et al. Bone progenitor dysfunction induces myelodysplasia and secondary leukaemia. *Nature*. 2010;464(7290):852-857.

147. Dong L, Yu WM, Zheng H, et al. Leukaemogenic effects of Ptpn11 activating mutations in the stem cell microenvironment. *Nature*. 2016.

148. Kode A, Manavalan JS, Mosialou I, et al. Leukaemogenesis induced by an activating beta-catenin mutation in osteoblasts. *Nature*. 2014;506(7487):240-244.

149. Frisch BJ, Ashton JM, Xing L, Becker MW, Jordan CT, Calvi LM. Functional inhibition of osteoblastic cells in an in vivo mouse model of myeloid leukemia. *Blood*. 2012;119(2):540-550.

150. Schepers K, Pietras EM, Reynaud D, et al. Myeloproliferative neoplasia remodels the endosteal bone marrow niche into a self-reinforcing leukemic niche. *Cell Stem Cell*. 2013;13(3):285-299.

151. Medyouf H, Mossner M, Jann JC, et al. Myelodysplastic cells in patients reprogram mesenchymal stromal cells to establish a transplantable stem cell niche disease unit. *Cell Stem Cell*. 2014;14(6):824-837.

152. Arranz L, Sanchez-Aguilera A, Martin-Perez D, et al. Neuropathy of haematopoietic stem cell niche is essential for myeloproliferative neoplasms. *Nature*. 2014;512(7512):78-81.

153. Hanoun M, Zhang D, Mizoguchi T, et al. Acute myelogenous leukemia-induced sympathetic neuropathy promotes malignancy in an altered hematopoietic stem cell niche. *Cell Stem Cell*. 2014;15(3):365-375.

154. Raaijmakers MH. Myelodysplastic syndromes: revisiting the role of the bone marrow microenvironment in disease pathogenesis. *Int J Hematol*. 2012;95(1):17-25.

155. Bartl R, Frisch B, Baumgart R. Morphologic classification of the myelodysplastic syndromes (MDS): combined utilization of bone marrow aspirates and trephine biopsies. *Leuk Res*. 1992;16(1):15-33.

156. Mangi MH, Mufti GJ. Primary myelodysplastic syndromes: diagnostic and prognostic significance of immunohistochemical assessment of bone marrow biopsies. *Blood*. 1992;79(1):198-205.

157. Bellamy WT, Richter L, Sirjani D, et al. Vascular endothelial cell growth factor is an autocrine promoter of abnormal localized immature myeloid precursors and leukemia progenitor formation in myelodysplastic syndromes. *Blood*. 2001;97(5):1427-1434.

158. Tsimberidou AM, Estey E, Wen S, et al. The prognostic significance of cytokine levels in newly diagnosed acute myeloid leukemia and high-risk myelodysplastic syndromes. *Cancer*. 2008;113(7):1605-1613.

159. Benito AI, Bryant E, Loken MR, et al. NOD/SCID mice transplanted with marrow from patients with myelodysplastic syndrome (MDS) show long-term propagation of normal but not clonal human precursors. *Leuk Res*. 2003;27(5):425-436.

160. Thanopoulou E, Cashman J, Kakagianne T, Eaves A, Zoumbos N, Eaves C. Engraftment of NOD/SCID-beta2 microglobulin null mice with multilineage neoplastic cells from patients with myelodysplastic syndrome. *Blood*. 2004;103(11):4285-4293.

161. Kerbauy DM, Lesnikov V, Torok-Storb B, Bryant E, Deeg HJ. Engraftment of distinct clonal MDS-derived hematopoietic precursors in NOD/SCID-beta2-microglobulin-deficient mice after intramedullary transplantation of hematopoietic and stromal cells. *Blood*. 2004;104(7):2202-2203.

162. Muguruma Y, Matsushita H, Yahata T, et al. Establishment of a xenograft model of human myelodysplastic syndromes. *Haematologica*. 2011;96(4):543-551.

163. Blau O, Baldus CD, Hofmann WK, et al. Mesenchymal stromal cells of myelodysplastic syndrome and acute myeloid leukemia patients have distinct genetic abnormalities compared with leukemic blasts. *Blood*. 2011;118(20):5583-5592.

164. Blau O, Hofmann WK, Baldus CD, et al. Chromosomal aberrations in bone marrow mesenchymal stroma cells from patients with myelodysplastic syndrome and acute myeloblastic leukemia. *Exp Hematol*. 2007;35(2):221-229.

165. Aanei CM, Flandrin P, Eloae FZ, et al. Intrinsic growth deficiencies of mesenchymal stromal cells in myelodysplastic syndromes. *Stem Cells Dev*. 2012;21(10):1604-1615.

166. Li X, Marcondes AM, Gooley TA, Deeg HJ. The helix-loop-helix transcription factor TWIST is dysregulated in myelodysplastic syndromes. *Blood*. 2010;116(13):2304-2314.

167. da Costa SV, Roela RA, Junqueira MS, Arantes C, Brentani MM. The role of p38 mitogen-activated protein kinase in serum-induced leukemia inhibitory factor secretion by bone marrow stromal cells from pediatric myelodysplastic syndromes. *Leuk Res*. 2010;34(4):507-512.

168. Marcondes AM, Mhyre AJ, Stirewalt DL, Kim SH, Dinarello CA, Deeg HJ. Dysregulation of IL-32 in myelodysplastic syndrome and chronic myelomonocytic leukemia modulates apoptosis and impairs NK function. *Proc Natl Acad Sci U S A*. 2008;105(8):2865-2870.

# 2

# MASSIVE PARALLEL RNA SEQUENCING OF HIGHLY PURIFIED MESENCHYMAL ELEMENTS IN LOW-RISK MDS REVEALS TISSUE-CONTEXT DEPENDENT ACTIVATION OF INFLAMMATORY PROGRAMS

Si Chen,[1] Noemi A. Zambetti,[1] Eric M.J. Bindels,[1] Keane Kenswil,[1] Athina M. Mylona,[1] Niken M. Adisty,[1] Remco M. Hoogenboezem,[1] Mathijs A. Sanders,[1] Eline M.P. Cremers,[2] Theresia M. Westers,[2] Joop H. Jansen,[3] Arjan A. van de Loosdrecht,[2] and
Marc H.G.P, Raaijmakers[1]

[1]Department of Hematology, Erasmus MC Cancer Institute, Rotterdam, the Netherlands;
[2]Department of Hematology, VU University Medical Center, Amsterdam, the Netherlands
[3]Laboratory of Hematology, Department of Laboratory Medicine, Radboud University Nijmegen Medical Centre and Centre for Molecular Life Sciences, Nijmegen, the Netherlands

*Leukemia 2016 June 30: 1938–1942*

Myelodysplastic syndromes (MDS) have long been considered hematopoietic cell-autonomous disorders in which disease initiation and progression is exclusively driven by hematopoietic cell intrinsic genetic events. Recent experimental findings have challenged this view, implicating mesenchymal elements in the bone marrow microenvironment in disease pathogenesis. Specifically, genetic perturbation of mesenchymal cells has the ability to induce MDS and acute myeloid leukemia (AML), establishing an experimental concept of 'niche-induced' oncogenesis.[1, 2] Alternatively, primary alterations in hematopoietic cells have the ability to alter mesenchymal niche components such that niche cells facilitate disease propagation in the context of xenograft transplantation.[3] Together, these observations challenge the view that ineffective hematopoiesis and leukemic progression is exclusively driven by hematopoietic-cell autonomous events in human MDS. Translation of experimental findings to human disease is complicated by a lack of insight in the molecular wiring of primary, non-expanded, mesenchymal cells in MDS. Insights into the biology of mesenchymal elements in human MDS, and other hematopoietic disorders, thus far, have been derived from studies investigating *ex vivo* expanded mesenchymal cells derived from the diseased bone marrow. The hierarchic, biologic and molecular relationship between these *ex vivo* expanded cells and their in situ counterparts, however, has remained largely unknown. Here, we describe massive parallel transcriptome sequencing of prospectively isolated mesenchymal elements from human low risk MDS (LR-MDS), revealing a common molecular signature, distinct from both normal and *ex vivo* expanded cells, characterized by cellular stress and upregulation of genes encoding inflammation-associated secreted factors with established inhibitory effects on hematopoiesis.

Mesenchymal cells were prospectively FACS-sorted from bone marrow aspirates of LR-MDS patients (n=12, Supplementary Table S1) and normal controls (n=10) using previously established markers of primary bone marrow mesenchymal cells (Figure 1A).[4] The frequency of $CD45^-/7AAD^-/CD235a^-/CD31^-/CD271^+/CD105^+$ mesenchymal cells in LR-MDS was not significantly different from normal bone marrow (Figure 1B) (0.019%±0.0086% vs. 0.022%±0.0066% of mononuclear cells (MNCs), $p$=0.819 by unpaired student t-test), and these cells comprised a small subset of $CD45^-/7AAD^-/CD235a^-$ 'niche' cells (10.41%±4.086% vs. 12.30%±5.052, $p$=0.771) with the major constituent being $CD31^+$ endothelial cells (43.80%±7.243% vs. 38.28%±9.424%, $p$=0.816).

RNA was extracted from highly purified mesenchymal elements and cDNA synthesis was performed using the SMARTer Ultra Low RNA kit for Illumina Sequencing (Clonetech) (Supplementary Methods). Quality of RNA-sequencing data was shown to be similar for normal and LR-MDS derived samples using various quality parameters including the number of aligned bases, base composition, coverage coefficient and full-length transcript coverage (from 5' end to 3' end) reflecting no systematic 5'-end or 3'-end bias (Supplementary Figure S1).

The mesenchymal identity of $CD45^-/7AAD^-/CD235a^-/CD31^-/CD271^+/CD105^+$ cells was confirmed molecularly by whole transcriptome analysis demonstrating significant abundance of transcripts encoding defining membrane proteins (Figure 1C), established markers of mesenchymal stem cells (Figure 1D)[4, 5], essential 'niche' factors governing the behavior of hematopoietic stem and progenitor cells (HSPCs) (Figure 1E) and osteolineage markers (Figure 1F) compared to endothelial cells. Collectively, the findings demonstrate the feasibility of prospective isolation and molecular characterization of highly purified primary mesenchymal elements in LR-MDS by massive parallel transcriptome sequencing.

Principle component analysis (PCA) of all transcriptomes demonstrated uniform clustering of normal mesenchymal cells, implying transcriptional homogeneity (Figure 2A). Strikingly, distinct and more heterogeneous clustering of mesenchymal transcriptomes was found in LR-MDS revealing that these cells are transcriptionally distinct from their normal counterparts. Gene set enrichment analysis (GSEA) was subsequently performed to define the molecular networks underlying the distinct transcriptional landscape of LR-MDS. Gene sets associated with inflammatory response and cellular stress were remarkably enriched in LR-MDS (Figure 2B-C; Supplementary Table S2). Cellular stress was reflected by a reduced capacity of the $CD271^+$ mesenchymal population in LR-MDS to form colonies (Figure 2D) with morphologic features reminiscent of cellular senescence (Figure 2E), as described earlier for expanded stromal cells in LR-MDS.[6, 7] Distinct hierarchical clustering and the signatures of cellular stress were not age-dependent, as these signatures remained statistically significant when examined in an age-matched sub-cohort of patients and controls (Supplementary Figure S2). Together, the data indicate that mesenchymal cells in LR-MDS are molecularly and functionally distinct from their normal counterparts, characterized by cellular stress, reflected by a reduced, *ex vivo,* capacity to form fibroblast colonies.

Thus far, molecular and biologic insights into the role of mesenchymal cells in the pathogenesis of human MDS have been derived from studies using *ex vivo* expanded, plastic adherent stromal cells. The molecular relationship between these expanded cells and their *in situ* mesenchymal counterparts has remained largely unknown. Elucidation of the transcriptome of mesenchymal elements in the MDS marrow allows us to compare our transcriptional data to sequencing data obtained from expanded cells in an age-matched cohort of LR-MDS published earlier (Supplementary Figure S3).[3]

Comparison of FDR-significant differentially expressed transcripts between the two datasets demonstrated limited overlap (Figure 2F), suggesting distinct molecular wiring between the two mesenchymal cell sources. To obtain insight into the biologic processes underlying differential gene expression, GO (gene ontologies) term analysis was performed focusing on cellular biologic processes. To correct for potential experimental differences affecting FPKM

values, we normalized expression of all genes in LR-MDS to the expression of the controls in the respective data sets as detailed in the Supplementary Methods section. Normalized expression was subsequently used to perform GO term analysis and GSEA, comparing sorted to expanded cells.

25 GO terms were significantly (FDR < 0.25) enriched in primary CD271$^+$ mesenchymal cells (while no signatures were enriched in the *ex vivo* expanded mesenchymal cells), many of which (8/25) reflected response to external stimuli, chemokine activity and immune regulation (Figure 2G). Transcript abundance analysis in CD271$^+$ cells in comparison to their normal counterparts indeed revealed significant upregulation of numerous cytokines (Supplementary Table S3), including a large number of inflammatory factors, such as IL6 and IL8, and a wide variety of factors previously demonstrated to be negative regulators of hematopoiesis, in particular erythropoiesis and B-lymphopoiesis, cell lineages that are typically affected in LR-MDS (Supplementary Table S3).

To obtain insight into the molecular pathways underlying the biologic processes identified, transcriptional network analysis (GSEA) was performed. This identified 504 gene sets that were significantly (FDR < 0.25) enriched in primary sorted LR-MDS stromal cells, whereas 16 signatures were enriched in expanded LR-MDS stromal cells. Again, gene signatures related to inflammation and cellular stress were enriched in CD271$^+$ cells with a remarkable abundance of signatures related to EGF, TGFß and TNF signaling (Supplementary Figure S4, Table S4).

Collectively, the data comprise, to our knowledge, the first comprehensive transcriptional network analysis of highly purified mesenchymal elements directly isolated from the marrow in human hematopoietic disease. They support the view that these cells are intricately implicated in MDS disease pathogenesis, stressing the relevance of considering the tissue context in generating a comprehensive understanding of the disease. The data further support the notion that inflammatory signaling is an important pathophysiologic factor in LR-MDS and implicate the mesenchyme in this process. Finally, the data complement findings derived from *ex vivo* stromal cells in this disease revealing preferential overexpression of inflammatory pathways and secreted factors in FACS-purified CD271$^+$ cells. This likely reflects active cross-talk with other cellular elements within the inflammatory bone marrow environment in LR-MDS[8], eliciting or maintaining these transcriptional programs, which may not be fully appreciated in *ex vivo* cultures.

The finding that secretory programs implicated in negative regulation of hematopoiesis are activated in CD271$^+$ cells may be of particular relevance given their close anatomical proximity with CD34$^+$ cells[9], potentially harboring the MDS initiating population.[10] The data warrant

future investigations unraveling the signaling between cellular elements in the MDS marrow driving these secretory programs. We anticipate that elucidation of the transcriptome of highly purified mesenchymal elements in MDS will thus be a valuable resource to the community, instructing the validation and discovery of novel pathophysiologic factors and putative therapeutic targets.[11]

## Acknowledgements

The authors thank O. Roovers, P. van Geel and Dr. W.J.C. Chikhovskaya - Rombouts for their technical support.

This work was supported by grants from the Dutch Cancer Society (KWF Kankerbestrijding) (EMCR 2010-4733), the Netherlands Organization of Scientific Research (NWO 90700422) and the Netherlands Genomics Initiative (40-41009-98-11062) to MHGPR.

## Authorship

S.C and M.H.G.P.R designed studies; S.C, N.A.Z, K.K, A.M.M, and N.M.A performed experiments and acquired data; S.C, R.M.H, E.M.J.B, and M.A.S provided technical guidance and bioinformatical analysis; T.M.W, E.M.P.C and A.vd.L provided patient material and clinical data; J.H.J performed mutational studies and provided molecular data of the patients; S.C and M.H.G.P.R. wrote the manuscript; all authors were involved in data interpretation and manuscript reviewing, M.H.G.P.R supervised the study.

Conflict-of-interest disclosure: The authors declare no competing financial interests

## REFERENCES:


1. Raaijmakers MHGP, Mukherjee S, Guo SQ, Zhang SY, Kobayashi T, Schoonmaker JA, et al. Bone progenitor dysfunction induces myelodysplasia and secondary leukaemia. Nature. 2010;464(7290):852-U58.
2. Kode A, Manavalan JS, Mosialou I, Bhagat G, Rathinam CV, Luo N, et al. Leukaemogenesis induced by an activating beta-catenin mutation in osteoblasts. Nature. 2014;506(7487):240-4.
3. Medyouf H, Mossner M, Jann JC, Nolte F, Raffel S, Herrmann C, et al. Myelodysplastic cells in patients reprogram mesenchymal stromal cells to establish a transplantable stem cell niche disease unit. Cell Stem Cell. 2014;14(6):824-37.
4. Tormin A, Li O, Brune JC, Walsh S, Schutz B, Ehinger M, et al. CD146 expression on primary nonhematopoietic bone marrow stem cells is correlated with in situ localization. Blood. 2011;117(19):5067-77.
5. Dominici M, Le Blanc K, Mueller I, Slaper-Cortenbach I, Marini FC, Krause DS, et al. Minimal criteria for defining multipotent mesenchymal stromal cells. The International Society for Cellular Therapy position statement. Cytotherapy. 2006;8(4):315-7.
6. Geyh S, Oz S, Cadeddu RP, Frobel J, Bruckner B, Kundgen A, et al. Insufficient stromal support in MDS results from molecular and functional deficits of mesenchymal stromal cells. Leukemia. 2013;27(9):1841-51.
7. Ferrer RA, Wobus M, List C, Wehner R, Schonefeldt C, Brocard B, et al. Mesenchymal stromal cells from patients with myelodyplastic syndrome display distinct functional alterations that are modulated by lenalidomide. Haematologica. 2013;98(11):1677-85.
8. Ganan-Gomez I, Wei Y, Starczynowski DT, Colla S, Yang H, Cabrero-Calvo M, et al. Deregulation of innate immune and inflammatory signaling in myelodysplastic syndromes. Leukemia. 2015;29(7):1458-69.
9. Flores-Figueroa E, Varma S, Montgomery K, Greenberg PL, Gratzinger D. Distinctive contact between CD34+ hematopoietic progenitors and CXCL12+ CD271+ mesenchymal stromal cells in benign and myelodysplastic bone marrow. Lab Invest. 2012;92(9):1330-41.
10. Woll PS, Kjallquist U, Chowdhury O, Doolittle H, Wedge DC, Thongjuea S, et al. Myelodysplastic syndromes are propagated by rare and distinct human cancer stem cells in vivo. Cancer Cell. 2014;25(6):794-808.
11. Mies A BE, Rogulj IM, Hofbauer LC, Platzbecker U. Alterations within the Osteo-Hematopoietic Niche in MDS and their Therapeutic Implications. Curr Pharm Des. 2016;Epub ahead of print.

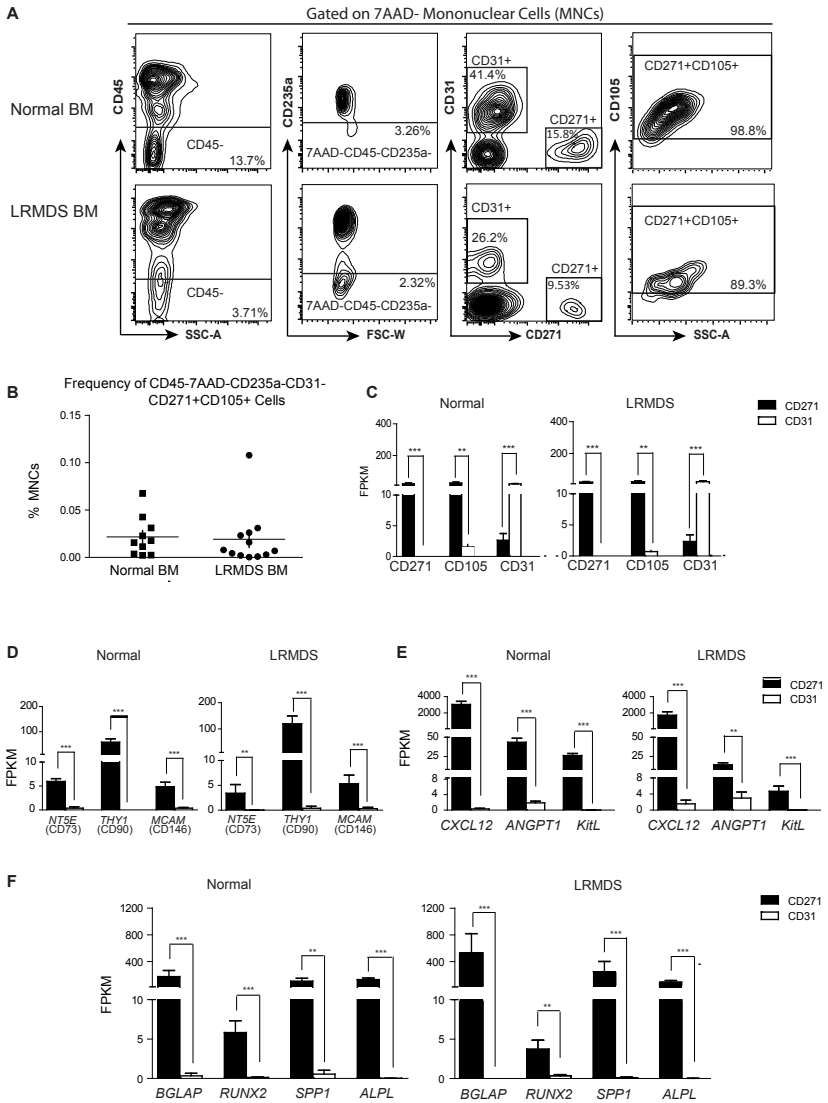


**Figure 1. Prospective isolation and molecular characterization of mesenchymal cells in LR-MDS.** (A) Gating strategy to identify and isolate 7AAD$^-$/CD45$^-$/CD235a$^-$/CD271$^+$/CD105$^+$ mesenchymal cells. (B) Frequency of mesenchymal cells in normal and MDS samples. (C-F) Transcriptional validation of the mesenchymal identity of 7AAD$^-$/CD45$^-$/CD235a$^-$/CD271$^+$/CD105$^+$ cells, revealing differential expression in comparison to endothelial subsets of (C) defining cell surface markers (CD271, CD105, CD31), (D) known mesenchymal markers (CD73, CD90, CD146), (E) established hematopoiesis-supporting cytokines (*CXCL12, ANGPT1, KITL*) and (F) bone lineage markers (*BGLAP, RUNX2, SPP1* and *ALPL*).

FPKM: fragments per kilobase of exon per million fragments mapped. CD73 (*NT5E*: ecto-5'-nucleotidase); CD90 (*THY1*: Thy-1 T-Cell Antigen); CD146 (*MCAM*: melanoma cell adhesion molecule); *CXCL12* (stromal cell-derived factor 1); *ANGPT1* (angiopoietin 1); *KITL* (KIT ligand); *BGLAP* (osteocalcin); *RUNX2* (runt-related transcription factor 2); *SPP1* (osteopontin); *ALPL* (alkaline phosphatase, liver/bone/kidney). Figure C to figure F: Normal samples (n=10); MDS samples (n=12). Black bar: CD271+ mesenchymal cells; white bar: CD31+ endothelial cells. ** FDR < .01; *** FDR < .001.

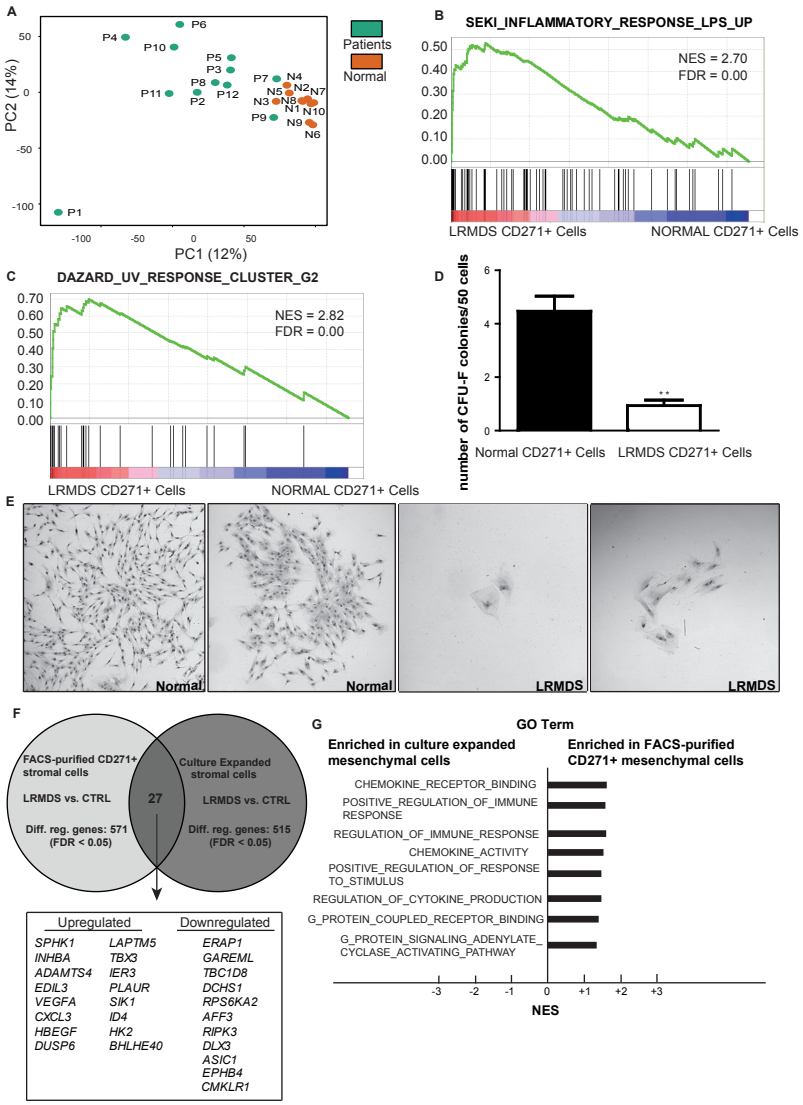


**Figure 2. Mesenchymal cells in LR-MDS display a distinct molecular signature characterized by cellular stress and inflammation.** (A) Principle component analysis (PCA) on the transcriptomes of normal and LR-MDS mesenchymal cells. Patient numbers in Figure 2A refer to LR-MDS patient IDs (Table S1). (B) Example of GSEA plot revealing inflammatory response in the mesenchymal cells from LR-MDS. (C) Representative GSEA plot demonstrating deregulation of the gene set associated with cellular stress in response to UV in LR-MDS mesenchymal cells. Gene set size, NES and FDR value of each gene set is listed. GSEA: gene sets enrichment analysis. NES: normalized enrichment score. FDR: false discovery rate. (D) Number of CFU-F colonies formed by normal (n=3) or LR-MDS (n=3) CD271+ mesenchymal cells. (E) Representative images of cell clusters and colonies formed by mesenchymal cells from healthy control (left panel) and LR-MDS patients (right panel). (F) Comparison of significantly differentially expressed genes in FACS-purified CD271+ versus culture-expanded mesenchymal cells in LR-MDS. The total number of differentially regulated transcripts in each data set is indicated and the overlapping differentially regulated genes in the two datasets are listed. (G) Biologic processes significantly enriched (FDR < 0.25) in FACS-purified CD271+ LR-MDS mesenchymal cells in comparison to expanded stromal cells defined by GO term analysis. ** P < .01

# SUPPLEMENTAL DATA

# SUPPLEMENTARY MATERIAL AND METHODS

## Patient and healthy donor bone marrow samples

Patient characteristics (median age: 65, range 38-80) are shown in Table S1. Control marrow was obtained from donors for allogeneic transplantation (median age: 45, range 35-61), after written informed consent. The use of human samples was approved by the Institutional Review Board of the Erasmus Medical Center, the Netherlands, in accordance with the declaration of Helsinki.

## Flow cytometry analysis

For cell sorting, bone marrow from patients and normal donors were stained on ice in the dark with the following antibodies using optimized dilutions: CD45-PE-Cy7 (1:200), CD235a-BV421-A (1:100), CD271-PE (1:100), CD105-APC (1:50), CD31-APC-CY7 (1:50). The indicated populations of interest were sorted using a FACS ARIAIII Cell Sorter (BD Biosciences). Dead cells were gated out using 7AAD (Stem-Kit Reagents) after mononuclear cell selection and doublets exclusion. The cells were directly sorted in 800µl Trizol (Ambion) for RNA isolation. RNAse free non-stick micro-tubes (Ambion) were used to prevent pre-digestion of RNA.

## RNA extraction and RNA quality control

Total sample RNA isolation was performed according to the standard protocol of RNA isolation with Trizol and GenElute LPA (Sigma). The RNA pellet was resuspended in 7.5µl of RNAse free water (Qiagen) and quality and quantity of the total RNA was checked on a 2100 Bio-analyzer (Agilent) using the Agilent RNA 6000 Pico Kit.

## RNA sequencing and gene expression profiling

SMARTer Ultra Low RNA Kit (Clonetech) for Illumina Sequencing was used to prepare the cDNA based on the manufacture's recommendation. Similar quantities of total RNA from each sample were used as starting material for the SMARTer procedure. cDNA preparation steps were performed according to the user manual in a PCR-clean room to avoid contamination. The Agilent 2100 Bio-analyzer and the High Sensitivity DNA kit were applied to determine the quantity and quality of the cDNA production. Once the cDNAs were obtained, the subsequent library preparation steps, sequencing and alignments were performed as previously described.[1, 2] In brief, prior to sequence alignment, the SMARTer adapters were trimmed using the cutadapt program.[3] The resulting sequences were aligned to the human RefSeq transcriptome using TopHat2.[4] Sequences that could not be aligned to the RefSeq transcriptome were aligned to the reference genome (build hg19). Normalization and quantification was performed using Cufflinks.[5] The resulting

gene expression values are measured as FPKM (Fragments per kilobase of exon per million fragments mapped). Fragment counts were determined per gene with HTSeq-count, utilizing the strict intersection option, and subsequently used for differential expression analysis using the DESeq2[6] package, with standard parameters, in the R environment. Multiple testing correction was performed with the Benjamini-Hochberg procedure to control the False Discovery Rate (FDR). Principle component analysis was performed on the fragment counts using the R environment. Finally gene set enrichment analysis (GSEA) was performed on the FPKM values using the curated C2 collection of gene sets within MSigDB.[7]

### Comparison between molecular data from primary and *ex vivo* expanded mesenchymal cells

We performed a direct comparison of transcriptional data obtained from FACS-isolated $CD271^+$ mesenchymal cells to transcriptional data obtained by RNAseq from culture-expanded stromal cells from an age-matched cohort of LR-MDS patients reported earlier.[8] BAM files containing the molecular data of *ex vivo* expanded stromal cells derived from LR-MDS patients (n=5) and normal controls (n=3)[8] were obtained from the European Genome-Phenome Archive data base (EGAS00001000716). Gene expression values quantified by the FPKM statistic were determined by Cufflinks as previously described (*vide supra*). Differential expression analysis was performed using the DESeq2 package.

To allow direct comparison of datasets and correct for potential technical/experimental variation affecting FPKM values, for both datasets, average gene FPKM values of MDS samples were normalized to average FPKM values observed in the normal control samples (FPKM MDS/FPKM control)and the normalized (fold-change) value subjected to GO term and GSEA.[7]

### CFU-F assay

Live $CD45^-/CD235a^-/CD271^+$ mesenchymal cells from bone marrow samples of LR-MDS patients (n=3) and normal controls (n=3) were sorted using a FACSARIA III cell sorter. On average, 20 cells per 0.32 $cm^2$ were plated in αMEM supplemented with 20% fetal bovine serum and 1% penicillin, streptomycin. On day 14, dishes were fixed and stained with Giemsa, and CFU-F colonies were counted as previously described.[9] Images of colonies and individual cell clusters were acquired on a Leica SP5 confocal laser scan microscope using a 40x objective. Images were analyzed using ImageJ software.

## SUPPLEMENTARY REFERENCE


1. Groschel S, Sanders MA, Hoogenboezem R, de Wit E, Bouwman BA, Erpelinck C, et al. A single oncogenic enhancer rearrangement causes concomitant EVI1 and GATA2 deregulation in leukemia. Cell. 2014;157(2):369-81.
2. Zambetti NA, Bindels EM, Van Strien PM, Valkhof MG, Adisty MN, Hoogenboezem RM, et al. Deficiency of the ribosome biogenesis gene Sbds in hematopoietic stem and progenitor cells causes neutropenia in mice by attenuating lineage progression in myelocytes. Haematologica. 2015;100(10):1285-93.
3. Marcel M. Cutadapt removes adapter sequences from high-throughput sequencing reads. EMBnet journal. 2011;17:10-2.
4. Kim D, Pertea G, Trapnell C, Pimentel H, Kelley R, Salzberg SL. TopHat2: accurate alignment of transcriptomes in the presence of insertions, deletions and gene fusions. Genome Biol. 2013;14(4):R36.
5. Trapnell C, Roberts A, Goff L, Pertea G, Kim D, Kelley DR, et al. Differential gene and transcript expression analysis of RNA-seq experiments with TopHat and Cufflinks. Nat Protoc. 2012;7(3):562-78.
6. Anders S, Huber W. Differential expression analysis for sequence count data. Genome Biol. 2010;11(10):R106.
7. Subramanian A, Tamayo P, Mootha VK, Mukherjee S, Ebert BL, Gillette MA, et al. Gene set enrichment analysis: A knowledge-based approach for interpreting genome-wide expression profiles. P Natl Acad Sci USA. 2005;102(43):15545-50.
8. Medyouf H, Mossner M, Jann JC, Nolte F, Raffel S, Herrmann C, et al. Myelodysplastic cells in patients reprogram mesenchymal stromal cells to establish a transplantable stem cell niche disease unit. Cell Stem Cell. 2014;14(6):824-37.
9. Tormin A, Li O, Brune JC, Walsh S, Schutz B, Ehinger M, et al. CD146 expression on primary nonhematopoietic bone marrow stem cells is correlated with in situ localization. Blood. 2011;117(19):5067-77.
10. Kim SJ, Letterio J. Transforming growth factor-beta signaling in normal and malignant hematopoiesis. Leukemia. 2003;17(9):1731-7.
11. Broxmeyer HE, Cooper S, Hangoc G, Kim CH. Stromal cell-derived factor-1/CXCL12 selectively counteracts inhibitory effects of myelosuppressive chemokines on hematopoietic progenitor cell proliferation in vitro. Stem Cells Dev. 2005;14(2):199-203.
12. Dimicoli S, Wei Y, Bueso-Ramos C, Yang H, Dinardo C, Jia Y, et al. Overexpression of the toll-like receptor (TLR) signaling adaptor MYD88, but lack of genetic mutation, in myelodysplastic syndromes. PLoS One. 2013;8(8):e71120.
13. Nishihara T, Ohsaki Y, Ueda N, Koseki T, Eto Y. Induction of apoptosis in B lineage cells by activin A derived from macrophages. J Interferon Cytokine Res. 1995;15(6):509-16.
14. Lambert MP, Rauova L, Bailey M, Sola-Visner MC, Kowalska MA, Poncz M. Platelet factor 4 is a negative autocrine in vivo regulator of megakaryopoiesis: clinical and therapeutic implications. Blood. 2007;110(4):1153-60.
15. Bruns I, Lucas D, Pinho S, Ahmed J, Lambert MP, Kunisaki Y, et al. Megakaryocytes regulate hematopoietic stem cell quiescence through CXCL4 secretion. Nat Med. 2014;20(11):1315-20.

## SUPPLEMENTAL TABLES AND FIGURES

**Table S1. Patient characteristics**

1a.

| Patient ID | Age | WHO | Cytogenetics | BM Blasts | IPSS | Genetic Aberrations |
|---|---|---|---|---|---|---|
| MDS01 | 62 | RCMD-RS | 46, XY[20] | 0% | 0 | *SF3B1, RUNX1, TET2* |
| MDS02 | 63 | RAEB-1 | 46, XX[20] | 5% | 1 | *DNMT3A, SRSF2* |
| MDS03 | 72 | RCMD-RS | 46, XX[20] | 1% | 0.5 | *SRSF2* |
| MDS04 | 75 | Isolated del(5q) | 46, XX, del(5)(q15q33)[10] | 1% | 0 | no mutations |
| MDS05 | 79 | RCMD-RS | 46, XX[10] | 0% | 0 | *SF3B1* |
| MDS06 | 66 | RARS | 46, XX[21] | 2% | 0 | *DNMT3A, SF3B1* |
| MDS07 | 56 | RARS | 46, XX[20] | 0% | 0 | *TET2, DNMT3A, SF3B1* |
| MDS08 | 80 | RCMD | 46, XY[20] | 3% | 0.5 | *TET2, ASXL1* |
| MDS09 | 65 | RCMD-RS | 46, XX[20] | 3% | 0.5 | *TET2, DNMT3A, SF3B1, Runx1* |
| MDS10 | 58 | RCMD-RS | 45,X,-Y[10]/46,XY[10] | 1% | 0 | no mutations |
| MDS11 | 38 | Isolated del(5q) | 46, XX, del(5)(q13q33)[25]/46,XX[5] | 2% | 0 | *ASXL1* |
| MDS12 | 65 | RCMD | 46, XX[20] | 2% | 0 | *EZH2* |

1b.

| Normal Samples | Age | Gender |
|---|---|---|
| N10410 (N1) | 58 | F |
| N10513 (N2) | 40 | M |
| N12723 (N3) | 48 | F |
| N15863 (N4) | 42 | M |
| N14207 (N5) | 61 | F |
| N16237 (N6) | 40 | F |
| N11703 (N7) | 39 | M |
| N08276 (N8) | 58 | M |
| N14167 (N9) | 48 | M |
| N12066 (N10) | 35 | M |

**Supplemental Table 1**. **Patient characteristics.** (A) Bone marrow was obtained at entry of a prospective clinical trial (HOVON89, Eudract nr. 2008-002195-10). The patient ID, age, WHO category (MDS WHO classification 2008), cytogenetic abnormalities, percentage of blasts in the bone marrow, the International Prognostic Scoring System for MDS (IPSS) and genetic aberrations of each patient are listed above (n=12). (B) Age and gender of each normal control sample is listed.

**Supplemental Table 2. Enrichment of transcriptional signatures reflecting inflammatory response and cellular stress in mesenchymal cells from LR-MDS patients.**

| Cellular process | Data Sets | Enrichment | Size | NES | NOM p-val | FDR q-Val |
|---|---|---|---|---|---|---|
| Inflammatory Response | SEKI_INFLAMMATORY_RESPONSE_LPS_UP | MDS | 76 | 2.70 | <0.001 | 0.00 |
| | NEMETH_INFLAMMATORY_RESPONSE_LPS_UP | MDS | 154 | 2.70 | <0.001 | 0.00 |
| | BIOCARTA_INFLAM_PATHWAY | MDS | 29 | 1.68 | <0.001 | 0.04 |
| DNA Damage & Stress Response | GHANDHI_DIRECT_IRRADIATION_UP | MDS | 106 | 2.40 | <0.001 | 6,38E-02 |
| | GHANDHI_BYSTANDER_IRRADIATION_UP | MDS | 83 | 2.30 | <0.001 | 0.001 |
| | DAZARD_UV_RESPONSE_CLUSTER_G24 | MDS | 26 | 2.26 | <0.001 | 0.001 |
| | DAZARD_UV_RESPONSE_CLUSTER_G4 | MDS | 21 | 2.08 | <0.001 | 0.006 |
| | DAZARD_UV_RESPONSE_CLUSTER_G28 | MDS | 20 | 2.44 | <0.001 | 3,54E-03 |
| | RASHI_RESPONSE_TO_IONIZING_RADIATION_1 | MDS | 45 | 1.68 | <0.001 | 0.04 |
| | RASHI_RESPONSE_TO_IONIZING_RADIATION_2 | MDS | 127 | 2.42 | <0.001 | 5,89E-03 |
| | GENTILE_UV_LOW_DOSE_UP | MDS | 27 | 2.68 | <0.001 | <0.001 |
| | GENTILE_UV_HIGH_DOSE_UP | MDS | 25 | 2.26 | <0.001 | 0.001 |
| | SESTO_RESPONSE_TO_UV_C3 | MDS | 20 | 2.13 | <0.001 | 0.004 |
| | SESTO_RESPONSE_TO_UV_C1 | MDS | 72 | 1.95 | <0.001 | 0.011 |
| | SESTO_RESPONSE_TO_UV_C5 | MDS | 46 | 1.79 | <0.001 | 0.026 |
| | SESTO_RESPONSE_TO_UV_C0 | MDS | 107 | 1.42 | <0.001 | 0.126 |
| | SMIRNOV_RESPONSE_TO_IR_2HR_UP | MDS | 50 | 2.62 | <0.001 | 0.049 |
| | SMIRNOV_RESPONSE_TO_IR_6HR_UP | MDS | 163 | 1.65 | <0.001 | <0.001 |
| | MURAKAMI_UV_RESPONSE_6HR_UP | MDS | 37 | 1.35 | 0.09 | 0.159 |
| | TSAI_RESPONSE_TO_RADIATION_THERAPY | MDS | 32 | 2.25 | <0.001 | 0.002 |
| | TSAI_RESPONSE_TO_IONIZING_RADIATION | MDS | 149 | 1.81 | <0.001 | 0.024 |

The size of each individual gene set, normalized enrichment score (NES), nominal p-value and false discovery rate (FDR) values are as listed.

**Supplemental Table 3. Differential expression of secreted factors and cytokines in primary LR-MDS mesenchymal cells**

| Gene Name | FC | FDR | Avg FPKM MDS | Avg FPKM CTRL | Differenitally expressed in Expanded MDS MSCs |
|---|---|---|---|---|---|
| *ADM* | 6.44 | 0.003 | 294.24 | 48.24 | No |
| *ADAMTS4* | 6.81 | 0.001 | 10.28 | 0.99 | Yes |
| *ANXA1* | 6.36 | 1.63E-011 | 773.02 | 116.31 | No |
| *EREG* | 8.93 | 0.006 | 5.07 | 0.61 | No |
| *CXCL3* | 6.21 | 0.026 | 206.06 | 33.63 | Yes |
| *CXCL10* | 4.00 | 0.034 | 27.48 | 6.25 | No |
| *CCL5* [e] | 2.71 | 0.036 | 101.15 | 39.08 | No |
| *CXCL14* | 5.56 | 0.023 | 39.68 | 3.08 | No |
| *F3* | 11.8 | <0.001 | 3.32 | 0.30 | No |
| *FTL* | 2.63 | 0.000 | 4610.60 | 2716.91 | No |
| *HBEGF* | 6.21 | 0.001 | 11.90 | 2.45 | Yes |
| *IL8* [b,e] | 7.24 | 4.36E-005 | 235.82 | 41.33 | No |
| *IL6* | 5.09 | 0.005 | 100.67 | 20.52 | No |
| *PLIN2* | 4.04 | 6.75E-005 | 104.73 | 54.95 | No |
| *SERPINB1* | 2.75 | 0.006 | 39.46 | 20.11 | No |
| *SOD2* | 3.18 | 0.002 | 379.00 | 152.55 | No |
| *SERPINE1* | 16.45 | 1.35E-006 | 43.23 | 2.58 | No |
| *VEGFA* | 2.67 | 0.000 | 10.67 | *3.05* | Yes |
| *BMP2* | 4.83 | 0.017 | 6.37 | 2.30 | No |
| *CCL3* [b] | 4.21 | 0.022 | 48.17 | 16.10 | No |
| *CXCL9* | 6.73 | 0.023 | 6.18 | 0.59 | No |
| *FTH1* [e] | 2.02 | 0.015 | 286.33 | 212.15 | No |
| *INHBA* [c] | 8.08 | 0.026 | 10.60 | 1.01 | Yes |
| *LTF* [e] | 6.58 | 0.017 | 23.95 | 2.74 | No |
| *PF4 (CXCL4)* [d] | 6.96 | 0.005 | 28.09 | 2.84 | No |
| *SLC16A1* | 3.24 | 0.012 | 4.59 | 1.66 | No |
| *S100A10* | 2.95 | <0.001 | 157.62 | 81.17 | Yes |
| *S100A6* | 3.06 | 0.006 | 428.18 | 219.92 | No |
| *SLC3A2* | 2.64 | 0.008 | 60.91 | 36.89 | No |
| *TGFB1* [a] | 4.44 | 0.048 | 1.92 | 0.32 | No |

Differential expression of different cytokines in primary LR-MDS mesenchymal cells comparing to the normal counterparts are listed. This list includes bona fide inflammatory cytokines known to be negative regulators of hematopoiesis (a), erythropoiesis (b), B-lymphopoiesis (c), megakaryopoiesis (d) and with myelosuppressive effects (e). [10-15] FC: Fold change; FDR: false discovery rate. Fold change, FDR significance and average FPKM value of each gene are as listed. FC: Fold change; FDR: false discovery rate.

**Supplemental Table 4. Signatures that are associated with stress, inflammation, TNF and EGF signaling within the top 100 signatures enriched in primary LR-MDS mesenchymal cells in comparison to culture expanded stromal cells**

| Signatures | Enrichment | Size | NES | FDR |
|---|---|---|---|---|
| NAGASHIMA_EGF_SIGNALING_UP | Purified CD271+ cells | 56 | 36.9 | 0.000 |
| PLASARI_TGFB1_TARGETS_1HR_UP | Purified CD271+ cells | 32 | 36.1 | 0.000 |
| PHONG_TNF_TARGETS_UP | Purified CD271+ cells | 60 | 3.53 | 0.000 |
| GENTILE_UV_LOW_DOSE_UP | Purified CD271+ cells | 25 | 31.0 | 0.000 |
| DAZARD_UV_RESPONSE_CLUSTER_G28 | Purified CD271+ cells | 19 | 30.5 | 0.000 |
| GALINDO_IMMUNE_RESPONSE_TO_ENTEROTOXIN | Purified CD271+ cells | 74 | 30.4 | 0.000 |
| KOBAYASHI_EGFR_SIGNALING_6HR_DN | Purified CD271+ cells | 17 | 29.8 | 0.000 |
| DAZARD_UV_RESPONSE_CLUSTER_G2 | Purified CD271+ cells | 25 | 29.6 | 0.000 |
| SEKI_INFLAMMATORY_RESPONSE_LPS_UP | Purified CD271+ cells | 70 | 2.94 | 0.000 |
| AMIT_EGF_RESPONSE_120_MCF10A | Purified CD271+ cells | 40 | 28.0 | 5,48E-02 |
| AMIT_EGF_RESPONSE_120_HELA | Purified CD271+ cells | 63 | 27.6 | 4,47E-00 |
| SESTO_RESPONSE_TO_UV_C3 | Purified CD271+ cells | 20 | 25.9 | 3,35E-03 |
| AMIT_EGF_RESPONSE_60_HELA | Purified CD271+ cells | 41 | 24.2 | 0.001 |
| AMIT_EGF_RESPONSE_240_MCF10A | Purified CD271+ cells | 20 | 23.1 | 0.002 |
| AMIT_EGF_RESPONSE_40_HELA | Purified CD271+ cells | 38 | 23.0 | 0.003 |
| AMIT_EGF_RESPONSE_60_MCF10A | Purified CD271+ cells | 37 | 22.8 | 0.003 |
| GHANDHI_BYSTANDER_IRRADIATION_UP | Purified CD271+ cells | 78 | 22.6 | 0.003 |
| MURAKAMI_UV_RESPONSE_6HR_DN | Purified CD271+ cells | 18 | 216 | 0.005 |
| NEMETH_INFLAMMATORY_RESPONSE_LPS_UP | Purified CD271+ cells | 85 | 2.09 | 0.008 |
| GENTILE_UV_HIGH_DOSE_UP | Purified CD271+ cells | 24 | 20.6 | 0.009 |

**Supplemental Figure 1. Comparable quality of RNA sequencing data obtained from MDS and normal mesenchymal cells.** (A) Number of aligned bases were calculated using aligned data of MDS (orange bars) *vs.* normal (blue bars) stromal samples. (B) Base composition including ribosomal bases (blue), coding bases (orange), UTR bases (yellow), intronic bases (green) and intergenic bases (red) is constructed for both MDS and normal stromal cell aligned sequencing data. (C) Median coefficient of variation (CV) value was computed indicating the level of coverage for LR-MDS and normal stromal cell aligned sequencing data. (D) Comparison of the transcript coverage from LR-MDS $CD271^+$ cells and control $CD271^+$ cells. Presented here are superimposed plots displaying the average read coverage from the total RNA of each sample library. The x-axis represents gene length normalized to 100%, where 0 is the 5'-end and 100 is the 3'end of each transcript.

**Figure S1**

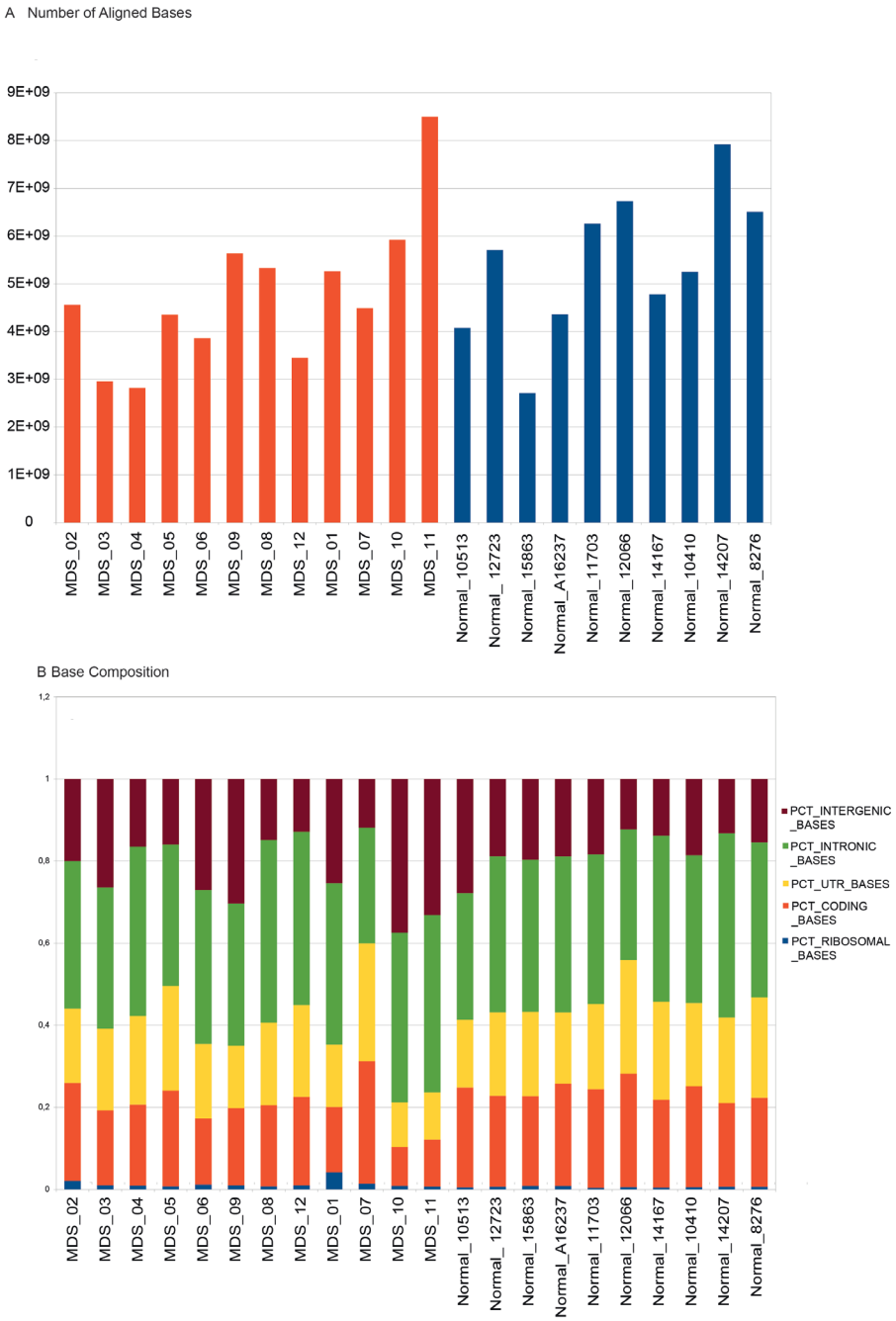
A Number of Aligned Bases
9E+09
8E+09
7E+09
6E+09
5E+09
4E+09
3E+09
2E+09
1E+09
0
MDS_02
MDS_03
MDS_04
MDS_05
MDS_06
MDS_09
MDS_08
MDS_12
MDS_01
MDS_07
MDS_10
MDS_11
Normal_10513
Normal_ 12723
Normal_15863
Normal_A16237
Normal_11703
Normal_12066
Normal_14167
Normal_10410
Normal_14207
Normal_8276
B Base Composition
1,2
1
0,8
0,6
0,4
0,2
0
PCT_INTERGENIC _BASES
PCT_INTRONIC _BASES
PCT_UTR_BASES
PCT_CODING _BASES
PCT_RIBOSOMAL _BASES

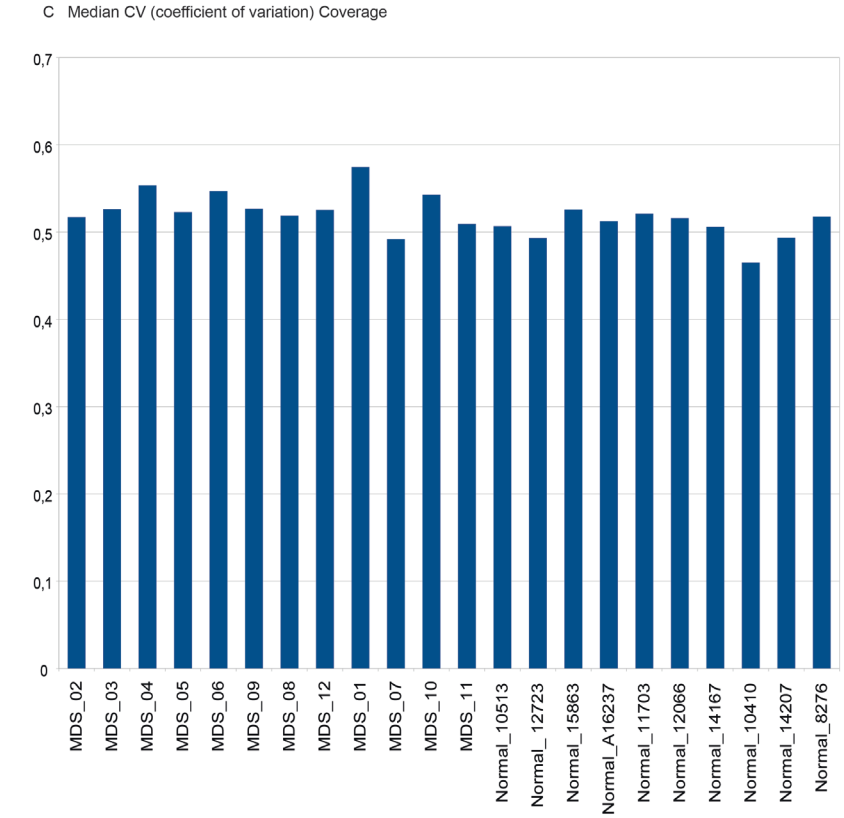
C Median CV (coefficient of variation) Coverage
0,7
0,6
0,5
0,4
0,3
0,2
0,1
0
MDS_02
MDS_03
MDS_04
MDS_05
MDS_06
MDS_09
MDS_08
MDS_12
MDS_01
MDS_07
MDS_10
MDS_11
Normal_10513
Normal_ 12723
Normal_15863
Normal_A16237
Normal_11703
Normal_12066
Normal_14167
Normal_10410
Normal_14207
Normal_8276

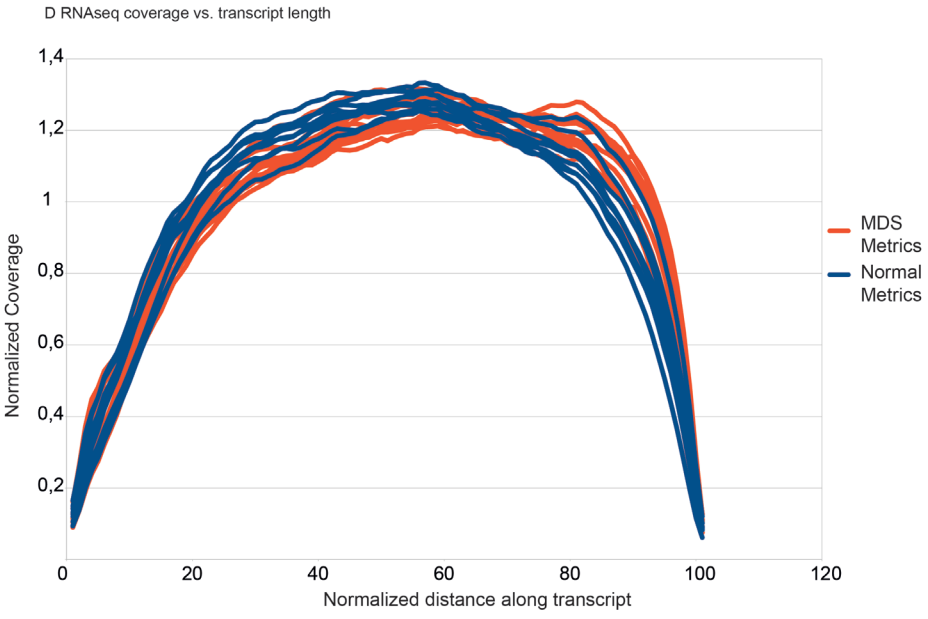
D RNAseq coverage vs. transcript length
1,4
1,2
1
0,8
0,6
0,4
0,2
Normalized Coverage
0
20
40
60
80
100
120
Normalized distance along transcript
MDS Metrics
Normal Metrics

**Figure S2**

A

| Patient ID | Age | Median (range) | Gender |
|---|---|---|---|
| MDS01 | 62 | 58 (38-63) | M |
| MDS02 | 63 | | F |
| MDS07 | 56 | | F |
| MDS10 | 58 | | M |
| MDS11 | 38 | | F |
| **Normal Donor** | **Age** | **Median (range)** | |
| N10410 (N1) | 58 | 58 (48-61) | F |
| N14207 (N5) | 61 | | F |
| N08276 (N8) | 58 | | M |
| N12723 (N3) | 48 | | F |
| N14167 (N9) | 48 | | M |

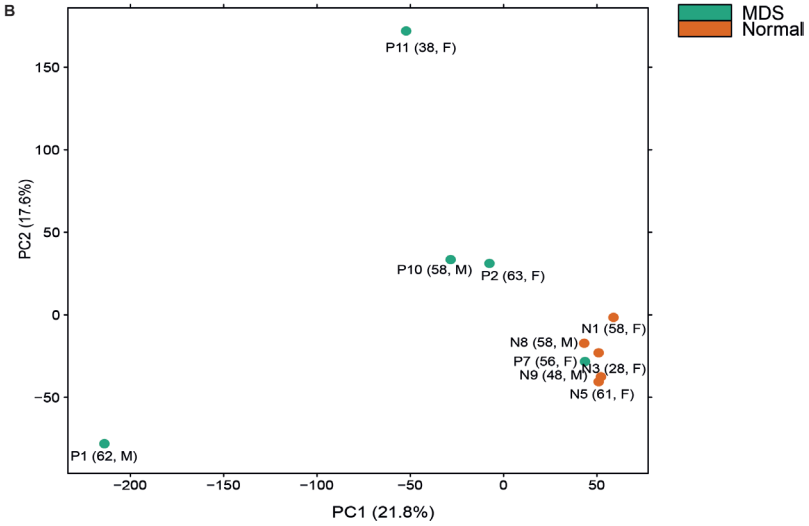


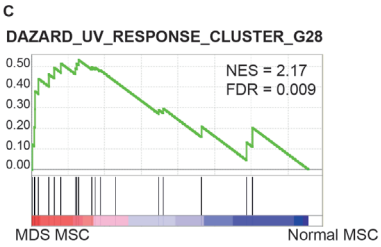


D

| Data Sets | Enrichment | Size | NES | NOM p-val | FDR q-Val |
|---|---|---|---|---|---|
| SESTO_RESPONSE_TO_UV_C3 | MDS MSC | 20 | 1.87 | 0.000 | 0.048 |
| DAZARD_UV_RESPONSE_CLUSTER_G2 | MDS MSC | 30 | 1.77 | 0.000 | 0.066 |
| GENTILE_UV_LOW_DOSE_UP | MDS MSC | 26 | 1.65 | 0.000 | 0.093 |
| DAZARD_UV_RESPONSE_CLUSTER_G24 | MDS MSC | 26 | 1.42 | 0.105 | 0.188 |
| GENTILE_UV_HIGH_DOSE_UP | MDS MSC | 24 | 1.40 | 0.053 | 0.201 |

**Supplemental Figure 2. Molecular signature of mesenchymal cells from LR-MDS patients compared to age-matched controls.** (A) Patient and control characteristics including median age and gender. (B) PCA. (Normal: orange; patient: green). The age and gender of each sample is indicated in the plot. (C) Representative GSEA plot indicating enriched stress response in LR-MDS mesenchymal cells compared to age-matched controls. NES and FDR value of each signature are listed. (D) List of GSEA signatures reflecting cellular stress in LR-MDS stromal cells in the age-matched cohort. GSEA: gene sets enrichment analysis. NES: normalized enrichment score. FDR: false discovery rate.

**Figure S3**

**A**

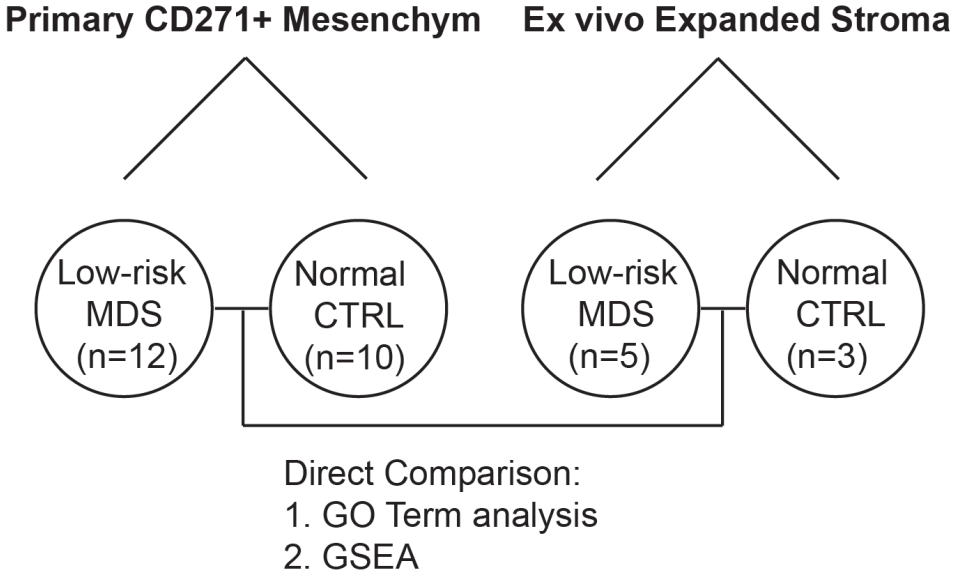


**B**

| Primary LRMDS CD271+ Cells | | | Expanded LRMDS MSCs | | |
|---|---|---|---|---|---|
| **Patient ID** | **Age** | **Median Age** | **Patient ID** | **Age** | **Median Age** |
| MDS01 | 62 | | | | |
| MDS02 | 63 | | MDS14 | 57 | |
| MDS03 | 72 | | MDS28 | 81 | |
| MDS04 | 75 | | MDS38 | 58 | |
| MDS05 | 79 | 65 | MDS52 | 79 | 72 |
| MDS06 | 66 | | MDS53 | 72 | |
| MDS07 | 56 | | | | |
| MDS08 | 80 | | | | |
| MDS09 | 65 | | | | |
| MDS10 | 58 | | | | |
| MDS11 | 38 | | | | |
| MDS12 | 65 | | | | |

**Supplemental Figure 3. Comparison of molecular profile between primary and expanded LR-MDS stromal cells[8]**
(A) Scheme illustrating the strategy of directly comparing RNA-seq data from primary mesenchymal cells to RNA-seq data obtained from culture expanded stromal cells in LR-MDS. (B) Age distribution of LR-MDS patients for the primary and expanded stromal cell data sets. (C) Gene sets differentially expressed (FDR< 0.25) in primary CD271$^+$ cells or *ex vivo* expanded MSCs from patients with LR-MDS.

**Figure S4**

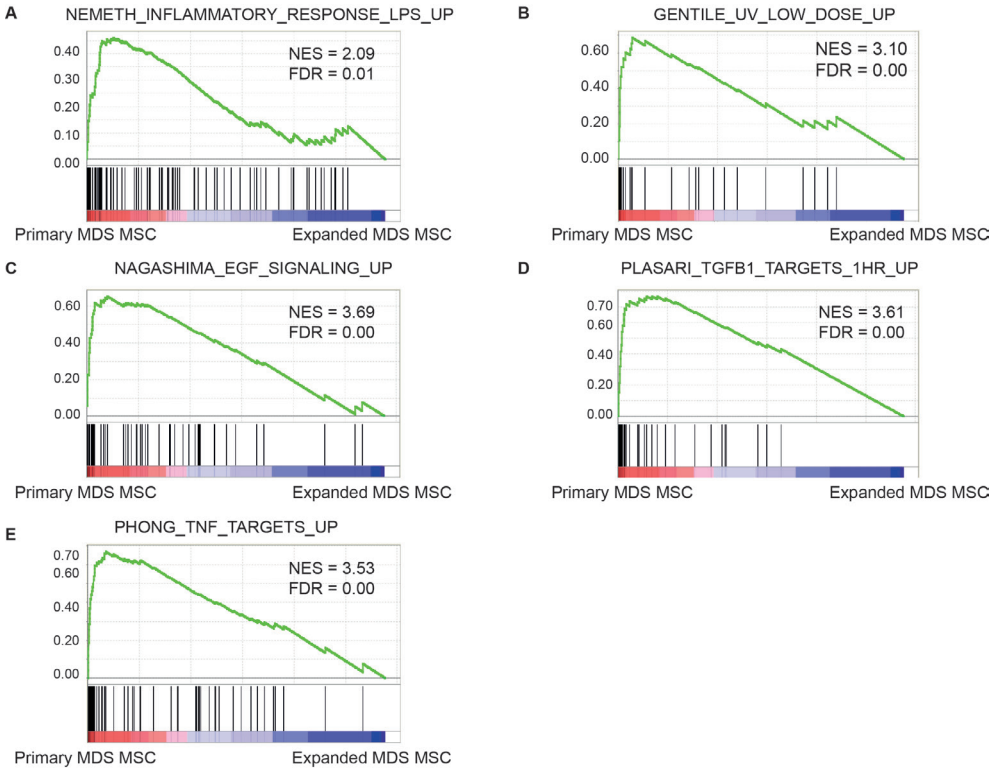


**Supplemental Figure 4. Gene signatures of inflammation and stress enriched in primary LR-MDS mesenchymal cells in comparison to expanded stromal cells.** Representative GSEA plot demonstrating enrichment of gene sets associated with inflammation (A), stress (B) and EGF, TGFß, TNF signaling (C-E) in primary LR-MDS mesenchymal cell comparing to expanded stromal cells. These plots are associated with Supplemental Table S4.

# 3

# MESENCHYMAL INFLAMMATION DRIVES GENOTOXIC STRESS IN HEMATOPOIETIC STEM CELLS AND PREDICTS DISEASE EVOLUTION IN HUMAN PRE-LEUKEMIA

Noemi A. Zambetti[1,*], Zhen Ping[1,*], Si Chen[1,*], Keane J. G. Kenswil[1], Maria A. Mylona[1], Mathijs A. Sanders[1], Remco M. Hoogenboezem[1], Eric M. J. Bindels[1], Maria N. Adisty[1], Paulina M. H. Van Strien[1], Cindy S. van der Leije[2], Theresia M. Westers[3], Eline M. P. Cremers[3], Chiara Milanese[4], Pier G. Mastroberardino[4], Johannes P. T. M. van Leeuwen[2], Bram C. J. van der Eerden[2], Ivo P. Touw[1], Taco W. Kuijpers[5], Roland Kanaar[6], Arjan A. van de Loosdrecht[3], Thomas Vogl[7] and Marc H. G. P. Raaijmakers[1,]

*Co-first author

[1]Department of Hematology, Erasmus MC Cancer Institute, Rotterdam 3015CN, The Netherlands
[2]Department of Internal Medicine, Erasmus MC Cancer Institute, Rotterdam 3015CN, The Netherlands
[3]Department of Hematology, VU University Medical Center, Cancer Center Amsterdam, Amsterdam 1081HV, The Netherlands
[4]Department of Molecular Genetics, Erasmus MC Cancer Institute, Rotterdam 3015CN, The Netherlands
[5]Department of Pediatric Hematology, Immunology and Infectious Diseases, Emma Children's Hospital, Academic Medical Centre (AMC), University of Amsterdam (UvA), Amsterdam 1105AZ, The Netherlands
[6]Department of Genetics, Cancer Genomics Center, Department of Radiation Oncology, Erasmus MC Cancer Institute, Rotterdam 3015CN, The Netherlands
[7]Institute of Immunology, University of Münster, Münster 48149, Germany

Running title: Oncogenic niche signaling in human pre-leukemia.

*Cell Stem Cell 2016 Nov 3;19(5):613-627*

## SUMMARY

Mesenchymal niche cells may drive tissue failure and malignant transformation in the hematopoietic system but the underlying molecular mechanisms and relevance to human disease remain poorly defined. Here, we show that perturbation of mesenchymal cells in a mouse model of the preleukemic disorder Shwachman-Diamond syndrome (SDS) induces mitochondrial dysfunction, oxidative stress and activation of DNA damage responses in hematopoietic stem and progenitor cells. Massive parallel RNA sequencing of highly purified mesenchymal cells in the SDS mouse model and a range of human preleukemic syndromes identified p53-S100A8/9-TLR inflammatory signaling as a common driving mechanism of genotoxic stress. Transcriptional activation of this signaling axis in the mesenchymal niche predicted leukemic evolution and progression-free survival in myelodysplastic syndrome (MDS), the principal leukemia predisposition syndrome. Collectively, our findings identify mesenchymal niche-induced genotoxic stress in heterotypic stem and progenitor cells through inflammatory signaling as a targetable determinant of disease outcome in human preleukemia.

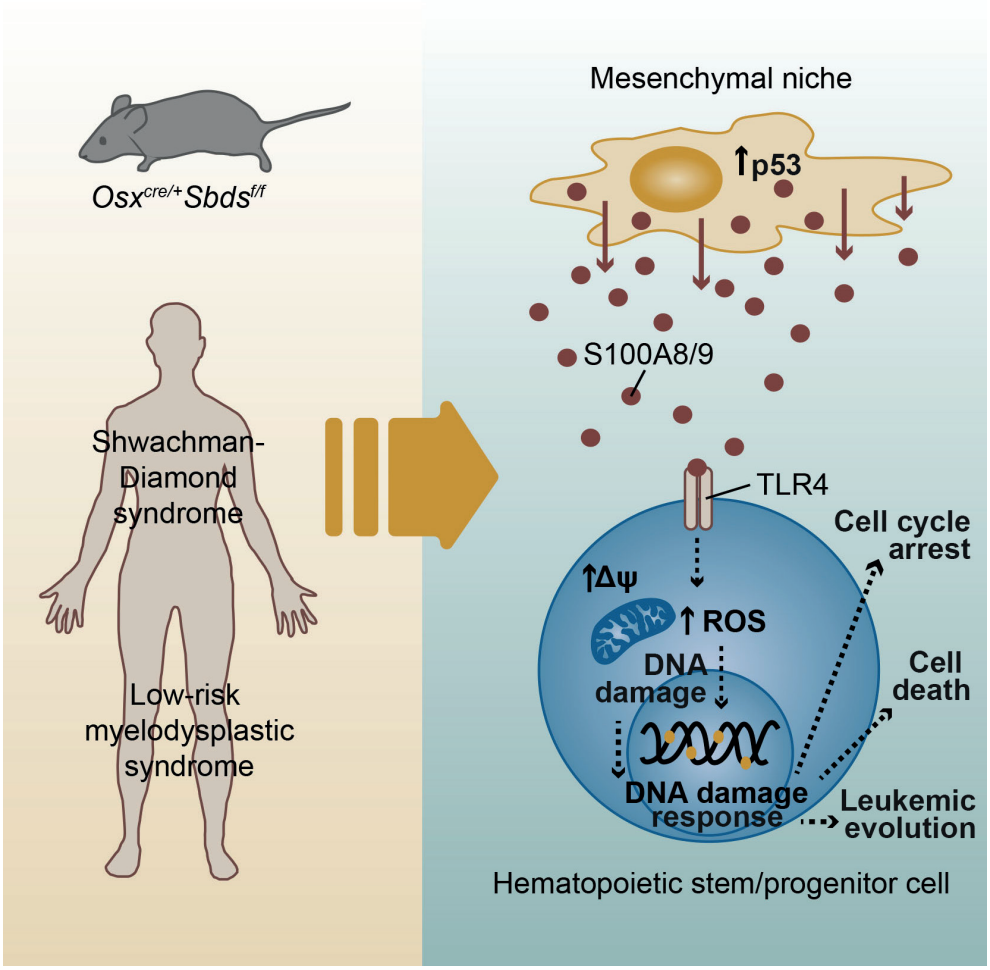
Osx^cre/+Sbds^f/f
Shwachman-Diamond syndrome
Low-risk myelodysplastic syndrome
Mesenchymal niche
↑p53
S100A8/9
TLR4
Cell cycle arrest
↑Δψ
↑ ROS
DNA damage
Cell death
DNA damage response
Leukemic evolution
Hematopoietic stem/progenitor cell

## INTRODUCTION

Genotoxic stress results in the accumulation of DNA lesions in hematopoietic stem and progenitor cells (HSPCs) over the lifespan of an organism, contributing to tissue failure and malignant transformation (Jaiswal et al., 2014; Rossi et al., 2007). The pathophysiological insults underlying genomic stress in HSPCs, however, remain incompletely understood. Perturbed signaling from their surrounding microenvironment may be implicated, but this has not been experimentally defined.

Components of the bone marrow microenvironment have emerged as key regulators of normal and malignant hematopoiesis (Arranz et al., 2014; Hanoun et al., 2014; Medyouf et al., 2014; Schepers et al., 2015; Walkley et al., 2007). We, and others, have shown that primary alterations of the mesenchymal niche can induce myelodysplasia and promote the emergence of acute myeloid leukemia (AML) with cytogenetic abnormalities in HSPCs (Kode et al., 2014; Raaijmakers et al., 2010), thus introducing a concept of niche-driven oncogenesis in the hematopoietic system.



To provide insights into the mechanisms that underlie this concept, as well as their relevance for human disease, we modeled the human leukemia predisposition disorder Shwachman-Diamond syndrome (SDS), caused by constitutive homozygous or compound heterozygous loss of function mutations in the *SBDS* gene, required for ribosome biogenesis (Boocock et al., 2003; Finch et al., 2011). SDS is characterized by skeletal defects in conjunction with a striking propensity to develop myelodysplastic syndrome (MDS) and AML at a young age, with a cumulative probability of >30% at the age of 30 years and a median onset at 18 years (Alter, 2007; Donadieu et al., 2012). Hematopoietic cell intrinsic loss of *Sbds* does not result in MDS or leukemia (Rawls et al., 2007; Zambetti et al., 2015), supporting the notion that cell-extrinsic factors contribute to malignant transformation. Deletion of *Sbds* from mesenchymal cells expressing the mesenchymal progenitor marker osterix (*Sp7*) in the bone marrow induced apoptosis in HSPCs and myelodysplasia, but the molecular mechanisms driving these observations and their relevance for human disease remained to be defined (Raaijmakers et al., 2010).

Here, we identify the endogenous damage-associated molecular pattern (DAMP) molecules S100A8 and S100A9, secreted from mesenchymal niche cells, as drivers of mitochondrial dysfunction, oxidative stress and DNA damage response (DDR) activation in HSPCs, with clinical relevance to the pathogenesis and prognosis of human bone marrow failure and leukemia predisposition syndromes.

## RESULTS

### Deletion of *Sbds* from mesenchymal progenitor cells (MPCs) recapitulates skeletal abnormalities of human SDS

SDS is characterized by bone abnormalities including low-turnover osteoporosis with reduced trabecular bone volume, low numbers of osteoblasts, and reduced amount of osteoid, leading to increased risk of fractures (Toiviainen-Salo et al., 2007). The cellular subsets driving these abnormalities and the underlying molecular mechanisms have remained largely undefined. We have previously shown that Cre-mediated deletion of *Sbds* from osterix$^{+}$ MPCs (*Sbds*$^{f/f}$ *Osx*$^{cre/+}$ mice, hereafter OCS$^{f/f}$ or mutants) disrupts the architecture of the marrow and cortical bone (Raaijmakers et al., 2010). Here, we first sought to better define the skeletal defects in these mice and their relevance to human disease.

OCS$^{f/f}$ mice presented growth retardation and reduced femur length compared to control *Sbds*$^{f/+}$ *Osx*$^{cre/+}$ (OCS$^{f/+}$) mice (Figure 1A and 1B) as observed in human patients (Aggett et al., 1980; Ginzberg et al., 1999). The runted phenotype was associated with a significantly limited lifespan, with lethality observed after the age of 4 weeks. Analyses were therefore performed in three week-old mice. The femur trabecular area was profoundly reduced in OCS$^{f/f}$ mice, with decreased bone volume, low number of trabeculae, increased trabecular spacing and reduced numbers of osteoblasts compared to controls (Figure 1C-1G, and 1I). The cortical bone of OCS mutants was also affected, as indicated by low bone mineral density values (Figure 1C-1D and 1H), attenuating the mechanical properties of the bone, which was found less resistant to fracture in three-point bending test (Figure 1J). A tendency for reduced stiffness in the long bones was also observed (Figure 1K). Taken together, the structural and mechanical defects indicate that *Sbds* deficiency in MPCs causes osteoporosis with a propensity for fracturing, in line with observations in SDS patients (Ginzberg et al., 1999; Mäkitie et al., 2004; Toiviainen-Salo et al., 2007). Impaired osteogenesis did not reflect a contraction of the bone progenitor cell pool as shown by frequency of CFU-F and Osx::GFP$^{+}$ cells (Figure S1A and S1B), but rather impairment of terminal osteogenic differentiation as suggested by transcriptional profiling of prospectively isolated osterix-expressing (GFP$^{+}$) cells (Figure S1C). Transcriptional data confirmed deregulated expression of genes related to ribosomal biogenesis and translation (Figure S1D and S1E), in line with the established role of *Sbds* in ribosome biogenesis. Collectively, this data supports a view in which bone abnormalities in SDS are caused by deficiency of *Sbds* in MPCs, which attenuates terminal differentiation towards matrix-depositing osteoblastic cells with a compensatory increase in the most primitive mesenchymal compartment.

### *Sbds* deficiency in the hematopoietic niche induces mitochondrial dysfunction, oxidative stress and activation of the DNA damage response in HSPCs

Having established that the OCS mice represent a *bona fide* model for bone abnormalities in human disease, we next investigated the hematopoietic consequences of these environmental alterations. HSPC number was unaltered in OCS mice (Figure S2A-S2C) and HSPCs displayed global preservation of their transcriptional landscape after exposure to the *Sbds*-deficient environment (Figure S2D-S2F). Transcriptional network analysis, however, revealed significant overlap with signatures previously defined as predicting leukemic evolution of human $CD34^+$ cells (Li et al., 2011), including pathways signaling mitochondrial abnormalities (Figure 2A; Table S1). Mitochondrial dysfunction was confirmed by measuring the mitochondrial membrane potential ($\Delta\psi$), indicating hyperpolarization of the mitochondria (Figure 2B and 2C). Mitochondrial hyperpolarization can result in reverse electron transfer, leading to the production of superoxide radicals, which can be further converted into other reactive oxygen species (ROS) (Murphy, 2009). In line with this, a marked increase in intracellular ROS levels was found in OCS mutant HSPCs (Figure 2D), more specifically superoxide radicals derived from mitochondria as shown by dihydroethidium (DHE) staining (Figure S2G) (Owusu-Ansah et al., 2008; Stowe and Camara, 2009). ROS can undermine the genomic integrity of HSPCs by inducing DNA damage (Ito et al., 2006; Walter et al., 2015; Yahata et al., 2011), to which normal HSPCs react by activating the DDR and DNA repair pathways (Rossi et al., 2007). Indeed, HSPCs (LKS-SLAM) cells from $OCS^{f/f}$ mice displayed accumulation of Ser139-phosphorylated H2AX histone (γH2AX), which forms at the sites of DNA damage (Figure 2E; Figure S2H). Treatment of OCS mutant animals with the ROS scavenger N-acetylcysteine (NAC) resulted in partial reduction in the accumulation of gH2AX (Figure S2I and S2J). Congruent with genotoxic effects of the mutant microenvironment, HSPCs displayed transcriptional modulation of DDR and DNA repair pathways (Table S2), including nucleotide excision repair programs, associated with ROS-induced lesions (Curtin, 2012) and signatures related to the master regulator of DDR and cell checkpoint activation ataxia telangiectasia and Rad3-related (ATR). Activation of the G1-S cell cycle checkpoint, resulting in cell cycle arrest, was suggested by depletion of S-phase transcriptional signatures (Figure 2F; Table S1), *in vivo* BrdU/Ki67 labeling (Figure 2G and 2H; Figure S2K) and downregulation of the Myc pathway, a critical regulator for this restriction point and the coordination of S–G2–M progression (Figure 2I; Table S3). Apoptosis of mutant HSPCs, as an alternative outcome of checkpoint activation, was earlier demonstrated (Raaijmakers et al., 2010). Together, the data indicate that the Sbds-deficient environment induces mitochondrial dysfunction, oxidative stress, DNA damage and genotoxic stress in HSPCs leading to activation of DDR pathways and G1-S checkpoint activation, reminiscent of a model in which mitochondrial dysfunction underlies an escalating cycle of increased ROS and genotoxic damage (Sahin and Depinho, 2010).

Short term exposure to the genotoxic environment did not attenuate HSPC function in DNA repair proficient cells, as demonstrated by competitive transplantation experiments (Figure S3A-S3C), suggesting efficient DNA-repair or elimination of functionally impaired HSPCs by the DDR-driven apoptosis and cell cycle arrest. Congruent with this notion, alkaline comet assays on sorted HSPCs failed to demonstrate structural DNA damage (Figure S3D and S3E).

## Activation of the p53 pathway drives bone abnormalities and genotoxic stress in OCS mice

Next, we sought to define the molecular programs underlying the bone and hematopoietic alterations in OCS mice. A proposed common molecular mechanism for the pathogenesis of ribosomopathies involves activation of the p53 tumor suppressor pathway (Raiser et al., 2014). The p53 protein was overexpressed in $GFP^+$ MPCs in OCS mutants, with activation of downstream transcriptional pathways and upregulation of canonical targets (Figure 3A-3C). To assess the pathophysiological role of p53 activation in MPCs, we intercrossed OCS with *Trp53*-floxed mice (Marino et al., 2000), generating a double conditional knock-out model where the deletion of p53 is localized in the *Sbds*-deleted stromal compartment (*Sbds*$^{f/f}$ *Trp53*$^{f/f}$ *Osx*$^{cre/+}$ mice; hence OCS$^{f/f}$ p53$^{\Delta}$) (Figure 3D). Genetic recombination of the *Trp53* locus was detected only in bone cells-containing samples, demonstrating the tissue specificity of p53 deletion in this model (Figure 3E). Genetic deletion of p53 from *Sbds*-deficient MPCs rescued the osteoporotic phenotype (Figure 3F-3J), but not cortical bone mineralization (Figure 3K), while it had only modest effects on bone mass in OCS control mice (Figure S4), in line with earlier observations (Wang et al., 2006). Rescue of the skeletal phenotype was linked to amelioration of genotoxic stress in HSPCs as demonstrated by a reduction of superoxide radicals derived from mitochondria and DNA damage (Figure 3L and 3M).

## Identification of the damage-associated molecular pattern genes *S100A8* and *S100A9* as candidate niche factors driving genotoxic stress in human leukemia predisposition syndromes

To identify human disease-relevant niche factors, downstream of p53 activation, driving genomic stress in HSPCs, we compared the transcriptomes of $GFP^+$ MPCs from OCS mice to those from prospectively FACS-isolated mesenchymal $CD271^+$ niche cells (Tormin et al., 2011) from human SDS patients (Figure 4A; Table S4). The mesenchymal nature of $CD271^+$ cells was confirmed by CFU-F capacity and differential expression of mesenchymal, osteolineage and HSPC-regulatory genes (Chen et al, 2016). RNA sequencing showed the presence of *SBDS* mutations (Figure 4B; Figure S5; Table S4) associated with reduced *SBDS* expression (Figure 4C), confirming molecular aspects of SDS in previous studies (Finch et al., 2011; Woloszynek et al., 2004). Virtually identical transcriptional signatures of disrupted ribosome biogenesis and translation were found in human niche cells (Figure 4D) and in $GFP^+$ cells from OCS mice (Figure S1E), confirming faithful recapitulation of human molecular disease characteristics

in the mouse model. Forty genes were differentially expressed both in the mouse model and human SDS, 25 of which were overexpressed, with a remarkable abundance of genes encoding proteins implicated in inflammation and innate immunity (Figure 4E).

To further delineate candidate genes driving genomic stress and leukemic evolution from this gene set, we performed whole transcriptome sequencing of $CD271^+$ cells in two related human bone marrow failure and leukemia predisposition disorders: (1) low-risk MDS, the principal human preleukemic disorder in which cell cycle exit (senescence), accumulation of ROS, DNA damage and apoptosis have been described (Head et al., 2011; Peddie et al., 1997; Xiao et al., 2013), reminiscent of HSPC phenotypes in OCS mice, and (2) DBA, like SDS, a ribosomopathy characterized by bone marrow failure, but with a much lower propensity to evolve into AML (<1% with longer latency than observed in SDS and MDS) (Vlachos et al., 2012) (Table S4). We reasoned that genes specifically overexpressed in mesenchymal niche cells from disorders with as strong propensity for leukemic evolution (SDS and MDS) might represent strong candidate drivers of genotoxic stress. Eleven such genes were found (Figure 4F), among which the damage-associated molecular pattern (DAMP) genes *S100A8* and *S100A9*, which were significantly ($P$<0.05) differentially expressed in $GFP^+$ cells from OCS mutant mice (Figure 4E-4G) and also represent a *bona fide* downstream transcriptional target of p53 (Li et al., 2009). Ex vivo shRNA experiments confirmed that upregulation of both p53 and S100A8/9 are direct, cell-intrinsic consequences of *Sbds* downregulation in mesenchymal precursor (OP9) cells (Figure S6A).



### Niche-derived S100A8/9 induces genotoxic stress in murine and human HSPCs

*S100A8* and *S100A9* belong to a subclass of proinflammatory molecules referred to as DAMP or alarmins. DAMPs are endogenous danger signals that are passively released or actively secreted in the microenvironment after cell death, damage or stress and bind pattern recognition receptors (PRR) to regulate inflammation and tissue repair (Srikrishna and Freeze, 2009). S100A8 and S100A9 proteins were overexpressed in mouse *Sbds*-deficient MPCs (Figure 5A and 5B) and increased plasma concentration of S100A8/9 indicated secretion of the heterodimer (Figure 5C). Its canonical receptor TLR4 (Vogl et al., 2007) is expressed in murine HSPCs (Figure S6B) and the canonical downstream signaling NF-κB and MAPK pathways were activated in HSPCs from $OCS^{f/f}$ mice (Figure S6C).

Exposure of HSPCs (LKS) cells to recombinant murine S100A8/9 resulted in increased DNA damage (number of γH2AX and 53BP1 foci) (Figure 5D; Figure S6D), which was replication-independent (Figure 5E), and apoptosis (Figure 5F), associated with activation of TLR signaling (Figure 5G; Table S5), recapitulating the *in vivo* HSPC phenotype (Raaijmakers et al., 2010). *In vivo*, blockage of TLR4 by neutralizing antibodies resulted in a reduction of γH2AX foci in LKS cells from $OCS^{f/f}$ mice (Figure 5H).

To provide formal experimental support for the view that S100A8/9 production by ancillary cells in the bone marrow microenvironment is sufficient to drive genotoxic stress in HSPCs in a paracrine manner, we next transplanted CD45.1$^+$ wild type hematopoietic cells into S100A9-GFP transgenic (S100A9Tg) mice, overexpressing both *S100A8* and *S100A9* under control of the MHC class I H2K promoter (Cheng et al., 2008) (Figure 6A). S100A8/9 (GFP) was expressed in a mesenchymal (CD45$^-$ CD31$^-$ Ter119$^-$ CD51$^+$ Sca1$^-$) niche population, previously shown to contain the Osterix-expressing cells (Schepers et al, 2013) (Figure 6B and 6C). The S100A8/9$^+$ microenvironment induced accumulation of superoxide radicals (DHE) and DNA-damage (γH2AX) in wild type (CD45.1$^+$) HSPCs (Figure 6D-6F), in particular in immunophenotypic HSCs, indicating that secretion of S100A8/9 from ancillary cells in the microenvironment is indeed sufficient to induce genotoxic stress in HSCs in a paracrine manner.

Translating these findings to human disease, exposure of human cord blood CD34$^+$ HSPCs to human recombinant S100A8/9 at clinically relevant concentrations (Chen et al., 2013 and Supplemental Experimental Procedures) resulted in DNA damage (increased γH2AX foci), apoptosis and impaired HSPC function (CFU-C) (Figure S7).

## Activation of the p53-S100A8/9-TLR axis in mesenchymal niche cells predicts leukemic evolution and clinical outcome in human low-risk MDS

To further define the biologic and clinical significance of these findings, we performed transcriptome sequencing of CD271$^+$ niche cells in a prospective, homogeneously treated cohort of low-risk MDS patients (*n* = 45, Figure 7A; Table S6). Expression of *S100A8* and *S100A9* was strongly correlated (Figure 7B, 7C), with a subgroup of MDS patients (17/45; 38%) demonstrating significant overexpression of *S100A8* and *S100A9* (Modified Thompson Tau outlier test) (Figure 7B and 7D), independent of established prognostic factors as defined by the revised International Prognostic Scoring System (IPSS-R) and the MD Anderson risk score (LR-PSS) (Table S6). Transcriptional pathway analysis (GSEA) comparing mesenchymal cells overexpressing S100A8/9 (*n* = 17) to those of niche S100A8/9$^-$ patients (*n* = 28) revealed activation of p53 and TLR programs in S100A8/9$^+$ mesenchymal cells (Figure 7E), in line with experimental data from the mouse model pointing at the existence of a p53-S100A8/9-TLR axis. Leukemic evolution, defined as the development of frank AML or excess of blasts to WHO RAEB1/ RAEB2 (refractory anemia with excess of blasts), occurred in 5/17 (29.4%) of niche S100A8/9$^+$ patients (3 AML, 2 RAEB1/RAEB2) vs. 4/28 (14.2%) in niche S100A8/9$^-$ patients (2AML, 2 RAEB1/RAEB2). Time to leukemic evolution was significantly shorter in niche S100A8/9$^+$ patients (average 3.4 (1-7.5) vs 18.5 (7-40); *P* = 0.03 by Exact Wilcoxon rank sum test) resulting in a significantly shorter progression-free survival of niche S100A8/9$^+$ patients (median 11.5 vs 53 months, *P* = 0.03) (Figure 7F and 7G). Collectively, the data establish activation of p53-S100A8/9 signaling in mesenchymal niche cells as an independent predictor of disease outcome in human MDS.

## DISCUSSION

Genomic stress and the ensuing DNA damage play a pivotal role in the attenuation of normal hematopoiesis in ageing and disease. Mutations accumulate in HSPCs over the lifespan of an organism, but the (patho)physiological sources of genomic stress in HSPCs and their relationship with human bone marrow failure remain incompletely understood. Here, we show that specific inflammatory signals from the mesenchymal niche can induce genotoxic stress in heterotypic stem/progenitor cells and relate this concept to the pathogenesis of two human bone marrow failure and leukemia predisposition syndromes, SDS and MDS.
The data indicate that the mesenchymal niche may actively contribute to the formation of a 'mutagenic' environment, adding to our understanding of how a premalignant environment facilitates cancer initiation and evolution. The data argue that this may not only occur through facilitated selection and expansion of genetic clones that stochastically emerge in a permissive environment, but that the mesenchymal niche may be an active participant in driving the genotoxic stress underlying tissue failure and malignant transformation of parenchymal cells.



Notably, leukemic transformation was not observed in mice with targeted deficiency of *Sbds* in mesenchymal cells. Earlier, in a related mouse model of targeted *Dicer1* deletion in MPCs, leukemic transformation was a rare event (Raaijmakers et al., 2010). In the light of our current findings, these observations are likely explained by several factors. First, prolonged exposure to a mutagenic niche, beyond the limited lifespan of OCS mice, may be necessary for the accumulation of genetic damage required for full transformation. Additionally, the data argue that DNA repair-proficient HSPCs are able to cope with the mutagenic stress induced by their environment through activation of the DDR (as shown by molecular activation of cell cycle checkpoints and apoptosis), preventing the accumulation of stable genetic damage (as demonstrated by comet assays) and maintaining the functional integrity of HSPCs (as shown by repopulation assays).

We propose that in SDS (and possibly other congenital bone marrow failure syndromes) genetically aberrant hematopoietic and niche elements cooperate in driving bone marrow failure and leukemic evolution. Our mouse models of SDS support a view in which hematopoietic cell autonomous loss-of-function of *Sbds* drives neutropenia (Zambetti et al., 2015), while niche alterations in this disease drive myelodysplastic alteration and genotoxic stress. It is conceivable that loss-of-function mutations in *Sbds* in HSPCs further sensitizes HSPCs to the genotoxic effects of the *Sbds*-deficient environment, perhaps through attenuation of DNA damage repair mechanisms. It will thus be of considerable interest to test the hypothesis that a mutagenic environment cooperates with aberrant HSPCs, compromised in their ability to cope with inflammatory genotoxic stress, in leukemia

evolution. In this context, the propensity of *Sbds*-deficient cells to accumulate ROS (Ambekar et al., 2010), and their reduced ability to cope with various cellular stressors such as mitotic spindle destabilizing agents, endoplasmic reticulum stress activators, topoisomerase inhibitors and UV irradiation (Austin et al., 2008; Ball et al., 2009) is noteworthy.

The current findings add to emerging insights into the role of innate immune TLR-signaling in the pathogenesis of human MDS. TLR4 and other TLRs are overexpressed in HSPCs from MDS patients (Maratheftis et al., 2007; Wei et al., 2013) and TLR4 expression was shown to correlate with apoptosis in $CD34^+$ hematopoietic cells. TLR signaling is constitutively activated in MDS mice with deletion of chromosome 5 (del5q) (Starczynowski et al., 2010) and multiple TLR downstream signaling pathways have been shown to be activated in MDS and related to loss of progenitor cell function (Ganan-Gomez et al., 2015).

Our findings implicate the DAMP S100A8/9 derived from the mesenchymal niche as a driver of TLR signaling in this disease. The unbiased identification of S100A8/9 seems to independently converge with an earlier report implicating S100A8/9 in the pathogenesis of MDS (Chen et al., 2013). In this study it was shown that the plasma concentration of S100A9 was significantly increased in MDS patients (Chen et al., 2013) and S100A8/9 was shown to drive expansion and activation of myeloid-derived suppressor cells (MDSCs) that contributed to cytopenia and myelodysplasia in a murine model of S100A9 overexpression through secretion of suppressive cytokines. It is therefore an intriguing possibility that additional, indirect, biologic effects of S100A8/9 contribute to the hematopoietic phenotype of OCS mice. This may include engagement of other cognate receptors of the protein, including expansion of MDSCs through CD33 signaling (Chen et al., 2013).

In our study S100A8/9 was aberrantly overexpressed in a rare population of mesenchymal niche cells, both in the mouse model and human disease. Typically, expression of the protein is found in myeloid cells, raising the question why S100A8/9 production by (rare) niche cells is more relevant to the biology of HSPC than secretion from myeloid/erythroid cells. While the answer to this question remains speculative in the absence of *in vivo* targeted overexpression studies, it is noteworthy that, in contrast to most cytokines, chemokines and other pro-inflammatory molecules, the local accumulation of S100A8/9 in the environment is very high (up to 100µg/ml and about 50 to 100-fold higher than systemic concentrations), likely caused by attachment to extracellular matrices such as proteoglycans (Vogl et al., 2014). This implicates that the exposure of HSPCs to S100A8/9 is projected to relate strongly to their anatomical proximity to a producing cell. $CD271^+$ mesenchymal cells are directly adjacent to $CD34^+$ HSPC in human bone marrow (Flores-Figueroa et al., 2012). This notion of 'spatial relevance' may also be congruent with recent observations that aberrant overexpression of S100A8/9 in hematopoietic (erythroid) cells within the erythroid island

in a model of human 5q$^-$ syndrome leads to a predominant erythroid, anemic, phenotype (Schneider at al., 2016).

The mechanisms of S100A8/9 induced DNA damage remain to be fully elucidated. Our experiments using NAC to reduce ROS burden suggest an incomplete association between oxidative stress and DNA damage, suggesting that S100A8/9 secretion may attenuate genomic integrity through additional mechanisms. Similarly, it is conceivable that other ligands secreted from mesenchymal cells contribute to the induction of DNA damage in HSPCs in the mouse model. We found a striking abundance of transcripts encoding other DAMPs and cytotoxic proteins in both the mouse model and mesenchymal elements isolated from SDS patients. Ongoing investigations will have to assess whether other selected ligands can evoke genomic stress in heterotypic HSPCs and in such a fashion contribute to the generation of a mutagenic environment in these disorders.



Finally, our findings establish molecular characteristics of the mesenchymal environment as an important determinant of disease outcome in humans. S100A8/9 expression, associated with activated p53 and TLR signaling, in mesenchymal cells predicted leukemic evolution and progression-free survival in a cohort of homogeneously treated low-risk MDS patients. This is of considerable clinical relevance because low-risk MDS is a heterogeneous disease-entity with a subset of patients having a particular dismal prognosis not identified by current risk-stratification strategies (Bejar et al., 2012). Gene expression of S100A8/9 may identify a substantial subset of patients with a survival typically associated with ‘high-risk’ patients and, if confirmed in larger independent cohorts, could guide therapeutic decision making in MDS. The data thus provide a strong rationale for niche–instructed therapeutic targeting of inflammatory signaling in human preleukemic disease.

## EXPERIMENTAL PROCEDURES

### Mice and *in vivo* procedures

OCS, *Trp53*$^{f/f}$ and S100A9Tg mice have been previously described (Cheng et al., 2008; Jonkers et al., 2001; Raaijmakers et al., 2010). *Ptprc*$^{a}$*Pepc*$^{b}$*/BoyCrl* (B6.SJL) mice were purchased from Charles River. Animals were maintained in specific pathogen free conditions in the Experimental Animal Center of Erasmus MC (EDC). For *in vivo* cell cycle analysis, OCS mice received intraperitoneal injections of BrdU (1.5 mg in PBS, BD Biosciences) and sacrificed after 15 h. For TLR4 studies, 2 week-old mice were intraperitoneally injected with a double dose (100 µg and 35 µg, 48 h interval) of TLR4-neutralizing antibody (clone MTS510, eBioscience) or isotype control (clone eBR2a, eBioscience) and sacrificed after 60h. For NAC rescue studies, 2-week-old mice received daily intraperitoneal injections of NAC (Sigma-Aldrich, 320 mg/kg in saline) until the day of the analysis and at least for 5 days. All mice were sacrificed by cervical dislocation. Animal studies were approved by the Animal Welfare/Ethics Committee of the EDC in accordance with legislation in the Netherlands (Approval No. EMC 2067, 2714, 2892, 3062).

µCT analysis

Femur bones were isolated, fixated in 3% PFA/PBS for 24 h and stored in 70% ethanol. µCT analysis was performed using a SkyScan 1172 system (SkyScan) using previously described settings (Tudpor et al., 2015). Bone microarchitectural parameters relative to the trabecular and the cortical area were determined in the distal metaphysis and the mid-diaphysis of each femur, respectively, using software packages from Bruker MicroCT (NRecon, CtAn and Dataviewer).

### Human bone marrow samples

Bone marrow aspirates were obtained from SDS and DBA patients during routine follow-up. All MDS patients were treated with lenalidomide (10 mg/day, d 1-21 in a 4-week schedule) in the context of an ongoing prospective clinical trial for patients with low or intermediate-1 risk MDS according to IPSS criteria (HOVON89; www.hovon.nl; www.trialregister.nl as NTR1825; EudraCT No. 2008-002195-10). Bone marrow specimens were collected at study entry and disease diagnosis and staging confirmed by central board reviewing. Leukemic evolution was assessed according to WHO criteria; development of RAEB1 (refractory anemia with excess of blast) or RAEB-2 (if RAEB1 at entry) was considered progression of disease. Leukemia (AML) was diagnosed according to standard WHO criteria (≥20% myeloblasts in blood/bone marrow). Bone marrow cells from allogeneic transplantation donors were used as normal controls. Patients and healthy donor characteristics are described in Table S4 and S6. All specimens were collected with informed consent, in accordance with the Declaration of Helsinki

## Gene expression profiling

Osx::GFP cells from bone cell suspensions of OCS mice were sorted in TRIzol Reagent (Life Technologies) and RNA was extracted according to the manufacturer's recommendations. Linear amplification of mRNA was performed using the Ovation Pico WTA System (NuGEN). cDNA was fragmented and labelled with Encore™ Biotin Module (NuGEN). The biotinylated cDNA was hybridized to the GeneChip Mouse Genome 430 2.0 Array (Affymetrix eBioscience). Signal was normalized and differential gene expression analysis was performed with the limma package (Ritchie et al., 2015). Gene expression array data derived from murine Osterix:GFP cells is available at ArrayExpress (www.ebiac.uk/arrayexpress) under accession number E-MTAB-5023. RNA sequencing experiments were performed as previously described (Zambetti et al., 2015). Human transcripts were aligned to the Ref Seq transcriptome (hg19) and analyzed with DESeq2 (Love et al., 2014), while mouse transcripts were aligned to the Ensembl transcriptome (mm10) and analyzed with EdgeR (Robinson et al., 2010) in the R environment. FPKM values were calculated using Cufflinks (Trapnell et al., 2010). Principal component analysis was performed in the R environment on the raw fragment counts extracted from the BAM files by HTSeq-count (Anders et al., 2015). RNA-Seq data derived from murine $CD48^{-}/CD48^{+}$ LSK cells have been deposited at the European Nucleotide Archive (ENA, http://www.ebi.ac.uk/ena/), which is hosted by the EBI, under accession number PRJEB15060. RNA-seq data derived from human LR-MDS, SDS and DBA specimens have been deposited at the European Genome-phenome Archive (EGA, https://www.ebi.ac.uk/ega/), which is hosted by the EBI, under accession number EGAS00001001926. For Gene Set Enrichment Analysis (Subramanian et al., 2005) (GSEA, Broad Institute), normalized intensity values (microarray data) and FPKM values (RNA sequencing) were compared to the curated gene sets (C2) and the Gene Ontology gene sets (C5) of the Molecular Signature Database (MsigDB) using the Signal2Noise metric and 1000 gene set-based permutations. For HSPCs GO-term analysis, genes with significantly differential expression ($P<0.05$) were interrogated using g:Profiler web-based software (Reimand et al., 2011; Reimand et al., 2007).

## Immunofluorescence microscopy

HSPCs were harvested in PBS+0.5%FBS, cytospun on a glass slide for 3 min at 500 rpm using a Cytospin 4 centrifuge (Thermo Scientific) and fixed in 3% PFA/PBS for 15 min on ice. After 3 washing steps in PBS, cells were permeabilized for 2 min in 0.15% Triton-X100/PBS. Aspecific binding sites were blocked by incubation in 1%BSA/PBS for 1 h at room temperature. Cells were next stained overnight at 4°C with either anti-phospho-histone H2A.X (Ser139) mouse monoclonal antibody (clone JBW301, Merck Millipore, diluted 1:1000 in 1%BSA/PBS) or with anti-53BP1 rabbit polyclonal antibody (Novus Biologicals, diluted 1:1000 in 1%BSA/PBS). Slides were washed twice in PBS for 5 min and incubated for 1 h at 37°C with either

Alexa Fluor 488-conjugated goat anti-mouse antibody (Cat. A10667, Life Technologies) or goat anti-rabbit antibody (Cat. A11008, Life Technologies), both diluted 1:200 in 1%BSA/PBS. After 2 washes in PBS, slides were mounted in VECTASHIELD Mounting Medium with DAPI (Vector Laboratories). Z-series images were acquired with a Leica TCS SP5 confocal microscope (63X objective lens) using the LAS software (Leica Microsystems). γH2AX and 53BP1 foci were counted manually from the maximum projection view.

### Survival analysis

The low-risk MDS patient subgroup with S100 niche signature was defined by the Modified Thompson Tau test for outlier detection. In brief, *S100A8* statistics from the control cases were combined to define the rejection region, demarcating FPKM values to be considered as outliers. MDS cases with *S100A8* FPKM values within the rejection region were thus defined as niche-signature$^{+}$. To determine the significance difference in time to progression we used the Wilcoxon signed rank test accounting for tied observations. Event-free survival was determined by specifying leukemic progression or death as events. Patients experiencing a non-hematological related death (e.g., cardiac failure), where censored on the date of this event. Patients remaining alive were censored on the date of last consultation. Kaplan-Meier curves were used to estimate the survival functions through time. Statistical differences in the survival distributions was assessed with the Mantel-Cox log-rank test. All calculations were performed in the R environment.

### Statistics

Statistical analysis was performed using Prism 5 (GraphPad Software). Unless otherwise specified, unpaired, 2-tailed Student's t test (single test) or 1-way analysis of variance (multiple comparisons) were used to evaluate statistical significance, defined as $P<0.05$. All results in bar graphs are mean value ± standard error of the mean.

## SUPPLEMENTAL INFORMATION

Supplemental Information includes Supplemental Experimental Procedures, five figures, and six tables.

### AUTHOR CONTRIBUTIONS

Conceptualization: N.A.Z. and M.H.G.P.R.; Methodology: N.A.Z., Z.P., S.C., K.J.G.K., M.A.M., E.M.J.B., B.V.D.E., J.P.T.M.V.L., R.K., T.V., and M.H.G.P.R.; Investigation: N.A.Z., Z.P., S.C., M.A.M., E.M.J.B., M.N.A., P.M.H.V.S., C.V.D.L., B.V.D.E., and T.V.; Resources: T.M.W., E.M.P.C., C. M., P. G. M., J.P.T.M.V.L, I.P.T., T.W.K., R.K., A.V.D.L., and T.V.; Data curation: M.A.S., R.M.H., T.M.W., E.M.P.C., T.W.K., and A.V.D.L.; Writing: N.A.Z. and M.H.G.P.R; Visualization: N.A.Z., Z.P., S.C, and R.H.M. ; Supervision and Funding Acquisition: M.H.G.P.R.



### ACKNOWLEDGEMENTS

Prof. Johanna M. Rommens donated *Sbds*-floxed mice; Dr Eric Braakman and Mariette ter Borg provided $CD34^+$ cells; Dr Elwin Rombouts, Onno Roovers, Peter van Geel, Kirsten van Lom, Marijke Koedam, Nicole van Vliet, Charlie Laffeber and Gert-Jan Kremers provided technical assistance; Dr Marc Bierings and Dr Valerie de Haas on behalf of the 'Stichting Kinderoncologie Nederland (SKION)' provided DBA samples; Pearl F.M. Mau Asam helped with SDS bone marrow collection; Dr Dana Chitu of the HOVON data center helped with clinical data; members of the Erasmus MC Department of Hematology provided scientific discussion; members of the Erasmus MC animal core facility EDC helped with animal care. This work was supported by grants from the Dutch Cancer Society (KWF Kankerbestrijding), Amsterdam, The Netherlands (grant EMCR 2010-4733 to M.H.G.P.R.), the Netherlands Organization of Scientific Research (NWO 90700422 to M.H.G.P.R.) and the Netherlands Genomics Initiative (Zenith grant no 40-41009-98-11062 to M.H.G.P.R.).

## REFERENCES

Aggett, P.J., Cavanagh, N.P.C., Matthew, D.J., Pincott, J.R., Sutcliffe, J., and Harries, J.T. (1980). Shwachmans Syndrome - a Review of 21 Cases. Arch. Dis. Child. *55*, 331-347.

Alter, B.P. (2007). Diagnosis, genetics, and management of inherited bone marrow failure syndromes. Hematology Am. Soc. Hematol. Educ. Program, 29-39.

Ambekar, C., Das, B., Yeger, H., and Dror, Y. (2010). SBDS-deficiency results in deregulation of reactive oxygen species leading to increased cell death and decreased cell growth. Pediatr. Blood Cancer *55*, 1138-1144.

Anders, S., Pyl, P.T., and Huber, W. (2015). HTSeq--a Python framework to work with high-throughput sequencing data. Bioinformatics *31*, 166-169.

Arranz, L., Sanchez-Aguilera, A., Martin-Perez, D., Isern, J., Langa, X., Tzankov, A., Lundberg, P., Muntion, S., Tzeng, Y.S., Lai, D.M*., et al.* (2014). Neuropathy of haematopoietic stem cell niche is essential for myeloproliferative neoplasms. Nature *512*, 78-81.

Austin, K.M., Gupta, M.L., Jr., Coats, S.A., Tulpule, A., Mostoslavsky, G., Balazs, A.B., Mulligan, R.C., Daley, G., Pellman, D., and Shimamura, A. (2008). Mitotic spindle destabilization and genomic instability in Shwachman-Diamond syndrome. J. Clin. Invest. *118*, 1511-1518.

Ball, H.L., Zhang, B., Riches, J.J., Gandhi, R., Li, J., Rommens, J.M., and Myers, J.S. (2009). Shwachman-Bodian Diamond syndrome is a multi-functional protein implicated in cellular stress responses. Hum. Mol. Genet. *18*, 3684-3695.

Bejar, R., Stevenson, K.E., Caughey, B.A., Abdel-Wahab, O., Steensma, D.P., Galili, N., Raza, A., Kantarjian, H., Levine, R.L., Neuberg, D*., et al.* (2012). Validation of a prognostic model and the impact of mutations in patients with lower-risk myelodysplastic syndromes. J. Clin. Oncol. *30*, 3376-3382.

Boocock, G.R., Morrison, J.A., Popovic, M., Richards, N., Ellis, L., Durie, P.R., and Rommens, J.M. (2003). Mutations in SBDS are associated with Shwachman-Diamond syndrome. Nat. Genet. *33*, 97-101.

Chen, S., Zambetti, N.A., Bindels, E.M., Kenswill, K., Mylona A.M., Adisty, N.M., Hoogenboezem, R.M., Sanders, M.A., Cremers, E.M., Westers, T.M., *et al*. (2016). Massive parallel RNA sequencing of highly purified mesenchymal elements in low-risk MDS reveals tissue-context-dependent activation of inflammatory programs. Leukemia http://dx.doi.org/10.1038/leu.2016.91.

Chen, X., Eksioglu, E.A., Zhou, J., Zhang, L., Djeu, J., Fortenbery, N., Epling-Burnette, P., Van Bijnen, S., Dolstra, H., Cannon, J*., et al.* (2013). Induction of myelodysplasia by myeloid-derived suppressor cells. J. Clin. Invest. *123*, 4595-4611.

Cheng, P., Corzo, C.A., Luetteke, N., Yu, B., Nagaraj, S., Bui, M.M., Ortiz, M., Nacken, W., Sorg, C., Vogl, T., et al. (2008). Inhibition of dendritic cell differentiation and accumulation of myeloid-derived suppressor cells in cancer is regulated by S100A9 protein. J. Exp. Med. *205*, 2235-2249.

Curtin, N.J. (2012). DNA repair dysregulation from cancer driver to therapeutic target. Nat. Rev. Cancer *12*, 801-817.

Donadieu, J., Fenneteau, O., Beaupain, B., Beaufils, S., Bellanger, F., Mahlaoui, N., Lambilliotte, A., Aladjidi, N., Bertrand, Y., Mialou, V*., et al.* (2012). Classification of and risk factors for hematologic complications in a French national cohort of 102 patients with Shwachman-Diamond syndrome. Haematologica *97*, 1312-1319.

Finch, A.J., Hilcenko, C., Basse, N., Drynan, L.F., Goyenechea, B., Menne, T.F., Fernandez, A.G., Simpson, P., D'Santos, C.S., Arends, M.J*., et al.* (2011). Uncoupling of GTP hydrolysis from eIF6 release on the ribosome causes Shwachman-Diamond syndrome. Genes Dev. *25*, 917-929.

Flores-Figueroa, E., Varma, S., Montgomery, K., Greenberg, P.L., Gratzinger, D. (2012). Distinctive contact between CD34+ hematopoietic progenitors and CXCL12+ CD271+ mesenchymal stromal cells in benign and myelodysplastic bone marrow. Lab. Invest. *92*, 1330-1341.

Ganan-Gomez, I., Wei, Y., Starczynowski, D.T., Colla, S., Yang, H., Cabrero-Calvo, M., Bohannan, Z.S., Verma, A., Steidl, U., and Garcia-Manero, G. (2015). Deregulation of innate immune and inflammatory signaling in myelodysplastic syndromes. Leukemia *29*, 1458-1469.

Ginzberg, H., Shin, J., Ellis, L., Morrison, J., Ip, W., Dror, Y., Freedman, M., Heitlinger, L.A., Belt, M.A., Corey, M.*, et al.* (1999). Shwachman syndrome: phenotypic manifestations of sibling sets and isolated cases in a large patient cohort are similar. J. Pediatr. *135*, 81-88.

Hanoun, M., Zhang, D., Mizoguchi, T., Pinho, S., Pierce, H., Kunisaki, Y., Lacombe, J., Armstrong, S.A., Duhrsen, U., and Frenette, P.S. (2014). Acute myelogenous leukemia-induced sympathetic neuropathy promotes malignancy in an altered hematopoietic stem cell niche. Cell Stem Cell *15*, 365-375.

Head, D.R., Jacobberger, J.W., Mosse, C., Jagasia, M., Dupont, W., Goodman, S., Flye, L., Shinar, A., McClintock-Treep, S., Stelzer, G.*, et al.* (2011). Innovative analyses support a role for DNA damage and an aberrant cell cycle in myelodysplastic syndrome pathogenesis. Bone Marrow Res. *2011*, 950934.

Ito, K., Hirao, A., Arai, F., Takubo, K., Matsuoka, S., Miyamoto, K., Ohmura, M., Naka, K., Hosokawa, K., Ikeda, Y.*, et al.* (2006). Reactive oxygen species act through p38 MAPK to limit the lifespan of hematopoietic stem cells. Nat. Med. *12*, 446-451.

Jaiswal, S., Fontanillas, P., Flannick, J., Manning, A., Grauman, P.V., Mar, B.G., Lindsley, R.C., Mermel, C.H., Burtt, N., Chavez, A.*, et al.* (2014). Age-related clonal hematopoiesis associated with adverse outcomes. N. Engl. J. Med. *371*, 2488-2498.

Jonkers, J., Meuwissen, R., van der Gulden, H., Peterse, H., van der Valk, M., and Berns, A. (2001). Synergistic tumor suppressor activity of BRCA2 and p53 in a conditional mouse model for breast cancer. Nat. Genet. *29*, 418-425.

Kode, A., Manavalan, J.S., Mosialou, I., Bhagat, G., Rathinam, C.V., Luo, N., Khiabanian, H., Lee, A., Murty, V.V., Friedman, R.*, et al.* (2014). Leukaemogenesis induced by an activating beta-catenin mutation in osteoblasts. Nature *506*, 240-244.

Li, C., Chen, H., Ding, F., Zhang, Y., Luo, A., Wang, M., and Liu, Z. (2009). A novel p53 target gene, S100A9, induces p53-dependent cellular apoptosis and mediates the p53 apoptosis pathway. Biochem. J. *422*, 363-372.

Li, L., Li, M., Sun, C., Francisco, L., Chakraborty, S., Sabado, M., McDonald, T., Gyorffy, J., Chang, K., Wang, S.*, et al.* (2011). Altered hematopoietic cell gene expression precedes development of therapy-related myelodysplasia/acute myeloid leukemia and identifies patients at risk. Cancer Cell *20*, 591-605.

Love, M.I., Huber, W., and Anders, S. (2014). Moderated estimation of fold change and dispersion for RNA-seq data with DESeq2. Genome Biol. *15*, 550.

Mäkitie, O., Ellis, L., Durie, P.R., Morrison, J.A., Sochett, E.B., Rommens, J.M., and Cole, W.G. (2004). Skeletal phenotype in patients with Shwachman-Diamond syndrome and mutations in SBDS. Clin. Genet. *65*, 101-112.

Maratheftis, C.I., Andreakos, E., Moutsopoulos, H.M., and Voulgarelis, M. (2007). Toll-like receptor-4 is up-regulated in hematopoietic progenitor cells and contributes to increased apoptosis in myelodysplastic syndromes. Clin. Cancer Res. *13*, 1154-1160.

Marino, S., Vooijs, M., van der Gulden, H., Jonkers, J., and Berns, A. (2000). Induction of medulloblastomas in p53-null mutant mice by somatic inactivation of Rb in the external granular layer cells of the cerebellum. Genes Dev. *14*, 994-1004.

Medyouf, H., Mossner, M., Jann, J.C., Nolte, F., Raffel, S., Herrmann, C., Lier, A., Eisen, C., Nowak, V., Zens, B.*, et al.* (2014). Myelodysplastic cells in patients reprogram mesenchymal stromal cells to establish a transplantable stem cell niche disease unit. Cell Stem Cell *14*, 824-837.

Murphy, M.P. (2009). How mitochondria produce reactive oxygen species. Biochem. J. *417*, 1-13.

Owusu-Ansah, E., Yavari, A., Mandal, S., and Banerjee, U. (2008). Distinct mitochondrial retrograde signals control the G1-S cell cycle checkpoint. Nat Genet. *40*, 356-361.

Peddie, C.M., Wolf, C.R., McLellan, L.I., Collins, A.R., and Bowen, D.T. (1997). Oxidative DNA damage in CD34+ myelodysplastic cells is associated with intracellular redox changes and elevated plasma tumour necrosis factor-alpha concentration. Br. J. Haematol. *99*, 625-631.

Raaijmakers, M.H., Mukherjee, S., Guo, S., Zhang, S., Kobayashi, T., Schoonmaker, J.A., Ebert, B.L., Al-Shahrour, F., Hasserjian, R.P., Scadden, E.O.*, et al.* (2010). Bone progenitor dysfunction induces myelodysplasia and secondary leukaemia. Nature *464*, 852-857.

Raiser, D.M., Narla, A., and Ebert, B.L. (2014). The emerging importance of ribosomal dysfunction in the pathogenesis of hematologic disorders. Leuk. Lymphoma *55*, 491-500.

Rawls, A.S., Gregory, A.D., Woloszynek, J.R., Liu, F.L., and Link, D.C. (2007). Lentiviral-mediated RNAi inhibition of Sbds in murine hematopoietic progenitors impairs their hematopoietic potential. Blood *110*, 2414-2422.

Reimand, J., Arak, T., and Vilo, J. (2011). g:Profiler--a web server for functional interpretation of gene lists (2011 update). Nucleic Acids Res. *39*, W307-315.

Reimand, J., Kull, M., Peterson, H., Hansen, J., and Vilo, J. (2007). g:Profiler--a web-based toolset for functional profiling of gene lists from large-scale experiments. Nucleic Acids Res. *35*, W193-200.

Ritchie, M.E., Phipson, B., Wu, D., Hu, Y., Law, C.W., Shi, W., and Smyth, G.K. (2015). limma powers differential expression analyses for RNA-sequencing and microarray studies. Nucleic Acids Res. *43*, e47.

Robinson, M.D., McCarthy, D.J., and Smyth, G.K. (2010). edgeR: a Bioconductor package for differential expression analysis of digital gene expression data. Bioinformatics *26*, 139-140.

Rossi, D.J., Bryder, D., Seita, J., Nussenzweig, A., Hoeijmakers, J., and Weissman, I.L. (2007). Deficiencies in DNA damage repair limit the function of haematopoietic stem cells with age. Nature *447*, 725-729.

Sahin, E., and Depinho, R.A. (2010). Linking functional decline of telomeres, mitochondria and stem cells during ageing. Nature *464*, 520-528.

Schepers, K., Campbell, T.B., and Passegue, E. (2015). Normal and leukemic stem cell niches: insights and therapeutic opportunities. Cell Stem Cell *16*, 254-267.

Schepers, K., Pietras, E.M., Reynaud, D., Flach, J., Binnewies, M., Garg, T., Wagers, A.J., Hsiao, E.C., and Passegué, E. (2013). Myeloproliferative neoplasia remodels the endosteal bone marrow niche into a self-reinforcing leukemic niche. Cell Stem Cell *13*, 285-299.

Schneider, R.K., Schenone, M., Ferreira, M.V., Kramann, R., Joyce, C.E., Hartigan, C., Beier, F., Brümmendorf, T.H., Germing, U., Platzbecker, U. *et al.* (2016). Rps14 haploinsufficiency causes a block in erythroid differentiation mediated by S100A8 and S100A9. Nat. Med. *22*, 288-297.

Srikrishna, G., and Freeze, H.H. (2009). Endogenous damage-associated molecular pattern molecules at the crossroads of inflammation and cancer. Neoplasia *11*, 615-628.

Stowe, D.F., and Camara, A.K.S. (2009). Mitochondrial Reactive Oxygen Species Production in Excitable Cells: Modulators of Mitochondrial and Cell Function. Antioxid. Redox Signal. *11*, 1373-1414.

Subramanian, A., Tamayo, P., Mootha, V.K., Mukherjee, S., Ebert, B.L., Gillette, M.A., Paulovich, A., Pomeroy, S.L., Golub, T.R., Lander, E.S., *et al.* (2005). Gene set enrichment analysis: a knowledge-based approach for interpreting genome-wide expression profiles. Proc. Natl. Acad. Sci. USA *102*, 15545-15550.

Toiviainen-Salo, S., Mayranpaa, M.K., Durie, P.R., Richards, N., Grynpas, M., Ellis, L., Ikegawa, S., Cole, W.G., Rommens, J., Marttinen, E., *et al.* (2007). Shwachman-Diamond syndrome is associated with low-turnover osteoporosis. Bone *41*, 965-972.

Tormin, A., Li, O., Brune, J.C., Walsh, S., Schutz, B., Ehinger, M., Ditzel, N., Kassem, M., and Scheding, S. (2011). CD146 expression on primary nonhematopoietic bone marrow stem cells is correlated with in situ localization. Blood *117*, 5067-5077.

Starczynowski, D.T., Kuchenbauer, F., Argiropoulos, B., Sung, S., Morin, R., Muranyi, A., Hirst, M., Hogge, D., Marra, M., Wells, R.A., *et al*. (2010). Identification of miR-145 and miR-146a as mediators of the 5q- syndrome phenotype. Nat. Med. *16*, 49-58.

Trapnell, C., Williams, B.A., Pertea, G., Mortazavi, A., Kwan, G., van Baren, M.J., Salzberg, S.L., Wold, B.J., and Pachter, L. (2010). Transcript assembly and quantification by RNA-Seq reveals unannotated transcripts and isoform switching during cell differentiation. Nat. Biotechnol. *28*, 511-515.

Tudpor, K., van der Eerden, B.C., Jongwattanapisan, P., Roelofs, J.J., van Leeuwen, J.P., Bindels, R.J., and Hoenderop, J.G. (2015). Thrombin receptor deficiency leads to a high bone mass phenotype by decreasing the RANKL/OPG ratio. Bone *72*, 14-22.

Vlachos, A., Rosenberg, P.S., Atsidaftos, E., Alter, B.P., and Lipton, J.M. (2012). Incidence of neoplasia in Diamond Blackfan anemia: a report from the Diamond Blackfan Anemia Registry. Blood *119*, 3815-3819.

Vogl, T., Eisenblätter, M., Völler, T., Zenker, S., Hermann, S., van Lent, P., Faust, A., Geyer, C., Petersen, B., Roebrock, K., *et al*. (2014). Alarmin S100A8/S100A9 as a biomarker for molecular imaging of local inflammatory activity. Nat. Commun. *6*,4593.

Vogl, T., Tenbrock, K., Ludwig, S., Leukert, N., Ehrhardt, C., van Zoelen, M.A., Nacken, W., Foell, D., van der Poll, T., Sorg, C., *et al.* (2007). Mrp8 and Mrp14 are endogenous activators of Toll-like receptor 4, promoting lethal, endotoxin-induced shock. Nat. Med. *13*, 1042-1049.

Walkley, C.R., Olsen, G.H., Dworkin, S., Fabb, S.A., Swann, J., McArthur, G.A., Westmoreland, S.V., Chambon, P., Scadden, D.T., and Purton, L.E. (2007). A microenvironment-induced myeloproliferative syndrome caused by retinoic acid receptor gamma deficiency. Cell *129*, 1097-1110.

Walter, D., Lier, A., Geiselhart, A., Thalheimer, F.B., Huntscha, S., Sobotta, M.C., Moehrle, B., Brocks, D., Bayindir, I., Kaschutnig, P., *et al.* (2015). Exit from dormancy provokes DNA-damage-induced attrition in haematopoietic stem cells. Nature *520*, 549-552.

Wang, X., Kua, H.Y., Hu, Y., Guo, K., Zeng, Q., Wu, Q., Ng, H.H., Karsenty, G., de Crombrugghe, D., Yeh, J., *et al.* (2006). p53 functions as a negative regulator of osteoblastogenesis, osteoblast-dependent osteoclastogenesis, and bone remodeling. J. Cell. Biol. *172*, 115-125.

Wei, Y., Dimicoli, S., Bueso-Ramos, C., Chen, R., Yang, H., Neuberg, D., Pierce, S., Jia, Y., Zheng, H., Wang, H., *et al.* (2013). Toll-like receptor alterations in myelodysplastic syndrome. Leukemia *27*, 1832-1840.

Woloszynek, J.R., Rothbaum, R.J., Rawls, A.S., Minx, P.J., Wilson, R.K., Mason, P.J., Bessler, M., and Link, D.C. (2004). Mutations of the SBDS gene are present in most patients with Shwachman-Diamond syndrome. Blood *104*, 3588-3590.

Xiao, Y., Wang, J., Song, H., Zou, P., Zhou, D., and Liu, L. (2013). CD34+ cells from patients with myelodysplastic syndrome present different p21 dependent premature senescence. Leuk. Res. *37*, 333-340.

Yahata, T., Takanashi, T., Muguruma, Y., Ibrahim, A.A., Matsuzawa, H., Uno, T., Sheng, Y., Onizuka, M., Ito, M., Kato, S., *et al.* (2011). Accumulation of oxidative DNA damage restricts the self-renewal capacity of human hematopoietic stem cells. Blood *118*, 2941-2950.

Zambetti, N.A., Bindels, E.M., Van Strien, P.M., Valkhof, M.G., Adisty, M.N., Hoogenboezem, R.M., Sanders, M.A., Rommens, J.M., Touw, I.P., and Raaijmakers, M.H. (2015). Deficiency of the ribosome biogenesis gene Sbds in hematopoietic stem and progenitor cells causes neutropenia in mice by attenuating lineage progression in myelocytes. Haematologica *100*, 1285-1293.

## FIGURE LEGENDS

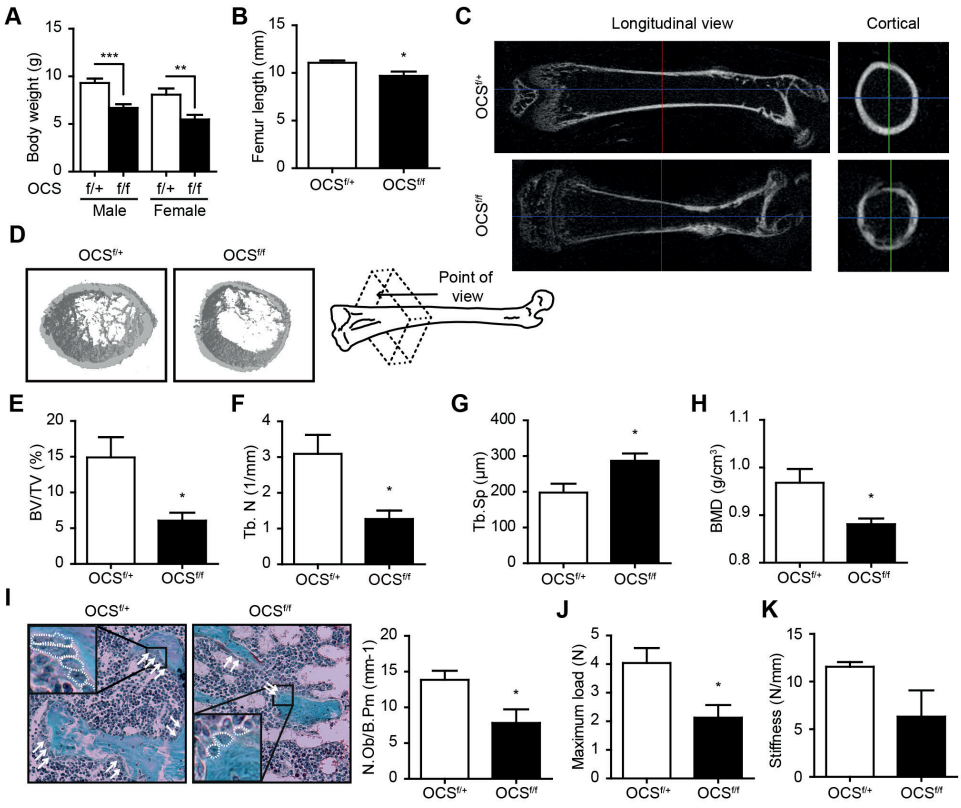


**Figure 1. Deletion of *Sbds* in MPCs recapitulates skeletal defects in human SDS.** (A-B) Impaired growth in $OCS^{f/f}$ mice: (A) body weight ($n$ = 9) and (B) femur length ($n$ = 5). (C-H) Femur µCT analysis of $OCS^{f/+}$ ($n$ = 5) and $OCS^{f/f}$ ($n$ = 4) mice. (C) Representative 2D-images. Left: longitudinal view. Right: cortical bone. (D) 3D-image. (E) Bone volume per tissue volume (BV/TV). (F) Trabecular number (Tb. N). (G) Trabecular spacing (Tb. Sp). (H) Cortical bone mineral density (BMD). (I) Goldner osteoblast staining ($OCS^{f/+}$, $n$ = 6; $OCS^{f/f}$, $n$ = 8). Left: representative images (arrows: osteoblasts; with white dashed line in the magnified region). Right: number of osteoblasts per bone perimeter (N.Ob/B.Pm). (J-K) 3-point bending test indicating (J) reduced resistant to fracture and (K) decreased stiffness of $OCS^{f/f}$ bone ($OCS^{f/+}$, $n$ = 5; $OCS^{f/f}$, $n$ = 4). *$P$<0.05. **$P$< 0.01. ***$P$<0.001. Data are mean ± SEM. See also Figure S1.

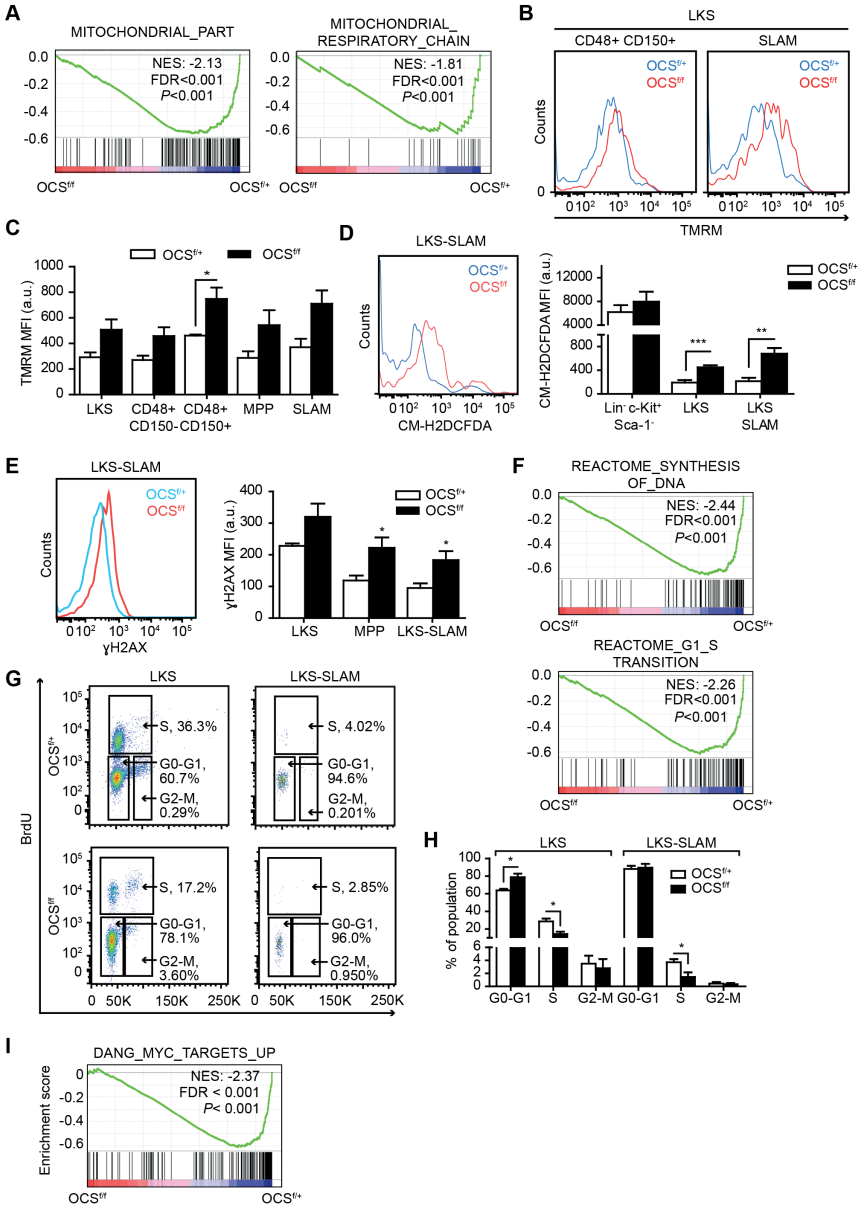


**Figure 2. *Sbds*-deficient mesenchymal cells induce genotoxic stress in HSPCs.** (A) Transcriptional network analysis indicating mitochondrial dysregulation in mutant HSPCs. NES: Normalized Enrichment Score. (B-C) Increased mitochondrial potential (TMRM) in HSPCs: (B) representative plots; (C) mean fluorescence intensity (MFI) ($n$ = 3). (D) ROS quantification by CM-H2DCFDA ($OCS^{f/+}$, $n$ = 6; $OCS^{f/f}$, $n$ = 7). (E) Increased γH2AX levels in mutant HSPCs. Left, representative FACS analysis. Right, MFI values ($n$ = 4). (F-I) Activation of DNA damage response in mutant HSPCs. (F) Transcriptional repression of G1-S checkpoint progression. (G, H) *In vivo* BrdU staining confirming impaired S-phase transition ($n$ = 4). (I) Downregulation of Myc signaling. GSEA data shown is from $CD48^-$ LKS cells. a.u., arbitrary units. †††FDR<0.001. *$P$<0.05. **$P$<0.01. ***$P$<0.001. Data in bar graphs are mean± SEM. See also Figure S2, S3, S6 and Table S1-S3.

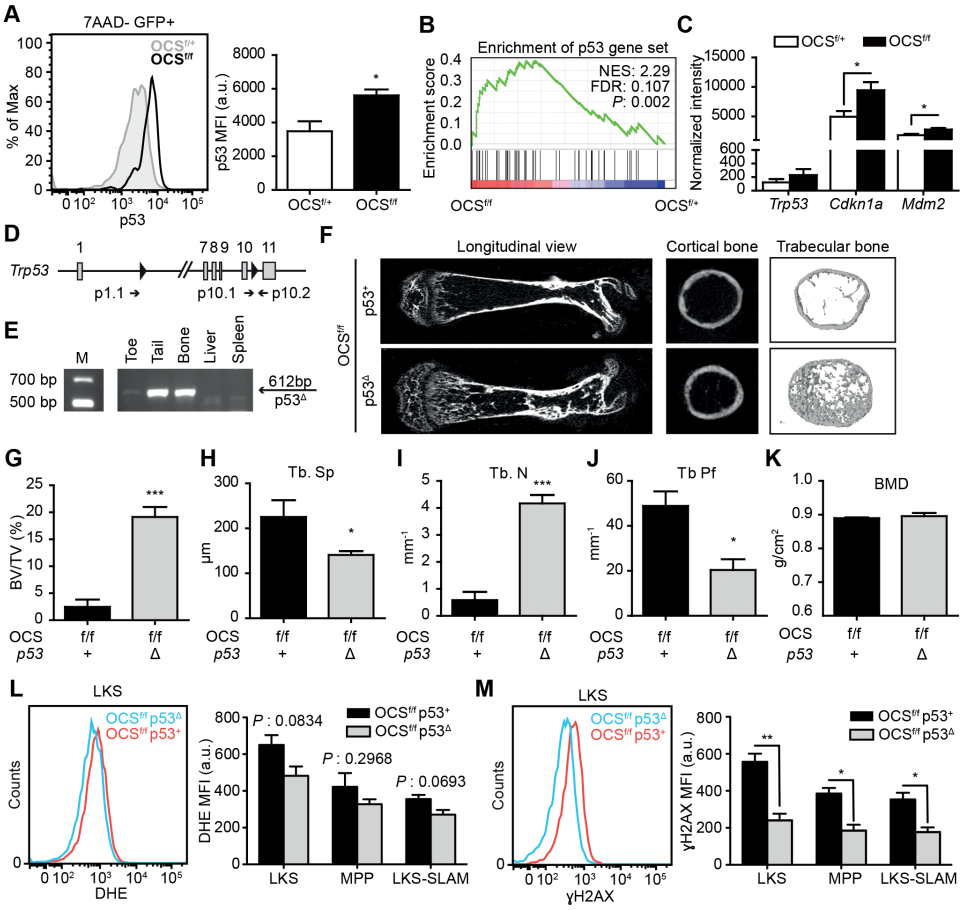


**Figure 3. Activation of p53 in MPCs drives skeletal and hematopoietic abnormalities in OCS mutants.** (A) p53 protein (FACS) accumulates in GFP⁺ cells from OCS$^{f/f}$ mice ($n$ = 3). (B-C) Activation of p53 in mutant GFP⁺ cells as demonstrated by (B) enrichment of a p53 GSEA signature and (C) overexpression of canonical p53 targets ($n$ = 3). (D) Schematic representation of the p53 floxed allele with indication of primers used to assess genotypes (p10.1-p10.2) and genomic deletion (p1.1-p10.2). (E) Specific deletion of p53 in bone-containing tissue in OCS$^{f/f}$ p53$^{\Delta}$ mice (genomic PCR). (F-J) Non-compiled µCT images indicating normalization of bone mass in OCS$^{f/f}$ mice upon genetic deletion of p53 (p53$^{+}$, $n$ = 3; p53$^{\Delta}$, $n$ = 5). Tb. Pf , Trabecular bone pattern factor. (K) Bone imineral density in OCS$^{f/f}$ mice is not rescued by p53 deletion. (L-M) Effects of p53 deficiency on OCS HSPCs. Tendency for reduced oxidative stress as assessed by DHE analysis (L) and significant reduction of γH2AX levels (M) in HSPCs from OCS$^{f/f}$ p53$^{\Delta}$ mice ($n$ = 3). MFI: mean fluorescence intensity. a.u., arbitrary units. *$P$ < 0.05. **$P$ <0.01. ***$P$ <0.001. Data are mean ± SEM. See also Figure S4.

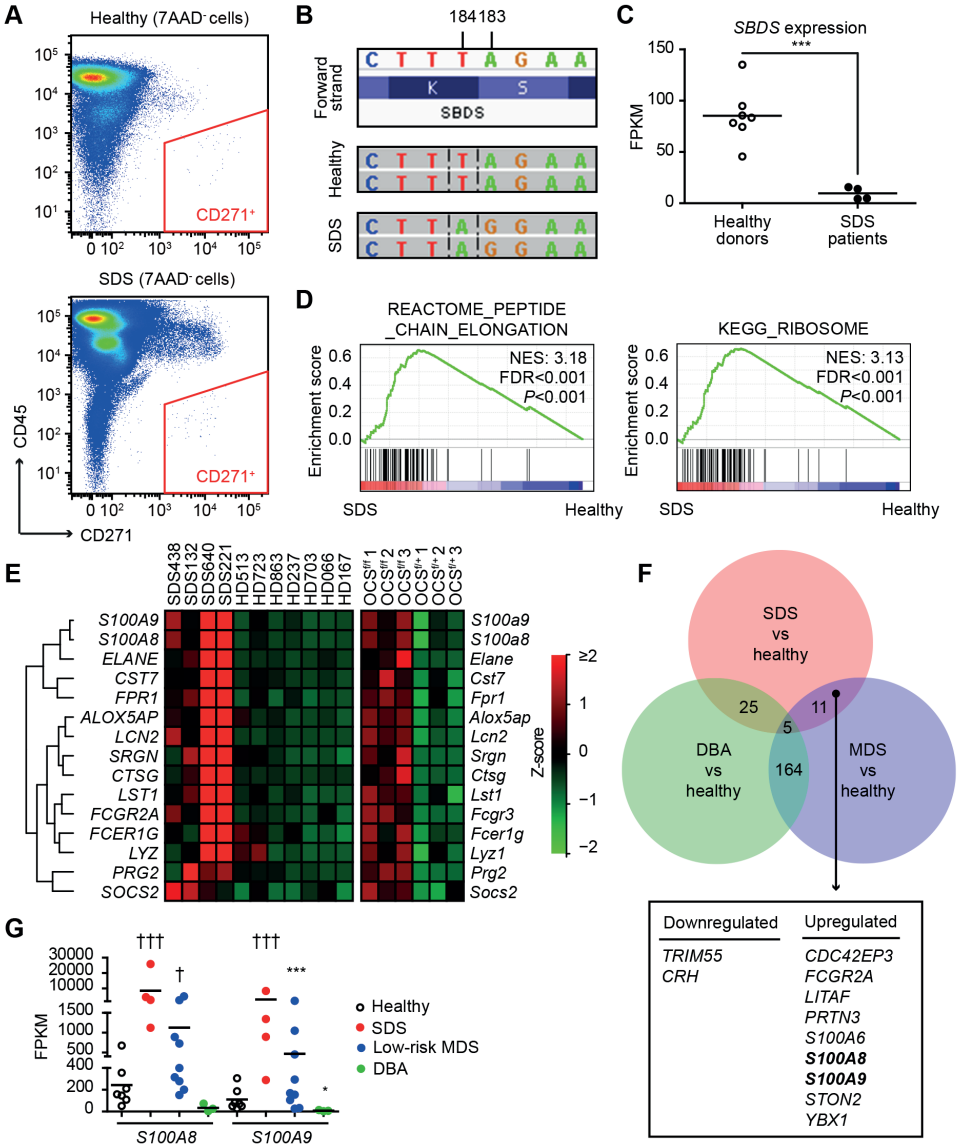


**Figure 4. Identification of *S100A8* and *S100A9* as candidate drivers of genotoxic stress in leukemia predisposition syndromes.** (A) Representative mesenchymal CD271$^+$ FACS gating. (B) Pathognomonic 183-184 TA>CT mutation in niche cells from a representative SDS patient (IGV plot). (C) Reduced *SBDS* expression in SDS niche cells. (D) Disruption of ribosome biogenesis and translation in SDS CD271$^+$ cells (GSEA). (E) Inflammation-related transcripts are upregulated in niche cells from SDS patients and OCS$^{f/f}$ mice. (F) Significantly differentially expressed genes in SDS ($n$ = 4), MDS ($n$ = 9) and DBA ($n$ = 3) in comparison to normal CD271$^+$ cells. (G) Expression of *S100A8* and *S100A9* in mesenchymal cells from SDS, low-risk MDS, and DBA patients. *$P$<0.05. ***$P$<0.001. $^{\dagger\dagger\dagger}$FDR-adjusted $P$<0.001. See also Figure S1, S5 and Table S4.

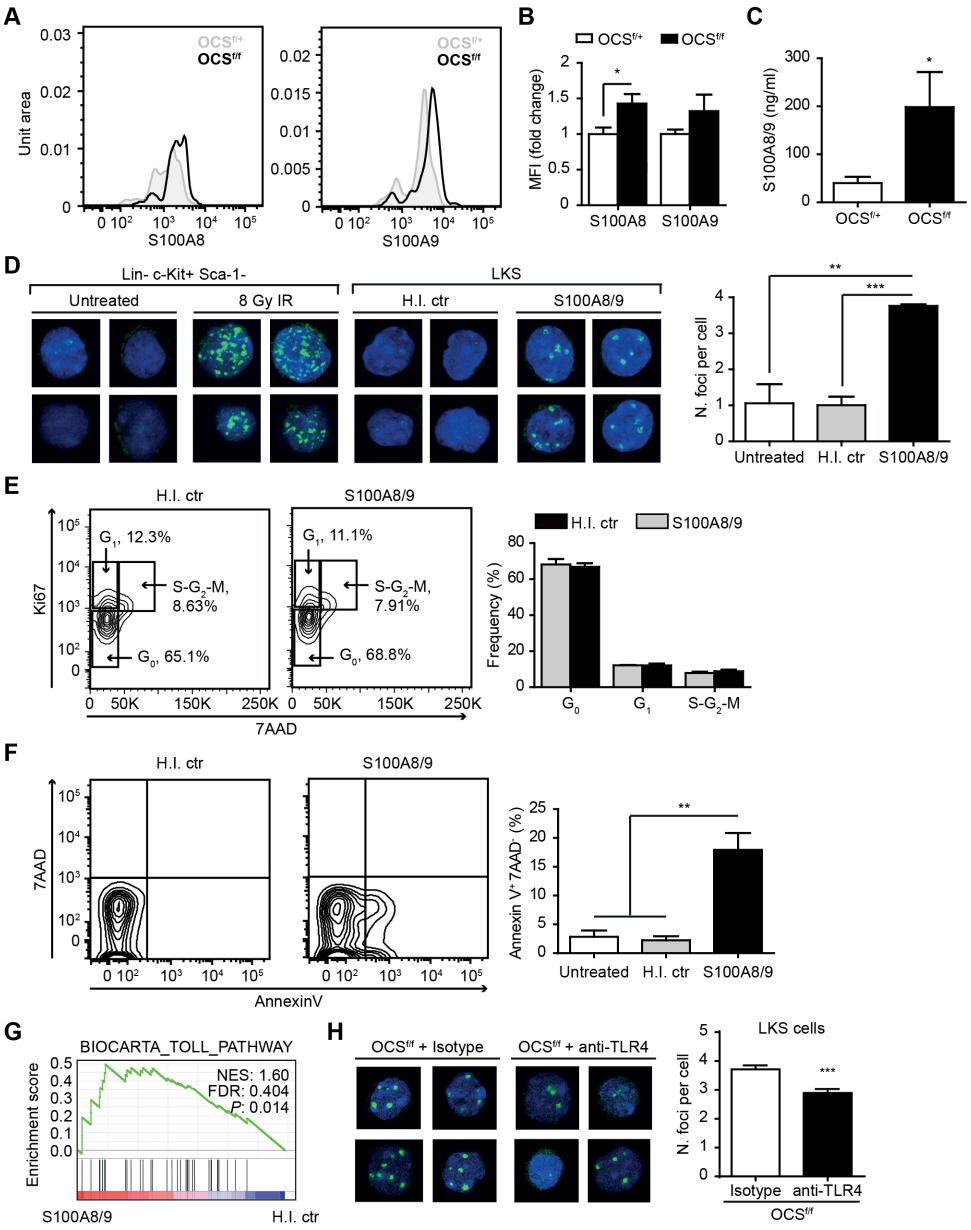


**Figure 5. S100A8/9 induces genotoxic stress in murine HSPCs through TLR4 signaling.** (A-B) Increased S100A8 and S100A9 levels in OCS$^{f/f}$ GFP$^{+}$ cells. (A) representative plots. (B) MFI values ($n$ = 5). (C) Increased plasma concentration of S100A8/9 by ELISA (OCS$^{f/+}$, $n$ = 5; OCS$^{f/f}$, $n$ = 4). (D) Left: representative γH2AX pictures after HSPCs in vitro exposure. Positive control: 8-Gγ irradiated Lin$^{-}$ c-Kit$^{+}$ Sca-1$^{-}$ cells. Negative controls: heat-inactivated S100A8/9 (H.I. ctr). Right: number of γH2AX foci ($n$ = 3). (E) S100A8/9 has no effect on cell cycle ($n$ = 2). (F) Increased apoptosis in S100A8/9-exposed LKS ($n$ = 3). (G) Activation of TLR signaling (GSEA). (H) TLR4-blocking antibodies limit DNA damage in OCS$^{f/f}$ mice ($n$ = 4). *$P$<0.05. *$P$<0.01. ***$P$<0.001. Data are mean ± SEM. See also Figure S6 and S7; Table S5.

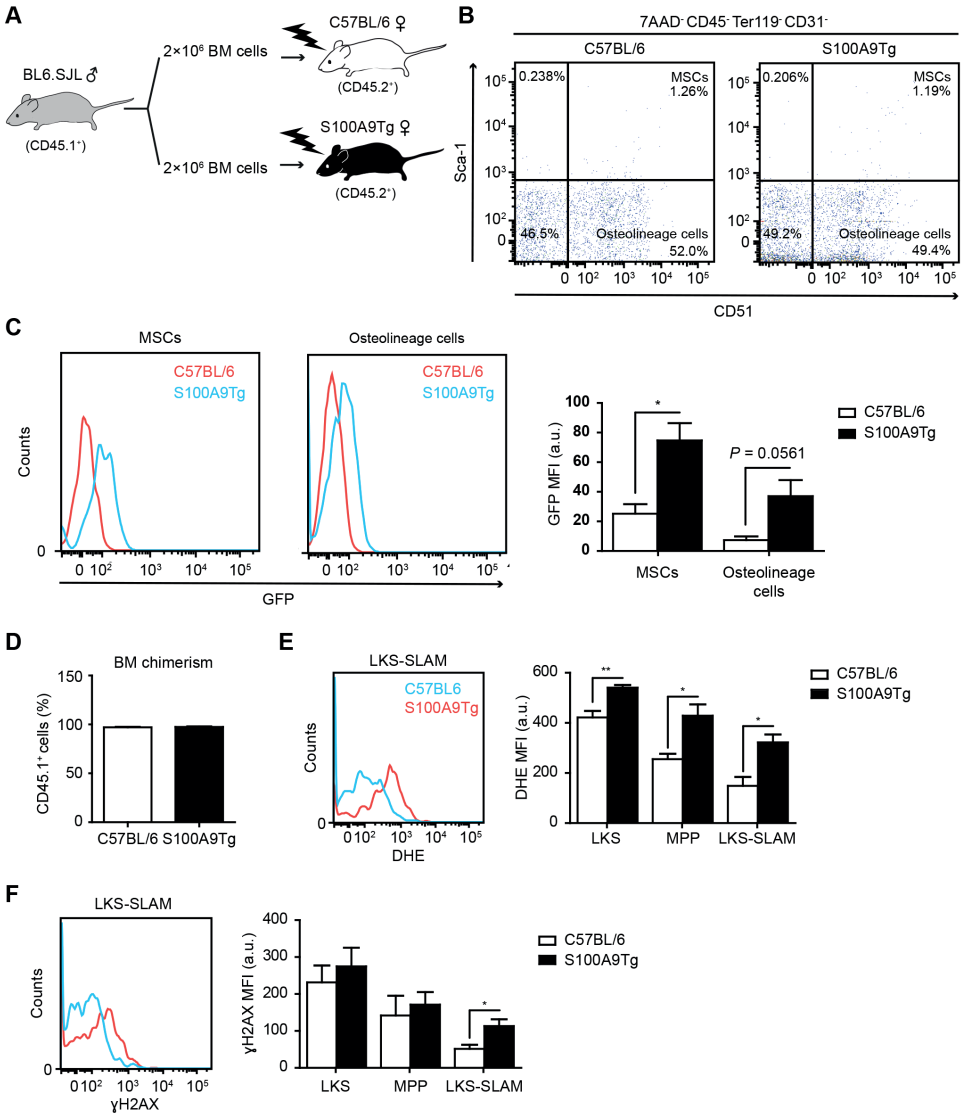


**Figure 6. Niche derived S100A8/9 induces oxidative and genotoxic stress in HSPCs.** (A) Schematic representation of wild type HSPCs transplantation in S100A9Tg mice. BM: bone marrow. (B-C) Mesenchymal cells from S100A9Tg mice express the S100A9-IRES-GFP construct. (B) Gating strategy defining CD51$^+$ Sca-1$^+$ mesenchymal 'stem' cells (MSC) and CD51$^+$ Sca-1$^-$ osteolineage cells in the microenvironment (C) Expression of GFP in S100A9Tg-derived mesenchymal compartments ($n$ = 3). (D) Transplantation efficiency as assessed by CD45.1$^+$ cell chimerism in the bone marrow (BM) of transplanted mice ($n$ = 4). (E) Accumulation of superoxide radicals in HSPCs exposed to S100A8/9-overexpressing microenvironment. Left, representative plot. Right, DHE MFI values ($n$ = 4). (F) Increased levels of γH2AX in immunophenotypically-defined HSCs. Left, representative plot. Right, DHE MFI values ($n$ = 4). *$P$<0.05. **$P$<0.01. Data are mean ± SEM.

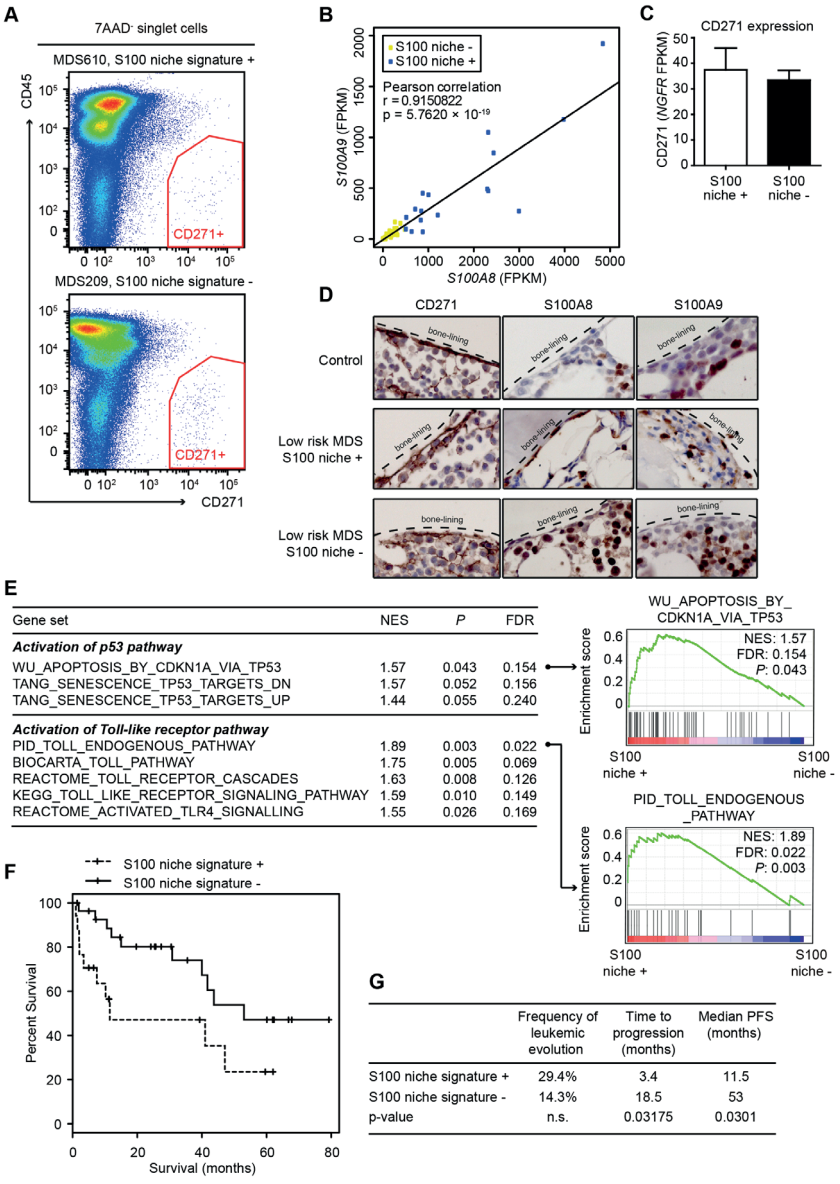


**Figure 7. Activation of the p53-S100A8/9-TLR axis in mesenchymal niche cells predicts leukemic evolution and clinical outcome in human low-risk MDS.** (A) Representative examples of FACS-isolated CD271$^+$ niche cells in human MDS. (B) Correlation plot of *S100A8* and *S100A9* expression levels in human low-risk MDS ($n$ = 45). (C) Expression of the defining gene *NGFR* (CD271) in mesenchymal cells (S100 niche +, $n$ = 17; S100 niche -, $n$ = 28). (D) Representative staining of S100A8 and S100A9 in endosteal (CD271$^+$) stromal cells. Intramedullary staining reflects expression of S100A8/9 in myeloid cells. (E) GSEA analysis indicating enrichment of p53 and TLR signatures in S100A8/9-overexpressing CD271$^+$ cells. Two representative GSEA plots are shown. NES: Normalized Enrichment Score. (F) Kaplan-Meier survival curve showing progression-free survival (G). Statistical analysis indicating significantly reduced time to progression and progression-free survival (PFS). Data are mean ± SEM. See also Table S6.

## SUPPLEMENTAL DATA ITEMS

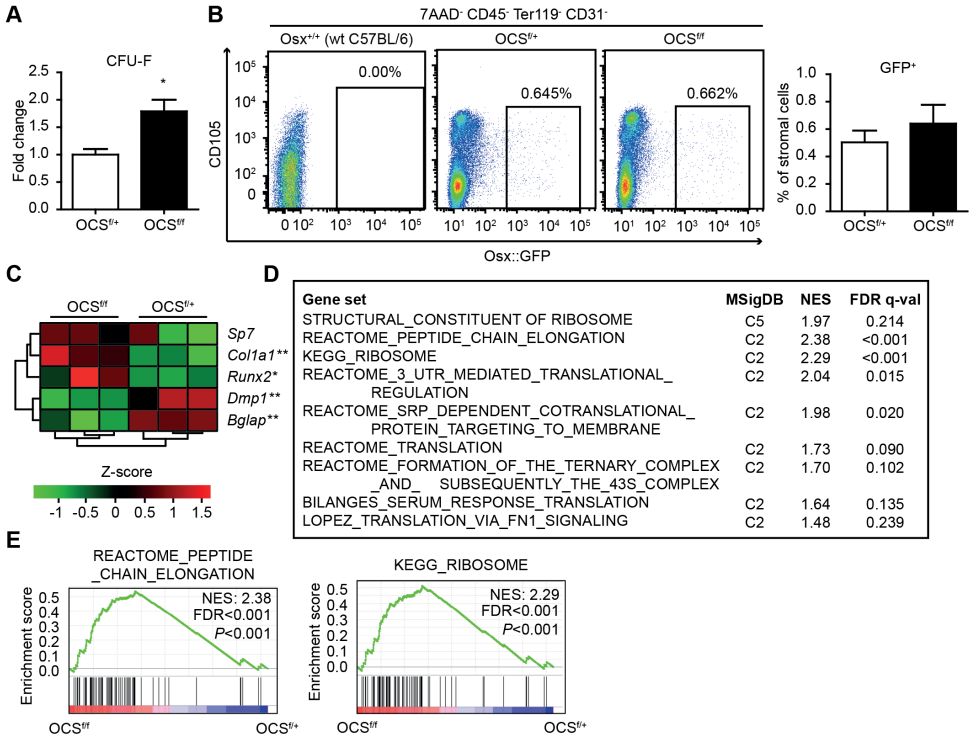


| Gene set | MSigDB | NES | FDR q-val |
|---|---|---|---|
| STRUCTURAL_CONSTITUENT OF RIBOSOME | C5 | 1.97 | 0.214 |
| REACTOME_PEPTIDE_CHAIN_ELONGATION | C2 | 2.38 | <0.001 |
| KEGG_RIBOSOME | C2 | 2.29 | <0.001 |
| REACTOME_3_UTR_MEDIATED_TRANSLATIONAL_REGULATION | C2 | 2.04 | 0.015 |
| REACTOME_SRP_DEPENDENT_COTRANSLATIONAL_PROTEIN_TARGETING_TO_MEMBRANE | C2 | 1.98 | 0.020 |
| REACTOME_TRANSLATION | C2 | 1.73 | 0.090 |
| REACTOME_FORMATION_OF_THE_TERNARY_COMPLEX_AND_SUBSEQUENTLY_THE_43S_COMPLEX | C2 | 1.70 | 0.102 |
| BILANGES_SERUM_RESPONSE_TRANSLATION | C2 | 1.64 | 0.135 |
| LOPEZ_TRANSLATION_VIA_FN1_SIGNALING | C2 | 1.48 | 0.239 |

**Figure S1. Related to Figure 1; Figure 4. Impairment of terminal osteogenic differentiation in OCS$^{f/f}$ mice.** (A) Increased CFU-F numbers ($n$ = 3) with (B) unaltered frequency of Osx::GFP$^+$ cells ($n$ = 4) in OCS$^{f/f}$ mice. (C) Depletion of transcripts defining terminal osteogenic differentiation (osteocalcin, *Bglap*) and dentin matrix acidic phosphoprotein 1 (*Dmp1*), critical for proper mineralization of bone, and enrichment of markers of bone progenitor cells or early osteoblasts (*Runx2* and *Col1a1*) in GFP$^+$ cells from OCS$^{f/f}$ mice. No statistically significant difference was observed in the expression of osterix (*Sp7*). (D) Significant (FDR<0.25) enrichment of ribosome and peptide chain elongation signatures in OCS$^{f/f}$ GFP$^+$ cells (GSEA) with (E) representative plots. *$P$<0.05. **$P$<0.01. Data are mean ± SEM.

**Figure S2. Related to Figure 2. Oxidative and genotoxic stress in HSPCs from OCS$^{f/f}$ mice.** (A-C) unaltered HSPC numbers in OCS$^{f/f}$ mice: (A) representative FACS plots, (B) bone marrow cellularity and (C) subset frequency (OCS$^{f/+}$, $n$ = 8 in A-B, $n$ = 7 in C; OCS$^{f/f}$, $n$ = 7). LK: Lin- c-Kit$^+$ Sca-1- cells. LKS: Lin- c-Kit$^+$ Sca-1$^+$ cells. MPP: multipotent progenitors, CD48$^-$ CD150- LKS cells. SLAM: CD48$^-$ CD150$^+$ LKS cells. (D) FACS isolation of CD48$^+$ and CD48$^-$ HSPC subsets for RNA-seq (OCS$^{f/+}$ CD48$^-$, $n$ = 3; other groups, $n$ = 4). (E) RNA-seq validation confirming CD48 and *Ptprc* (CD45) expression and the *Sbds*-proficient status of HSPCs from mutant mice. (F) Principal component analysis indicating global preservation of the transcriptome in HSPCs from OCS$^{f/f}$ mice. (G) Superoxide radical accumulation in HSPCs from OCS$^{f/f}$ mice as shown by DHE staining. (H) Increased number of γH2AX foci in HSPCs from mutants ($n$= 2; pooled data). (I-J) NAC treatment attenuates oxidative (I) and (non-significantly) genotoxic stress (J) of OCS$^{f/f}$ mice. NAC- controls were either treated with saline or not injected. (OCS$^{f/+}$ + NAC, $n$ = 3; OCS$^{f/f}$ + NAC, $n$ = 3;, $n$ = 4; other groups, $n$ = 5). (K) Ki67 analysis of OCS mice indicating no change in the frequency of G0 HSPCs (OCS$^{f/+}$, $n$ = 3; OCS$^{f/f}$, $n$ = 4). *$P$<0.05. **$P$<0.01. ***$P$<0.001. †††FDR-adjusted $P$<0.001. Data are mean ± SEM.

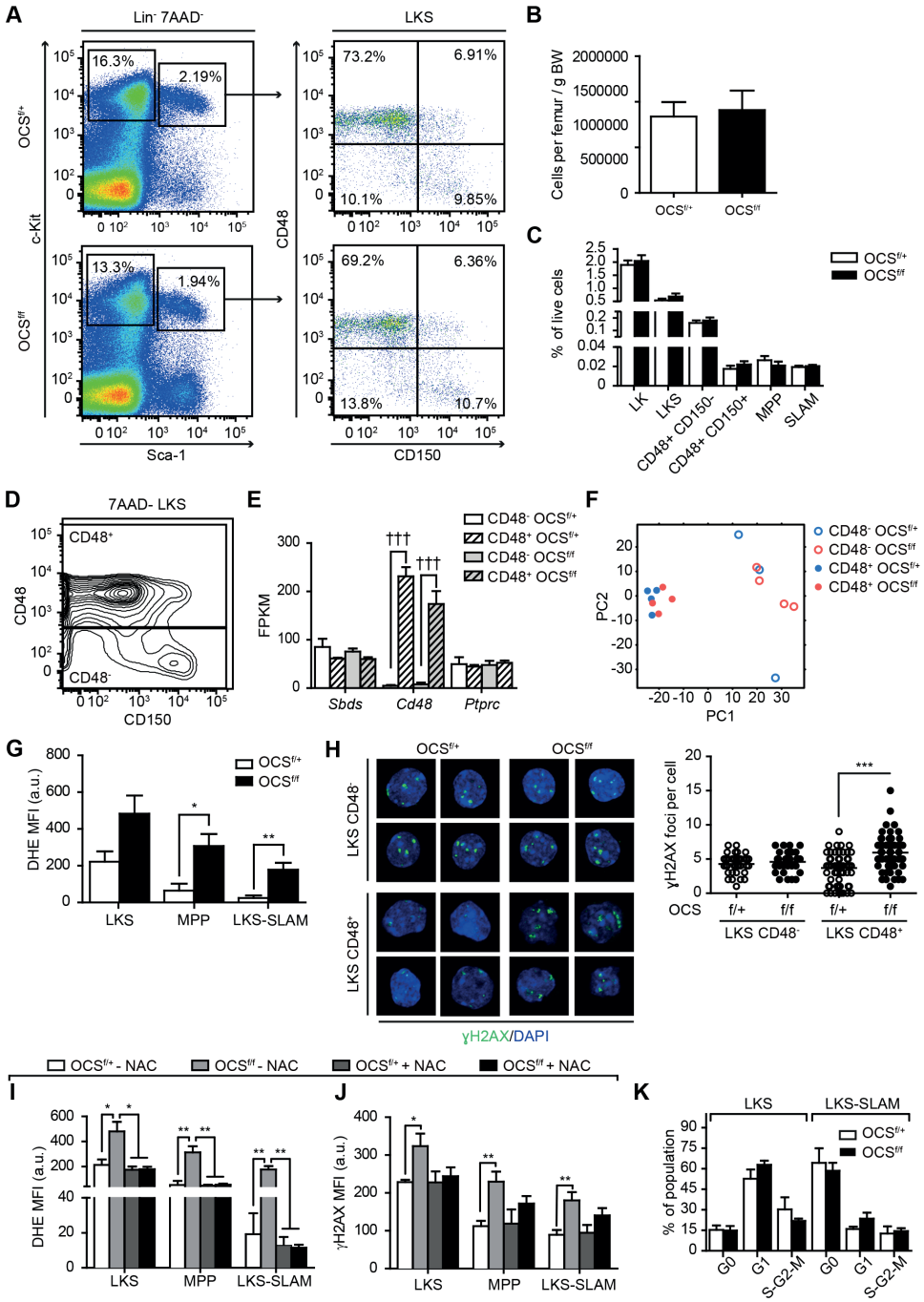
A
Lin- 7AAD-
LKS
16.3%
2.19%
73.2%
6.91%
10.1%
9.85%
13.3%
1.94%
69.2%
6.36%
13.8%
10.7%
OCSf/+
OCSf/f
c-Kit
CD48
Sca-1
CD150
B
Cells per femur / g BW
2000000
1500000
1000000
500000
0
OCSf/+
OCSf/f
C
% of live cels
OCSf/+
OCSf/f
LK
LKS
CD48+ CD150-
CD48+ CD150+
MPP
SLAM
D
7AAD- LKS
CD48+
CD48-
CD48
CD150
E
FPKM
CD48- OCSf/+
CD48+ OCSf/+
CD48- OCSf/f
CD48+ OCSf/f
Sbds
Cd48
Ptprc
F
PC2
PC1
CD48- OCSf/+
CD48- OCSf/f
CD48+ OCSf/+
CD48+ OCSf/f
G
DHE MFI (a.u.)
OCSf/+
OCSf/f
LKS
MPP
LKS-SLAM
H
OCSf/+
OCSf/f
LKS CD48-
LKS CD48+
γH2AX/DAPI
γH2AX foci per cell
OCS
f/+
f/f
LKS CD48-
LKS CD48+
OCSf/+ - NAC
OCSf/f - NAC
OCSf/+ + NAC
OCSf/f + NAC
I
DHE MFI (a.u.)
LKS
MPP
LKS-SLAM
J
γH2AX MFI (a.u.)
LKS
MPP
LKS-SLAM
K
LKS
LKS-SLAM
OCSf/+
OCSf/f
% of population
G0
G1
S-G2-M

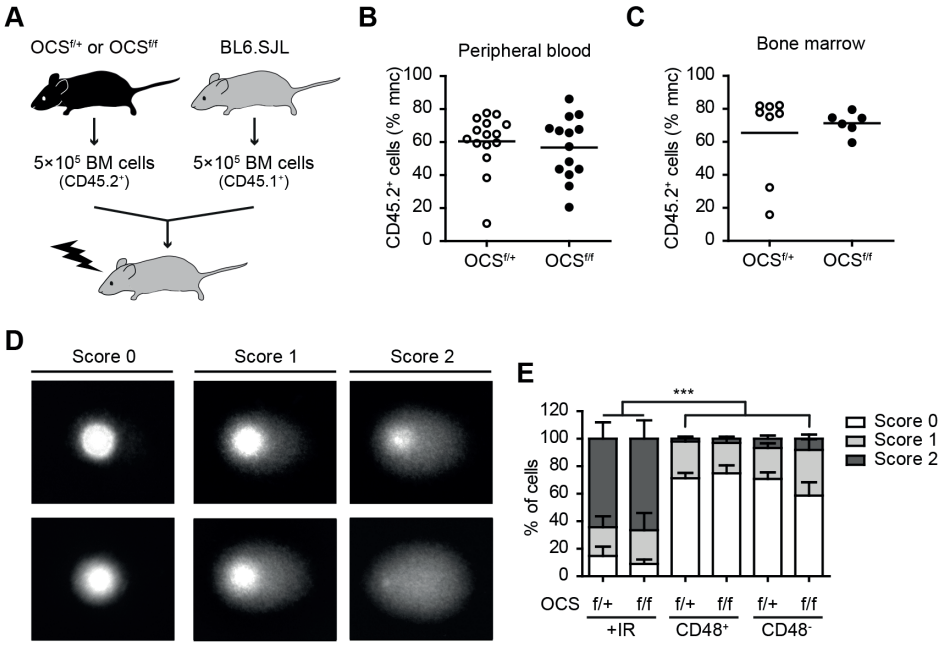


**Figure S3. Related to Figure 2. Niche-induced DNA damage does not affect HSPC function.** (A) Schematic representation of the competitive transplantation. BM: bone marrow. (B) Peripheral blood frequency of CD45.2$^+$ cells 16 weeks after transplantation. (C) Bone marrow frequency of CD45.2$^+$ cells (21-32 weeks after transplantation). Every circle represents one recipient mouse. (D) Manual scoring system applied to comet assay analysis. (E) Comet assay showing similar frequency of highly damaged HSPCs in OCS$^{f/+}$ and OCS$^{f/f}$ mice ($n$ = 5). +IR: 8-10 Gy irradiated positive control (LK cells). ***$P$<0.001. Data are mean ± SEM.

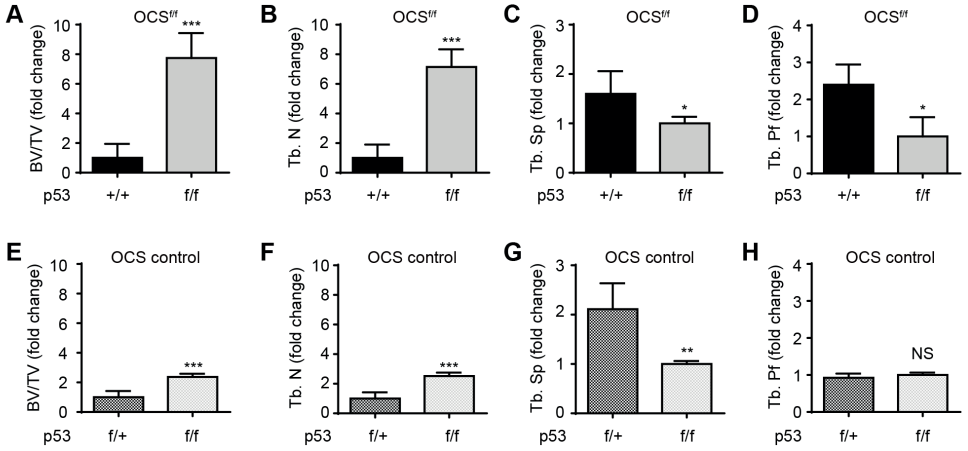


**Figure S4. Related to Figure 3. Bone effects of *Trp53* ablation in OCS mutant and control mice.** (A-D) Normalization of µCT parameters in OCS$^{f/f}$ p53$^{\Delta}$ mice shown as fold change (p53$^{+}$, *n* = 3; p53$^{\Delta}$, *n* = 5). (E-F) Modest increase in bone mass upon genetic deletion of p53 in OCS control mice, defined as *Osx*$^{cre/+}$ *Sbds*$^{f/+}$ or *Osx*$^{cre/+}$ *Sbds*$^{+/+}$ (p53$^{f/+}$, *n* = 8; p53$^{f/f}$, *n* = 3). **P*<0.05. ***P*<0.01. ****P*<0.001. Data are mean ± SEM.

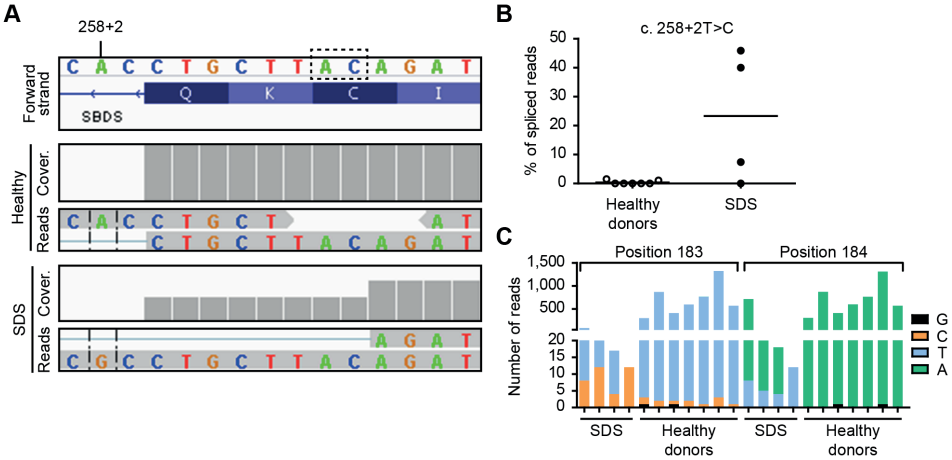


**Figure S5. Related to Figure 4. *SBDS* mutations in mesenchymal cells from SDS patients.** (A-B) Detection of 258+2 T>C mutation in SDS patients. (A) Representative IGV plot. Note that the coverage level after the cryptic site (dashed box) is reduced in SDS, indicating an 8-bp deletion. (B) Quantification of 258+2 T>C mutation as frequency of spliced reads with 8-bp deletion. Every circle represents a patient. (C) Nucleotide sequence in positions 183-184 from SDS patients and healthy donors.

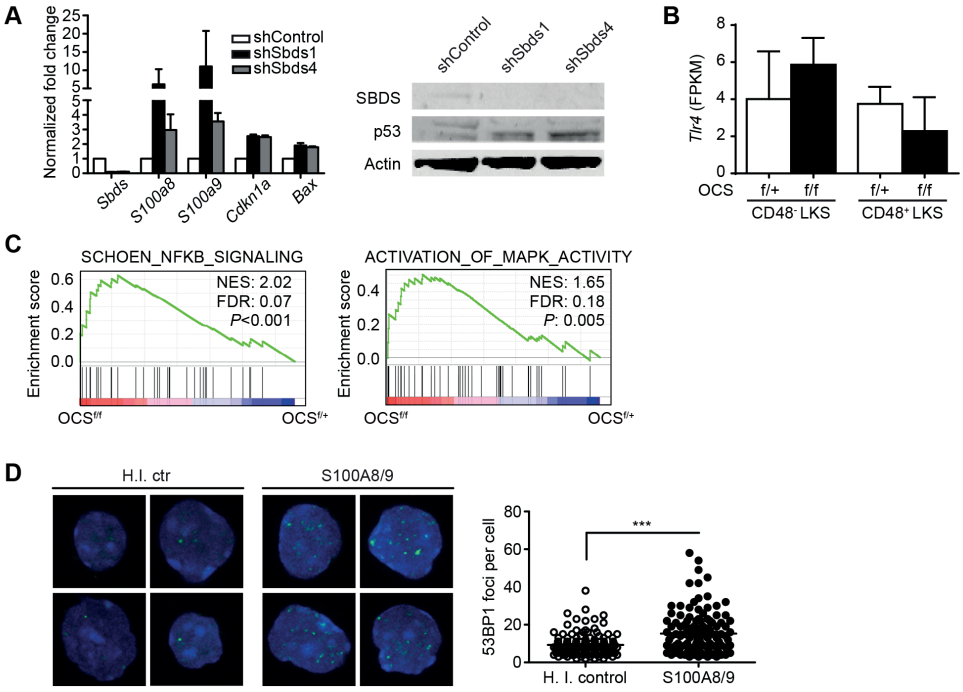


**Figure S6. Related to Figure 2; Figure 5. A p53-S100A8/9-TLR axis induces DNA damage in HSPCs.** (A) *Sbds*-knock down in OP9 cells induces expression of *S100a8*, *S100a9* and activation of p53 pathway. Left, expression analysis by qPCR (data normalized against shControl, $n$ = 3). Right, representative Western Blot analysis showing p53 accumulation upon *Sbds*-knock down. (B, C) TLR4 expression and activation of NF-κB and MAPK pathways in HSPCs from $OCS^{f/f}$ mice (GSEA). NES: normalized enrichment score. (D) *Ex-vivo* treatment with S100A8/9 induces 53BP1 foci of DNA damage in murine HSPCs (LKS cells), Left, representative images. Right, cumulative dot plots ($n$ = 2). ***$P$ <0.001. Data in bar graphs are mean ± SEM.

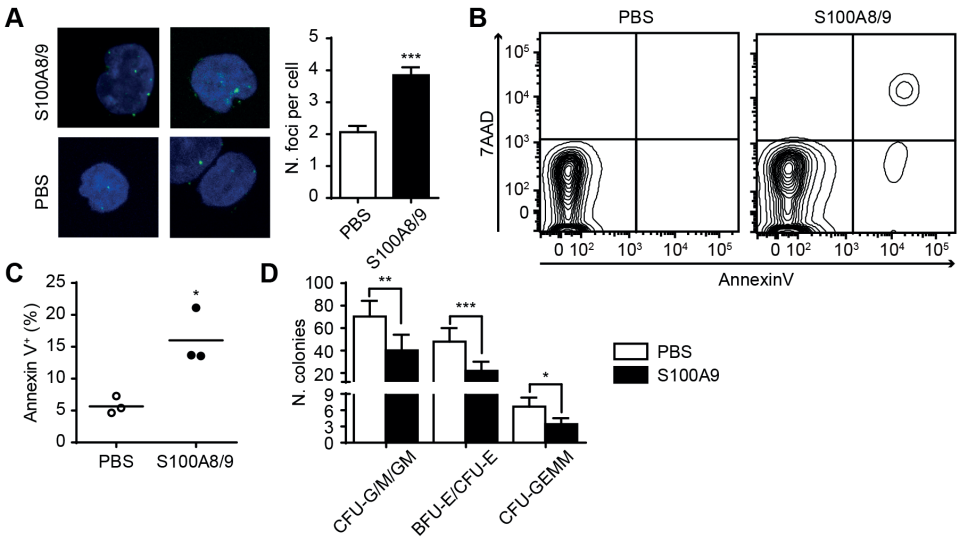


**Figure S7. Related to Figure 5. S100A8/9 drives genomic stress in human HSPCs.** (A-C) Treatment of human CD34$^+$ HSPCs with recombinant S100A8/9. (A) Induction of γH2AX foci ($n$ = 3). (B-C) Increased frequency of apoptotic cells. (B) Representative plot. (C) Quantification ($n$ = 3). (D) Reduced colony forming capacity of HSPCs as assessed by CFU-C assay ($n$ = 4 independent experiments in triplicate). Data are mean ± SEM. *$P$<0.05. **$P$<0.01. ***$P$<0.001.

T**able S1. Related to Figure 2. Transcriptional profiling of OCS-derived HSPCs reveals dysregulation of signatures previously identified as predictive for leukemia evolution. Provided as an Excel file.** Upregulation of G-protein-coupled receptors and cell adhesion-communication, and downregulation of mitochondrial oxidative phosphorylation, ribosome biogenesis, aminoacyl-tRNA synthetase activity, proteasomal degradation, citric acid cycle, cell cycle deregulation and hematopoietic stem cell programs. Normalized enrichment score (NES) and False Discovery Rate-adjusted q-value (FDR) are omitted when FDR > 0.25.

| Gene set | MSigDB collection | CD48- LKS | | CD48+ LKS | |
|---|---|---|---|---|---|
| | | NES | FDR | NES | FDR |
| Enriched in OCS mutants | | | | | |
| G-protein coupled receptors | | | | | |
| G_PROTEIN_COUPLED_RECEPTOR_PROTEIN_SIGNALING_PATHWAY | C5 | | | 1.63 | 0.180 |
| Cell adhesion-communication | | | | | |
| | | | | 1.84 | 0.170 |
| REACTOME_GAP_JUNCTION_ASSEMBLY | C2 | | | | |
| PID_INTEGRIN_CS_PATHWAY | C2 | | | 1.78 | 0.213 |
| SA_MMP_CYTOKINE_CONNECTION | C2 | | | 1.75 | 0.230 |
| KEGG_CELL_ADHESION_MOLECULES_CAMS | C2 | | | 1.70 | 0.236 |
| **Enriched in OCS controls** | | | | | |
| Mitochondria and oxidative phosphorylation | | | | | |
| MOOTHA_VOXPHOS | C2 | -2.49 | <0.001 | -1.93 | 0.001 |
| WONG_MITOCHONDRIA_GENE_MODULE | C2 | -2.46 | <0.001 | -2.19 | <0.001 |
| REACTOME_RESPIRATORY_ELECTRON_TRANSPORT_ATP_SYNTHESIS_BY_CHEMIOSMOTIC_COUPLING_AND_HEAT_PRODUCTION_BY_UNCOUPLING_PROTEINS_ | C2 | -2.44 | <0.001 | -2.02 | <0.001 |
| REACTOME_RESPIRATORY_ELECTRON_TRANSPORT | C2 | -2.43 | <0.001 | -1.91 | 0.002 |
| KEGG_OXIDATIVE_PHOSPHORYLATION | C2 | -2.37 | <0.001 | -1.75 | 0.012 |
| REACTOME_MITOCHONDRIAL_PROTEIN_IMPORT | C2 | -2.13 | <0.001 | -1.95 | 0.001 |
| MOOTHA_MITOCHONDRIA | C2 | -2.12 | <0.001 | -1.96 | 0.001 |
| HOUSTIS_ROS | C2 | -1.58 | 0.047 | -1.34 | 0.211 |
| REACTOME_RNA_POL_I_RNA_POL_III_AND_MITOCHONDRIAL_TRANSCRIPTION | C2 | -1.50 | 0.076 | | |
| GARGALOVIC_RESPONSE_TO_OXIDIZED_PHOSPHOLIPIDS_TURQUOISE_DN | C2 | -1.48 | 0.083 | | |
| MOOTHA_HUMAN_MITODB_6_2002 | C2 | | | -2.01 | <0.001 |
| GALLUZZI_PREVENT_MITOCHONDIAL_PERMEABILIZATION | C2 | | | -1.30 | 0.248 |
| MITOCHONDRIAL_MEMBRANE_PART | C5 | -2.21 | <0.001 | -1.83 | 0.016 |
| MITOCHONDRIAL_INNER_MEMBRANE | C5 | -2.15 | <0.001 | -1.99 | 0.003 |
| MITOCHONDRIAL_PART | C5 | -2.13 | <0.001 | -2.07 | 0.001 |
| MITOCHONDRIAL_MEMBRANE | C5 | -2.07 | <0.001 | -2.02 | 0.003 |

| Gene set | MSigDB collection | CD48- LKS | | CD48+ LKS | |
|---|---|---|---|---|---|
| | | NES | FDR | NES | FDR |
| MITOCHONDRIAL_ENVELOPE | C5 | -1.98 | 0.002 | -2.01 | 0.003 |
| MITOCHONDRIAL_MATRIX | C5 | -1.97 | 0.002 | -1.81 | 0.020 |
| MITOCHONDRIAL_LUMEN | C5 | -1.96 | 0.002 | -1.81 | 0.019 |
| MITOCHONDRIAL_RIBOSOME | C5 | -1.87 | 0.008 | -1.64 | 0.060 |
| MITOCHONDRION | C5 | -1.85 | 0.010 | -2.01 | 0.002 |
| MITOCHONDRIAL_RESPIRATORY_CHAIN | C5 | -1.81 | 0.015 | -1.87 | 0.013 |
| MITOCHONDRION_ORGANIZATION_AND_BIOGENESIS | C5 | -1.54 | 0.121 | -1.50 | 0.133 |
| ELECTRON_CARRIER_ACTIVITY | C5 | | | -1.73 | 0.034 |
| MITOCHONDRIAL_TRANSPORT | C5 | | | -1.55 | 0.099 |
| Ribosomes | | | | | |
| BILANGES_SERUM_RESPONSE_TRANSLATION | C2 | -1.64 | 0.028 | | |
| REACTOME_DEADENYLATION_DEPENDENT_MRNA_DECAY | C2 | -1.63 | 0.032 | | |
| REACTOME_ELONGATION_ARREST_AND_RECOVERY | C2 | -1.58 | 0.046 | | |
| REACTOME_TRANSLATION | C2 | -2.47 | <0.001 | | |
| KEGG_RIBOSOME | C2 | -2.42 | <0.001 | | |
| REACTOME_PEPTIDE CHAIN ELONGATION | C2 | -2.42 | <0.001 | | |
| REACTOME_NONSENSE_MEDIATED_DECAY_ENHANCED_BY_ THE_EXON_JUNCTION_COMPLEX | C2 | -2.37 | <0.001 | | |
| REACTOME_FORMATION_OF_THE_TERNARY_COMPLEX_ AND_SUBSEQUENTLY_THE_43S_COMPLEX | C2 | -2.19 | <0.001 | | |
| MCGOWAN_RSP6_TARGETS_UP | C2 | | | -1.76 | 0.011 |
| STRUCTURAL_CONSTITUENT_OF_RIBOSOME | C5 | -2.33 | <0.001 | | |
| RIBOSOME | C5 | -2.04 | 0.001 | -1.68 | 0.045 |
| RIBOSOME_BIOGENESIS_AND_ASSEMBLY | C5 | -2.02 | 0.001 | -1.78 | 0.023 |
| ORGANELLAR_RIBOSOME | C5 | -1.89 | 0.007 | -1.63 | 0.067 |
| RIBONUCLEOPROTEIN_COMPLEX_BIOGENESIS_AND_ ASSEMBLY | C5 | -1.83 | 0.012 | -2.11 | 0.002 |
| RIBOSOMAL_SUBUNIT | C5 | -1.78 | 0.019 | -1.62 | 0.071 |
| TRANSLATION | C5 | -1.56 | 0.118 | | |
| PROTEIN_POLYMERIZATION | C5 | -1.53 | 0.126 | | |
| RIBONUCLEOPROTEIN_COMPLEX | C5 | | | -2.09 | 0.001 |
| PROTEIN_RNA_COMPLEX_ASSEMBLY | C5 | | | -1.98 | 0.003 |
| TRANSLATIONAL_INITIATION | C5 | | | -1.73 | 0.034 |
| TRANSLATION_REGULATOR_ACTIVITY | C5 | | | -1.71 | 0.039 |
| TRANSLATION_FACTOR_ACTIVITY_NUCLEIC_ACID_BINDING | C5 | | | -1.70 | 0.044 |
| TRANSLATION_INITIATION_FACTOR_ACTIVITY | C5 | | | -1.67 | 0.048 |
| REGULATION_OF_TRANSLATIONAL_INITIATION | C5 | | | -1.55 | 0.100 |

| Gene set | MSigDB collection | CD48- LKS | | CD48+ LKS | |
|---|---|---|---|---|---|
| | | NES | FDR | NES | FDR |
| tRNA biosynthesis | | | | | |
| REACTOME_CYTOSOLIC_TRNA_AMINOACYLATION | C2 | | | -1.85 | 0.004 |
| REACTOME_TRNA_AMINOACYLATION | C2 | | | -1.72 | 0.015 |
| KEGG_AMINOACYL_TRNA_BIOSYNTHESIS | C2 | | | -1.64 | 0.030 |
| TRNA_METABOLIC_PROCESS | C5 | | | -1.69 | 0.044 |
| Proteasomal pathway | | | | | |
| KEGG_PROTEASOME | C2 | -2.18 | <0.001 | -1.99 | 0.001 |
| REACTOME_AUTODEGRADATION_OF_THE_E3_UBIQUITIN_ LIGASE_COP1 | C2 | -2.07 | <0.001 | -2.01 | <0.001 |
| BIOCARTA_PROTEASOME_PATHWAY | C2 | -1.92 | 0.002 | -2.14 | <0.001 |
| WONG_PROTEASOME_GENE_MODULE | C2 | | | -1.83 | 0.005 |
| REACTOME_ANTIGEN_PROCESSING_UBIQUITINATION_ PROTEASOME_DEGRADATION | C2 | | | -1.42 | 0.138 |
| PROTEASOME_COMPLEX | C5 | -1.47 | 0.168 | -1.52 | 0.113 |
| Cell cycle regulation | | | | | |
| REACTOME_SYNTHESIS_OF_DNA | C2 | -2.44 | <0.001 | -2.25 | <0.001 |
| REACTOME_S_PHASE | C2 | -2.42 | <0.001 | -2.31 | <0.001 |
| CHICAS_RB1_TARGETS_LOW_SERUM | C2 | -2.28 | <0.001 | | |
| ISHIDA_E2F_TARGETS | C2 | -2.27 | <0.001 | -2.11 | <0.001 |
| REACTOME_MITOTIC_G1_G1_S_PHASES | C2 | -2.27 | <0.001 | -2.37 | <0.001 |
| REACTOME_G1_S_TRANSITION | C2 | -2.26 | <0.001 | -2.31 | <0.001 |
| REACTOME_M_G1_TRANSITION | C2 | -2.26 | <0.001 | -2.17 | <0.001 |
| REACTOME_DNA_STRAND_ELONGATION | C2 | -2.23 | <0.001 | -2.05 | <0.001 |
| KEGG_DNA_REPLICATION | C2 | -2.21 | <0.001 | -2.02 | <0.001 |
| RAHMAN_TP53_TARGETS_PHOSPHORYLATED | C2 | -2.18 | <0.001 | -1.90 | 0.002 |
| REACTOME_CDK_MEDIATED_PHOSPHORYLATION_AND_ REMOVAL_OF_CDC6 | C2 | -2.17 | <0.001 | -2.00 | 0.001 |
| REACTOME_ASSEMBLY_OF_THE_PRE_REPLICATIVE_COMPLEX | C2 | -2.15 | <0.001 | -2.20 | <0.001 |
| KONG_E2F3_TARGETS | C2 | -2.14 | <0.001 | -2.19 | <0.001 |
| REACTOME_DNA_REPLICATION | C2 | -2.14 | <0.001 | -2.29 | <0.001 |
| REACTOME_CDT1_ASSOCIATION_WITH_THE_CDC6_ORC_ ORIGIN_COMPLEX | C2 | -2.13 | <0.001 | -2.10 | <0.001 |
| REACTOME_CYCLIN_E_ASSOCIATED_EVENTS_DURING_G1_S_ TRANSITION_ | C2 | -2.13 | <0.001 | -2.13 | <0.001 |
| MARKEY_RB1_ACUTE_LOF_DN | C2 | -2.11 | <0.001 | -2.27 | <0.001 |
| REACTOME_CELL_CYCLE_CHECKPOINTS | C2 | -2.10 | <0.001 | -2.11 | <0.001 |
| WHITFIELD_CELL_CYCLE_LITERATURE | C2 | -2.08 | <0.001 | -2.25 | <0.001 |

| Gene set | MSigDB collection | CD48- LKS | | CD48+ LKS | |
|---|---|---|---|---|---|
| | | NES | FDR | NES | FDR |
| EGUCHI_CELL_CYCLE_RB1_TARGETS | C2 | -2.03 | <0.001 | -1.97 | 0.001 |
| REACTOME_REGULATION_OF_MITOTIC_CELL_CYCLE | C2 | -2.03 | <0.001 | | |
| REACTOME_CELL_CYCLE_MITOTIC | C2 | -2.02 | <0.001 | -2.34 | <0.001 |
| REACTOME_LAGGING_STRAND_SYNTHESIS | C2 | -2.02 | <0.001 | -1.88 | 0.003 |
| REACTOME_CELL_CYCLE | C2 | -2.01 | <0.001 | -2.18 | <0.001 |
| REACTOME_MITOTIC_M_M_G1_PHASES | C2 | -2.00 | <0.001 | -2.23 | <0.001 |
| SCIAN_CELL_CYCLE_TARGETS_OF_TP53_AND_TP73_DN | C2 | -1.98 | 0.001 | -1.81 | 0.006 |
| ZHOU_CELL_CYCLE_GENES_IN_IR_RESPONSE_24HR | C2 | -1.90 | 0.002 | -2.12 | <0.001 |
| KAUFFMANN_DNA_REPLICATION_GENES | C2 | -1.87 | 0.003 | -1.96 | 0.001 |
| IGLESIAS_E2F_TARGETS_UP | C2 | -1.86 | 0.003 | -1.32 | 0.235 |
| CHANG_CYCLING_GENES | C2 | -1.85 | 0.004 | -2.10 | <0.001 |
| TANG_SENESCENCE_TP53_TARGETS_DN | C2 | -1.82 | 0.006 | -1.86 | 0.003 |
| MARKEY_RB1_CHRONIC_LOF_UP | C2 | -1.78 | 0.008 | -1.42 | 0.134 |
| REACTOME_G2_M_CHECKPOINTS | C2 | -1.78 | 0.008 | -1.71 | 0.017 |
| ZHOU_CELL_CYCLE_GENES_IN_IR_RESPONSE_6HR | C2 | -1.77 | 0.009 | -2.19 | <0.001 |
| REACTOME_CYCLIN_A_B1_ASSOCIATED_EVENTS_DURING_G2_M_TRANSITION | C2 | -1.68 | 0.022 | -1.39 | 0.160 |
| REACTOME_E2F_MEDIATED_REGULATION_OF_DNA_REPLICATION | C2 | -1.64 | 0.028 | -1.88 | 0.003 |
| MOLENAAR_TARGETS_OF_CCND1_AND_CDK4_DN | C2 | -1.62 | 0.033 | -2.32 | <0.001 |
| REACTOME_G1_S_SPECIFIC_TRANSCRIPTION | C2 | -1.62 | 0.034 | -1.94 | 0.001 |
| BIOCARTA_P53_PATHWAY | C2 | -1.59 | 0.044 | -1.31 | 0.246 |
| VERNELL_RETINOBLASTOMA_PATHWAY_UP | C2 | -1.58 | 0.045 | -1.96 | 0.001 |
| REACTOME_MEIOTIC_RECOMBINATION | C2 | -1.57 | 0.049 | | |
| KANNAN_TP53_TARGETS_DN | C2 | -1.56 | 0.052 | | |
| IWANAGA_E2F1_TARGETS_INDUCED_BY_SERUM | C2 | -1.54 | 0.059 | -1.40 | 0.155 |
| KEGG_CELL_CYCLE | C2 | -1.51 | 0.068 | -1.88 | 0.003 |
| BIOCARTA_MCM_PATHWAY | C2 | -1.49 | 0.079 | -1.54 | 0.068 |
| REACTOME_G0_AND_EARLY_G1 | C2 | -1.48 | 0.086 | -1.86 | 0.003 |
| PID_E2F_PATHWAY | C2 | -1.47 | 0.088 | -1.85 | 0.004 |
| MARKEY_RB1_CHRONIC_LOF_DN | C2 | -1.44 | 0.110 | | |
| CHICAS_RB1_TARGETS_GROWING | C2 | -1.42 | 0.121 | -1.72 | 0.015 |
| REACTOME_MITOTIC_PROMETAPHASE | C2 | -1.38 | 0.153 | -1.84 | 0.004 |
| REACTOME_G1_PHASE | C2 | -1.37 | 0.155 | -1.65 | 0.030 |
| BIOCARTA_CELLCYCLE_PATHWAY | C2 | -1.35 | 0.173 | -1.65 | 0.029 |
| HERNANDEZ_MITOTIC_ARREST_BY_DOCETAXEL_1_DN | C2 | -1.30 | 0.220 | | |
| WHITFIELD_CELL_CYCLE_G2 | C2 | -1.30 | 0.224 | -1.60 | 0.044 |

| Gene set | MSigDB collection | CD48- LKS | | CD48+ LKS | |
|---|---|---|---|---|---|
| | | NES | FDR | NES | FDR |
| SANCHEZ_MDM2_TARGETS | C2 | -1.28 | 0.249 | | |
| BENPORATH_PROLIFERATION | C2 | | | -2.15 | <0.001 |
| REACTOME_SCFSKP2_MEDIATED_DEGRADATION_OF_P27_P21 | C2 | | | -2.14 | <0.001 |
| REACTOME_APC_C_CDC20_MEDIATED_DEGRADATION_OF_MITOTIC_PROTEINS | C2 | | | -2.03 | <0.001 |
| REN_BOUND_BY_E2F | C2 | | | -1.89 | 0.002 |
| REACTOME_PROCESSIVE_SYNTHESIS_ON_THE_LAGGING_STRAND | C2 | -1.92 | 0.001 | -1.72 | 0.016 |
| REACTOME_MITOTIC_G2_G2_M_PHASES | C2 | | | -1.69 | 0.021 |
| REACTOME_ACTIVATION_OF_THE_PRE_REPLICATIVE_COMPLEX | C2 | -1.93 | 0.001 | -1.68 | 0.022 |
| CEBALLOS_TARGETS_OF_TP53_AND_MYC_UP | C2 | | | -1.67 | 0.025 |
| REACTOME_RECRUITMENT_OF_MITOTIC_CENTROSOME_PROTEINS_AND_COMPLEXES | C2 | | | -1.63 | 0.033 |
| REICHERT_MITOSIS_LIN9_TARGETS | C2 | | | -1.61 | 0.039 |
| PID_P53REGULATIONPATHWAY | C2 | | | -1.59 | 0.047 |
| BIOCARTA_G1_PATHWAY | C2 | | | -1.55 | 0.060 |
| SA_G1_AND_S_PHASES | C2 | | | -1.51 | 0.082 |
| WHITFIELD_CELL_CYCLE_G2_M | C2 | | | -1.48 | 0.099 |
| WHITFIELD_CELL_CYCLE_M_G1 | C2 | | | -1.48 | 0.099 |
| WHITFIELD_CELL_CYCLE_G1_S | C2 | | | -1.47 | 0.101 |
| BIOCARTA_G2_PATHWAY | C2 | | | -1.46 | 0.112 |
| GEORGES_CELL_CYCLE_MIR192_TARGETS | C2 | | | -1.45 | 0.116 |
| WHITFIELD_CELL_CYCLE_S | C2 | | | -1.40 | 0.155 |
| REGULATION_OF_CYCLIN_DEPENDENT_PROTEIN_KINASE_ACTIVITY | C5 | -1.99 | 0.001 | | |
| REPLICATION_FORK | C5 | -1.85 | 0.010 | -1.45 | 0.169 |
| DNA_REPLICATION | C5 | -1.83 | 0.012 | -1.58 | 0.088 |
| CELL_CYCLE_PROCESS | C5 | -1.74 | 0.031 | -1.51 | 0.127 |
| INTERPHASE | C5 | -1.67 | 0.057 | -1.45 | 0.171 |
| CELL_CYCLE_PHASE | C5 | -1.64 | 0.070 | -1.40 | 0.209 |
| CELL_CYCLE_GO_0007049 | C5 | -1.64 | 0.070 | -1.43 | 0.174 |
| MITOTIC_CELL_CYCLE | C5 | -1.63 | 0.070 | -1.51 | 0.122 |
| DNA_DEPENDENT_DNA_REPLICATION | C5 | -1.59 | 0.097 | -1.52 | 0.113 |
| INTERPHASE_OF_MITOTIC_CELL_CYCLE | C5 | -1.58 | 0.104 | -1.50 | 0.128 |
| M_PHASE | C5 | -1.54 | 0.122 | -1.34 | 0.250 |

| Gene set | MSigDB collection | CD48- LKS | | CD48+ LKS | |
|---|---|---|---|---|---|
| | | NES | FDR | NES | FDR |
| M_PHASE_OF_MITOTIC_CELL_CYCLE | C5 | -1.52 | 0.125 | -1.55 | 0.098 |
| CELL_PROLIFERATION_GO_0008283 | C5 | -1.46 | 0.176 | | |
| MITOSIS | C5 | -1.43 | 0.197 | -1.56 | 0.096 |
| DNA_METABOLIC_PROCESS | C5 | | | -1.46 | 0.160 |
| Metabolism | | | | | |
| REACTOME_TCA_CYCLE_AND_RESPIRATORY_ELECTRON_TRANSPORT | C2 | -2.19 | <0.001 | -2.08 | <0.001 |
| MOOTHA_TCA | C2 | -1.67 | 0.024 | -1.78 | 0.008 |
| REACTOME_CITRIC_ACID_CYCLE_TCA_CYCLE | C2 | -1.61 | 0.037 | -1.87 | 0.003 |
| KEGG_CITRATE_CYCLE_TCA_CYCLE | C2 | -1.55 | 0.054 | -1.79 | 0.007 |
| REACTOME_GLUCOSE_METABOLISM | C2 | -1.33 | 0.190 | | |
| REACTOME_PYRUVATE_METABOLISM_AND_CITRIC_ACID_TCA_CYCLE | C2 | | | -1.71 | 0.017 |
| Hematopoietic stem cells | | | | | |
| IVANOVA_HEMATOPOIESIS_INTERMEDIATE_PROGENITOR | C2 | -1.67 | 0.023 | -2.02 | <0.001 |
| BYSTRYKH_HEMATOPOIESIS_STEM_CELL_QTL_CIS | C2 | -1.45 | 0.103 | | |
| PARK_HSC_AND_MULTIPOTENT_PROGENITORS | C2 | -1.39 | 0.145 | -1.53 | 0.070 |
| BYSTRYKH_HEMATOPOIESIS_STEM_CELL_AND_BRAIN_QTL_CIS | C2 | | | -1.32 | 0.227 |

**Table S2. Related to Figure 2. Stress and DNA damage dysregulation in the transcriptome of HSPCs from OCS$^{f/f}$ mice.**

| ID | Description | CD48- LKS p-val | CD48+ LKS p-val |
|---|---|---|---|
| GO:0006310 | DNA recombination | NS | 4.68e-02 |
| GO:0006950 | response to stress | 4.69e-05 | 1.31e-10 |
| ├GO:0080134 | regulation of response to stress | 2.25e-03 | 9.78e-04 |
| └GO:0033554 | cellular response to stress | 5.53e-06 | 9.15e-05 |
| ├GO:0080135 | regulation of cellular response to stress | 2.82e-02 | NS |
| └GO:0006974 | cellular response to DNA damage stimulus | 4.11e-03 | 1.96e-03 |
| └GO:0006281 | DNA repair | 3.86e-02 | NS |
| └GO:0006301 | postreplication repair | NS | 2.78e-02 |
| REAC:5956042 | Cell Cycle Checkpoints | 1.27e-04 | 2.86e-04 |
| └REAC:5956049 | Activation of ATR in response to replication stress | 2.89e-02 | 4.10e-02 |
| ┌REAC:5956279 | Gap-filling DNA repair synthesis and ligation in GG-NER | 2.01e-02 | NS |
| └REAC:5956420 | Gap-filling DNA repair synthesis and ligation in TC-NER | 2.01e-02 | NS |

Genes with significantly different expression ($P$<0.05) between OCS$^{f/+}$ and OCS$^{f/f}$ mice within the CD48$^{-}$ or CD48$^{+}$ populations were interrogated for GO and Reactome term enrichment using g-profiler. P-val: p-value. NS: not significant ($P$≥0.05).

**Table S3. Related to Figure 2. Myc-related signatures depleted in OCSf/f HSPCs.**

| Gene set | Size | CD48- LKS | | CD48+ LKS | |
|---|---|---|---|---|---|
| | | NES | FDR q-val | NES | FDR q-val |
| DANG_MYC_TARGETS_UP | 140 | -2.3691 | <0.0001 | -2.3219 | <0.0001 |
| MENSSEN_MYC_TARGETS | 52 | -2.2803 | <0.0001 | -2.1716 | <0.0001 |
| YU_MYC_TARGETS_UP | 40 | -2.1026 | <0.0001 | -2.2127 | <0.0001 |
| ODONNELL_TARGETS_OF_MYC_AND_TFRC_DN | 45 | -1.9994 | 0.0004 | -1.9883 | 0.0006 |
| CAIRO_PML_TARGETS_BOUND_BY_MYC_UP | 23 | -1.9161 | 0.0015 | -1.6278 | 0.0344 |
| SCHUHMACHER_MYC_TARGETS_UP | 80 | -1.9014 | 0.0019 | -2.2771 | <0.0001 |
| SCHLOSSER_MYC_TARGETS_REPRESSED_BY_SERUM | 153 | -1.8948 | 0.0021 | -2.1315 | 0.0001 |
| BENPORATH_MYC_TARGETS_WITH_EBOX | 224 | -1.8805 | 0.0025 | -1.6005 | 0.0427 |
| SANSOM_APC_TARGETS_REQUIRE_MYC | 195 | -1.8271 | 0.0049 | -1.6294 | 0.0340 |
| PID_MYC_ACTIVPATHWAY | 77 | -1.7735 | 0.0088 | -1.7577 | 0.0107 |
| MORI_EMU_MYC_LYMPHOMA_BY_ONSET_TIME_UP | 102 | -1.7638 | 0.0098 | -1.9423 | 0.0012 |
| SCHLOSSER_MYC_AND_SERUM_RESPONSE_SYNERGY | 32 | -1.7246 | 0.0142 | -1.5919 | 0.0448 |
| KIM_MYC_AMPLIFICATION_TARGETS_UP | 192 | -1.6787 | 0.0216 | -1.8727 | 0.0027 |
| DANG_REGULATED_BY_MYC_UP | 69 | -1.5696 | 0.0484 | -1.7749 | 0.0091 |
| COLLER_MYC_TARGETS_UP | 25 | -1.5656 | 0.0498 | -2.0411 | 0.0003 |
| ACOSTA_PROLIFERATION_INDEPENDENT_MYC_TARGETS_UP | 77 | -1.4380 | 0.1081 | -1.4098 | 0.1455 |
| SCHLOSSER_MYC_TARGETS_AND_SERUM_RESPONSE_DN | 47 | -1.4123 | 0.1260 | -1.9374 | 0.0012 |
| BILD_MYC_ONCOGENIC_SIGNATURE | 193 | -1.4101 | 0.1277 | -1.3748 | 0.1735 |

**Table S4. Related to Figure 4. Human normal donor and patient characteristics.**

| Sample ID | Disease status | Age | Sex |
|---|---|---|---|
| HD513 | Healthy donor | 40 y | M |
| HD723 | Healthy donor | 48 y | F |
| HD863 | Healthy donor | 42 y | M |
| HD237 | Healthy donor | 40 y | M |
| HD703 | Healthy donor | 39 y | M |
| HD066 | Healthy donor | 35 y | M |
| HD167 | Healthy donor | 48 y | M |
| SDS438 | SDS patient[a] | 9 y | M |
| SDS132 | SDS patient[a] | 14 y | M |
| SDS640 | SDS patient[a] | 4 y | M |
| SDS221 | SDS patient[a] | 18 y | M |
| MDS247 | MDS patient[b] | 59 y | M |
| MDS006 | MDS patient[b] | 62 y | F |
| MDS020 | MDS patient[b] | 71 y | F |
| MDS159 | MDS patient[b] | 74 y | F |
| MDS209 | MDS patient[b] | 78 y | F |
| MDS222 | MDS patient[b] | 66 y | F |
| MDS610 | MDS patient[b] | 64 y | F |
| MDS627 | MDS patient[b] | 80 y | M |
| MDS008 | MDS patient[b] | 67 y | F |
| DBA044 | DBA patient | 1 y | F |
| DBA087 | DBA patient | 4 mo | M |
| DBA563 | DBA patient | 4 y | F |

[a]All SDS patients were genetically characterized by compound heterozygosity c.183_184TA>CT/c.258+2T>C. Patients did not receive G-CSF treatment and were not diagnosed with MDS or AML at the time of bone marrow sampling. All patients presented with pancreatic insufficiency (serum trypsinogen level <6 µg/L) and growth retardation (≤ 2 SD). All patients but SDS438 were neutropenic at sampling (absolute neutrophil counts, ANC < $1.5\times10^9$/l); SDS438 had ANC = $1.62\times10^9$/l).
[b]See Table S6 for further patient characteristics.

**Table S5. Related to Figure 5. In vitro exposure of HSPCs to S100A8/9 activates transcriptional signatures related to TLR signaling and cellular stress/apoptosis.**

| Gene set | NES | p-val | FDR q-val |
|---|---|---|---|
| ***Toll-like receptor signaling*** | | | |
| BIOCARTA_TOLL_PATHWAY | 1.60 | 0.014 | 0.404 |
| REACTOME_TOLL_RECEPTOR_CASCADES | 1.53 | 0.005 | 0.365 |
| PID_TOLL_ENDOGENOUS_PATHWAY | 1.49 | 0.043 | 0.380 |
| KEGG_TOLL_LIKE_RECEPTOR_SIGNALING_PATHWAY | 1.46 | 0.012 | 0.428 |
| REACTOME_ACTIVATED_TLR4_SIGNALING | 1.44 | 0.025 | 0.444 |
| REACTOME_INNATE_IMMUNE_SYSTEM | 1.56 | 0.0001 | 0.374 |
| ***Activation of p53 and apoptosis pathways*** | | | |
| REACTOME_P53_DEPENDENT_G1_DNA_DAMAGE_RESPONSE | 1.52 | 0.017 | 0.364 |
| INGA_TP53_TARGETS | 1.62 | 0.019 | 0.363 |
| RASHI_RESPONSE_TO_IONIZING_RADIATION_1 | 1.68 | 0.005 | 0.326 |
| DAZARD_UV_RESPONSE_CLUSTER_G2 | 1.69 | 0.006 | 0.314 |
| AMUNDSON_GAMMA_RADIATION_RESISTANCE | 1.71 | 0.009 | 0.316 |
| KEGG_APOPTOSIS | 1.74 | 0.001 | 0.260 |
| KEGG_P53_SIGNALING_PATHWAY | 1.78 | 0.001 | 0.217 |

**Table S6. Related to Figure 7. MDS patient characteristics. Provided as an Excel file.** All patients were treated with lenalidomide in the context of an ongoing prospective clinical trial (details in Experimental Procedures). Patient characteristics at study entry are listed. Progression free survival is calculated from date of study-entry. Hb, hemoglobin. PLT, platelets. WBC, white blood cells. ANC, absolute neutrophil count. *S100A8* and *S100A9* expression is obtained by RNA-sequencing data. P-values were calculated by Mann-Whitney (MW) test.

| Patient ID | WHO | Cyto-genetics | IPSS | Genetic Abnormalities | |
|---|---|---|---|---|---|
| S100 niche signature + | MDS020 | RCMD-RS | 46,XX[20] | 0 | SRSF2 mutation |
| | MDS486 | CMML-1 | 46,XX,t(3;3)(q21;q26)[10] | 0.5 | SF3B1 mutation |
| | MDS610 | RCMD-RS | 46,XX[20] | 0.5 | TET2, DNMT3A, SF3B1 and RUNX1 mutation |
| | MDS627 | RCMD | 46,XY[20] | 0 | TET2 and ASXL1 mutation |
| | MDS008 | RCMD | 46,XX[20] | 0.5 | ASXL1 and EZH2 mutation |
| | MDS092 | RAEB-1 | 46,XX,del(5)(q1?5q3?5)[15] | 0.5 | sequenced: no mutations found |
| | MDS174 | RCMD-RS | 47,XY,+19[9]/46,XY[11] | 1 | SETBP1 and U2AF1 mutation |
| | MDS176 | RCMD-RS | 46,XY[22] | 0 | Not Sequenced |
| | MDS019 | RCMD-RS | 46,XX[20] | 0 | SF3B1 mutation |
| | MDS061 | RAEB-1 | 46,XY[20] | 0.5 | DNMT3A, SF3B1 and TET2 mutation |
| | MDS069 | CMML-1 | 46,XY,der(13)t(1;13)(q11;p11)[10] | 1.0 | ASXL1, IDH2, SF3B1 and TET2 mutation |
| | MDS079 | RCMD | 47,XY,t(2;14)(q3?7;q2?2),idic(21)(p1?2),+idic(21)(p1?2)[8] | 1.0 | ASXL1 mutation |
| | MDS135 | RCMD-RS | 46,XX[20] | 0 | ASXL1, TET2 mutation |
| | MDS183 | MDS-U | 47,XX,+8[12] | 0.5 | ASXL1, IDH2 and SRSF2 mutation |
| | MDS203 | RCMD-RS | 46,XY,del(5)(q13q31)[7]/47,XY,del(5)(q13q31),+8[4]/46,XY[1] | 0.5 | ASXL1 and SF3B1 mutation |
| | MDS206 | Del(5q) | 46,XX,del(5)(q13q33)[7}/46,XX[13] | 0 | SF3B1 and TET2 mutation |
| | MDS010 | RCMD | 46,XY[20] | 0 | sequenced: no mutations found |
| S100 niche signature - | MDS006 | RAEB-1 | 46,XX[20] | 1 | DNMT3A and SRSF2 mutation |
| | MDS118 | RARS | 46,XX[20] | 0 | TET2, DNMT3A and SF3B1 mutation |
| | MDS159 | Del(5q) | 46,XX,del(5)(q15q33)[10] | 0 | sequenced, no mutations found |
| | MDS209 | RCMD-RS | 46,XX[10] | 0 | SF3B1 mutation |
| | MDS222 | RARS | 46,XX[21] | 0 | SF3B1 and 2 TET2 mutations |
| | MDS025 | RCMD-RS | 46,XY[20] | 0 | SF3B1 mutation |
| | MDS433 | RCMD-RS | 45,X,-Y[10]/46,XY[10] | 0 | sequenced: no mutations found |
| | MDS646 | RAEB-1 | 46,XX[20] | 1 | ASXL1 mutation |
| | MDS893 | RARS | 46,XX[20] | 0 | SF3B1 mutation |
| | MDS111 | RCMD | 46,XX[20] | 0 | sequenced: no mutations found |
| | MDS623 | RCMD | 46,XY[20] | 0.5 | sequenced: no mutations found |
| | MDS247 | RCMD-RS | 46,XY[20] | 0 | DNMT3A and SF3B1 mutation |
| | MDS150 | RCMD-RS | 46,XX[20] | 0.5 | not sequenced |
| | MDS158 | RCMD-RS | 46,XX[20] | 0 | DNMT3A, SF3B1 and TET2 mutation |
| | MDS172 | RARS | 46,XY[20] | 0 | SF3B1 and 2 TET2 mutations |
| | MDS022 | RAEB-1 | 46,XY[20] | 1.0 | sequenced: no mutations found |
| | MDS053 | RARS | 45,X,-Y][7]/46,XY[3] | 0.0 | SF3B1, TET2 mutation |
| | MDS055 | RCMD | 46,XY,der(22)(t(1;22)(q12;p11)[16]/46,XY,SL,del(20)(q12)[3] | 0.5 | sequenced: no mutations found |
| | MDS093 | RCMD | 46,XY[20] | 0.5 | TET2 mutation |
| | MDS101 | RCMD-RS | 46,XY[21] | 0.0 | ASXL1, DNMT3A and SF3B1 mutation |
| | MDS121 | RCMD | 46,XY[20] | 0.5 | sequenced: no mutations found |
| | MDS144 | RCMD | 47,XY,+19[6]/48,idem,+21[3]/46,XY[4] | 1.0 | ASXL1, U2AF1 mutation |
| | MDS167 | RCMD | 46,XY[21] | 0.0 | SF3B1 mutation |
| | MDS182 | RCMD | 46,XY,del(5)(q13q33)[10]/46,XY[10] | 0.0 | DNMT3A, TET2 mutation |
| | MDS201 | RCMD-RS | 46,XX[20] | 0.0 | SF3B1 mutation |
| | MDS001 | RCMD-RS | 46,XY[20] | 0.0 | SF3B1 mutation |
| | MDS007 | RCMD-RS | 46,XY[20] | 0.0 | SF3B1, TET2 mutation |
| | MDS013 | Del(5q) | 46,XX,del(5)(q13q33)[15]/46,XX[1] | 0.0 | sequenced: no mutations found |

## SUPPLEMENTAL EXPERIMENTAL PROCEDURES

### Mice genotyping and sample collection

DNA was extracted from mouse toes with DirectPCR Lysis Reagent (Viagen Biotech). Genotyping and Cre-mediated recombination were verified on genomic DNA samples using the primers listed in the table below. Mouse bone marrow and bone fraction cells were isolated as previously described (Raaijmakers et al., 2010). Red blood cells (RBC) were lysed with ACK lysing buffer (Lonza) before surface markers staining. Peripheral blood was collected from the submandibular vein in $K_2$EDTA-coated microtainers (BD) and analyzed using a Vet ABC counter (Scil Animal Care).

### Genotyping primers used in the study.

| Target | Allele | Primer ID | Sequence | Amplicon size, bp |
|---|---|---|---|---|
| *Sbds* | Wild type | a<br>b | CCAGGGTCACGTTAATACAAACC<br>TGAGTTTCAATCCTCAGCATCC | 329 |
| | Floxed | a<br>b | CCAGGGTCACGTTAATACAAACC<br>TGAGTTTCAATCCTCAGCATCC | 450 |
| | Recombined | c<br>d | TAAAACAAAGCTGCGGTCAAGA<br>ATCCTCAGCATCCCGAACAA | 319 |
| *Osx* | Wild type | e<br>f | CTCTTCATGAGGAGGACCCT<br>GCCAGGCAGGTGCCTGGACAT | No band |
| | Cre | e<br>f | CTCTTCATGAGGAGGACCCT<br>GCCAGGCAGGTGCCTGGACAT | 500 |
| *Trp53* | Wild type | 10.1<br>10.2 | GTTAAGGGGTATGAGGGACA<br>GAAGACAGAAAAGGGGAGGG | 400 |
| | Floxed | 10.1<br>10.2 | GTTAAGGGGTATGAGGGACA<br>GAAGACAGAAAAGGGGAGGG | 600 |
| | Recombined | 1.1<br>10.2 | CACAAAAACAGGTTAAACCCAG<br>GAAGACAGAAAAGGGGAGGG | 612 |

### Bone mineral density and 3-point bending test analysis

Cortical BMD was calculated from µCT cortical data on the basis of a calibration scanning obtained using two phantoms with known density (0.25 g/cm$^3$ and 0.75 g/cm$^3$; Bruker MicroCT) under identical conditions as for the femurs. For the bending test, femurs were placed in a custom-modified Single Column Lloyd LRX System bending device (Lloyd Instruments) and analyzed as previously reported (van der Eerden et al., 2013) using CtAnalyzer software (Bruker MicroCT).

### Goldner's Masson trichrome staining

Femurs were embedded in methylmetacrylate as indicated before (Derkx et al., 1998). Sections of 6 µm were deacrylated, hydrated and stained accordingly to the previously described protocol (Gruber, 1992). Images of the metaphysial area were captured with a Nikon Eclipse E400 system (Nikon) using a 20X objective lens. Data was analyzed using Image J software (http://imagej.nih.gov/ij/). Briefly, the bone surface was manually selected and the perimeter length calculated. Osteoblasts were manually identified based on staining and morphology. The frequency of osteoblasts was calculated as percentage of osteoblast area in the bone surface and as number of osteoblasts per mm of bone.



### CFU-F assay

Primary bone fraction cells were resuspended in growth medium, consistent of αMEM, 20% FBS (Life Technologies), and Penicillin-Streptomycin solution (Life Technologies), and cultured under hypoxic conditions (5% $O_2$, 5% $CO_2$) in 24-well plates (seeding density: 6.5 x $10^4$ cells/$cm^2$). After 24h, the medium was changed to eliminate non-adherent cells. Colonies were stained after 7 days of culture. Briefly, medium was removed and cells were fixed 5' in methanol, stained in a 1:20 dilution of Giemsa staining (Merck Millipore) in distilled water and rinsed with tap water. Colonies were counted with an Olympus CK2 inverted microscope, using a 10X magnification.

### Primary cell isolation and flow cytometry

All FACS antibodies incubations were performed in PBS+0.5%FCS for 20 min on ice. To identify hematopoietic stem and progenitor cells (HSPCs), bone marrow cells were first co-stained with a cocktail of biotin-labelled antibodies against the following lineage (Lin) markers: Gr1 (RB6-8C5), Mac1 (M1/70), Ter119 (TER-119), CD3e (145-2C11), CD4 (GK1.5), CD8 (53-6.7) and B220 (RA3-6B2) (all from BD Biosciences). After washing, cells were incubated with Pacific Orange-conjugated streptavidin (Life Technologies) and the following antibodies: Pacific Blue anti-Sca1 (D7), FITC or PE anti-CD48 (HM48-1), PE-Cy7 anti-CD150 (TC15-12F12.2) (all from Biolegend), APC anti-c-Kit (2B8, BD Biosciences). Dead cells were excluded based on 7AAD staining.

To analyze differentiated cells and define chimerism, we used FITC anti-Gr1 (RB6-8C5), APC anti-Mac1 (M1/70), PE anti-B220 (RA3-6B2), APC-Cy7 anti-CD45.1 (A20), PE-Cy7 anti-CD45.2 (104), all from Biolegend. To identify stromal cells, bone fraction cell suspension was stained with the following antibodies: APC-Cy7 anti-CD45.2 (104), BV510 anti-Ter119 (TER-119), PE-Cy7 anti-CD105 (MJ7/18), PE anti-CD51 (RMV-7), Pacific Blue anti-Sca1 (D7) (all from Biolegend), PE-CF594 anti-CD31 (MEC 13.3, BD Biosciences).

For human mesenchymal cell isolation, bone marrow aspirates were diluted 1:25 with red

blood cell lysis solution ($NH_4Cl$ 0.155 M, $KHCO_3$ 0.01 M, EDTA-Na2.2H2O 0.1 M, pH 7.4) and incubated for 10 min at room temperature. Cells were collected by centrifugation and washed once with PBS+0.5%FBS. For FACS sorting, immunostaining was performed with the same protocol used for murine bone marrow, using PE CD271 (ME20.4) and PE-Cy7 CD45 (HI30) antibodies (Biolegend). $CD271^+$ cells did not contain erythroid cells based on staining with BV421 CD235a (GA-R2, BD Biosciences).

Apoptosis was assayed with FITC Annexin V Apoptosis Detection Kit I (BD Biosciences) according to the recommendation of the manufacturer.

The content of p53 in stromal cells was analyzed after cell surface antibody staining and cell permeabilization, obtained with Cytofix/Cytoperm Fixation/Permeabilization Solution Kit (BD Biosciences), by incubating cells with Alexa Fluor 647 anti-p53 (1C12) diluted in 1X Perm/Wash buffer (BD Biosciences).

γH2AX levels were assessed in cells fixed and permeabilized with Cytofix/Cytoperm Fixation/ Permeabilization Solution Kit (BD Biosciences) by incubating cells with Alexa Fluor 647 anti-γH2AX (N1-431, BD Biosciences) diluted in 1X Perm/Wash buffer (BD Biosciences).

All FACS events were recorded using a BD LSR II Flow Cytometer and analyzed with FlowJo 7.6.5 software (Tree Star). Cells were sorted with a BD FACSAria III.

### *SBDS* mutation analysis

Mutations in *SBDS* were evaluated in the RNA sequencing data of SDS patients and healthy controls using the Integrative Genomics Viewer (IGV) (Robinson et al., 2011). The c.183_184TA>CT mutation was quantified by annotating the number of reads presenting each of the four different nucleotides for both the positions 183 and 184. Because of its intronic position, the c.258+2T>C mutation was assessed by quantifying the usage of the 251-252 cryptic donor site (Boocock et al., 2003). Specifically, we quantified the fraction of spliced reads with an 8-bp deletion (nucleotides 251-258) as an indication of the mutated genotype.

### Mitochondrial membrane potential quantification

After staining cells for surface antigens, cells were washed in PBS+0.5%FBS and centrifuged. Cells were resuspended in PBS+0.5%FBS and tetramethylrhodamine methyl ester (TMRM, ThermoFisher Scientific) was added from a 50 mM stock solution in DMSO to a final non-quenching concentration of 100 nM. After incubation for 20 min at 37°C, cells were washed with PBS+0.5%FBS and analyzed. Cells treated with 1 µM p-trifluoromethoxy carbonyl cyanide phenyl hydrazone (FCCP) were used as positive control for membrane depolarization.

### ROS detection

After surface antigen staining, cells washed in PBS+0.5%FBS and centrifuged. A stock solution of 2.5 µg/µl 5-(and-6)-chloromethyl-2',7'-dichlorodihydrofluorescein diacetate

acetyl ester (CM-H2DCFDA, Life Technologies) in DMSO was diluted with PBS+0.5%FBS to a final concentration of 3 ng/µl. Cells were resuspended with the CM-H2DCFDA solution and stained for 20 min at 37°C, washed in PBS+0.5%FBS and analyzed.
For dihydroethidium (DHE) studies, the compound (Sigma-Aldrich) was reconstituted to a 100 mM solution in DMSO. After surface antigen staining and washing, cells were resuspended in 500 µl of diluted DHE solution (1:100,000 in HBSS) and incubated at 37°C for 30 min, then washed in PBS+0.5%FBS and analyzed.

### Cell cycle analysis

Mice labeled *in vivo* by BrdU were sacrificed and bone marrow cells were stained for surface antigen. BrdU staining was performed using the FITC BrdU Flow Kit (BD Biosciences) following the manufacturer's instructions.
For Ki67-based cell cycle analysis, cultured or freshly isolated cells were first stained for surface markers and then fixed and permeabilized with Cytofix/Cytoperm Fixation/ Permeabilization Solution Kit (BD Biosciences). After washing, cells were incubated with FITC anti-Ki67 (B56, BD Biosciences) diluted in 1X Perm/Wash buffer (BD Biosciences) for 20 min and then washed. Cells were resuspended in PBS+0.5%FBS and 7AAD was added to detect DNA.



### Alkaline comet assay

HSPCs were resuspended in 0.7% low melting agarose (Sigma-Aldrich) in PBS at a concentration of $10^5$ cells/ml. 50 µl of cell suspension were spread on CometSlides (Trevigen) and the agarose was allowed to solidify for 30 min at 4°C. Slides were incubated for 1 h at 4°C in lysis buffer (1% Triton-X100 freshly added to 2.5M NaCl, 100 mM EDTA, 10 mM Tris/pH10 solution) protected from light and placed in an electrophoresis tray. After 20 min incubation in alkaline solution (200mM NaOH, 1mM EDTA, freshly prepared), unwound DNA was run in the same solution for 30 min at 1 V/cm. After electrophoresis, slides were washed twice in distilled water for 5 min, fixated in 70% ethanol for 5 min and allowed to dry at 37°C. DNA was stained for 5 min in SYBR Gold (Life Technologies), washed in distilled water and allowed to dry in the dark. Images were captured with a Leica DMRXA fluorescent microscope (10X magnification). DNA damage severity was manually quantified according to the score system depicted in Figure S3D.

### Bone marrow transplantation

For serial (competitive) transplantation studies, bone marrow cells from OCS and BL6.SJL mice were isolated and RBC-depleted as described above. BL6.SJL cells were mixed in a 1:1 ratio with cells from $OCS^{f/+}$ or $OCS^{f/f}$ mice. 9 week-old B6.SJL mice were lethally irradiated (8.5Gy) and transplanted with a total of $10^6$ bone marrow cells.
For transplantation in S100A9Tg mice, donor bone marrow cells were isolated from 12-week

old BL6.SJL mice and transplanted into lethally irradiated (8.5Gy) C57BL/6 or S100A9Tg mice (F10 backcross in C57BL76). Each mouse received $2x10^6$ bone marrow cells by tail vein injection and was sacrificed one month after transplantation.
In all transplantation experiment, recipients received antibiotics in the drinking water for 2 weeks after transplantation.

### S100A8/9 measurements

To quantify intracellular levels of S100A8/9 proteins, bone fraction cell suspensions were first stained for surface markers and next fixated and permeabilized with Cytofix/Cytoperm Fixation/Permeabilization Solution Kit (BD Biosciences) according to the manufacturer's instructions. Cells were then resuspended in 1X Perm/Wash buffer (BD Biosciences) and incubated for 20 min with polyclonal rabbit antibodies against mouse S100A8 or S100A9 (Vogl et al., 2014). After washing, cells were incubated for 20 min with Pacific Orange-labelled goat anti-rabbit secondary antibody (Life Technologies) diluted in 1X Perm/Wash buffer, washed and resuspended in PBS+0.5%FBS and analyzed by FACS.
To analyze the concentration of S100A8/9 in the plasma, peripheral blood was collected in Microtainer PST tube (BD) and centrifuged to collect the plasma fraction. Samples were stored at -80°C until the moment of analysis. S100A8/9 was quantified by ELISA as previously described (Vogl et al., 2014).
Immunohistochemical staining of low-risk MDS and age-matched controls (biopsies obtained for disease staging from lymphoma patients without evidence of intramedullary localization) were performed on 5 µm bone marrow sections, which were deparaffinized in xylene and hydrated in a graded series of alcohol. Antigen retrieval was achieved by microwave treatment in citrate buffer (10mM pH 6.0) and blocking of the endogenous peroxidases was performed with 3% $H_2O_2$ in PBS. Sections were blocked using 10% normal human and goat serum (DAKO) in Teng-T solution followed by overnight incubation at 4°C with primary antibody anti-S100A8 and S100A9 (Vogl et al., 2014) diluted 1:500, CD271 (Sigma-Aldrich) diluted 1:200, or normal rabbit immunoglobulin (DAKO) diluted accordingly. Immunoreactions were detected using biotinylated secondary antibody (goat anti-rabbit, 1:2000 dilution) with Vectastain ABC Elite Kit (Vector Laboratories) and 3,3'-diaminobenzidine tetrahydrochloride (Sigma-Aldrich). For all stainings, nuclei were counterstained with haematoxylin (Vector Laboratories). Images of the stained tissue were acquired using a Leica DM5500B upright microscope with 40x lenses and LAS-AF image acquisition software.

### *Sbds*-knockdown and expression analysis in OP9 cells

OP9 cells were grown in DMEM+10%FBS+1%PenStrep. *Sbds* RNA interference was achieved by lentiviral transduction. Briefly, short hairpin RNAs against *Sbds* (shSbds1:TRCN0000108586; and shSbds4:TRCN0000316346) and a commercial non-target control (shControl: SHC002 [SHC]), cloned in the pLKO.1 backbones, were selected from the Mission TRC shRNA library

(Sigma-Aldrich). Lentiviral shRNAs were produced in HEK293T cells after cotransfection of shControl, shSbds1, or shSbds4 together with the packaging plasmids pSPAX2 and pMDG.2. OP9 cells were infected with lentivirus for 72 hours in the presence of 4 µg/mL polybrene and selected 72 hours with 2 µg/mL puromycin.

RNA isolation, conversion to cDNA and qPCR were performed accordingly to previously described methods (Zambetti et al., 2015), using the SuperScript II Reverse Transcriptase (Thermo Fisher Scientific) for conversion to cDNA. For qPCR, expression levels were obtained using the ddCt method using GAPDH as internal control and shControl sample as calibrator. The following primers were used: *Sbds*-Fw: GCGCTTCGAAATCGCCTG; *Sbds*-Rv: TCTGGTCGTCTGTCCCAAATG; *S100a8*-Fw: ATCACCATGCCCTCTACAAGAATG; *S100a8*-Rv: GTCCAATTCTCTGAACAAGTTTTCG; *S100a9*-Fw: AAGCTGCATGAGAACAACCCA; *S100a9*-Rv: CCCAGAACAAAGGCCATTGA; *Cdkn1a*-Fw: CCTGGTGATGTCCGACCTG; *Cdkn1a*-Rv: CCATGAGCGCATCGCAATC; *Bax*-Fw: CCGGCGAATTGGAGATGAACT; *Bax*-Rv: CCAGCCCATGATGGTTCTGAT.

For protein analysis, cells were lysed in Carin lysis buffer (20 mM Tris-HCl pH 8.0, 138 mM NaCl, 10mM EDTA, 100 mM NaF, 1% NP-40, 10% glycerol, 2mM sodium vanadate) supplemented with 0.5 mM DTT and the protease inhibitor SigmaFast (Sigma-Aldrich). 32 µg of protein per condition were denatured and separated on a Novex NuPage 4-12% Bis-Tris Gradient gel (Life Technologies) and transferred to Protran BA83 blotting paper (GE Healthcare Sciences). After blocking, membranes were incubated overnight at 4°C with the following primary antibodies: goat polyclonal anti-SBDS (Santa Cruz, S-15, 1:200); rabbit polyclonal anti- p53 (Leica, CM5, 1:2000). Beta-actin was used as a loading control (mouse monoclonal anti-beta-actin, clone AC-15, Sigma-Aldrich, 1:10,000 dilution). After washing, blots were incubated with the following secondary antibody: IRDye 800CW Donkey anti-Goat IgG (H + L), IRDye® 800CW Donkey anti-Rabbit IgG (H + L), and IRDye 800CW Donkey anti-mouse IgG (H + L) (all from Li-COR and diluted 1:10,000). After final washing steps, Western blots were scanned and processed using an Odyssey Infrared Imager (Li-COR Biosciences).

### HSPCs in vitro culture, S100A8/9 exposure and CFU-C assay

LKS and $Lin^-$ c-$Kit^+$ $Sca\text{-}1^-$ cells were sorted from wild type C57BL/6 mice and cultured in a serum-free medium, with the following composition: X-Vivo 15 (Lonza), 1% detoxified BSA, 50 µM β-mercaptoethanol (Life Technologies), 1:100 GlutaMAX™ Supplement (Life Technologies), 20 ng/ml recombinant murine SCF (Peprotech), 100 ng/ml recombinant murine Flt3-Ligand (Peprotech), 1:100 penicillin-streptomycin mixture (Life Technologies). The medium was supplemented with recombinant murine S100A8/9, produced with the same methods described earlier (Vogl et al., 2006), at a final, clinically relevant concentration of 25-50 µg/ml, in the range of concentrations measured in the bone marrow supernatants of MDS patients (List, 2014). A heat-inactivated control was obtained by incubating S100A8/9 at 80°C for 30 min; the protein was cooled-down and next added to the HSPC medium

with the same concentration and volume as S100A8/9. LKS and $Lin^-$ c-$Kit^+$ Sca-$1^-$ cells were cultured in 96-well plates at a cell density of $2.5x10^4$ cells/well.

For human studies, cryopreserved $CD34^+$ cells were used, which were isolated from cord blood obtained under informed consent by Ficoll gradient and MACS separation (Miltenyi Biotec). Thawed cells were resuspended in StemSpan SFEM II (STEMCELL Technologies) and recombinant human S100A8/9 was added (R&D systems) at a final concentration of 50 µg/ml. For the control medium, an equal volume of vehicle (PBS) was added. Cells were seeded in flat bottom 96 well-plates ($5x10^4$ cells/well).

For both mouse and human studies, cells were harvested at 4h for γH2AX and cell cycle studies and at 24 h for apoptosis assay.

To assess the effect of S100A9 on HSPC function, $CD34^+$ cord blood cells were resuspended in SFEM1 medium (Stemcell Technologies) containing SCF (50 ng/ml) and human recombinant S100A9 (2.5 µg/ml,ProSpec) or PBS control and seeded in 96-well plates ($2x10^4$ cells/well). After one week of preconditioning (37ºC, 5% $CO_2$), cells were pooled. 2,000 cells per condition were resuspended in 400 µl IMDM and transferred to 3.6 ml of MethoCult H84434 (Stemcell Technologies). Cells were plated in triplicate on 1 $cm^2$ petri-dishes (1 ml/dish) and incubated at 37ºC/5% CO2. Colonies were counted after 12-14 days.

## SUPPLEMENTAL REFERENCES

Derkx, P., Nigg, A.L., Bosman, F.T., Birkenhager-Frenkel, D.H., Houtsmuller, A.B., Pols, H.A., and van Leeuwen, J.P. (1998). Immunolocalization and quantification of noncollagenous bone matrix proteins in methylmethacrylate-embedded adult human bone in combination with histomorphometry. Bone *22*, 367-373.

Gruber, H.E. (1992). Adaptations of Goldner's Masson trichrome stain for the study of undecalcified plastic embedded bone. Biotech Histochem *67*, 30-34.

List, A. (2014). Myeloid-Derived Suppressor Cells & Altered Innate Immunity in MDS Pathogenesis. http://www.mds-foundation.org/wp-content/uploads/manual/ASH2014/6ListMDSF-ASH-253 12-5-14.pdf

Robinson, J.T., Thorvaldsdottir, H., Winckler, W., Guttman, M., Lander, E.S., Getz, G., and Mesirov, J.P. (2011). Integrative genomics viewer. Nat Biotechnol *29*, 24-26.

van der Eerden, B.C., Oei, L., Roschger, P., Fratzl-Zelman, N., Hoenderop, J.G., van Schoor, N.M., Pettersson-Kymmer, U., Schreuders-Koedam, M., Uitterlinden, A.G., Hofman, A.*, et al.* (2013). TRPV4 deficiency causes sexual dimorphism in bone metabolism and osteoporotic fracture risk. Bone *57*, 443-454.

Vogl, T., Eisenblatter, M., Voller, T., Zenker, S., Hermann, S., van Lent, P., Faust, A., Geyer, C., Petersen, B., Roebrock, K.*, et al.* (2014). Alarmin S100A8/S100A9 as a biomarker for molecular imaging of local inflammatory activity. Nat Commun *5*, 4593.

Vogl, T., Leukert, N., Barczyk, K., Strupat, K., and Roth, J. (2006). Biophysical characterization of S100A8 and S100A9 in the absence and presence of bivalent cations. Biochim Biophys Acta *1763*, 1298-1306.

# 4

# ACTIVATION OF NF-κB DRIVEN INFLAMMATORY PROGRAMS IN MESENCHYMAL ELEMENTS IS A BIOLOGIC COMMONALITY IN LOW-RISK MYELODYSPLASTIC SYNDROMES

Si Chen,[1] Zhen Ping,[1] Keane Kenswil,[1] Sjoerd J.F. Hermans,[1] Eric M.J. Bindels,[1] Athina M. Mylona,[1] Niken M. Adisty,[1] Remco M. Hoogenboezem,[1] Mathijs A. Sanders,[1] Eline M.P. Cremers,[3] Theresia M. Westers,[3] Dicky J. Lindenbergh-Kortleve,[2] Janneke N. Samsom,[2] Arjan A. van de Loosdrecht,[3] and Marc H.G.P Raaijmakers[1]

[1]Department of Hematology, Erasmus MC Cancer Institute, Rotterdam, the Netherlands;
[2]Laboratory of Pediatrics, Division of Gastroenterology and Nutrition, Erasmus MC University Medical Center, Rotterdam, the Netherlands;
[3]Department of Hematology, VU University Medical Center, Amsterdam, the Netherlands

Correspondence: Marc H.G.P, Raaijmakers, MD, PhD.
Faculty Building Rm Ee-1393
Department of Hematology and Erasmus Stem Cell Institute
Erasmus University Medical Center
Wytemaweg 80, 3015 CN, Rotterdam
the Netherlands
m.h.g.raaijmakers@erasmusmc.nl

*Manuscript submitted*

## KEY POINTS:

1. Activation of NF-κB signaling in mesenchymal cells is a biologic commonality in LR-MDS.

2. Activation of NF-κB in mesenchymal cells leads to transcriptional overexpression of inflammatory factors including negative regulators of hematopoiesis.

3. Activation of NF-κB attenuates HSPC numbers and function *ex vivo.*

## ABSTRACT

Myelodysplastic syndromes (MDS) are bone marrow failure states characterized by ineffective hematopoiesis and the propensity for malignant transformation. Accumulating evidence supports a contribution of the mesenchymal microenvironment to disease pathogenesis. Mesenchymal inflammation has been demonstrated to play an important role but the underlying programs driving these inflammatory alterations remain incompletely understood.

Here, we show that activation of NF-κB signaling in mesenchymal cells is a biologic commonality in low-risk MDS, driving transcriptional activation of inflammatory programs and attenuating HSPC function. Gene set enrichment analysis of the transcriptome of highly purified mesenchymal cells from 45 low-risk MDS patients revealed activation of NF-κB signaling and upregulation of putative downstream genes encoding inflammatory factors. Overexpression of the *NFκBIA* gene, reflecting activation of the NF-κB pathway, supported the notion that the pathway is overexpressed in mesenchymal cells in the vast majority of patients. Experimental activation of NF-κB signaling in mesenchymal precursor cells *ex vivo*, recapitulated transcriptional activation of inflammatory factors and negative regulators of hematopoiesis observed in patient cells. Finally, mesenchymal activation of NF-κB attenuated normal HSPC function in co-culture systems.

Collectively, the data provide human disease relevance to murine studies implicating NF-κB activation in ancillary cells in bone marrow failure and support the notion that NF-κB is a potential therapeutic target in MDS.

## INTRODUCTION

Myelodysplastic syndromes (MDS) are clonal disorders characterized by ineffective hematopoiesis and the propensity for leukemic transformation. Cumulating evidence has challenged the traditional view that MDS is exclusively driven by hematopoietic cell intrinsic factors. Mesenchymal cells in the bone marrow (BM) microenvironment have emerged as key players in disease pathogenesis, as either initiating or contributing factors.[1-5] We have earlier demonstrated that the transcriptional landscape of highly purified mesenchymal elements from human low risk MDS (LR-MDS) is distinct from normal mesenchymal cells and characterized by cellular stress and the upregulation of inflammatory molecules with known inhibitory effects on normal hematopoiesis.[5] Specifically, mesenchymal overexpression of the alarmins S100A8/9 was shown to drive genotoxic stress in hematopoietic stem/progenitor cells (HSPCs) and are related to leukemic evolution in a subset of LR-MDS patients.[4] An important question emerging from these findings is the nature of the upstream drivers of cellular stress and inflammatory programs in LR-MDS mesenchyme. Here, we show that activation of NF-κB in mesenchymal cells is a biologic commonality in LR-MDS, driving transcriptional activation of inflammatory programs and attenuating HSPC function.



## RESULTS AND DISCUSSION

### Mesenchymal NF-κB activation is a biologic commonality in LR-MDS

We earlier reported on the elucidation of the transcriptome of highly purified mesenchymal cells isolated from LR-MDS patients (n=45) by massive parallel RNA sequencing[4], suggesting inflammation in these mesenchymal elements. In order to identify candidate master regulatory pathways upstream of inflammatory programs in LR-MDS, we performed Gene Set Enrichment Analysis (GSEA) comparing the transcriptomes of these 45 patients to mesenchymal cells purified from healthy controls (n=10).[5] In total, 120 gene signatures were significantly enriched in the LR-MDS mesenchyme, while 8 signatures were enriched in normal mesenchymal cells. Among the signatures upregulated in LR-MDS patients was a remarkable abundance of signatures related to the activation of the Nuclear Factor-kappa B (NF-κB) family of transcription factors in LR-MDS (Figure 1A, 1B). To corroborate the notion of activation of this pathway and provide better insight into the heterogeneity within the population, we assessed the expression levels of NF-κB inhibitor *NFκBIA* (also known as *IκB-α*), which forms an autoregulatory loop with activated NF-κB transcription factors and therefore directly reflects activation of NF-κB signaling.[6-8] Overexpression of *NFκBIA* was found in the vast majority of patients, suggesting that mesenchymal NF-κB activation is probably not specific to a subgroup of patients but a general feature in LR-MDS (Figure 1C). To confirm functional activation of NF-κB in mesenchymal elements

in LR-MDS, we demonstrated increased phosphorylation of p65, a component of the activated NF-κB complex, in intramedullary located CD271$^+$ mesenchymal cells (Figure 1D) as well as in bone-lining CD271$^+$ stromal cells (Figure 1E-F). Moreover, our earlier report has demonstrated that many of the overexpressed inflammatory cytokines and negative regulators of hematopoiesis (including *IL6, IL8, CXCL4, CCL3, INHBA, FTH1, LTF* and *CCL5*)[5] in LR-MDS mesenchyme are *bona fide* NF-κB downstream targets.

To begin understanding whether activation of NF-κB signaling is an intrinsic feature of the mesenchyme, or rather dependent on the tissue context, we compared the transcriptome of *ex vivo* expanded mesenchymal cells from LR-MDS patients (n=5)[3] to the transcriptome of the n=45 mesenchymal cells directly sorted from LR-MDS bone marrow. This analysis revealed significant enrichment of NF-κB pathway and genes encoding inflammatory factors in then tissue-sorted cells (Figure S1), suggesting that activation of NF-κB in mesenchymal cells is dependent on signaling in the diseased marrow.

## Activation of NF-κB in mesenchymal cells induces transcriptional upregulation of inflammatory cytokines

While the genes encoding inflammatory factors and negative regulators of hematopoiesis[5] are *bona fide* downstream targets of NF-κB signaling in other systems, we next wanted to provide experimental support for the view that NF-κB activation specifically in mesenchymal precursor cells results in upregulation of these targets. To this end, we designed a strategy of activating NF-κB signaling in OP9 mesenchymal progenitor cells by stably overexpressing the constitutively active form of IKK2 (FLAG-IKK2SE), a kinase upstream regulator of NF-κB, via a lentiviral vector (Figure 2A, Figure S2A-C).[9-11] OP9 cells, like CD271$^+$ cells[5] express osteolineage commitment markers as well as HSPC regulatory factors and robustly support the expansion of human HSPCs.[12] NF-κB activation in OP9 cells resulted in overexpression of the canonical NF-κB downstream targets and several negative regulators of hematopoiesis, including *Il6*, *Cxcl2* (murine homologue of *IL8*), *Ccl3*, *Inhba, Fth1, Ltf, Ccl5 and Cxcl4* (Figure 2B). Interestingly, activation of NF-κB in OP9 cells also resulted in transcriptional upregulation of the alarmins *S100a8* and *S100a9* (Figure 2B) recently described by us to drive genotoxic stress in HSPCs associated with increased likelihood of leukemic transformation.[4] Similar to results in OP9 cells, activation of NF-κB in human mesenchymal cells (HS5 cell line and expanded bone-marrow-derived primary mesenchymal cells) (Figure S2D) also resulted in upregulation of NF-κB downstream targets including negative regulators of hematopoiesis such as *IL6, IL8, CCL3, S100A9, INHBA*, and *CCL5*. (Figure S2E). Together, the data link the transcriptional landscape of inflammatory alterations in mesenchymal cells to activation of NF-κB in LR-MDS.

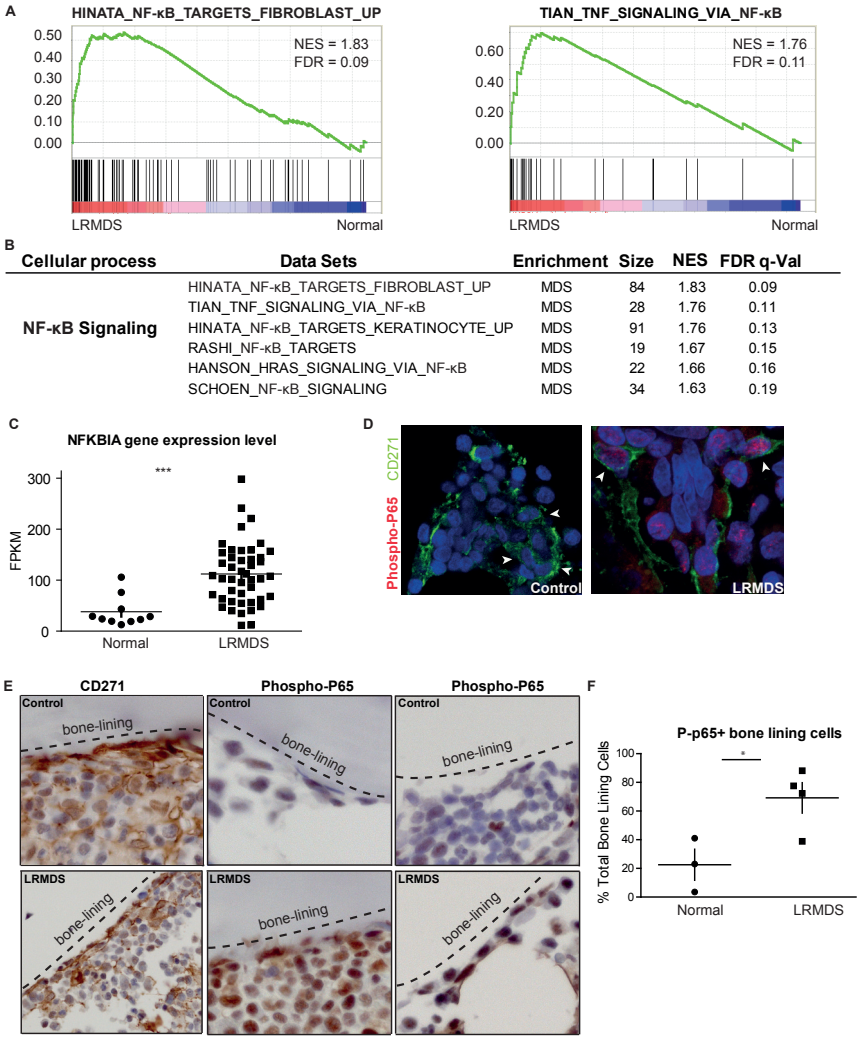


**Figure 1. Activation of NF-κB mediated signaling in LR-MDS mesenchymal cells.** (A) Representative GSEA plots demonstrating activation of NF-κB signaling in mesenchymal cells from LR- MDS. (B) Summary of gene sets implicating NF-κB activation in mesenchymal cells from 45 LR-MDS patients. Gene set size, NES, and FDR value of each gene set are as listed. GSEA: gene sets enrichment analysis. NES: normalized enrichment score. FDR: false discovery rate. (C) Gene expression level (in FPKM) of NFKBIA in normal and LR-MDS samples. (D) Representative images showing immunofluorescence staining of CD271 and phospho-p65 in both age-matched control (left panel) and LR-MDS patient (ight panel) bone marrow slides confirming activation of NF-κB in mesenchymal cells. The white arrow indicates the absence or presence of nuclear phospho-p65 signal (red) in $CD271^+$ (green) mesenchymal cells. The nuclei were counterstained with DAPI. (E) Representative photomicrographs of the distribution of $CD271^+$ mesenchymal cells (left panels). These cells are enriched at the endosteal surface (marked by bone-lining area) and have a spindle-shaped morphology. Representative immuno-histochemical analysis of phospho-p65 (middle and right panels) in age-matched controls (top) and LR-MDS (bottom) patients, demonstrating NF-κB activation in spindle-shaped endosteal cells in LR-MDS. (F) The percentage of phospho-p65+ bone lining cells as a fraction of the total bone lining cells in LR-MDS (n=4) compared to age-matched controls (n=3). *** $P < .001$ * $P < .05$ FPKM: fragments per kilobase of exon per million fragments mapped. *NFKBIA*: NF-Kappa-B Inhibitor Alpha

### Mesenchymal activation of NF-κB attenuates HSPC numbers and function

As earlier reported, in human MDS, the majority of $CD34^+$ HSPCs is in direct contact with $CD271^+$ mesenchymal cells.[13] To assess the effect of NF-κB activation in mesenchymal cells on the biology of normal HSPC, we performed co-culture experiments with cord blood $CD34^+$ HSPCs and OP9 cells transduced with IKK2SE or empty vector (EV) (Figure 2C). Co-culture for 7 days on IKK2SE-transduced OP9 cells resulted in significantly reduced numbers of immunophenotypically-defined HSPC in comparison to EV-transduced mesenchymal cells (Figure 2D). This included the fraction enriched for long-term hematopoietic stem cells (LT-HSCs) defined by the markers $CD34^+CD38^-CD45^-CD90^-$, as well as primitive ($CD34^+CD38^-$) and committed $CD34^+CD38^+$ progenitor cells (Figure 2D). In addition, reduced HSPC number was reflected in a reduced number of CFU-Cs (Figure 2E), indicating attenuation of progenitor function in this setting.

Collectively, in this brief communication, we demonstrate that mesenchymal NF-κB activation is a biological commonality in LR-MDS patients leading to transcriptional upregulation of inflammatory programs associated with negative regulation of hematopoiesis and attenuation of HSPC numbers and function.

Demonstration of mesenchymal activation of NF-κB provides human disease relevance to a number of murine studies implicating NF-κB activation in ancillary cells to the pathogenesis of hematopoietic disease. NF-κB activation in non-hematopoietic cells has been shown to induce 'MDS-like' myeloproliferative disease (MPD) in mice.[14] In another study, NF-κB activation in bone marrow mesenchymal cells and endothelial cells, as a result of elevated levels of the microRNA miR-155, generated a persistent pro-inflammatory state of the bone marrow niche leading to a MPD-like disease in a Notch/RBPJ loss-of-function mouse model.[15] In addition to a potential role in driving myeloid hematopoietic disease, other studies have implicated stromal NF-κB activation in the survival and chemoresistance of malignant cells in chronic lymphocytic leukemia (CLL) and AML.[16,17] Our experimental data demonstrate that NF-κB activation in the mesenchyme attenuates normal hematopoiesis, which is of key relevance as a common feature of LR-MDS is characterized by cytopenia. The implication of mesenchymal NF-κB activation in the pathogenesis of MDS may also point towards common mechanisms between the pathogenesis of MDS and oncogenesis in other systems. NF-κB mediated chronic tissue inflammation has been shown to drive cancer initiation and progression via secretion of cytokines and soluble factors in models of several other forms of cancer,[18-20] including skin, prostate and colon cancer.[21-23] In these models, activation of NF-κB signaling, specifically in fibroblasts, promoted malignant features in heterotypic (pre) cancerous cells, supporting the hypothesis that mesenchymal inflammation may facilitate tumorigenesis in the hematopoietic system as well.

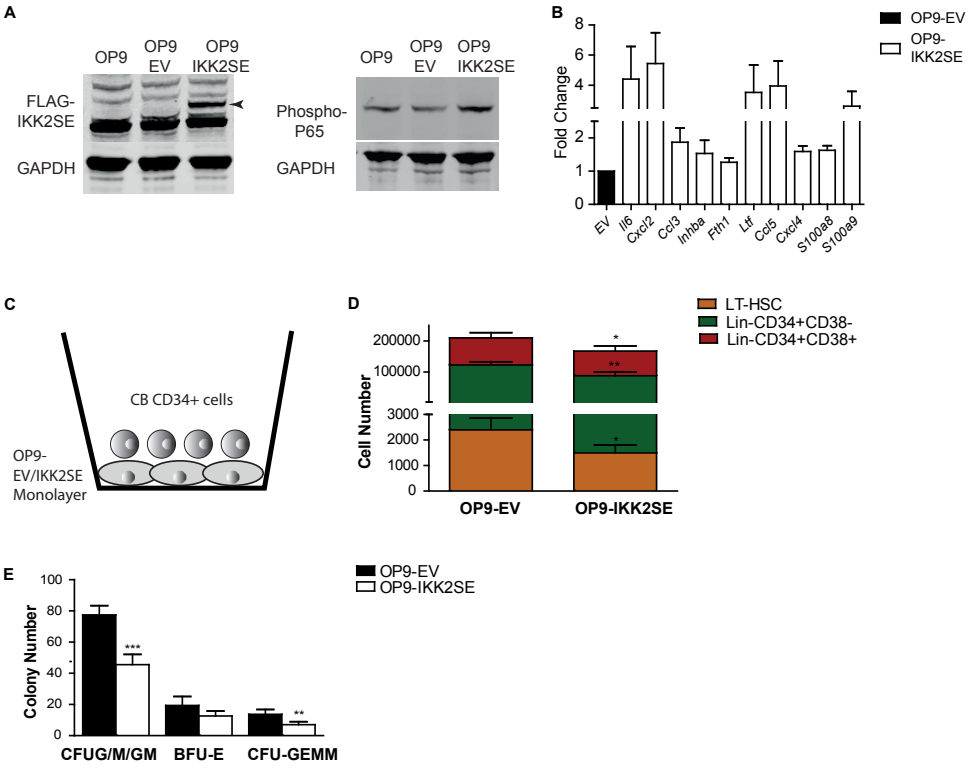


**Figure 2. Activated NF-κB signaling in mesenchymal cells attenuates HSPC number and function.** (A) Western blot analysis showing the overexpression of Flag-IKK2SE and nuclear phospho-p65, the phosphorylated (active) form of NF-κB, in IKK2SE transduced OP9 cells in comparison to empty vector (EV)-transduced or wild-type cells (B) Expression level of NF-κB downstream targets (*Il6, Cxcl2*) and disease-relevant negative regulators of hematopoiesis[4,5] in OP9 cells transduced with IKK2SE. Fold change relative to EV is presented. (n=3 for each transcript) (C) Experimental strategy of co-culture experiments with cord blood CD34+ HSPCs and OP9 stromal cells transduced with either EV or IKK2SE. The co-culture took place for 7 days before analysis. (D) The absolute number of immunophenotypically defined HSPCs subsets ($Lin^-CD34^+CD38^+$ progenitors, $Lin^-CD34^+CD38^-$ HSPCs, $Lin^-CD34^+CD38^-CD45^-CD90^-$ LT-HSCs) on day 7 after co-culturing with OP9-EV or OP9-IKK2SE (n=4). (E) The total number of CFU-C after 7 days co-culture (n=4). *** $P < .001$ ** $P < .01$ * $P < .05$

The activation of NF-κB signaling in mesenchymal cells in most LR-MDS patients raises intriguing questions about the events driving this activation. This includes the question whether mesenchymal cell-intrinsic alterations or extrinsic events are driving NF-κB activation. While the answer to this question remains speculative in the absence of experimental evidence (and may vary between patients), our finding that NF-κB activation separates *in situ* mesenchymal elements from their *ex vivo* expanded counterparts may argue for cell-extrinsic determinants. This notion is supported by recent findings where activation of the NF-κB pathway in $CD34^+$ HSPCs is implicated in MDS pathogenesis[24] and $CD271^+$ mesenchymal cells co-localize with $CD34^+$ HSPC in the bone marrow section of MDS patients.[13] It is therefore reasonable to hypothesize that activated NF-κB pathway in HSPCs signals to the adjacent mesenchymal elements, resulting in NF-κB activation in mesenchymal cells. As NF-κB activation is likely maintained through autocrine/paracrine feedback signaling networks, other cellular types that anatomically localize with the activated HSPCs and mesenchymal elements are probably involved as well, suggesting diverse cellular components may participate in this crosstalk. The combined findings suggest that in LR-MDS, activation of NF-κB occurs in both hematopoietic and mesenchymal cells, likely through autocrine and paracrine feedback signaling networks, leading to a NF-κB-mediated inflammatory milieu in the LR-MDS bone marrow and an overexpression of a repertoire of secreted negative hematopoietic regulators. Among these, was S100A8/9, recently shown by us to induce NF-κB activation and genotoxic stress in HSPC and to be associated with an increased likelihood of leukemic transformation. Regulation of S100A8/9 in mesenchymal cells, however, is likely to be more complex in order to explain the heterogeneity of overexpression between LR-MDS patients and may include upstream TP53 activation.[4]

Taken together, the findings support the notion that mesenchymal factors, in addition to hematopoietic cell autonomous characteristics, may be therapeutically targeted in LR-MDS and warrant ongoing experiments defining the contribution of NF-κB activation and inflammation to ineffective hematopoiesis and leukemic evolution in MDS.

**Acknowledgements**

The authors thank O. Roovers, P. van Geel and Dr. W.J.C. Chikhovskaya - Rombouts for their technical support, Dr. King Lam for providing healthy and MDS bone marrow biopsies, Dr. H. Schepers and dr. J.J.. Schuringa for providing the retroviral construct pMIG HA-IKK-2 S177E S181E and prof. I. Touw for helpful comments on the manuscript.

This work was supported by grants from the Dutch Cancer Society (KWF Kankerbestrijding) (EMCR 2010-4733), the Netherlands Organization of Scientific Research (NWO 90700422) and the Netherlands Genomics Initiative (40-41009-98-11062) to MHGPR.

**Authorship**

S.C and M.H.G.P.R designed studies; S.C, Z.P., K.K, E.M.J.B., A.M.M, D.J.L-K and S.J.F.H performed experiments and acquired data; S.C, R.M.H, E.M.J.B, and M.A.S provided technical guidance and bioinformatical analysis; J.N.S provided helpful insights in immunohistochemical data analysis; T.M.W, E.M.P.C and A.vd.L provided patient material; S.C and M.H.G.P.R. wrote the manuscript; all authors were involved in data interpretation and manuscript reviewing, M.H.G.P.R supervised the study.

Conflict-of-interest disclosure: The authors declare no competing financial interests

## REFERENCES


1. Raaijmakers MH, Mukherjee S, Guo S, et al. Bone progenitor dysfunction induces myelodysplasia and secondary leukaemia. *Nature*. 2010;464(7290):852-857.
2. Kode A, Manavalan JS, Mosialou I, et al. Leukaemogenesis induced by an activating beta-catenin mutation in osteoblasts. *Nature*. 2014;506(7487):240-244.
3. Medyouf H, Mossner M, Jann JC, et al. Myelodysplastic cells in patients reprogram mesenchymal stromal cells to establish a transplantable stem cell niche disease unit. *Cell Stem Cell*. 2014;14(6):824-837.
4. Zambetti NA, Ping Z, Chen S, et al. Mesenchymal Inflammation Drives Genotoxic Stress in Hematopoietic Stem Cells and Predicts Disease Evolution in Human Pre-leukemia. *Cell Stem Cell*. 2016;19(5):613-627.
5. Chen S, Zambetti NA, Bindels EM, et al. Massive parallel RNA sequencing of highly purified mesenchymal elements in low-risk MDS reveals tissue-context-dependent activation of inflammatory programs. *Leukemia*. 2016;30(9):1938-1942.
6. Brown K, Park S, Kanno T, Franzoso G, Siebenlist U. Mutual regulation of the transcriptional activator NF-kappa B and its inhibitor, I kappa B-alpha. *Proc Natl Acad Sci U S A*. 1993;90(6):2532-2536.
7. Paciolla M, Boni R, Fusco F, et al. Nuclear factor-kappa-B-inhibitor alpha (NFKBIA) is a developmental marker of NF-kappa B/p65 activation during in vitro oocyte maturation and early embryogenesis. *Human Reproduction*. 2011;26(5):1191-1201.
8. Sun SC, Ganchi PA, Ballard DW, Greene WC. Nf-Kappa-B Controls Expression of Inhibitor I-Kappa-B-Alpha - Evidence for an Inducible Autoregulatory Pathway. *Science*. 1993;259(5103):1912-1915.
9. Bosman MC, Schepers H, Jaques J, et al. The TAK1-NF-kappaB axis as therapeutic target for AML. *Blood*. 2014;124(20):3130-3140.
10. Schepers H, Eggen BJ, Schuringa JJ, Vellenga E. Constitutive activation of NF-kappa B is not sufficient to disturb normal steady-state hematopoiesis. *Haematologica*. 2006;91(12):1710-1711.
11. Mercurio F, Zhu H, Murray BW, et al. IKK-1 and IKK-2: cytokine-activated IkappaB kinases essential for NF-kappaB activation. *Science*. 1997;278(5339):860-866.
12. Vodyanik MA, Bork JA, Thomson JA, Slukvin, II. Human embryonic stem cell-derived CD34+ cells: efficient production in the coculture with OP9 stromal cells and analysis of lymphohematopoietic potential. *Blood*. 2005;105(2):617-626.
13. Flores-Figueroa E, Varma S, Montgomery K, Greenberg PL, Gratzinger D. Distinctive contact between CD34+ hematopoietic progenitors and CXCL12+ CD271+ mesenchymal stromal cells in benign and myelodysplastic bone marrow. *Lab Invest*. 2012;92(9):1330-1341.
14. Rupec RA, Jundt F, Rebholz B, et al. Stroma-mediated dysregulation of myelopolesis in mice lackingk l kappa B alpha. *Immunity*. 2005;22(4):479-491.
15. Wang L, Zhang H, Rodriguez S, et al. Notch-dependent repression of miR-155 in the bone marrow niche regulates hematopoiesis in an NF-kappaB-dependent manner. *Cell Stem Cell*. 2014;15(1):51-65.
16. Jacamo R, Chen Y, Wang Z, et al. Reciprocal leukemia-stroma VCAM-1/VLA-4-dependent activation of NF-kappaB mediates chemoresistance. *Blood*. 2014;123(17):2691-2702.
17. Lutzny G, Kocher T, Schmidt-Supprian M, et al. Protein kinase c-beta-dependent activation of NF-kappaB in stromal cells is indispensable for the survival of chronic lymphocytic leukemia B cells in vivo. *Cancer Cell*. 2013;23(1):77-92.

18. DiDonato JA, Mercurio F, Karin M. NF-kappaB and the link between inflammation and cancer. *Immunol Rev*. 2012;246(1):379-400.

19. Karin M, Greten FR. NF-kappaB: linking inflammation and immunity to cancer development and progression. *Nat Rev Immunol*. 2005;5(10):749-759.

20. Pikarsky E, Porat RM, Stein I, et al. NF-kappaB functions as a tumour promoter in inflammation-associated cancer. *Nature*. 2004;431(7007):461-466.

21. Erez N, Truitt M, Olson P, Arron ST, Hanahan D. Cancer-Associated Fibroblasts Are Activated in Incipient Neoplasia to Orchestrate Tumor-Promoting Inflammation in an NF-kappaB-Dependent Manner. *Cancer Cell*. 2010;17(2):135-147.

22. Bohonowych JE, Hance MW, Nolan KD, Defee M, Parsons CH, Isaacs JS. Extracellular Hsp90 mediates an NF-kappaB dependent inflammatory stromal program: implications for the prostate tumor microenvironment. *Prostate*. 2014;74(4):395-407.

23. Mueller L, Goumas FA, Affeldt M, et al. Stromal fibroblasts in colorectal liver metastases originate from resident fibroblasts and generate an inflammatory microenvironment. *Am J Pathol*. 2007;171(5):1608-1618.

24. Wei Y, Chen R, Dimicoli S, et al. Global H3K4me3 genome mapping reveals alterations of innate immunity signaling and overexpression of JMJD3 in human myelodysplastic syndrome CD34+ cells. *Leukemia*. 2013;27(11):2177-2186.

# SUPPLEMENTARY MATERIALS

## SUPPLEMENTARY MATERIAL AND METHODS

### Patient and healthy donor bone marrow samples

Bone marrow samples from LR-MDS patients and healthy donors were obtained as previously described, including the clinical characteristics of the patients and information about the healthy donors.[1,2] In short, all 45 patients were part of the HOVON89 clinical trial (HOVON89; www.hovon.nl; www.trialregister.nl as NTR1825; EudraCT No. 2008-002195-10) where patients with low or intermediate-1 risk MDS based on IPSS criteria were recruited. The healthy controls were obtained from donors for allogeneic transplantation. All samples were collected with informed consent, approved by the Institutional Review Board of the Erasmus Medical Center, the Netherlands, in accordance with the declaration of Helsinki.

### Flow cytometry analysis

Sorting of the mesenchymal cells from the bone marrow of patients and normal donors were performed by FACS as previously described.[1,2] The cells were directly sorted in 800µl Trizol (Ambion) for RNA isolation.

For immunophenotyping of CD34+ HSPCs after 7 days of co-culture, the following antibodies were used based on earlier work with optimized dilutions: Lin-APC (1:25), CD34-PE-Cy7 (1:30), CD38-PercP-Cy5.5 (1:60), CD90-PE (1:30) and CD45RA-APC-H7 (1:30).[3] Live cells were selected based on the DAPI (1:5000) gate. The gating strategy defining the different subsets of HSPCs is illustrated in supplemental Figure 2F-G. The OP9 stromal cells were excluded based on ZsGreen expression, as the transduced OP9 cells (higher than 99% efficiency) were ZsGreen (GFP) positive (Figure S2C). The data was acquired using a LSRII flow cytometer (BD) and analyzed using FlowJo software.

Counting of the cells after 7 days of co-culture was accurately obtained with flow-count fluorosphere beads (Beckman Coulter), in combination with the following antibodies: CD34-PE-Cy7 (1:30) and CD45-PB (1:50). The gating strategy is shown in Figure S2H. The data was acquired using a LSRII flow cytometer (BD Biosciences) and analyzed using FlowJo software. The number of cells was calculated based on the following formula: CD34+ cells per µl = (Live CD34+ events x bead concentration)/number of acquired single beads/(volume beads/volume cells). The number of total mononuclear cells (MNCs) determined by cell counting with beads and frequency of each HSPCs subpopulation from immunophenotyping were combined to obtain the number of cells present in individual subpopulations.

### RNA extraction and RNA quality control

Total sample RNA isolation was performed according to the standard protocol of RNA isolation with Trizol and GenElute LPA (Sigma). In the end, the RNA pellet was resuspended in 7.5µl of RNAse free water (Qiagen) and quality and quantity of the total RNA was checked on a 2100 Bio-analyzer (Agilent) using the Agilent RNA 6000 Pico Kit.

### RNA sequencing and gene expression profiling

RNA sequencing and the downstream data processing were as previously described.[1,2] In short, SMARTer Ultra Low RNA Kit (Clonetech) for Illumina Sequencing was used to prepare the cDNA based on the manufacture's protocol. Once the cDNAs were obtained, the subsequent library preparation steps, sequencing and alignments were performed as earlier described, using a range of tools including the cutadapt program, TopHat2 and cufflinks.[4] The resulting gene expression values are measured as FPKM (Fragments per kilobase of exon per million fragments mapped). Fragment counts were determined per gene with HTSeq-count, utilizing the strict intersection option, and subsequently used for differential expression analysis using the DESeq2 package, with standard parameters, in the R environment. Multiple testing correction was performed with the Benjamini-Hochberg procedure to control the False Discovery Rate (FDR). Finally gene set enrichment analysis (GSEA) was performed on the FPKM values using the curated C2 collection of gene sets within MSigDB.5

Direct comparison between gene expression data from purified and ex vivo expanded LR-MDS mesenchymal cells was performed as previously described.[2] In brief, BAM files containing the molecular data of *ex vivo* expanded stromal cells derived from LR-MDS patients (n=5)[6] were obtained from the European Genome-Phenome Archive data base (EGAS00001000716). Gene set enrichment analysis (GSEA) was then performed comparing our gene expression data of the purified LR-MDS mesenchymal cells (n=45) to the gene expression data of expanded stromal cells (n=5).[5]

### Immunohistochemistry and immunofluorescence

Immunohistochemical and immunofluorescence stainings of LR-MDS and control paraffin-embedded bone marrow slides were performed as previously described (supplemental Methods).[7] CD271 and phospho-p65 antibodies were used to mark the stromal cells of interest with their corresponding phospho-p65 status. Immunohistochemical single staining facilitated the enumeration of phospho-p65$^+$ bone lining stromal cells; whereas the immunofluorescence double staining demonstrated the co-localization of CD271$^+$ and phospho-p65$^+$ cells in patient and control sections.

All the bone marrow sections (5-µm) were deparaffinized in xylene and hydrated in a graded series of alcohol. Antigen retrieval was achieved by microwave treatment in citrate buffer (10mM pH 6.0) and blocking of the endogenous peroxidases was performed with 3% $H_2O_2$ in PBS. For IHC staining, sections were blocked using 10% normal human and goat serum (DAKO) in Teng-T solution (10 mM Tris, 5 mM EDTA, 0.15 M SodiumCl, 0.25 % gelatine, 0.05 % Tween-20) followed by an overnight incubation at 4°C with primary antibody: rabbit anti-human phospho Serine 276 of p65 (p-p65, active form; Santa Cruz Biotechnology) diluted 1:400, CD271 (Sigma Aldrich) diluted 1:200, or normal rabbit immunoglobulin (DAKO) diluted accordingly. Immunoreactions were detected using biotinylated secondary antibody (goat anti-rabbit, 1:2000 dilution) with Vectastain ABC Elite Kit (Vector Laboratories) and 3,3'-diaminobenzidine tetrahydrochloride (Sigma Aldrich). For all stainings, nuclei were counterstained with haematoxylin (Vector Laboratories). Images of stained tissues were acquired using a Leica DM5500B upright microscope with 40x lenses and LAS-AF image acquisition software (Leica). The number of phospho-p65+ bone lining cells were manually quantified using ImageJ software from x40 photomicrographs of blindly selected trabecular bone area. Unpaired t-test was performed and $p < .05$ was considered significant.

For IF staining, sections were blocked with 10% normal human, goat and horse serum (DAKO) in Teng-T solution followed by an overnight incubation at 4°C with a primary antibody directed against phospho Serine 276 of p65. The next day, biotinylated goat anti-rabbit secondary antibody and streptavidin-Dylight 594 (1:200, Vector Laboratories) were incubated consecutively. This was followed by an additional incubation with a primary mouse anti-human antibody directed against CD271 (1:100, eBioscience) followed by conjugated horse anti-mouse Dylight 488 (1:200, Vector Laboratories). Counterstain with DAPI and mounting were performed using Vectashield mounting medium (Vector Laboratories, H-1200). Control slides with single stains for the primary antibodies CD271 or phospho-p65 combined with all conjugated secondary antibodies were performed as a background control. Images were acquired on a Leica SP5 confocal laser scan microscope equipped with Diode/Argon/HeNe lasers using a 40x planapochromat oil immersion objective. Images were analyzed using ImageJ software.

### Lentiviral transduction of OP9, HS5 and primary expanded stromal cells

The plasmid containing mutant form of IKK-2 (FlagIKK-2 S177E S181E; referred hereafter as IKK2SE), which has previously been demonstrated to result in constitutive NF-κB activation, was obtained from Addgene.[8,9] The Flag-IKK2SE fragment was recloned into the pHAGE ires ZsGreen lentiviral vector (kindly provided by Dr. R. Delwel). Stable transduction of OP9 cells with pHAGE-EV and IKK2SE was performed and transduction efficiency was determined by FACS measuring ZsGreen expression of the cells (Figure S2C). Overexpression of IKK2SE was confirmed by Western blotting against Flag-tag and the subsequent activation of NF-κB was verified using an antibody against the active form of NF-κB: phospho-p65 (Ser 536; Cell Signaling).

Lentivirus for both pHage-EV or pHage IKK2SE (Flag-tagged IKK2 S177E S181E) was produced in 293T cells, by means of transient transfection of the pHage EV or pHage IKK2SE, together with the packaging plasmids pSPAX and pMD2.G. OP9 cells were transduced with equal titer lentivirus and 3 days later OP9-EV or OP9-IKK2SE were used for subsequent co-culture experiments.

The same transduction procedures were carried out for human HS5 stromal cell line and primary expanded stromal cells.

**Luciferase Reporter Assay**

We performed NF-κB responsive luciferase reporter assays to test the functionality of the recloned pHage IKK2SE construct. HEK293T cells were transiently co-transfected with a luciferase vector containing three NF-κB responsive elements together with either pHage EV or pHage IKK2SE. Cells were harvested after 48 hours and luciferase activity was measured with the Dual-Luciferase Reporter Assay System (Promega) using a Victor3 plate reader (PerkinElmer). As a control for the luciferase assay pMIG EV and pMIG HA-IKK2SE were used (Figure S2A and S2B). Luciferase vector containing 3x NF-κB responsive elements and pMIG HA-IKK2SE were kindly provided by Dr. H. Schepers and J.J. Schuringa.[10]

## Western Blotting

Protein extracts were made by lysing cells in Carin lysis buffer (20 mM Tris-HCl pH 8.0, 138 mM NaCl, 10mM EDTA, 100 mM NaF, 1% Nonidet P-40, 10% glycerol, 2mM NA-vanadate) supplemented with 0.5 mM DTT and the protease inhibitor SigmaFast (Sigma Aldrich)and Equal amounts of proteins were denatured and separated on a Novex NuPage 4-12% Bis-Tris Gradient gel (Life Technologies) and transferred to Protran BA83 blotting paper (GE Healthcare Sciences). Primary antibodies mouse anti-Flag (1:1000) (Sigma Aldrich) or Rabbit anti-phospho p65 S536 (1:1000) (Cell Signaling) were incubated overnight at 4°C after necessary blocking step. Flag antibody was used to confirm transfection or transduction efficiency; whereas phospho-P65 was used to demonstrate phospho-p65 overexpression in IKK2SE transduced cells. As secondary antibodies (1:10000 for both) donkey anti-mouse 800 or goat anti-rabbit 800 (Li-COR Biosciences) were used. GAPDH (Santa Cruz Biotechnologies) was used as a loading control (primary: rat anti-GAPDH (1:1000), secondary: donkey anti-rat 680 (1:10000). After the final incubation, Western blots were scanned and processed using an Odyssey Infrared Imager (Li-COR Biosciences).

## Quantitative PCR

Total RNA of OP9-EV, OP9-IKK2SE, HS5-EV, HS5-IKK2SE, primary stroma-EV, primary stroma-IKK2SE cells was isolated 3 days after transduction using Trizol reagent (Ambion), followed by cDNA synthesis using SuperScript II Reverse Transcriptase II kit (Invitrogen). Q-PCR was

performed using Fast SYBR Green master mix (Applied Biosystems) on a 7500 Fast Real-Time PCR system (Applied Biosystems) with the following primer sets:
Murine: *Il6*: Fw 5'-TCGGAGGCTTAATTACACA-3' Rv 5'-CTGGCTTTGTCTTTCTTGTT-3; *Cxcl2* (murine homologue of IL8): Fw 5'-GCGCCCAGACAGAAGT-3' Rv 5'-CGGGTGCTGTTTGTTTT-3'; *Ccl3*: Fw 5'-TTCTCTGTACCATGACACTCTGC-3' Rv 5'-CGTGGAATCTTCCGGCTGTAG-3'; *Inhba*: Fw 5'-TCACCATCCGTCTATTTCAGCA-3' Rv 5'-CTTCCGAGCATCAACTACTTTCT-3'; *Fth1*: Fw 5'-CAAGTGCGCCAGAACTACCA-3' Rv 5'-GCCACATCATCTCGGTCAAAA-3'; *Ltf*: Fw 5'-TGAGGCCCTTGGACTCTGT-3' Rv 5'-ACCCACTTTTCTCATCTCGTTC-3' *Ccl5*: Fw 5'-GCTGCTTTGCCTACCTCTCC-3' Rv 5'-TCGAGTGACAAACACGACTGC-3'; validated all-in-one murine C*xcl4* (PF4) primers (Genecopoeia).
Human*: IL6*: Fw 5'-CCCCCAGGAGAAGATTC-3' Rv 5'- GCTGCTTTCACACATGTTACT-3'; *IL8*: Fw 5'- CCGGAAGGAACCATCT-3' Rv 5'-TTGGGGTGGAAAGGTT-3'; *CCL3*: Fw 5'-GCAACCAGTTCTCTGCATCA-3' Rv 5'-TGGCTGCTCGTCTCAAAGTA-3'; *INHBA*: Fw 5'-ACGGGTATGTGGAGATAGAGGA-3' Rv 5'- GGACTTTTAGGAAGAGCCAGACT-3'; *CCL5*: Fw 5'-CGCTGTCATCCTCATTGCTA-3' Rv 5'-CCATTTCTTCTCTGGGTTGG-3'; *S100A9*: Fw 5'-TTC AAA GAG CTG GTG CGA AAA G-3' Rv 5'-GCA TTT GTG TCC AGG TCC TCC-3'; *Ikk2SE*: Fw 5'-GGTGAGCAGATTGCCATCAAG-3' Rv 5'- ACCCTCAGTTCGCTGGTCTCG-3'

The expression level of each molecule was normalized against the housekeeping gene *Hprt* (in OP9) or *GAPDH* (in HS5 or primary expanded stromal cells) and the fold change of the expression level of each gene in IKK2SE-transduced cells was calculated relative to EV transduced cells.

### Isolation and culture of cord blood CD34+ cells

Informed consent was obtained to use cord blood provided by the Sanquin Bloedbank (the Netherlands). Cord blood mononuclear cells were isolated by Ficoll lymphoprep (Axis-shield) density gradient centrifugation. $CD34^+$ cells were selected by MiniMacs (Miltenyi Biotec) followed by LS and MS MACS separation columns (Miltenyi Biotec) to achieve optimal purity. In the co-culture setting, 15.000 $CD34^+$ cells per 1.9$cm^2$ were directly plated on either a OP9-EV or a OP9-IKK2SE monolayer (Figure 2C). The OP9-EV and OP9-IKK2SE monolayers were at comparable confluence on day 1 and 7 of coculture (data not shown). Culture medium consisted of αMEM supplemented with 20% fetal bovine serum (FBS), 1% penicillin/streptomycin, 50 ng/ml stem cell factor (SCF), 50 ng/ml FLT3 and 50 ng/ml thrombopoietin. All experiments were carried out in triplicates. Cultures were kept at 37°C in a 5% $CO_2$ incubator for 7 days until analysis.

**CFU-C**

On day 7 of the co-culture, 4000 mononuclear cells (MNCs) from each condition were collected and resuspended in IMDM medium. This cell suspension was added to MethoCult™ GF H84434, which allows the growth of colonies from all three lineages, (StemCell Technologies) and triplicate dishes were plated. The methocult plates were kept at 37°C in a 5% $CO_2$ incubator for 2 weeks until colony counting.

## SUPPLEMENTARY FIGURES

A

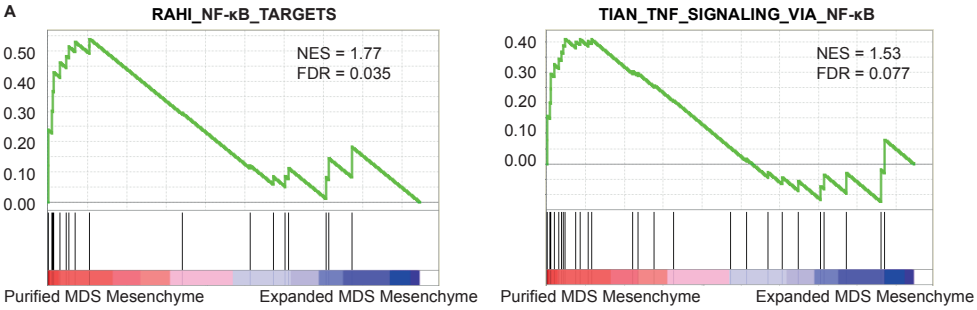


B

| Data Sets | Enrichment | Size | NES | FDR |
|---|---|---|---|---|
| SEKI_INFLAMMATORY_RESPONSE_LPS_UP | Purified MDS Mesenchyme | 76 | 1.84 | 0.030 |
| RASHI_NFKB1_TARGETS | Purified MDS Mesenchyme | 19 | 1.77 | 0.035 |
| DEBOSSCHER_NFKB_TARGETS_REPRESSED_BY_GLUCOCORTICOIDS | Purified MDS Mesenchyme | 24 | 1.74 | 0.041 |
| TIAN_TNF_SIGNALING_VIA_NFKB | Purified MDS Mesenchyme | 28 | 1.53 | 0.077 |

**Supplemental Figure 1. Enrichment of NF-κB signatures in purified (n=45) LR-MDS mesenchymal cells in comparison to expanded (n=5) stromal cells.** (A) Representative GSEA plot demonstrating enrichment of NF-κB signatures in purified LR-MDS mesenchymal cell comparing to expanded stromal cells. (B) A list of NF-κB signatures enriched in purified MDS mesenchyme comparing to the expanded counterparts. NES: normalized enrichment score; FDR: False Discovery Rate.

**Supplemental Figure 2. Activation of NF-κB signaling in OP9, HS5 and expanded primary stromal cells.** (A) Western blot analysis showing the overexpression of Flag-IKK2SE transfected 293T cells in comparison to pHage-empty vector (EV) transfected 293T cells. As a reference for the protein size of Flag-IKK2SE, lysates of pMIG EV and pMIG HA-IKK2SE transfected 293T cells were included. (B) Level of NF-κB luciferase response in pHage-EV and pHage-Flag IKK2 transfected 293T cells (right panel). NF-κB luciferase response in pMIG EV and pMIG HA-IKK2SE transfected 293T cells were included as a positive control. (C) Transduction efficiency of phage EV and pHage-Flag IKK2SE in OP9 cells measured by ZsGreen expression comparing to non-transfected OP9 cells. (D) Expression level of IKK2SE in HS5 and expanded primary mesenchyme transduced with either EV or IKK2SE. (E) Expression level of NF-kB downstream targets and disease-relevant negative regulators of hematopoiesis in HS5 mesenchymal cell lines (left panel) and expanded primary mesenchyme (right panel) transduced with EV or IKK2SE. Fold change relative to EV is presented. (F-G) Representative FACS plots showing the immunophenotypically defined HSPCs subsets after exposing to OP9-EV/IKK2SE in both direct cell contact (F) and transwell system (G). The presented plots were gated on live/OP9-/Lin- mononuclear cells (MNCs). The HSPCs subfractions are defined as: CD34+CD38+ progenitor population, $CD34^{+}CD38^{-}$ HSPCs and $CD34^{+}CD38^{-}CD45^{-}CD90^{-}$ LT-HSCs (long-term hematopoietic stem cells). (H) Representative FACS plot demonstrating the cell counting approach by flow-count fluorosphere beads. Information concerning total number of beads and MNCs were obtained during acquiring on LSRII. OP9 cells were gated out from the MNCs by ZsGreen expression and live cells were selected by 7AAD staining. CD45 and CD34 antibodies were applied to identify the frequency of $CD34^{+}$ HSPCs

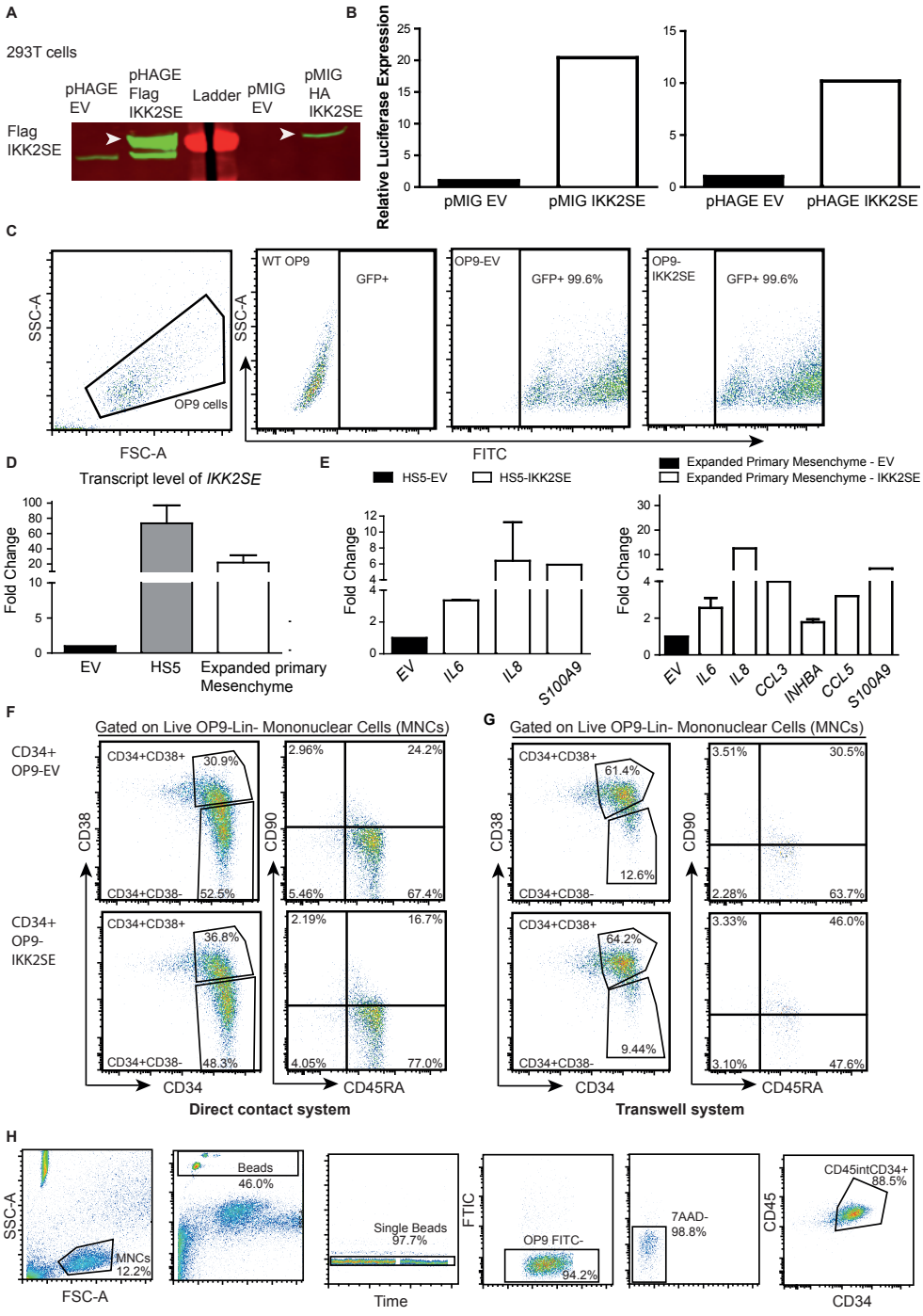
A
293T cells
pHAGE EV
pHAGE Flag IKK2SE
Ladder
pMIG EV
pMIG HA IKK2SE
Flag IKK2SE
B
Relative Luciferase Expression
pMIG EV
pMIG IKK2SE
pHAGE EV
pHAGE IKK2SE
C
SSC-A
FSC-A
OP9 cells
WT OP9
GFP+
OP9-EV
GFP+ 99.6%
OP9-IKK2SE
GFP+ 99.6%
FITC
D
Transcript level of IKK2SE
Fold Change
EV
HS5
Expanded primary Mesenchyme
E
HS5-EV
HS5-IKK2SE
Expanded Primary Mesenchyme - EV
Expanded Primary Mesenchyme - IKK2SE
Fold Change
EV
IL6
IL8
S100A9
CCL3
INHBA
CCL5
F
Gated on Live OP9-Lin- Mononuclear Cells (MNCs)
CD34+ OP9-EV
CD34+ OP9-IKK2SE
CD38
CD90
CD34
CD45RA
Direct contact system
G
Gated on Live OP9-Lin- Mononuclear Cells (MNCs)
Transwell system
H
SSC-A
FSC-A
MNCs 12.2%
Beads 46.0%
Single Beads 97.7%
Time
FITC
OP9 FITC- 94.2%
7AAD- 98.8%
CD45
CD34
CD45intCD34+ 88.5%

## REFERENCES


1. Zambetti NA, Ping Z, Chen S, et al. Mesenchymal Inflammation Drives Genotoxic Stress in Hematopoietic Stem Cells and Predicts Disease Evolution in Human Pre-leukemia. *Cell Stem Cell*. 2016;19(5):613-627.
2. Chen S, Zambetti NA, Bindels EM, et al. Massive parallel RNA sequencing of highly purified mesenchymal elements in low-risk MDS reveals tissue-context-dependent activation of inflammatory programs. *Leukemia*. 2016;30(9):1938-1942.
3. Doulatov S, Notta F, Eppert K, Nguyen LT, Ohashi PS, Dick JE. Revised map of the human progenitor hierarchy shows the origin of macrophages and dendritic cells in early lymphoid development. *Nat Immunol*. 2010;11(7):585-593.
4. Groschel S, Sanders MA, Hoogenboezem R, et al. A single oncogenic enhancer rearrangement causes concomitant EVI1 and GATA2 deregulation in leukemia. *Cell*. 2014;157(2):369-381.
5. Subramanian A, Tamayo P, Mootha VK, et al. Gene set enrichment analysis: a knowledge-based approach for interpreting genome-wide expression profiles. *Proc Natl Acad Sci U S A*. 2005;102(43):15545-15550.
6. Medyouf H, Mossner M, Jann JC, et al. Myelodysplastic cells in patients reprogram mesenchymal stromal cells to establish a transplantable stem cell niche disease unit. *Cell Stem Cell*. 2014;14(6):824-837.
7. van Dieren JM, Simons-Oosterhuis Y, Raatgeep HC, et al. Anti-inflammatory actions of phosphatidylinositol. *European Journal of Immunology*. 2011;41(4):1047-1057.
8. Mercurio F, Zhu H, Murray BW, et al. IKK-1 and IKK-2: cytokine-activated IkappaB kinases essential for NF-kappaB activation. *Science*. 1997;278(5339):860-866.
9. Bosman MC, Schepers H, Jaques J, et al. The TAK1-NF-kappaB axis as therapeutic target for AML. *Blood*. 2014;124(20):3130-3140.

# 5

# NICHE ALTERATIONS IN A HEMATOPOIETIC CELL - AUTONOMOUS MOUSE MODEL OF MDS DO NOT IMPAIR NORMAL HEMATOPOIESIS

Si Chen,[1] Yongyi Wang,[1] Shikhar Aggarwal,[1] Athina M. Mylona,[1] Niken M. Adisty,[1] Remco M. Hoogenboezem,[1] Marc H.G.P, Raaijmakers[1]

[1]Department of Hematology, Erasmus MC Cancer Institute, Rotterdam, the Netherlands

Key points:

1. Hematopoiesis in NHD13$^{+}$ MDS mice is characterized by loss of HSPCs

2. Niche alterations induced by MDS hematopoietic cells, however, do not impair numbers and function of normal HSPC

*Manuscript in preparation*

## ABSTRACT

Mounting evidence suggest that alterations in the bone marrow microenvironment (BMME) may contribute to disease pathogenesis in myelodysplastic syndromes (MDS). Mice with hematopoietic cell autonomous expression of the transgene NUP98-HOXD13 (NHD13) present a *bona fide* model of MDS. Here, we used NHD13 mice to address the question whether primary alterations in hematopoietic cells in MDS can induce alterations in the BMME that result in the attenuation of normal hematopoiesis. NHD13 mice have reduced numbers of HSPCs but transplantation of normal HSPCs in NHD13 recipients did not result in altered differentiation. Secondary transplant experiments revealed normal numbers and function of wildtype HSPC after exposure to the NHD13$^{+}$ BMME. Together, the findings in this particular mouse model of MDS do not support the notion that hematopoietic cells in MDS induce long-term effects on niche cells attenuating normal hematopoiesis.

## INTRODUCTION

It is increasingly evident that the bone marrow microenvironment (BMME) plays a pivotal role in the disease pathogenesis of a wide range of hematopoietic malignancies, including myelodysplastic syndromes (MDS).[1-9] MDS is the principal pre-leukemic malignancy that is characterized by ineffective hematopoiesis, dysplasia, cytopenia and a high propensity for clonal evolution to acute myeloid leukemia (AML).[10,11] Summarizing data derived from genetic mouse models studying the contribution of the BMME to leukemogenesis, two concepts have been proposed including "niche-induced " and "niche-facilitated" leukemogenesis. On one hand, primary alterations in the specific cellular component of the BMME can induce the development of MDS and secondary AML in mice[1]. Several models have demonstrated that genetic alterations of mesenchymal niche cells can drive the pathogenesis of MDS by inducing myelodysplasia and leukemic transformation of hematopoietic cells. Vice versa, whether hematopoietic elements in MDS can drive alterations in niche cells and how this would contribute to MDS pathogenesis remains understudied. Xenotransplantation models demonstrated that only when MDS hematopoietic cells co-inject with MDS stroma, efficient engraftment of MDS cells can be achieved.[3] In human MDS patients, a series of *in vitro* experiments showed that stromal cells isolated from MDS patients are dysfunctional.[12-15] However, the cellular and molecular mechanisms underlying the remodeling effect of MDS cells on their niche and the contribution of such remodeled niche to leukemogenesis remain incompletely understood. Here, we used the hematopoietic cell-autonomous model of MDS – the *Vav-NUP98-HOXD13* (NHD13) model to investigate the effects of altered HSPCs on its BMME and how this may contribute to bone marrow failure and leukemogenesis. To this end, NHD13 serves as an ideal model as the expression of the disease-causing fusion gene *NUP98-HOXD13* is driven by the hematopoietic-cell specific *Vav1* promoter and these mice recapitulate key clinical features in MDS patients including multilineage cytopenias and dysplasia with a high penetrance of leukemic transformation.[16-18]



## MATERIAL AND METHODS

### Mice and Transplant Experiments

All mice were maintained by the Experimental Animal Facility of Erasmus Medical Center (EDC) in specific pathogen free conditions. Wild-type and NHD13 mice in the C57BL/6 background were purchased from Jackson laboratory. B6.SJL (CD45.1) mice were purchased from Charles River. For the transplantation experiments, donor cells were freshly isolated whole bone marrow cells after red blood cell lysis with ACK buffer (Lonza). For the competitive transplant, 500,000 donor cells were isolated from 9 months old NHD13 mice and mixed in a 1:1 ratio with wildtype (WT) competitor CD45.1$^{+}$ cells isolated from 8 weeks old B6.SJL mouse.

The recipients were followed for 28 weeks. Recipient mice that died earlier were analyzed as described. For the non-competitive transplantation, 1 million CD45.1$^+$ healthy donor cells isolated from 8 weeks old B6.SJL mouse were injected into CTRL (7 or 10 months old) or NHD13 (7 or 10 months old) recipients. After 7 weeks, the CD45.1$^+$ cells from primary CTRL or NHD13 recipients were FACS sorted and competitively injected into healthy secondary recipients mixed with CD45.2 WT competitor cells. All recipients received lethal irradiation of 9 Gy and received antibiotic water for the first 2 weeks post transplantation. All mice were sacrificed by cervical dislocation and all the animal experiments were approved by the Animal Welfare/Ethics Committee of the EDC in accordance with legislation in the Netherlands. The work-flow of the transplant recipients includes blood counts, bone marrow cellularity, spleen isolation and analysis, flow cytometric analysis of CD45.1/CD45.2 chimerism, stem cell composition and differentiation in the peripheral blood and bone marrow as previously described.[1,19,20] Flow cytometric analysis defining the BM niche components including arterial and sinusoidal endothelial cells (CD45$^-$Ter119$^-$CD31$^+$Sca1$^-$, CD45$^-$Ter119$^-$CD31$^+$Sca1$^-$ CD31$^+$Sca1$^+$), osteoblasts (CD45$^-$Ter119$^-$CD51$^+$Sca1$^-$) and mesenchymal stem cells (MSCs: CD45$^-$Ter119$^-$CD51$^+$Sca1$^+$) are performed as previously described.[20,21]

## RESULTS

### Loss of the HSPC compartment in NHD13 mice

NHD13 mice recapitulate key characteristics of human MDS including leukopenia, macrocytic anemia, thrombocytopenia, and dysplasia, (Figure 1A and data not shown) fulfilling the Bethesda criteria[22] for MDS in mice, as previously reported.[16,17] Immunophenotypic analysis reveals a myeloid bias in the peripheral blood of 4-6 months old NHD13 mice: an increase in the frequency of Gr1$^+$Mac1$^+$ myeloid cells is accompanied by lower frequency of B220$^+$ lymphoid cells (Figure 1B). In addition, the biphenotypic B220$^+$Mac1$^+$ and B220$^+$Gr1$^+$ cells are elevated in the bone marrow (BM) of NHD13 mice (Figure 1C), as previously reported, with undefined functional relevance.[17,23,24] Earlier work has demonstrated an immunophenotypic reduction in the different subsets of hematopoietic stem progenitor cells (HSPCs) in 5 months' old NHD13 mice.[17,21] To examine if this phenotype persists as MDS progresses, we investigated the different HSPC subsets in 10 months' old NHD13 mice at the late MDS stage. It is worth noting that the BM of these mice are normocellular comparing to age-matched control (CTRL) mice (data not shown). Based on flow cytometry analysis (Figure 1D), we observed a significant decrease in the LKS (Lin$^-$C-kit$^+$Sca-1$^+$) population, nearly complete depletion of the short-term (LKSCD48$^-$CD150$^-$) and long-term HSCs (LKSCD48$^-$CD150$^+$, also known as the LKSSLAM). Together, the data reveal a progressive loss of the HSPC compartment upon disease progression in NHD13 mice. Investigating the cellular architecture of the niche in NHD13+ mice, we observed increased

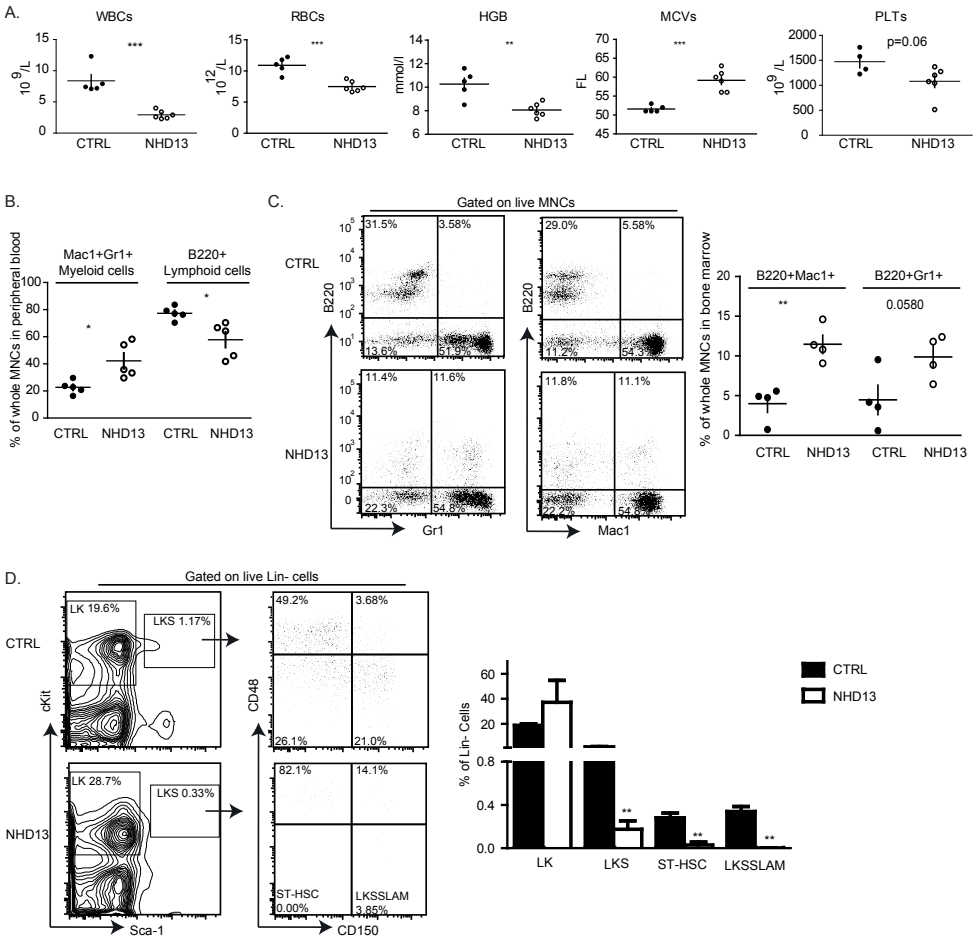


**Figure 1. NHD13 mice develop cytopenia accompanied by the loss of HSPCs.** (A) 4-6 months old NHD13 mice develop bone marrow failure as indicated by leukopenia, macrocytic anemia and thrombopenia. (B) NHD13+ mice present myeloid skewing with higher frequency of $Mac1^+$ $Gr1^+$ myeloid cells and lower frequency of $B220^+$ lymphoid cells. (C) In NHD13+ mice, hematopoietic cells with bi-phenotypic characteristics ($B220^+Mac1^+$ cells and $B220^+Gr1^+$ cells) are observed starting from 4 months. Representative FACS plots are shown on the left. (D) Representative FACS plots showing the HSPC compartment of CTRL and NHD13 mice (left panel) at 10 months. Bar graph demonstrating the loss of immunophenotypically defined HSPCs in NHD13 mice (right panel) (n=3 pairs).
MNCs: mononuclear cells; WBCs: white blood cells; RBCs: red blood cells; HGB: hemoglobin; MCVs: mean corpuscular volume; PLTs: platelets; LK: $lin^-c\text{-}kit^+$; LKS: $lin^-c\text{-}kit^+sca\text{-}1^+$; ST-HSC: short-term HSC ($lin^-c\text{-}kit^+sca\text{-}1^+CD48^-CD150^-$); LKSSLAM: long-term HSC ($lin^-c\text{-}kit^+sca\text{-}1^+CD48^-CD150^+$); * p<0.05; **p<0.01; ***p<0.0001

frequencies of different niche components including arteriolar and sinusoidal endothelial cells, osteoblasts and mesenchymal stem cells (Figure S1), congruent with earlier findings.[21] The functional relevance of this expansion in niche subsets remains to be defined,

## The BMME exposed to NHD13$^+$ hematopoietic cells does not impair normal hematopoiesis

Next, we wanted to investigate whether the altered cellular composition in the BM niche, induced by NHD13+ hematopoietic cells contribute to the loss of HSPC in the NHD13+ models. To test this, we performed a competitive transplantation assay with donor CD45.2$^+$ NHD13 cells (9 months old, late MDS stage) and competitor wild-type (WT) BM cells obtained from congenic B6.SJL mice that express CD45.1 into lethally irradiated age-matched (5 months) control (CTRL, n=5) or NHD13 recipients (n=6) (Figure 2A). We followed these recipients for approximately 28 weeks post transplantation. All CTRL recipients survived until analysis (Figure 2B). 3/6 NHD13 recipients died earlier at week 16, 17 and 21 respectively, indicating a higher mortality rate when cells were competitively transplanted into NHD13 recipients. The cause of death is likely due to the development of CD45.2-derived leukemia characterized by leukocytosis, anemia and thrombocytopenia in the blood, infiltration of CD45.2$^+$ myeloblasts in the bone marrow and spleen, accompanied by splenomegaly (Figure S2). Whether this leukemia arises from residual NHD13+ hematopoietic cells (surviving conditioning) or are of donor origin remains speculative. However, of the three NHD13 recipients that survived until analysis, CD45.2$^+$ NHD13 donor cells were outcompeted by the WT competitor cells, indicated by the nearly 100% CD45.1 chimerism in the BM of both CTRL and NHD13 recipients (Figure 2C).

To examine if the CD45.1$^+$ competitor cells are affected by the NHD13 BMME, we evaluated the differentiation capacity and HSPC composition of CD45.1$^+$ cells in both CTRL and NHD13 recipients. Both the differentiation capacity (Figure 2D) and the stem cell composition (Figure 2E) of the WT competitor cells are not strongly affected by the NHD13 BMME, except a trend of two-fold expansion in the LKS fraction (Figure 2E).

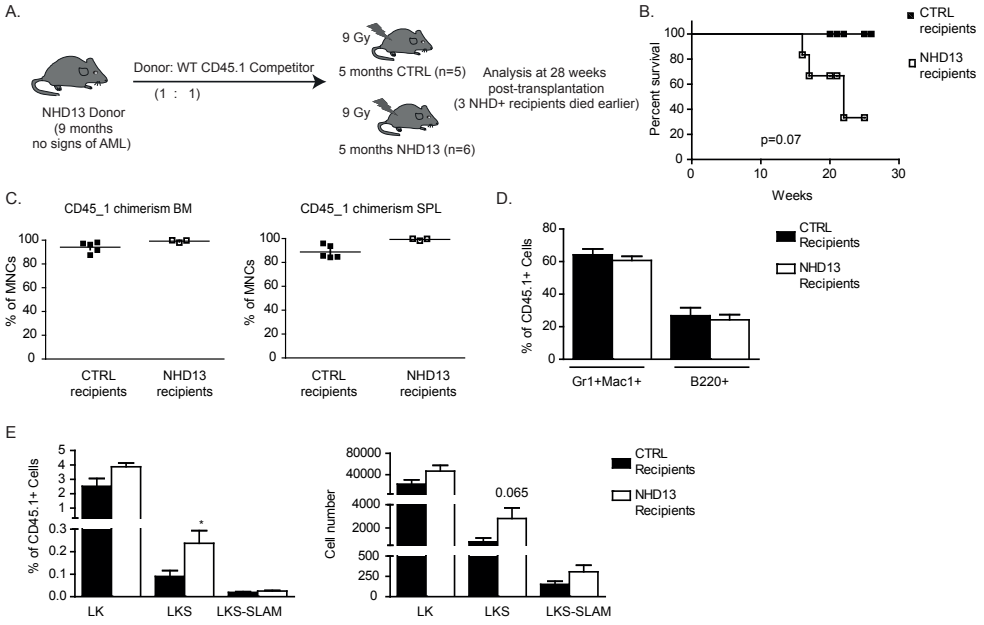


**Figure 2. The BMME of NHD13+ mice does not attenuate lineage progression of normal hematopoiesis.** (A) Scheme of the competitive transplantation of NHD13 hematopoietic cells (CD45.2$^+$) and wildtype competitor hematopoietic cells (CD45.1$^+$) into either CTRL (n=5) or NHD13 recipients (n=6). (B) Survival curves of CTRL and NHD13 recipients demonstrating reduced survival of NHD13 recipients. Premature death was observed in 3/6 NHD13+ recipients, likely due to the development of acute leukemia of CD45.2 NHD13$^+$ origin as indicated in supplementary figure 1. (C) Chimerism of CD45.1 WT competitor cells in the BM and SPL of CTRL (n=5) and NHD13 recipients (n=3) that survived until the time of analysis. (D) In the NHD13 recipients that survived, the differentiation capacity of competitor CD45.1$^+$ cells is comparable to the cells in CTRL recipients. (E) The CD45.1$^+$ HSPC composition in frequency (left panel) and cell number (right panel) in both CTRL and NHD13 recipients. * p<0.05
SPL: spleen

## The BMME of NHD13+ mice does not affect HSPC number and function

To further investigate the effect of the BMME exposed to NHD13$^+$ cells (at late MDS stage) on normal hematopoietic cells, we performed a non-competitive transplantation experiment where WT CD45.1$^+$ donor cells were introduced into 10 months old lethally irradiated CTRL (n=6) or NHD13 recipients (n=6) (Figure 3A). Seven weeks post-transplant, CD45.1 cells were isolated from recipient mice and used for secondary transplant to assess HSC function. Peripheral blood analysis of primary recipients at 7 weeks revealed moderate leukopenia and macrocytic anemia in NHD13 recipients (Figure 3B), reminiscent of the MDS phenotype in NHD13 mice. This cytopenia was, at least partially, explained by limited chimerism of CD45.1$^+$ cells (reached only 50% in the peripheral blood and less than 20% in the BM of NHD13 recipients) (Figure 3C), suggesting an incomplete engraftment of WT donor cells into lethally irradiated 10 months old NHD13 recipients. The differentiation status (Figure 3D) and HSPC composition (Figure 3E) of the engrafted CD45.1$^+$ donor cells in NHD13 recipients,

however, was not affected, in line with observations in the competitive transplant (figure 1). To assess the function of normal CD45.1 HSCs exposed to the NHD13 environment, we conducted a secondary transplantation experiment by isolating the $CD45.1^+$ donor cells from either CTRL or NHD13 primary recipients and competitively introduced these $CD45.1^+$ cells with WT $CD45.2^+$ competitor cells into healthy secondary recipients (Figure 3A). We followed these secondary recipients monthly for four months. $CD45.1^+$ cells isolated from the NHD13 primary recipients consistently showed a competitive advantage comparing to their counterparts from the CTRL primary recipients (Figure 3F), perhaps reflecting the (non-significant) increase of HSPC frequencies (Figure 3E).

In parallel, we performed similar primary and secondary transplantation experiments with 7 months old CTRL and NHD13 recipients (n=7 pairs) (less advanced MDS stage). In these recipients, efficient engraftment was observed accompanied by full rescue of the peripheral blood parameters (Figure S3A-C). Similarly, CD45.1 differentiation capacity and HSPC composition were not affected in the younger NHD13 recipients (Figure S3D, S3E) and $CD45.1^+$ donor cells isolated from NHD13 recipients at the intermediate MDS stage showed a competitive advantage in the secondary transplant recipients (Figure S3F). Together, these data suggest that the NHD13 MDS BMME does not attenuate normal hematopoiesis.

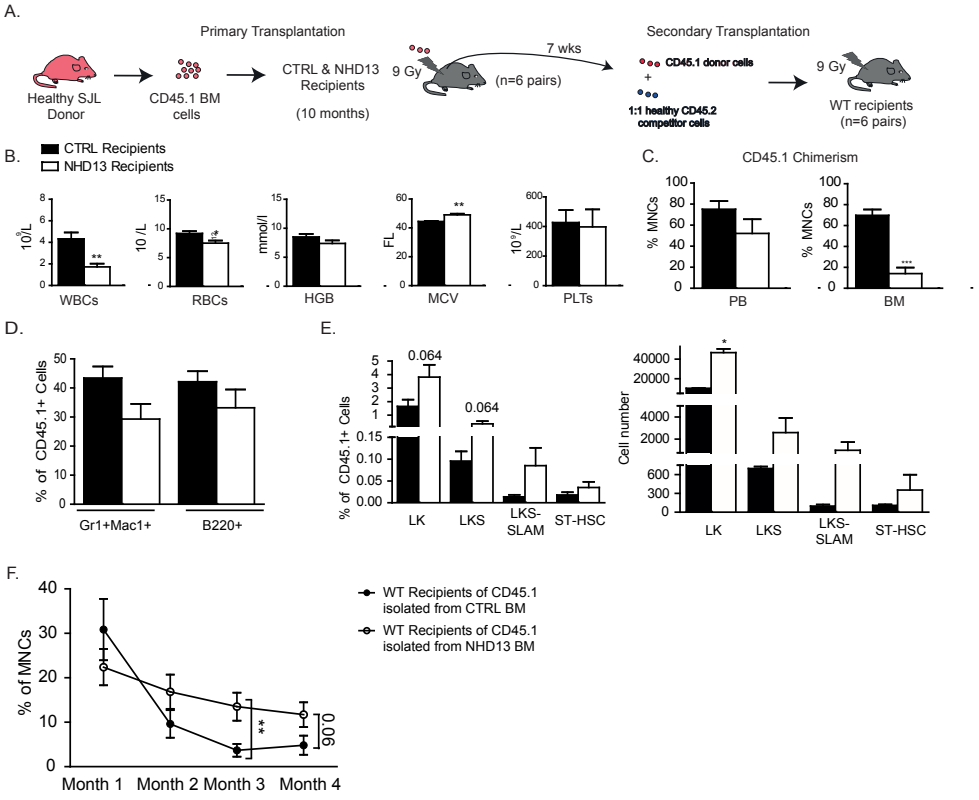


**Figure 3. The BMME of NHD13+ mice does not affect HSPC number and function.** (A) Scheme of primary transplantation of CD45.1⁺ normal hematopoietic cells into 10 months old CTRL (n=6) or NHD13 (n=6) recipients for 7 weeks, followed by secondary competitive transplantation of the isolated CD45.1⁺ BM cells into WT secondary recipients (n=6 pairs) with 16 weeks follow-up. (B) Whole blood counts of primary CTRL and NHD13 recipients (C) Peripheral blood (PB) and BM chimerism of CD45.1⁺ cells in the primary recipients at 7 weeks, indicating insufficient CD45.1 engraftment. (D) Differentiation capacity of CD45.1⁺ BM hematopoietic cells in CTRL and NHD13 recipients. (E) The composition of immunophenotypically defined BM CD45.1⁺ HSPCs in frequency (left panel) and cell number (right panel) in primary control and mutant recipients. (F) Chimerism of CD45.1⁺ cells isolated from CTRL or NHD13 primary recipients in the PB of secondary recipients for 16 weeks of follow-up period.

## DISCUSSION

The hematopoietic cell autonomous effects of the disease-causing transgene *Nup98-Hoxd13* have been extensively studied in the NHD13 MDS mouse model. However, the impact of the NHD13$^+$ MDS cells on their BMME and the contribution of this BMME to leukemogenesis and bone marrow failure in this model remains incompletely understood. Here, we conducted transplantation experiments to test the hypothesis that NHD13$^+$ hematopoietic cells affect the BMME in such a way that they attenuate normal hematopoiesis but failed to provide experimental support for this view. The data derived from both competitive and non-competitive transplantation assays suggest that the BMME of NHD13$^+$ mice does not impair the number and function of normal HSPCs, indicating the loss of the NHD13$^+$ HSPCs in NHD13 mice is probably a cell autonomous effect caused by the transgene, although niche interactions specific to genetically aberrant NHD13$^+$ hematopoietic cells cannot be completely excluded.

In the non-competitive transplantation assay, we introduced normal CD45.1$^+$ donor cells into primary CTRL or NHD13 recipients, at late (10 months) or less advanced (7 months) MDS stage. In the 10 months old primary NHD13 recipients, poor engraftment of CD45.1$^+$ donor cells were observed. The small pool of engrafted donor HSPCs displayed a compensatory expansion in the primitive compartment to support hematopoiesis, partially rescuing the peripheral blood parameters. The increased donor HSPC fraction was reflected in a competitive advantage in reconstituting healthy secondary recipients. In the NHD13 recipients at the less advanced (7 months) MDS stage, efficient CD45.1 engraftment was achieved and these cells resulted in higher chimerism in secondary recipients as well. The exact reason behind this discrepancy in the engraftment efficiency remains unclear. Since these two experiments were performed in parallel, irradiation effects are unlikely to be the cause. It could be that at a later MDS stage, the NHD13 cells are more resistant to irradiation or the BMME becomes less favorable for the engraftment of normal hematopoietic cells. In either case, regardless of the MDS stage, or engraftment efficiency, the NHD13 BMME shows no durable adversary effects on normal hematopoiesis.

Interestingly, we observed increased mortality and leukemic progression when NHD13$^+$ and WT cells were competitively transplanted into NHD13+ recipients (in comparison to WT recipients). The finding is reminiscent of recent data reported by the Calvi lab[21], although we cannot exclude the possibility that reduced survival was caused by leukemic transformation of residual CD45.2 NHD13$^+$ hematopoietic cells that survived conditioning by irradiation. Investigating the CD45.1$^+$ competitor cells in the NHD13 recipients that survived until analysis, the differentiation capacity and HSPC composition of these cells seemed to be preserved in the NHD13 recipients in our studies. However, in Calvi's report, a myeloid

bias of the CD45.1$^{+}$ competitor cells in NHD13 recipients was described. This discrepancy could be due to differences in transplantation procedures, such as the irradiation scheme given to the recipients (one time 9 Gy vs. 5 Gy split dose) or the post-transplant follow-up time (28 weeks vs 16 weeks). These factors may influence the level of residual MDS cells in the NHD13 recipients, potentially affecting the healthy competitor cells in addition to the BMME. Or in our study, the longer follow-up time may allow the competitor cells to correct the myeloid/lymphoid bias. Interestingly, however, we did observe an increased frequency of CD45.1 biphenotypic cells (expressing both myeloid and lymphoid markers) in the NHD13$^{+}$ environment (data not shown). The relevance of this remains to be shown but it is noteworthy that cells with this phenotype have been associated with dysplasia and leukemic transformation.[16,17,25]

Taken together, our data do not support the initial hypothesis, but instead suggest that the BMME of NHD13+ mice does not attenuate normal hematopoiesis, at least in the particular transplantation settings described here. This indicates that MDS pathogenesis in this model may be more cell intrinsic. Previous work has demonstrated that NHD13 MDS can be transferred to WT recipients and the NHD13$^{+}$ HSPCs are characterized by elevated apoptosis, accumulation of reactive oxygen species (ROS) and DNA damage response,[26,27] suggesting NHD13+ MDS can be cell autonomously propagated. In the meantime, our main conclusion should be seen in the light of several experimental limitations. Here, we only investigated one particular MDS model driven by the *nup98-hoxd13* gene fusion (infrequently reported in patients with therapy-related AML,) so the conclusion of NHD13+ BMME has no effect on normal hematopoiesis cannot be extrapolated to other pre-leukemic models. In addition, in this particular model, the disease-facilitating effect (remains to be proven) of the altered niche cells are short-term and may rely on continuous contacts with MDS cells. Once this contact is disrupted, the BMME no longer has an adversary effect, likely suggesting NHD13+ MDS cells do no elicit epigenetic or genetic alterations in their niche.

## REFERENCES


1. Raaijmakers MH, Mukherjee S, Guo S, et al. Bone progenitor dysfunction induces myelodysplasia and secondary leukaemia. *Nature*. 2010;464(7290):852-857.
2. Zambetti Noemi A, Ping Z, Chen S, et al. Mesenchymal Inflammation Drives Genotoxic Stress in Hematopoietic Stem Cells and Predicts Disease Evolution in Human Pre-leukemia. *Cell Stem Cell*. 2016;19(5):613-627.
3. Medyouf H, Mossner M, Jann JC, et al. Myelodysplastic cells in patients reprogram mesenchymal stromal cells to establish a transplantable stem cell niche disease unit. *Cell Stem Cell*. 2014;14(6):824-837.
4. Arranz L, Sanchez-Aguilera A, Martin-Perez D, et al. Neuropathy of haematopoietic stem cell niche is essential for myeloproliferative neoplasms. *Nature*. 2014;512(7512):78-81.
5. Hanoun M, Zhang D, Mizoguchi T, et al. Acute myelogenous leukemia-induced sympathetic neuropathy promotes malignancy in an altered hematopoietic stem cell niche. *Cell Stem Cell*. 2014;15(3):365-375.
6. Schepers K, Pietras EM, Reynaud D, et al. Myeloproliferative neoplasia remodels the endosteal bone marrow niche into a self-reinforcing leukemic niche. *Cell Stem Cell*. 2013;13(3):285-299.
7. Walkley CR, Olsen GH, Dworkin S, et al. A microenvironment-induced myeloproliferative syndrome caused by retinoic acid receptor gamma deficiency. *Cell*. 2007;129(6):1097-1110.
8. Kode A, Manavalan JS, Mosialou I, et al. Leukaemogenesis induced by an activating beta-catenin mutation in osteoblasts. *Nature*. 2014;506(7487):240-244.
9. Dong L, Yu WM, Zheng H, et al. Leukaemogenic effects of Ptpn11 activating mutations in the stem cell microenvironment. *Nature*. 2016.
10. Bejar R, Steensma DP. Recent developments in myelodysplastic syndromes. *Blood*. 2014;124(18):2793-2803.
11. Goldberg SL, Chen E, Corral M, et al. Incidence and clinical complications of myelodysplastic syndromes among United States Medicare beneficiaries. *J Clin Oncol*. 2010;28(17):2847-2852.
12. Ferrer RA, Wobus M, List C, et al. Mesenchymal stromal cells from patients with myelodyplastic syndrome display distinct functional alterations that are modulated by lenalidomide. *Haematologica*. 2013;98(11):1677-1685.
13. Geyh S, Oz S, Cadeddu RP, et al. Insufficient stromal support in MDS results from molecular and functional deficits of mesenchymal stromal cells. *Leukemia*. 2013;27(9):1841-1851.
14. Flores-Figueroa E, Gutierrez-Espindola G, Montesinos JJ, Arana-Trejo RM, Mayani H. In vitro characterization of hematopoietic microenvironment cells from patients with myelodysplastic syndrome. *Leuk Res*. 2002;26(7):677-686.
15. Tennant GB, Walsh V, Truran LN, Edwards P, Mills KI, Burnett AK. Abnormalities of adherent layers grown from bone marrow of patients with myelodysplasia. *Br J Haematol*. 2000;111(3):853-862.
16. Lin YW, Slape C, Zhang Z, Aplan PD. NUP98-HOXD13 transgenic mice develop a highly penetrant, severe myelodysplastic syndrome that progresses to acute leukemia. *Blood*. 2005;106(1):287-295.
17. Chung YJ, Choi CW, Slape C, Fry T, Aplan PD. Transplantation of a myelodysplastic syndrome by a long-term repopulating hematopoietic cell. *Proc Natl Acad Sci U S A*. 2008;105(37):14088-14093.
18. Beachy SH, Aplan PD. Mouse models of myelodysplastic syndromes. *Hematol Oncol Clin North Am*. 2010;24(2):361-375.
19. Zambetti NA, Bindels EM, Van Strien PM, et al. Deficiency of the ribosome biogenesis gene Sbds in hematopoietic stem and progenitor cells causes neutropenia in mice by attenuating lineage progression in myelocytes. *Haematologica*. 2015;100(10):1285-1293.
20. Zambetti NA, Ping Z, Chen S, et al. Mesenchymal Inflammation Drives Genotoxic Stress in Hematopoietic Stem Cells and Predicts Disease Evolution in Human Pre-leukemia. *Cell Stem Cell*. 2016;19(5):613-627.
21. Balderman SR, Li AJ, Hoffman CM, et al. Targeting of the bone marrow microenvironment improves outcome in a murine model of myelodysplastic syndrome. *Blood*. 2016;127(5):616-625.
22. Kogan SC, Ward JM, Anver MR, et al. Bethesda proposals for classification of nonlymphoid hematopoietic neoplasms in mice. *Blood*. 2002;100(1):238-245.

23. Balciunaite G, Ceredig R, Massa S, Rolink AG. Frontline: A B220(+) CD117(+) CD19(-) hematopoietic progenitor with potent lymphoid and myeloid developmental potential. *European Journal of Immunology*. 2005;35(7):2019-2030.
24. Anderson K, Rusterholz C, Mansson R, et al. Ectopic expression of PAX5 promotes maintenance of biphenotypic myeloid progenitors coexpressing myeloid and B-cell lineage-associated genes. *Blood*. 2007;109(9):3697-3705.
25. Watanabe-Okochi N, Kitaura J, Ono R, et al. AML1 mutations induced MDS and MDS/AML in a mouse BMT model. *Blood*. 2008;111(8):4297-4308.
26. Choi CW, Chung YJ, Slape C, Aplan PD. Impaired differentiation and apoptosis of hematopoietic precursors in a mouse model of myelodysplastic syndrome. *Haematologica*. 2008;93(9):1394-1397.
27. Chung YJ, Robert C, Gough SM, Rassool FV, Aplan PD. Oxidative stress leads to increased mutation frequency in a murine model of myelodysplastic syndrome. *Leuk Res*. 2014;38(1):95-102.

## SUPPLEMENTARY FIGURES

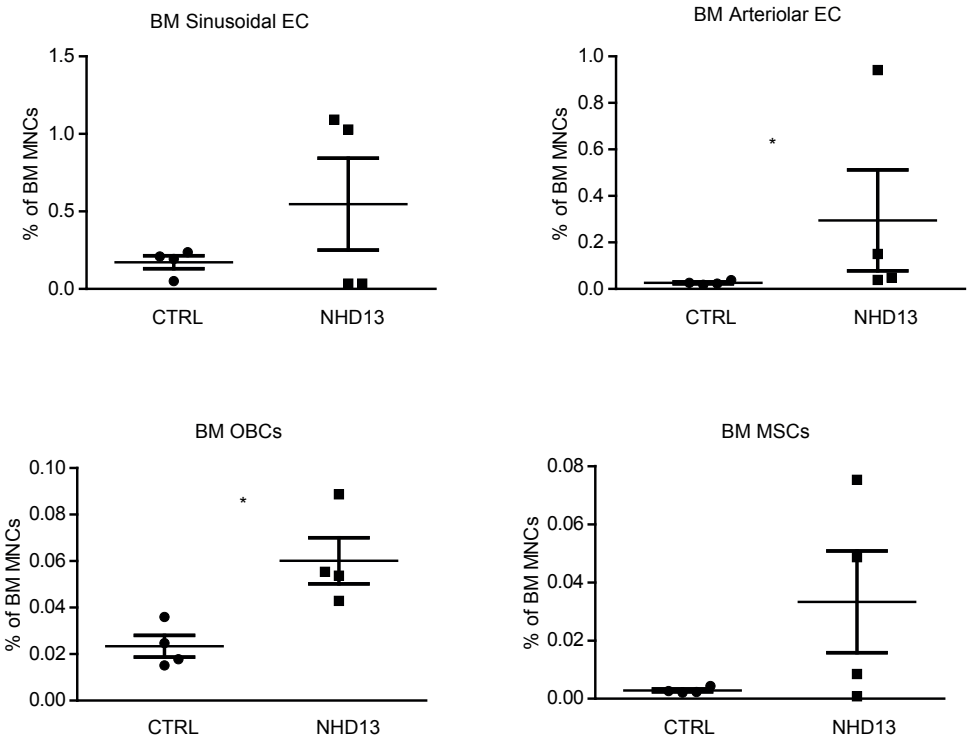


**Supplemental Figure 1. Cellular composition of the BM niche in CTRL and NHD13+ mice.** Frequency of the BM niche components in both CTRL and NHD13+ mice as a percentage of the total BM MNCs. The investigated niche components include sinusoidal endothelial cells (SEC: $CD45^-Ter119^-CD31^+Sca1^-$), arteriolar endothelial cells (AEC: $CD45^-Ter119^-CD31^+Sca1$-$CD31^+Sca1^+$), osteoblasts (OBCs: $CD45^-Ter119^-CD51^+Sca1^-$) and mesenchymal stem cells (MSCs: $CD45^-Ter119^-CD51^+Sca1^+$).

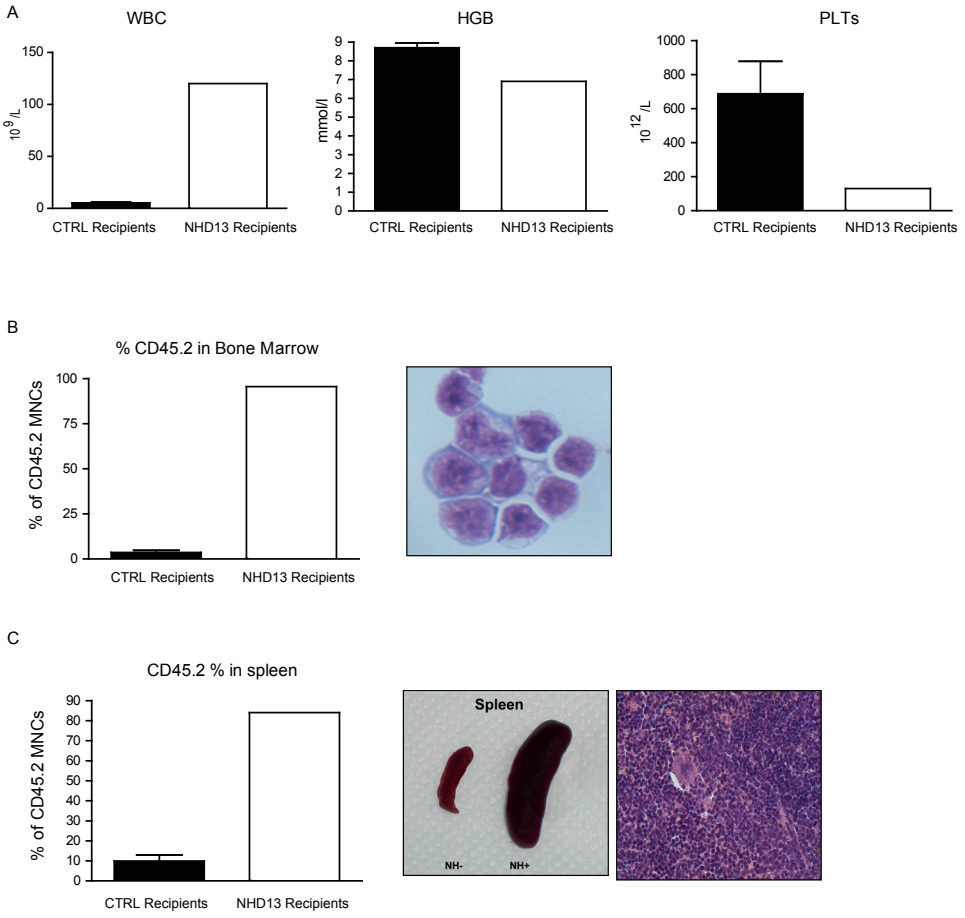


**Supplemental Figure 2. Development of acute leukemia of CD45.2 NHD13⁺ origin in NHD13+ recipient mice.** Figures show data from one NHD13 recipient with leukemia development and n=5 CTRL recipients. (A) peripheral blood counts demonstrating leukocytosis, anemia and thrombopenia in the NHD13⁺ recipient with leukemia in comparison to the control recipients. (B) Percentage of CD45.2⁺ MNCs in the bone marrow (left panel) of control and NHD13⁺ recipients; and representative image of myeloblasts (right panel) in the bone marrow of the NHD13⁺ recipient with leukemia development. (C) Percentage of CD45.2⁺ MNCs in the spleen (left panel) of the control and NHD13⁺ recipients; and splenomegaly (middle panel) due to infiltration of leukemic blasts of CD45.2 origin in the NHD13⁺ recipient.

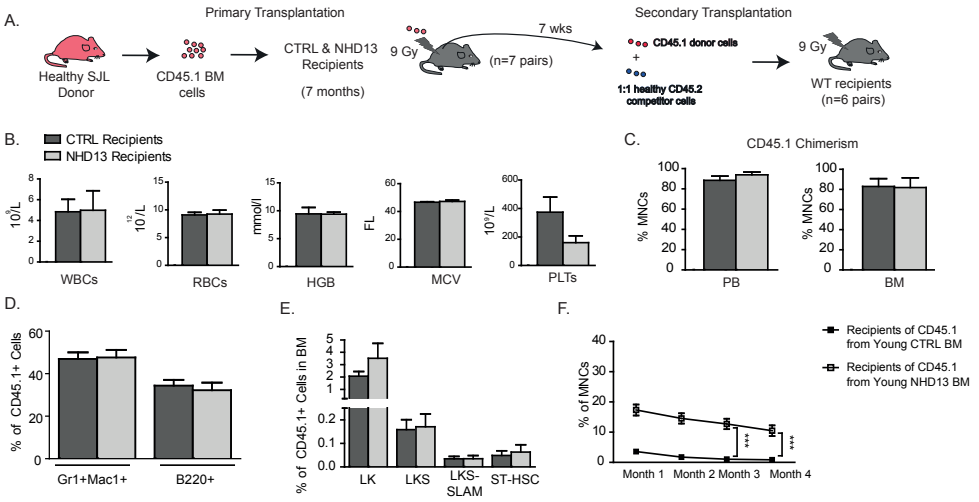


**Supplemental Figure 3. The NHD13 BMME supports normal hematopoietic cell function in a transplantation setting.** (A) Scheme of primary transplantation of CD45.1$^+$ normal hematopoietic cells into 7 months old CTRL (n=7) or NHD13 (n=7) recipients for 7 weeks, followed by secondary competitive transplantation of the isolated CD45.1$^+$ BM cells into WT secondary recipients (n=6 pairs) with 16 weeks follow-up. (B) Whole blood counts of primary CTRL and NHD13 recipients. (C) Peripheral blood (PB) and BM chimerism of CD45.1$^+$ cells in the primary recipients at 7 weeks. (D) Differentiation capacity of CD45.1$^+$ BM hematopoietic cells in CTRL and NHD13 recipients. (E) The composition of immunophenotypically defined BM CD45.1$^+$ HSPCs in primary control and mutant recipients. (F) Chimerism of CD45.1$^+$ cells isolated from CTRL or NHD13 primary recipients in the PB of secondary recipients for 16 weeks of follow-up period.

# 6

# SUMMARY AND GENERAL DISCUSSION

## 1. SUMMARY

The work presented in this thesis focused on the role of the bone marrow niche, mainly comprising different types of mesenchymal cells, in the development of MDS and Shwachman Diamond syndrome, conditions that are prone to progress towards leukemia.

MDS is the principal pre-leukemic disorder where mesenchymal elements have been implicated in disease initiation[1] and development[2], at least in mouse models. Insights into the involvement of the mesenchyme in the development of MDS in humans have long been limited to data derived from *ex vivo* expanded stromal cells, with unknown relevance to the complex *in vivo* bone marrow architecture. Translation of findings from the mouse models to human disease has been hampered by the lack of insight into non-expanded, purified mesenchymal cells from MDS patients. To bridge this gap, in **chapter 2**, we prospectively purified $CD271^{+}$ mesenchymal cells from low-risk MDS (LR-MDS) patients (n=12) and normal controls (n=10) and performed extensive transcriptome analysis. Strikingly, MDS mesenchymal cells are transcriptionally distinct from their normal counterparts, characterized by inflammatory signaling and cellular stress, reflected in reduced *in vitro* CFU-F capacity. In addition, in comparison to *ex vivo* expanded MDS stromal cells (published earlier)[2], purified MDS mesenchyme is enriched in signatures like response to external stimuli, chemokine activity and immune regulation. This data likely reflects active cross-talk of the mesenchymal cells with other cellular elements within the inflammatory bone marrow environment in LR-MDS[3], eliciting or maintaining these transcriptional programs, which may not be fully appreciated in *ex vivo* cultures.

Earlier work supporting the concept of "niche-induced" leukemogenesis has shown that primary dysfunction in the mesenchymal niche can induce myelodysplasia and AML with cytogenetic abnormalities in HSPCs.[1,4] To understand the underlying mechanism behind the concept, and to assess its relevance to human disease, in **Chapter 3**, we modelled Shwachman-diamond syndrome (SDS) – a monogenic disease caused by compound heterozygous or homozygous loss of function mutation in the gene *Sbds* required for ribosome biogenesis as outlined in Chapter 1. A recent study from our group in a conditional knockout mouse model (*Cebpa*-Cre-driven *Sbds* deletion) showed that hematopoietic cell intrinsic loss of *Sbds* resulted in neutropenia, but the mice failed to develop MDS or AML[5]. These findings raised the possibility that *Sbds*-deficient niche cells may contribute to the malignant transformation of SDS. To address this hypothesis, we specifically deleted *Sbds* in the osterix-expressing mesenchymal progenitor cells (MPCs) by generating the mouse model $OCS^{f/f}$ (mutant: $Sbds^{f/f}Osx^{cre/+}$) and $OCS^{f/+}$ (control: $Sbds^{f/+}Osx^{cre/+}$). As a result of mesenchymal *Sbds* deletion, the mutant mice developed an osteoporotic bone phenotype and a myelodysplastic hematopoietic phenotype, faithfully recapitulating the typical clinical

features in SDS patients. Investigating the HSPCs in the OCS model further, we observed accumulation of mitochondrial dysfunction, oxidative stress and DNA damage, along with G1-S cell cycle checkpoint activation. These data implicate disruptions in the mesenchymal niche can induce genotoxic stress in the HSPCs, which may play a pivotal role in the disease pathogenesis of SDS, MDS and/or AML.

Next, we defined the molecular mechanism associated with the bone and hematopoietic phenotype. Upon *Sbds* deletion, we observed activation of the p53 pathway, a molecular mechanism commonly associated with ribosomopathies. To test if the phenotypes we observed were p53 driven, we performed genetic rescue study by creating a double transgenic mouse model where deletion of *Sbds* and *p53* occurred in the same mesenchymal cells. We observed a rescue of the osteoporotic bone phenotype and genotoxic stress hematopoietic phenotype, suggesting the phenotypes we observed are p53 dependent. Then we investigated the potential molecules downstream of p53 driving these genotoxic stress in HSPCs. By comparing gene expression data from the mouse model to human SDS patients, where we performed transcriptional profiling of the human equivalent ($CD271^+$) of murine MPCs, we observed common overexpression of many inflammatory molecules including the alarmins (also known as DAMPs) *S100a8* and *S100a9* – bona fide p53 downstream targets.[6] Niche-derived S100A8 and S100A9 induced genotoxic stress in HSPCs in an *in vivo* transplantation assay, which is in line with the *in vitro* data showing that S100A8/9 induces DNA damage and apoptosis in HSPCs. Interestingly, the canonical S100A8/9 receptor TLR4 is partially involved here, as *in vivo* blocking of this receptor resulted in a partial reduction of DNA damage.

Because SDS is a rare congenital disease, we explored the broader relevance of our findings to human disease by analyzing the molecular profile of BM $CD271^+$ MPCs purified from 45 LR-MDS patients. Intriguingly, gene expression analysis revealed a subset of LR-MDS patients with high mesenchymal S100A8/9 expression, p53 and TLR activation. Patients in this subset are clinically undiscernible from the rest based on classical risk scores. However, patients in this subset with mesenchymal S100A8/9 overexpression have a higher frequency of leukemic evolution, significantly shorter time to leukemic progression and a shorter event-free survival. Taken together, our findings reveal the novel concept of inflammatory niche-induced genotoxic stress in HSPCs, suggesting a potential underlying mechanism supporting the model of niche-induced leukemogenesis and the human relevance of this concept. In addition to our study where inflammatory niche-derived P53-S100A8/9-TLR feedback loop is implicated in human pre-leukemic disorders, two other recent studies also showed the relevance of S100A8/9 overexpression in the pathogenesis of MDS.[7,8]

Continuing the work discussed in chapter 2 and chapter 3, **Chapter 4** aims to further dissect the molecular mechanism(s) potentially driving inflammation by comparing the transcriptional analysis of the mesenchymal cells isolated from 45 LR-MDS patients to the normal counterparts (n=10). Interestingly, activation of NF-κB mediated inflammatory signaling

appears to be a biological commonality in MDS mesenchymal cells. To test the functional relevance of this observation, we activated NF-κB pathway in mesenchymal cells *ex vivo*. We observed transcriptional upregulation of several inflammatory molecules, among which are the negative regulators of hematopoiesis observed in LR-MDS mesenchyme (**Chapter 2**) and S100A8/9, shown (in **Chapter 3**) to cause genotoxic stress in HSPCs. In a co-culture setting, mesenchymal NF-κB activation attenuated the number and function of normal HSPCs. These data implicate activation of NF-κB signaling may underlie the inflammatory phenotypes of LR-MDS mesenchyme, although unlikely to explain the overexpression of S100A8/9 in a subset of MDS patients described in Chapter 3. The cause of NF-κB activation in the LR-MDS mesenchymal elements remains to be established. However, earlier demonstration of activated NF-κB signaling in $CD34^+$ HSPCs in MDS patients[9] suggests a possible NF-κB-mediated inflammatory feedback loop as an important pathophysiological factor in MDS bone marrow. The data in this chapter suggest primary disruptions (e.g. NF-κB activation) in MDS HSPCs can remodel their niche (e.g. induce mesenchymal NF-κB activation) into a disease-supporting niche that impairs normal hematopoiesis and contributes to disease pathogenesis. We then tested this hypothesis in an *in vivo* MDS model in the next chapter.

In **Chapter 5**, we used the hematopoietic cell-autonomous model of MDS – the *Vav-NUP98-HOXD13* (NHD13) model to address the question whether primary disruptions in hematopoietic cells in MDS can induce alterations in the bone marrow microenvironment (BMME) that impair normal hematopoiesis. The NHD13 model serves as an ideal model to test our hypothesis as expression of the disease-causing fusion gene *NUP98-HOXD13* is driven by the hematopoietic-cell specific *Vav1* promoter and these mice recapitulate key clinical features in MDS patients. NHD13 mice present progressive loss of HSPCs; however, transplantation of normal HSPCs in NHD13 recipients did not result in altered differentiation and secondary transplant experiments revealed normal numbers and function of wildtype HSPC after exposure to the NHD13+ BMME. The data in this particular mouse model of MDS do not support our hypothesis that hematopoietic cells in MDS induce long-term effects on niche cells attenuating normal hematopoiesis, indicating the loss of the $NHD13^+$ HSPCs in NHD13 mice is probably a cell autonomous effect caused by the transgene. This is supported by previous work demonstrating NHD13+ MDS can be cell autonomously propagated.[10,11] However, we cannot completely exclude the niche interactions specific to genetically aberrant $NHD13^+$ hematopoietic cells and our main conclusion should be seen in the light of several experimental limitations. Here, we only investigated one particular MDS model, so the conclusion of NHD13+ BMME has no effect on normal hematopoiesis cannot be extrapolated to other MDS models. In addition, in this NHD13 MDS model, the effect of the altered niche cells may be short-term relying on the continuous contacts with MDS cells. This transient contacts-dependent niche effect likely suggests NHD13+ MDS cells do no elicit epigenetic or genetic alterations in their niche.

## 2. Mesenchymal inflammation in the development of myeloid malignancies – broader relevance to cancer-related inflammation

It is now generally accepted that inflammation plays an important role in tumorigenesis and an inflammatory microenvironment is an essential component of many tumors, although a direct causal relationship is yet to be proven in some tumor types.[12,13] In some cases, inflammatory conditions precede the occurrence of malignant changes; whereas in other types of cancer, oncogenic alterations in the malignant cells induce an inflammatory microenvironment contributing to tumor development.[12,13] The pro-tumorigenic effect of inflammatory signaling is often coupled with other mechanisms including senescence, immunity, angiogenesis, metabolism and cytokine/chemokine interactions, together contributing to the hallmarks of cancer.[13-15] Most of these hallmarks are enabled and sustained through reciprocal communications between the cancer (stem) cells and the tumorigenic microenvironment.[16] The stromal constituents of the tumor microenvironment are complex containing a wide range of diverse subcellular types. Three general classes have been defined including infiltrating immune cells, angiogenic vascular cells and cancer-associated fibroblasts (CAFs).[16] All three stromal classes have been indicated in an inflammatory tumor microenvironment, however, the importance and function of each of these classes vary with tumor types and disease states. Although the role of an inflammatory tumor microenvironment is increasingly appreciated, many important questions remain unanswered among which include a) whether inflammation is sufficient for cancer development; b) What are the cellular and molecular components that are common to all cancer-promoting inflammatory responses, and which are specific to particular tissues and tumor types.[12] The work discussed in this thesis provides new insights into the contribution of an inflammatory bone marrow niche, emphasizing the importance of the stem cell niche to the pathogenesis of pre-leukemic disorders and highlights the mesenchymal niche as a direct active participant in creating a disease-relevant inflammatory BMME. Our findings add new insights into the link between mesenchymal niche inflammation and oncogenesis (in the hematopoietic system), revealing mechanistic commonalities between our findings to the role of the inflammatory microenvironment in solid tumors.

**Chapter 2** revealed inflammation and cellular stress in mesenchymal elements purified from LR-MDS patients comparing to the normal counterparts. **Chapter 3** uncovered mesenchymal inflammation driving genotoxic stress in HSPCs in both pre-leukemic mouse models and human patients, contributing to leukemogenesis. In **Chapter 4**, we defined NF-κB mediated mesenchymal inflammation as a biological commonality in the bone marrow of LR-MDS patients. Together, mesenchymal inflammation in pre-leukemic disorders seems to be a converging theme in this dissertation. In the meantime, our findings invigorate the ongoing conundrum in the field whether (a) mesenchymal inflammation corrupts HSPCs through direct or indirect mechanisms; (b) inflammation in the niche is a primary event

or secondary to the primary alterations in the HSPCs; (b) an inflammatory niche induces malignant transformation of HSPCs or selects specific already-present malignant clones allowing clonal evolution. While these conundrums remain to be further explored, this discussion aims to speculate that these mechanisms may not be mutually exclusive, but act synergistically together in driving bone marrow failure and leukemogenesis. To start with, our data suggests a direct genotoxic effect of the mesenchymal-derived inflammatory molecules S100A8/9 on HSPCs; however, they are unlikely to be the only drivers. In fact, upregulation of genes encoding other inflammatory factors in the mesenchymal cells are observed in human MDS and the SDS model as detailed below. Thus, in addition to the direct effect of the niche-produced inflammatory factors as we described, indirect effects of these molecules are anticipated.

### 2.1 Deregulated immunity and inflammatory cytokines derived from mesenchymal cells are essential factors in myeloid malignancies through direct and/or indirect mechanisms

Congruent with our findings, several other studies have implicated inflammatory cytokines produced by the HSPC niche in initiating or facilitating myeloid malignancies. A recent study modeling Noonan syndrome showed that activating mutation of the RAS signaling mediator *PTPN11* in mesenchymal cells and osteoprogenitors can drive MPN progression. This process involves excessive production of CCL3 by the activated mesenchymal cells, recruiting inflammatory monocytes, which hyperactivate HSPCs by secreting the inflammatory cytokine IL-1ß, responsible for disease progression.[17] Interestingly, similar inflammatory cascades have been implicated in solid tumors. Stromal expression of CCL3 - an inflammatory chemoattractant - together with CCL2, CCL4 and CCL5 have been shown to affect the macrophage composition of tumors by recruiting monocytes and other immature myeloid cells into the tumor microenvironment.[18] Together with T cells, tumor-associated macrophages (TAMs) are among the most frequently found immune cells within the tumor microenvironment and are generally pro-tumorigenic by promoting processes like angiogenesis, tumor invasion and metastasis.[19] It is therefore conceivable that a comparable mechanism could take place in MPN, via mesenchymal-derived inflammation.

In addition to the niche-induced MPN model mentioned above, the inflammatory cytokine IL-1ß has been implicated in several other models of myeloid malignancies. In an inducible BCR/ABL CML mouse model, CML cells alter the function of osteoblasts and remodel these cells into an inflammatory osteoblastic niche, secreting pro-inflammatory molecules including IL-1ß, which amplifies MPN progression to the leukemic stage.[20] In this model, osteoblasts in CML mice fail to support normal HSCs due to reduced *Cxcl12* expression, but favor LSC expansion, partially via the secretion of inflammatory cytokines. In another study of the JAK2(V617F) MPN model, the mutated hematopoietic cells "created" an inflammatory environment by secreting molecules such as IL-1ß, causing neuropathy in the

BM and subsequent loss of nestin$^+$ mesenchymal cells. Such an inflammatory environment adversely contributed to MPN development.[21] IL-1ß is a pleiotropic inflammatory cytokine that is often upregulated in the microenvironment of solid tumors, including breast, colon, lung, head/neck cancers and melanomas. Its accumulation in the tumor microenvironment is often correlated with worse prognosis.[22] Though the exact mechanisms of this cytokine are being explored, it is increasingly evident that IL-1ß activates the expression of pro-tumorigenic factors including metastatic genes matrix metalloproteinases (MMPs), angiogenic factors and inflammatory cytokines by adjacent cells.[22]

Interestingly, we also observed upregulation of CCL3 and IL-1ß in the *Sbds* deleted MPCs in our OCS mouse model and CD271$^+$ mesenchymal cells from SDS patients (**Figure 1A**). Along with CCL3, CCL4 and CCL5, which are also involved in monocyte recruitment during inflammation, are upregulated in patient mesenchymal cells as well (**Figure 1B**). Furthermore, in the OCS model where CCL3 and IL-1ß are overexpressed in the mutant MPCs, CCL3 receptor CCR1 and IL-1ß receptors IL-1RI and IL-1RII are overexpressed in the mutant HSPCs (**Figure 1C**), suggesting an inflammatory crosstalk between the mesenchymal elements and HSPCs. In addition to SDS patients, CCL3, is also enriched in mesenchymal cells purified from LR-MDS patients (**Chapter 2**, Supplementary Table 3). This may be regulated via the NF-κB pathway, as *ex vivo* activation of NF-κB signaling in mesenchymal cells resulted in CCL3 upregulation (**Chapter 4**, Figure 2B). Interestingly, NF-κB activation is also present in the MDS hematopoietic cells[9]. CCL3 has long been recognized as a canonical NF-κB downstream target[23] suggesting a possible feedback/feedforward loop reinforcing an inflammatory milieu in the bone marrow relevant to MDS pathogenesis.

In addition to the CCL family of chemoattractants, many alarmins, including S100A8 and S100A9, have been reported to attract immune cells, such as monocytes and macrophages.[24] Specifically in lung cancer, the release of S100A8 and S100A9 can recruit CD11b$^+$ myeloid cells, which subsequently promote tumor invasion and metastasis.[25] In **Chapter 3**, our finding of S100A8/9 derived from the mesenchymal niche as a driver of myelodysplasia converge with another report showing S100A8/9 drive the expansion of CD11b$^+$ myeloid-derived suppressor cells (MDSCs), which directly contributed to the myelodysplasia phenotype.[26] In line with our findings, immunological alterations accompanied by perturbed cytokine regulation are key factors contributing to the transition from normal to aberrant hematopoiesis.[27] Altered cytokine networks within the bone marrow have been implicated in clonal stem cell disorders, as well as the expansion of LSCs.[28] Notably, deregulation of TLRs – critical for innate immune signaling – is a common feature in MDS and leukemia.[29]
For example, in MDS, TLR1, 2, and 6 upregulation have been observed and activation of TLR2 signaling axis is associated with elevated IL-8 expression; likewise, elevated levels of TNF-α, IFN-ɣ, TGF-ß and IL-6 have also been reported.[30-32] Furthermore, these receptors are important for the cooperative regulation of pro-inflammatory cytokines and chemokines.

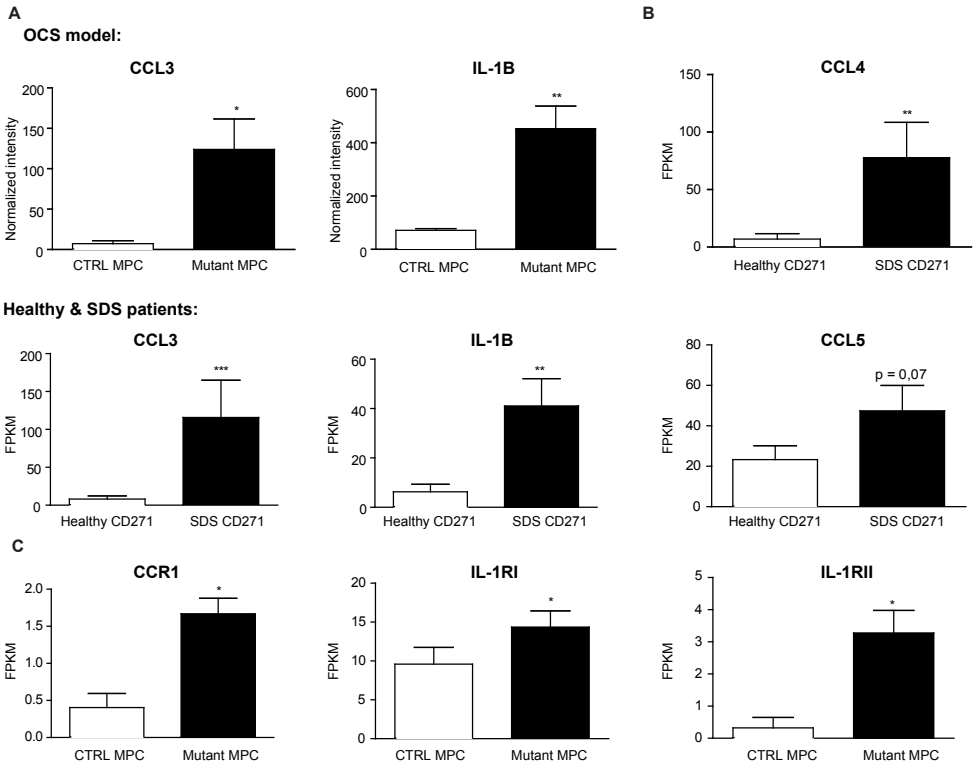


**Figure 1: Upregulation of inflammatory cytokines/chemokines and the binding receptors in the MPCs and HSPCs from OCS mice and SDS patients.** (A) Upregulation of CCL3 and IL-1ß in the MPCs isolated from mutant OCS mice (upper panel) and the $CD271^+$ mesenchymal cells from SDS patients (lower panel). (B) Upregulation of CCL4 and CCL5 in the purified $CD271^+$ mesenchymal cells from SDS patients comparing to healthy donors. (C) Upregulation of receptors CCR1 (for chemokine CCL3), IL-1RI and IL-1RII (for cytokine IL-1ß) in HSPCs from mutant OCS mice comparing to the control counterparts.

Dysfunction of these receptors have been implicated in MDS pathogenesis where signal transduction of key proliferative and apoptotic pathways is not properly activated.[33] Markedly, the S100A8/9-TLR4 axis is implicated in our mouse model of niche-induced genotoxic stress (**Chapter 3**) and upregulation of IL-6, IL8 and TGF-ß is observed in LR-MDS mesenchymal elements (**Chapter 2**), suggesting cytokine imbalances and dysregulated activation of TLRs contribute to the formation of an inflammatory genotoxic niche.

Taken together, in the OCS model, it is reasonable to hypothesize that other inflammatory factors in addition to S100A8/9 cooperating with deregulated TLR signaling may contribute to the genotoxic milieu exerting a direct effect on HSPCs. In addition, these secreted factors may exert indirect effects by recruiting immune cells like monocytes or MDSCs to the site, secreting additional inflammatory molecules and suppressive cytokines that can further compromise the functional integrity of adjacent HSPCs, promoting disease progression.

Similar interplay may be extrapolated to SDS and MDS patients, specifically the subsets of patients with enriched S100A8/9 expression in mesenchymal cells. Therefore, in relation to the inflammatory microenvironment in solid tumors, we suggest an inflammatory cascade in the HSPC niche of SDS and MDS patients, where diverse inflammatory cytokines and diverse cellular subsets are involved, including recruited immune cells. This cascade could have direct and/or indirect effects in disrupting normal hematopoiesis and perhaps support the expansion of leukemic clones (**Figure 2**).

### 2.2 Mesenchymal-inflammation associated tumorigenesis

Our findings indicating that inflammation in the bone marrow niche may contribute to oncogenesis in the hematopoietic system concur with a similar concept and mechanism identified in solid tumors. In fact, the notion of niche-induced tumorigenesis in solid tumors has been proposed already twenty years ago in the context of colon[34] and prostate cancers.[35] For instance, Bhowmick *et al* demonstrated that deletion of the gene encoding TGF-ß receptor type II (*Tgfbr2*) in fibroblasts resulted in epithelial tumors in prostate and forestomach in a conditional mouse model.[36] A follow-up study using the same model uncovered the underlying mechanism.[37] *Tgfbr2* deletion in stromal cell resulted in inflammation-induced DNA damage and cell cycle alterations due to epigenetic silencing of *p21* in the heterotypic epithelial cells, directly causing increased epithelial proliferation and ultimately the development of epithelial tumor formation in specific organ tissues.[37] These findings demonstrated that stromal alterations, specifically inflammation-mediated mechanisms, have significant genetic and epigenetic impact on the adjacent epithelial compartment critical for tumor initiation and development.

In parallel, another study investigating skin cancer demonstrated that mesenchymal loss of *Notch/CSL* signaling (specifically *CSL/RPB-Jk* gene, a key *Notch* effector) in mice triggered spontaneous formation of multifocal epithelial tumors in the skin via the recruitment of macrophages, upregulation of inflammatory factors (including MMPs) and diffusible growth factors.[38] Interestingly, in this model the suppression of inflammation delayed tumor formation, suggesting inhibition of inflammation may prevent secondary tumor development.

These data indicated that the stroma can play a primary role in the progression and initiation of cancer, supporting the longstanding concept of “field cancerization” that was first introduced in 1953 in squamous cell carcinomas with important clinical implications.[39] Field cancerization is defined as broader tissue and organ changes beyond localized neoplastic areas of tumor development resulting in multifocal and recurrent tumors.[40,41] While the mechanisms underlying this concept remain to be fully revealed, recent studies (including our own work) where primary stromal alterations are shown to induce tumorigenesis

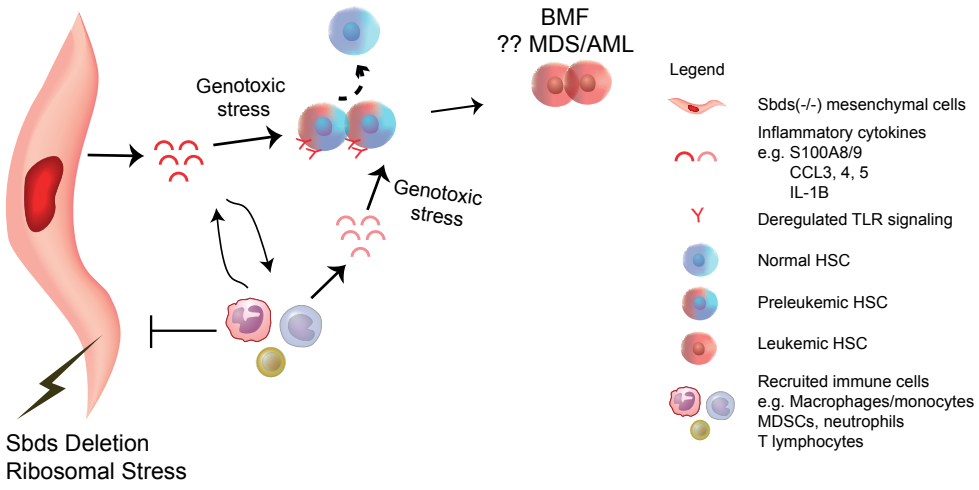


**Figure 2: Inflammation in the mesenchymal HSPC niche drives genotoxicity in HSPCs through direct and/or indirect mechanisms contributing to disease pathogenesis.** Ribosomal stress (e.g. *Sbds* deletion) in the HSPC mesenchymal niche results in elevated secretion of a wide range of inflammatory cytokines (e.g. S100A8/9, CCL3, 4, 5 and IL-1ß) and activation of TLR signaling, resulting in (a) direct induction of genotoxic stress in the heterotypic HSPCs; or (b) recruitment of immune cells s
uch as inflammation-associated macrophages/monocytes, MDSCs, neutrophils or T-lymphocytes secreting inflammatory or suppressive cytokines that further contribute to the inflammatory-genotoxic milieu. Such an inflammatory cascade within the HSPC niche contributes to the initiation and/or progression of BMF and MDS/AML development. In addition, inflammatory cytokines secreted from the recruited immune cells could corrupt the architecture of the HSPC niche (e.g. reduced nestin$^+$ mesenchymal cells due to IL-1ß induced neuropathy), further compromising the niche support to normal HSPC function.

may help explain the concept of "field cancerization", i.e., the occurrence of multifocal and recurrent tumors that are preceded by and associated with spreading alterations in surrounding parenchymal and stromal tissues.[40] It is worth noting that both in our OCS model and the abovementioned stromal-Notch/CSL skin cancer model, all mesenchymal cells were genetically altered/targeted. Although the translation of such models to human patients remains to be further investigated, based on these findings we may begin to appreciate that epigenetic or genetic alterations in one mesenchymal cell can perhaps spread into a field affecting the surrounding stroma and contribute to the process of "field cancerization".

In the meantime, stromal inflammation seems to significantly contribute to the phenomenon of field cancerization. In addition to the aforementioned mouse models where niche-derived inflammatory signaling resulted in tumorigenesis, a few other models have been described. In a mouse model with gastric-specific overexpression of the proinflammatory cytokine IL-1ß, these transgenic mice developed gastric cancer through a cascade of NF-κB-activating inflammatory cytokines and associated recruitment of MDSCs.[42] Interestingly, increased expression of IL-1ß resulted in increased proliferation

and transformation of the gastric epithelium, as well as severe atrophy in the stroma. Later work revealed that stromal atrophy and associated fibroblast senescence are important contributing factors in field cancerization process.[40]

Although alterations in mesenchymal stromal cells are usually assumed to play a more secondary reactive role, in some cases, especially for UV-induced skin cancer where the UV light can directly affect the dermal (stroma in the skin) compartment, stromal cell senescence acts as a putative tumor-promoting or –triggering mechanism.[43] The gene expression programs of senescent fibroblasts overlap with that of cancer-associated fibroblasts (CAFs), including the production of senescence-associated-secretory-phenotype (SASP) factors, mediating immune cell recruitment, angiogenesis and tumorigenesis.[44,45] For example, the overexpression of SASP factor IL-6 can promote inflammation and proliferation of neighboring parenchymal tumor cells by cooperating with transcription factor C/EBPß.[46] CAFs express a proinflammatory gene signature in a range of cancer types including skin, breast and pancreatic cancer. In a transgenic mouse model of squamous cell carcinoma, the tumor-promoting effect of CAFs is mediated via NF-κB signaling where inhibition of this pathway abolished the tumor-enhancing effect of CAFs.[47] To our interest, LR-MDS mesenchymal cells displayed a number of signatures indicating response to UV irradiation (**Chapter 2**, supplemental table 2). In addition, the molecular profiles of these cells are reminiscent of senescent fibroblasts, including the upregulation of numerous SASP factors such as IL-6, discussed in detail later on.

Additional analysis on the GSEA signatures from **Chapter 2** revealed several programs indicating "field cancerization", "tumor field effect" in $CD271^+$ mesenchymal cells in LR-MDS patients compared to the normal counterparts (**Figure 3A-B**). The observed "field cancerization" signatures in MDS mesenchymal cells suggest that in MDS patients, there could be a "field" of altered stroma (e.g. characterized by NF-kB activation as in **Chapter 4**) contributing to MDS pathogenesis. Data derived from **Chapter 3** supports the concept of niche-induced leukemogenesis, indicating a primary role the stroma can play in both leukemia progression and initiation, proposing a new aspect of the multi-hit hypothesis of cancer. A hit can occur outside of the cancer cells themselves, indicating a cell non-autonomous contribution to the emergence of malignancy.[48] However, such hypothesis is derived from data in mouse models, where the relevance to human patients remains to be formally demonstrated.

## 2.3 The mechanism behind inflammation-associated tumorigenesis

### What drives S100A8/9 expression?

The alarmins S100A8/9 are overexpressed in the mesenchymal cells from the mutant OCS mice and SDS patients, driving genotoxic stress in HSPCs. Interestingly, we found that mesenchymal overexpression of these two DAMP proteins identified a subset of MDS patients with worse clinical outcome (**Chapter 3**). Our data indicate that the mesenchymal niche may actively contribute to the formation of a "mutagenic" environment that facilitates cancer initiation and progression. At this moment, the question what drives the upregulation of the inflammatory molecules S100A8/9 in these two related yet distinct pre-leukemic disorders remains to be answered.

In the OCS model, we specifically deleted *Sbds* in the MPCs; whereas in SDS patients, *SBDS* deletion is intrinsic to nearly every cell including the mesenchymal elements. Therefore, it seems that ribosomal stress due to loss of *Sbds* in the mesenchymal cells could cause the inflammatory response, including the activation of TLR signaling and upregulation of DAMP proteins S100A8/9. Our data further demonstrated that inflammation induced by ribosomal stress in the mesenchymal cells is dependent on the p53 pathway, a common molecular mechanism associated with ribosomal defects. This finding is in agreement with another study investigating the effect of ribosomal defect in the context of $5q^-$ syndrome - a subset of MDS. In this study, a mouse model of *Rps14* (component of small ribosomal subunit) deletion in the erythroid progenitors was generated, resulting in impaired erythropoiesis, which was mediated via p53 activation and downstream S100A8/9 overexpression. The data linked *Rps14* haploinsufficiency to the activation of innate immunity and the induction of S100A8/9 overexpression, leading to defects in erythroid differentiation in a p53 dependent manner.[8] Together, it is reasonable to postulate that S100A8/9 induction in ribosomopathies SDS and $5q^-$ syndrome could be driven by stress signaling due to ribosomal dysfunction and subsequent p53 activation in specific cellular types.

In LR-MDS, transcriptome comparison of mesenchymal cells from S100-niche$^+$ patients (n=17) to patients in the S100-niche$^-$ group (n=28) revealed potential molecular pathways leading to DAMP signaling (**Chapter 3**, Figure 7). Interestingly, activation of p53 pathway and TLR signaling are observed in the S100-niche$^+$ mesenchyme, in line with findings in the OCS model, *Rps14* mice and SDS patients, suggesting p53 activation may be a common pathway driving S100A8/9 overexpression in pre-leukemic disorders. It is worth noting that in other systems, S100A8 and S100A9 have been identified to be *bona fide* p53 downstream targets, the above-mentioned data confirmed this finding in the mesenchymal HSPC niche component.[6] In SDS and $5q^-$ syndrome, p53 activation in the mesenchymal niche could be driven by stress associated with ribosomal dysfunction due to *Sbds* or *Rps14* deficiency; whereas in MDS, it

could reflect activation of senescence programs in the LR-MDS mesenchymal cells (**Figure 3 C-E**), as indicated by the upregulation of numerous SASP factors (**Table 1**) and activation of NF-kB pathway (Chapter 4). Data in **Chapter 4** (Figure 2) suggests *ex vivo* activation of NF-kB pathway in mesenchymal cells could drive transcriptional upregulation of S100A8/9, in line with a mouse model of hepatocellular carcinoma where NF-kB activation induced S100A8/9 overexpression. In this model, NF-kB-induced S100A8/9 overexpression resulted in higher level of reactive oxygen species (ROS)-dependent signaling that contributed to malignant progression of the hepatocellular tumor cells.[49]

This senescence-associated inflammatory feature of MDS mesenchymal cells is probably the result of being in contact with aberrant hematopoietic or other surrounding cells, as signatures of inflammation and cytokine stimulation are enriched in purified MDS CD271$^+$ mesenchyme compared to the *in vitro* expanded stroma, emphasizing the relevance of tissue context in this case (**Chapter 2**, Figure 2). It has been shown that in LR-MDS, senescence programs also characterize hematopoietic cells, including HSPCs.[50,51] Therefore, it is possible that senescence is initially established in the hematopoietic compartment due to MDS, and then propagated to the BMME via the production of SASP factors[52]; this senescent environment could then contribute to disease progression. Like in solid tumors, senescent fibroblasts could sustain the growth of parenchymal tumor cells[53-55], and promote the malignant transformation, invasion and metastasis of tumor cells.[56,57]

A recent study suggested that one of the hallmarks of MDS – activation of NLRP3 inflammasome in the HSPCs resulted in elevated secretion of IL-1ß, inducing the upregulation of DAMP molecules S100A8/9 and the accumulation of ROS. These processes are associated with the inflammasome-mediated HSPC pyroptosis, which significantly contributes to disease progression.[7] This link between S100A8/9 expression and inflammation has been supported by a broad range of studies, specifically in association with acute and chronic inflammatory disease.[58-60] Lately, alarmins S100A8 and S100A9 have been recognized as biomarkers for local inflammatory activity.[61] Typically, alarmins S100A8/9 are secreted by immune cells (e.g. neutrophils) in response to external insults. However, increasing evidence including our own data has demonstrated that the secretion of S100A8/9 by non-hematopoietic niche-derived elements could be stimulated by inflammatory factors such as prostaglandin E2 (PGE2)[62], IL-1ß, FGF-2 and TGFß[63]. In addition, in the skin tissue, expression of S100A8/9 could be induced by UV irradiation[64,65]. Interestingly, signatures of response to UV irradiation are enriched in the MDS CD271$^+$ mesenchymal cells (**Chapter 2**, supplementary Table 4).

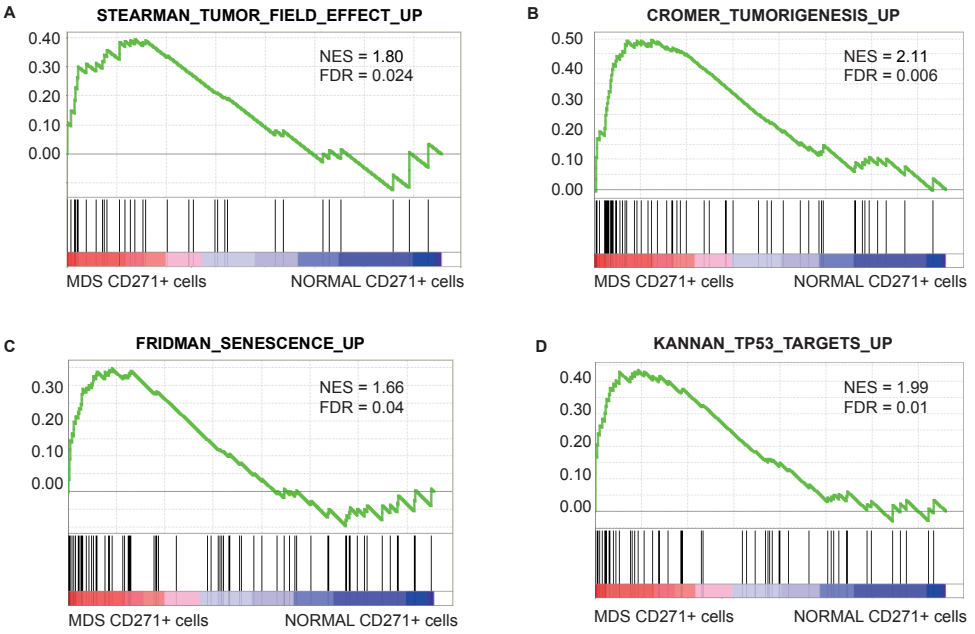


E

| Data Sets | Enrichment | Size | NES | NOM p-val | FDR q-Val |
|---|---|---|---|---|---|
| KANNAN_TP53_TARGETS_UP | MDS MSC | 58 | 1.90 | 0.0 | 0.016 |
| INGA_TP53_TARGETS | MDS MSC | 17 | 1.98 | 0.007 | 0.011 |
| ONGUSAHA_TP53_TARGETS | MDS MSC | 38 | 1.32 | 0.036 | 0.177 |
| SCHAVOLT_TARGETS_OF_TP53_AND_TP63 | MDS MSC | 16 | 1.55 | 0.062 | 0.067 |
| TANG_SENESCENCE_TP53_TARGETS_UP | MDS MSC | 33 | 1.24 | 0.081 | 0.237 |
| PID_P53DOWNSTREAMPATHWAY | MDS MSC | 136 | 1.40 | 0.0 | 0.132 |
| AMUNDSON DNA DAMAGE RESPONSE TP53 | MDS MSC | 16 | 1.39 | 0.091 | 0.137 |

**Figure 3: Signatures associated with field cancerization and senescence are enriched in MDS mesenchymal elements.** (A-B) Representative GSEA signatures indicating "field cancerization" and "tumor-field-effect" in the CD271$^+$ mesenchymal cells isolated from LR-MDS patients. (C-D) Representative GSEA plots implicating the activation of senescence programs in MDS CD271$^+$ mesenchymal cells. (E) A list of GSEA signatures showing upregulation of P53-associated senescence programs in MDS CD271$^+$ mesenchymal cells.
NES: Normalized Enrichment Scores; FDR: False Discovery Rate

Taken together, the data from our work and that of others suggest that stress signaling due to inflammation or ribosomal dysfunction could directly or indirectly induce S100A8/9 expression in the HSPC niche of SDS and MDS patients. These DAMP molecules, together with other inflammatory cytokines are important components of a premalignant inflammatory environment that critically contributes to leukemogenesis while compromising normal hematopoiesis. Therefore, better understanding of the working mechanisms underlying these inflammatory components and the upstream driving force may offer new avenues for therapeutic strategies.

| SASP factors | Genes | FC | FDR |
|---|---|---|---|
| Soluble Factors & Chemokines (CXCL, CCL) | *IL6* (Interleukin 6) | 5.10 | 0.005 |
| | *IL8* (Interleukin 8) | 7.24 | 4,36E-005 |
| | *CCL3* (Chemokine (C-C motif) ligand 3) (MIP-1a) | 4.21 | 0.022 |
| | *CCL7* (Chemokine (C-C motif) ligand 7) (MCP-3) | 9.65 | 0.006 |
| | *CXCL-4* (Chemokine (C-X-C motif) ligand 4) (PF4) | 6.96 | 0.005 |
| | *CXCL14* (Chemokine (C-X-C motif) ligand 14) | 5.54 | 0.023 |
| | *CXCL3* (Chemokine (C-X-C motif) ligand 3) | 6.23 | 0.026 |
| Growth Factors & Regulators | *VEGFa* (Vascular endothelial gorwth factor A) | 6.36 | <0.001 |
| | *IGFBP-3* (Insulin-like growth factor binding protein 3) | 2.53 | 0.010 |
| | *IGFBP-4* (Insulin-like growth factor binding protein 4) | 2.17 | 0.004 |
| | *IGFBP-7* (Insulin-like growth factor binding protein 7) | 2.00 | 0.016 |
| Proteases & Regulators | *TIMP-1* (Tissue Inhibitor Of Metalloproteinases 1) | 2.22 | 0.012 |
| | *ISG15* (ISG15 ubiquitin-like modifier) | 2.45 | 0.014 |
| | *SERPINB2* (Serpin peptidase inhibitor, member 2) | 4.11 | 0.029 |
| | *SMURF2* (SMAD specific E3 ubiquitin protein ligase 2) | 2.46 | 0.029 |
| Soluble or Shed Receptors & Ligands | *ICAM1* (Intercellular adhesion molecule 1) | 2.51 | 0.010 |
| | *PLAUR* (Plasminogen activator, urokinase receptor) (uPAR) | 3.36 | <0.001 |
| Insoluble Factors (ECM) | *FN1* (fibronectin) | 2.00 | 0.037 |
| | *Col1a1* (Collagen, type I, alpha 2) | 3.27 | 0.005 |
| Other | *CLTB* (Clathrin, light chain (Lcb) | 3.20 | 0.009 |
| | *Cryab* (Crystallin, alpha B) | 3.18 | 0.012 |
| | *Cyp1b1* (Cytochrome P450, family 1, subfamily B, polypeptide 1) | 2.22 | *0.004* |
| | *Map1lc3b* (Micotubule-associated protein 1 light chain 3, beta) | 2.75 | 0.016 |
| | *Nme2* (NME/NM23 nucleoside diphosphate kinase 2) | 1.83 | 0.020 |
| | *RAC1* (Ras-related C3 botulinum toxin substrate 1, rho family, small GTP binding protein) | 1.75 | 0.020 |
| | *Vim* (Vimentin) | 2.00 | 0.003 |
| | *MDM2* (Mdm2 p53 binding protein homolog) | 2.13 | 0.029 |

**Table 1:** List of SASP factors upregulated at the transcript level in MDS CD271$^+$ Mesenchymal cells compared to the normal counter parts.

## The mechanism behind inflammation-associated tumorigenesis - induction of genotoxic stress?

Tumorigenesis typically requires more than one single mutation to occur, providing specific clone(s) the survival and proliferative advantage to expand and escape from immune surveillance.[14] An inflammatory microenvironment containing activated inflammatory cells (mainly neutrophils and macrophages) serves as a source of ROS and reactive nitrogen intermediates (RNI) that are capable of inducing genomic instability, enhancing the proliferation of mutated cells and increasing mutation rates.[13,66,67] The infiltrating immune cells such as neutrophils and macrophages have been considered to be the main cellular sources of such genotoxic effects. Our work adds the mesenchymal niche components to this notion, as inflammation in the BM mesenchymal elements, specifically the DAMPs S100A8/9 actively induced genotoxic stress in HSPCs characterized by mitochondrial dysfunction, accumulation of ROS and DNA damage (**Chapter 3**). Not limited to hematological malignancies, in breast cancer, overexpression of MMP-3 (also known as stromelysin) in the tumor microenvironment causes genomic instabilities in the parenchymal cells, resulting in malignant transformation.[68,69] In the mouse model of MMP-3 overexpression in the stromal compartment, malignant transformation of mammary epithelial cells was observed.[68] A later study investigating the mechanistic insight reveals that the overexpression of stromal

MMP-3 exerted several genotoxic effects in the parenchymal epithelial cells characterized by accumulation of ROS mediated by the activation of GTPase Rac1b, stimulation of epithelial-to-mesenchymal transition (EMT), mitochondrial dysfunction and DNA damage.[69] Our data link mesenchymal inflammation to genotoxicity in HSPCs highlighting the stem cell niche as a cellular source of genotoxic effects.

In the OCS model, S100A8/9 act partially via their canonical receptor TLR4 – known pattern recognition receptor; in MDS patients, TLR signaling is activated in the mesenchymal cells with high levels of S100A8/9 expression (**Chapter 3,** Figure 5 & 7). Interestingly, in addition to our study, a recent work showed continuous stimulation of TLR4 with LPS treatment resulted in high level of ROS associated DNA damage in BM HSCs, linking chronic inflammation or severe infection to hematopoietic dysfunction and expansion of malignant HSC.[70] These data together indicate that genotoxic signaling is intimately related to the activation of innate immunity. A well-recognized effect of S100A8/9 binding to TLR4 or RAGE is the activation of NF-κB pathway (**Chapter 3**, supplemental Figure 6), which often results in the consequent secretion of NF-κB-associated inflammatory factors such as TNF-α, TGF-ß, IL-1ß and MMPs.[26,71,72] These inflammatory factors can recruit immune cells (as discussed in section 2.1), which augment S100A8/9 production[73], but they may also be relevant for inducing genotoxic stress in HSPCs. For instance, an inflammatory molecule *Lcn2* – upregulated in the niche cells from mutant OCS mice and SDS patients (**Chapter 3**, Figure 4), can be induced upon S100A8 stimulation[74] and has been recently shown to promote oxidative stress and DNA damage in hematopoietic cells in the context of MPN.[75,76] Therefore, in concert with S100A8/9, other inflammatory factors and TLR ligands may also contribute to the creation of a genotoxic environment, essential for leukemogenesis to take place (**Figure 2**). Our finding of the stem cell niche as the source of genotoxic insults is particularly relevant as recent work has demonstrated that under stress conditions such as infection or inflammation, HSPCs can directly respond to environmental cytokines by adapting their functions (incl. HSPC mobilization, proliferation and differentiation) and producing diverse cytokines for the regulation of stress hematopoiesis.[77-80] In addition, chronic inflammation in the BM can promote the exit of HSCs from dormancy, resulting in the accumulation of oxidative stress and DNA damage, eventually hematopoietic dysfunction and malignant transformation.[81,82] Our data indicate inflammatory molecules derived from the HSPC niche may equally contribute to HSPC DNA damage.

On the other hand, mouse models of solid tumors have shown that DNA damage can also lead to inflammation and thereby promote tumorigenesis, indicating the connection between inflammation and tumor initiation is bi-directional. For example, in the model of hepatocellular carcinoma induced by the carcinogen diethylnitrosamine (DEN), DNA damage in tumor cells resulted in accumulation of ROS and subsequent necrotic cell death, which

promoted an inflammatory reaction further contributing to tumorigenesis.[83,84] Deficiency of the gene flap endonuclease 1 (*Fen1*) resulted in elevated DNA damage due to impaired DNA-damage repair response, which led to a pro-tumorigenic inflammatory response, most likely through the activation of a pattern recognition receptor.[85] Therefore, it is possible for the HSPCs suffering from niche-derived genotoxic stress to undergo apoptosis, which in turn further promote inflammation, like a two-way street, forming a feedforward inflammatory loop that accelerates leukemogenesis.

### The mechanism behind inflammation-associated tumorigenesis – deregulation of epigenetic programs?

Besides inducing genotoxicity, some reports have linked inflammation to epigenetic reprogramming. For example, upon stimulation of inflammatory cytokines, inflammation-associated macrophages express the Jmjc-domain protein Jmjd3 – a H3K27me demethylase and a NF-kB target, associated with the silencing of polycomb group (PcG) target genes.[86] In a mouse model of intestinal cancer, inflammation can also induce DNA methyltransferase (DNMT)-dependent DNA methylation and silencing of a group of PcG target genes, some of which overlap with genes silenced by methylation in human colon cancer.[87] Interestingly, recent work demonstrated that overexpression of Jmjd3 in LR-MDS HSPC regulates the expression level of several NF-kB targets and is associated with impaired erythropoiesis, a key clinical feature in LR-MDS patients.[9] Still, the exact contribution of inflammation-induced epigenetic reprogramming to tumor initiation remains to be established, either in a relevant mouse model or through prospective analysis of human samples.[13]

Taken together, an inflammatory microenvironment is crucial for tumorigenesis and our findings suggest the stem cell niche in addition to the infiltrating immune cells are key components to this microenvironment. DAMPs S100A8/9 in concert with other inflammatory factors may play a critical role in attenuating normal hematopoiesis and driving leukemogenesis via mechanisms such as genotoxic stress and epigenetic reprogramming among others. It is therefore reasonable to hypothesize that an inflammatory "mutagenic" environment may serve as an active participant in driving mutagenesis.

## 3. Can niche-induced inflammatory signaling drive or facilitate the selection and/or expansion of dominant HSPC clones with specific mutations?

Bone marrow failure (BMF) syndromes are characterized by ineffective hematopoiesis, clonal evolution and malignant transformation to leukemia. In this dissertation, we focused on MDS and SDS, two major BMF syndromes with striking propensity for developing AML. As discussed in **Chapter 1**, a number of most frequently mutated genes has been identified in MDS, among which are the epigenetic/chromatin remodeling regulator genes *DNMT3A, TET2,* and *ASXL1*. Mutations in the classical tumor suppressor gene TP53 are associated

with poor prognosis and treatment resistance (Chapter 1 section 3.2). Interestingly, recent large-scale studies of population-based whole-exome sequencing revealed that somatic mutations of these four genes that are mutated in patients with myeloid cancers are recurrently mutated in apparently healthy people (termed as Clonal Hematopoiesis of Indeterminate Potential or 'CHIP'), suggesting these mutations may represent early events in driving the development of hematologic cancers. Mutations in these genes are increasingly prevalent as people age and this age-related clonal hematopoiesis is often associated with increased risks of hematologic cancer and death.[88,89,90] These emerging insights could reflect Darwinian selection, where the "failed" bone marrow environment selects a highly biased set of mutations and enables malignant evolution of these "selected" clones. However, the factors driving the emergence, selection and evolution of these mutational clones remain a mystery.

In **Chapter 3**, high level of mesenchymal S100A8/9 expression independently predicted poor clinical outcome in MDS patients, suggesting the possibility of an inflammatory niche favoring hematopoietic cells carrying certain mutations associated with worse clinical outcome. In addition, abundance of S100A8/9 is associated with aging in a wide range of mouse and human tissues, linking chronic inflammation as a novel mechanism to aging.[91] To investigate whether high level of mesenchymal S100A8/9 expression selects for certain MDS clone, we can compare MDS mutations in S100 niche$^+$ patients to S100 niche$^-$ patients. Interestingly, from this comparison, the frequency of ASXL1 mutation is clearly higher in S100 niche$^+$ patients (43.8% vs. 11.1%) (**Table 2**). *ASXL1* mutations are found in CHIP, suggesting mutations in this gene could be an early driver event for leukemogenesis, supported by data from a mouse model of global *ASXL1* deletion. ASXL(-/-) mice developed MDS-like phenotype via reduced HSC self-renewal and elevated apoptosis in myeloid-committed progenitors.[92,93] In MDS, *ASXL1* mutations are frequent molecular aberrancies that predict an adverse prognostic outcome.[94,95] Our data open the possibility that inflammation in the HSPC niche, specifically S100A8/9 overexpression, might favor the expansion of *ASXL1* mutated cells as they could be resistant to insults like genotoxic stress allowing them to expand while other cells are eliminated in this inflammatory niche.

Mutations in gene *DNMT3A* is another CHIP mutation. Notably, recent work has shown *DNMT3A* mutations resulted in the inability to sense and repair DNA torsional stress in response to daunorubicin (causing double-stranded breaks at higher concentration), resulting in increased mutagenesis.[96] Interestingly, the inability of *DNMT3A* mutant cells to respond to DNA damage signaling is mediated via attenuation of p53 response and γH2AX accumulation[96], indicating *DNMT3A* mutant cells could bypass S100A8/9-induced genotoxic stress, as similar mechanisms were implicated in our data. However, whether *DNMT3A* mutation in the MDS cells is associated with an inflammatory niche remains to be

investigated. Taken together, while our data on one hand supports niche-induced BMF or leukemogenesis mediated via inflammatory signaling, it is conceivable to speculate that in the meantime, this inflammatory "mutagenic" stem-cell niche provides selective pressure on certain clones that are resistant to such an environment driving clonal expansion while eliminating the "less fit" clones.

| | Patient ID | WHO | Cytogenetics | IPSS | Genetic Abnormalities |
|---|---|---|---|---|---|
| S100 niche signature + | MDS020 | RCMD-RS | 46,XX[20] | 0 | SRSF2 mutation |
| | MDS486 | CMML-1 | 46,XX,t(3;3)(q21;q26)[10] | 0.5 | SF3B1 mutation |
| | MDS610 | RCMD-RS | 46,XX[20] | 0.5 | TET2, DNMT3A, SF3B1 and RUNX1 mutation |
| | MDS627 | RCMD | 46,XY[20] | 0 | TET2 and ASXL1 mutation |
| | MDS008 | RCMD | 46,XX[20] | 0.5 | ASXL1 and EZH2 mutation |
| | MDS092 | RAEB-1 | 46,XX,del(5)(q1?5q3?5)[15] | 0.5 | sequenced: no mutations found |
| | MDS174 | RCMD-RS | 47,XY,+19[9]/46,XY[11] | 1 | SETBP1 and U2AF1 mutation |
| | MDS176 | RCMD-RS | 46,XY[22] | 0 | Not Sequenced |
| | MDS019 | RCMD-RS | 46,XX[20] | 0 | SF3B1 mutation |
| | MDS061 | RAEB-1 | 46,XY[20] | 0.5 | DNMT3A, SF3B1 and TET2 mutation |
| | MDS069 | CMML-1 | 46,XY,der(13)t(1;13)(q11;p11)[10] | 1.0 | ASXL1, IDH2, SF3B1 and TET2 mutation |
| | MDS079 | RCMD | 47,XY,t(2;14)(q3?7;q2?2),idic(21)(p1?2),+idic(21)(p1?2)[8] | 1.0 | ASXL1 mutation |
| | MDS135 | RCMD-RS | 46,XX[20] | 0 | ASXL1, TET2 mutation |
| | MDS183 | MDS-U | 47,XX,+8[12] | 0.5 | ASXL1, IDH2 and SRSF2 mutation |
| | MDS203 | RCMD-RS | 46,XY,del(5)(q13q31)[7]/47,XY,del(5)(q13q31),+8[4]/46,XY[1] | 0.5 | ASXL1 and SF3B1 mutation |
| | MDS206 | Del(5q) | 46,XX,del(5)(q13q33)[7]/46,XX[13] | 0 | SF3B1 and TET2 mutation |
| | MDS010 | RCMD | 46,XY[20] | 0 | sequenced: no mutations found |
| S100 niche signature - | MDS006 | RAEB-1 | 46,XX[20] | 1 | DNMT3A and SRSF2 mutation |
| | MDS118 | RARS | 46,XX[20] | 0 | TET2, DNMT3A and SF3B1 mutation |
| | MDS159 | Del(5q) | 46,XX,del(5)(q15q33)[10] | 0 | sequenced, no mutations found |
| | MDS209 | RCMD-RS | 46,XX[10] | 0 | SF3B1 mutation |
| | MDS222 | RARS | 46,XX[21] | 0 | SF3B1 and 2 TET2 mutations |
| | MDS025 | RCMD-RS | 46,XY[20] | 0 | SF3B1 mutation |
| | MDS433 | RCMD-RS | 45,X,-Y[10]/46,XY[10] | 0 | sequenced: no mutations found |
| | MDS646 | RAEB-1 | 46,XX[20] | 1 | ASXL1 mutation |
| | MDS893 | RARS | 46,XX[20] | 0 | SF3B1 mutation |
| | MDS111 | RCMD | 46,XX[20] | 0 | sequenced: no mutations found |
| | MDS623 | RCMD | 46,XY[20] | 0.5 | sequenced: no mutations found |
| | MDS247 | RCMD-RS | 46,XY[20] | 0 | DNMT3A and SF3B1 mutation |
| | MDS150 | RCMD-RS | 46,XX[20] | 0.5 | not sequenced |
| | MDS158 | RCMD-RS | 46,XX[20] | 0 | DNMT3A, SF3B1 and TET2 mutation |
| | MDS172 | RARS | 46,XY[20] | 0 | SF3B1 and 2 TET2 mutations |
| | MDS022 | RAEB-1 | 46,XY[20] | 1.0 | sequenced: no mutations found |
| | MDS053 | RARS | 45,X,-Y[7]/46,XY[3] | 0.0 | SF3B1, TET2 mutation |
| | MDS055 | RCMD | 46,XY,der(22)(t(1;22)(q12;p11)[16]/46,XY,SL,del(20)(q12)[3] | 0.5 | sequenced: no mutations found |
| | MDS093 | RCMD | 46,XY[20] | 0.5 | TET2 mutation |
| | MDS101 | RCMD-RS | 46,XY[21] | 0.0 | ASXL1, DNMT3A and SF3B1 mutation |
| | MDS121 | RCMD | 46,XY[20] | 0.5 | sequenced: no mutations found |
| | MDS144 | RCMD | 47,XY,+19[6]/48,idem,+21[3]/46,XY[4] | 1.0 | ASXL1, U2AF1 mutation |
| | MDS167 | RCMD | 46,XY[21] | 0.0 | SF3B1 mutation |
| | MDS182 | RCMD | 46,XY,del(5)(q13q33)[10]/46,XY[10] | 0.0 | DNMT3A, TET2 mutation |
| | MDS201 | RCMD-RS | 46,XX[20] | 0.0 | SF3B1 mutation |
| | MDS001 | RCMD-RS | 46,XY[20] | 0.0 | SF3B1 mutation |
| | MDS007 | RCMD-RS | 46,XY[20] | 0.0 | SF3B1, TET2 mutation |
| | MDS013 | Del(5q) | 46,XX,del(5)(q13q33)[15]/46,XX[1] | 0.0 | sequenced: no mutations found |

**Table 2: Summary of genetic abnormalities in LR-MDS patients divided in S100 niche+/- group.** (Associated with Chapter 3, Supplemental Table 6)

Summarizing this discussion chapter, a metaphor from the botanical garden proposed by Dotto *et al*. could be of relevance: when a bad plant (weed) is difficult to eradicate, it could be because of its many roots deeply embedded in the terrain or by the spreading of multiple bad seeds. It is, however, also possible that a bad soil could corrupt properties of otherwise perfectly good plants or favor the growth of bad plants. In the latter case, unless the soil is corrected, different interventions are of little or no use (**Figure 4**).[40]

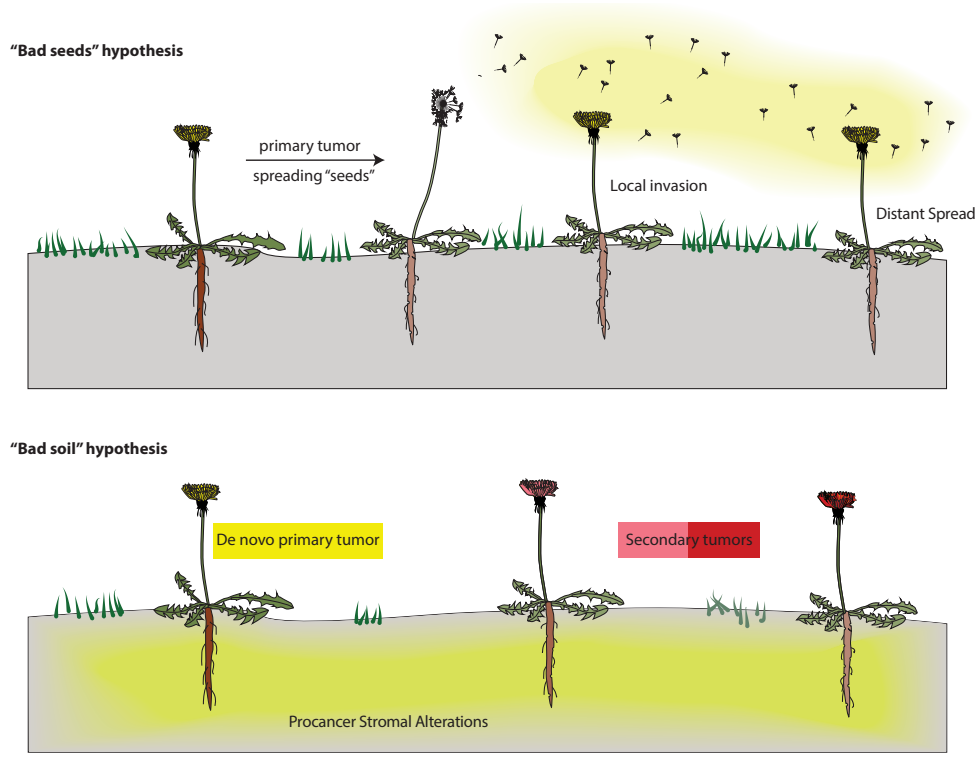


**Figure 4. Metaphorical hypothesis of bad plant and bad soil.** (Created based on Dotto, 2014)[40] (A) The bad seeds hypothesis suggests the ability of the primary tumors to root deeply in the soil and "spread bad seeds" to neighboring or distant cells (plants), transforming them into tumor. These primary tumors are likely to grow in many conditions. (B) On the other hand, the bad soil hypothesis suggests the initial insults and alterations occur in the stroma (soil) allowing the growth of various tumors of monoclonal (primary tumors) or polyclonal (secondary tumors) origin.

## 4. Perspective and future directions

This dissertation deals with the role of the HSPC niche in leukemia predisposition syndromes, particularly SDS and MDS. Our data uncovered an important novel concept of niche-induced inflammation driving genotoxic stress in HSPCs as a potential mechanism with relevance to human pre-leukemic disorders. In the meantime, our findings intrigued further questions and hypothesis worth investigating. First of all, leukemia transformation was not observed in the OCS model, likely due to a) the limited lifespan (~28 days) of these mice precluding long-term exposure of HSPCs to the mutagenic niche or b) the DNA repair-proficient HSPCs can overcome the mutagenic stress preventing the accumulation of stable genetic damage. To prolong the lifespan of the OCS mice, the tetracycline-off (TetO)-cassette in the *Osterix*-cre construct could be utilized. So *Sbds* deletion from the mesenchymal cells in the OCS model could be achieved postnatally, allowing the mice to age. As a result, the prolonged

exposure of the HSPCs to a genotoxic milieu may lead to complete HSPC dysfunction and eventually leukemia transformation from the myelodysplasia stage observed in the current OCS model. For a long time, we wanted to test in our model if leukemia evolution would be the result of a mutagenic environment cooperating with the aberrant HSPCs, unable to cope with the inflammatory genotoxic stress. Interestingly, a recent work supported our idea. This report demonstrated that mice with *PTPN11* mutations in both hematopoietic cells and mesenchymal elements reached malignant transformation much more rapidly than mice with *PTPN11* mutations in either one of the cellular compartments alone.[17] To test our idea, an experimental model where *Sbds* deficient mesenchymal microenvironment is combined with *Sbds* deficient HSPCs could generate interesting insights. This could be achieved by introducing *Sbds(-/-)* HSPCs[5] into the OCS recipients via intrahepatic transplantation into the newborn OCS mice, considering the short lifespan of the OCS mice. Alternatively, if the Tet-off system proves efficient, transplantation of *Sbds(-/-)* HSPCs into the adult Tet-off Osterix$^{cre}$*Sbds*$^{f/f}$ recipients could be performed and interrogated following the typical scheme of transplantation and leukemia-watch analysis. In addition, in a transplantation assay using S100A9Tg mice, we demonstrated niche-derived S100A8/9 is sufficient in driving genotoxic stress in HSPCs. Thus, it would also be interesting to transplant the DNA repair deficient *Sbds(-/-)* HSPCs into S100A9Tg recipients and examine if such cooperation would result in leukemic transformation.

As discussed earlier, other inflammatory cytokines such as CCL3, CCL4, CCL5 and IL-1ß are likely to contribute to the inflammatory-genotoxic milieu in addition to S100A8/9. Therefore, it is worth investigating if niche-derived S100A8/9 is required to induce genotoxicity (our data showed they are sufficient in inducing genotoxicity), particularly in the new models proposed above where leukemogenesis might be observed. Anti-TLR4 antibodies could be used, as suggested in Chapter 3. However, it is worth noting that in the OCS model, a partial rescue was observed suggesting S100A8/9 might engage other cognate receptors like CD33 in addition to TLR4, or other inflammatory factors may be invovled.[26] Small molecule inhibitors of S100A8/9 could be considered as well, such as the quinolone-3-carboxamide derivatives (ABR-215050 and ABR-215757) which have recently been tested as potential treatments in prostate cancer and inflammatory diseases.[97-99] Such studies will provide new insights into the possibility of targeting niche-derived S100A8/9 as therapeutic strategies in pre-leukemic patients.

In addition to the described mesenchymal inflammation-induced genotoxic stress, it is worth investigating if impaired energy metabolism could be another underlying mechanism. In a mouse model of prostate cancer, reduced level of p62 (also known as sequestosome-1) in CAFs resulted in impaired stromal glucose and amino acid metabolism via the redox mTORC1/c-Myc pathway, which in turn led to higher stromal IL-6 production and consequent

tumor promotion.[100] These data suggest metabolic reprogramming in the stroma is linked to inflammation and tumorigenesis. Another study also revealed that adipocytes could engage in the "metabolic coupling" process with cancer cells via mitochondria metabolism, thereby promote tumor progression.[101,102] Furthermore, in solid tumors, the well-known "Warburg effect" of cancer cells can "educate" the CAFs to switch on aerobic glycolysis, secreting lactate and pyruvate, which in turn can serve as fuel for tumor cell proliferation.[103,104] This symbiotic relationship in energy metabolism between the tumor microenvironment and cancer cells seem to be bi-directional. Notably, HSPCs in the OCS model present deregulated mechanism of mitochondrial ATP generation characterized by downregulation of oxidative phosphorylation pathways; whereas MDS CD271$^+$ mesenchymal cells display strong hypoxic signatures, which can activate HIF response system stimulating aerobic glycolysis (data not shown).[16] Therefore, further pinpointing the metabolic dysfunctions in the mesenchymal niche and HSPCs in the OCS model could reveal if such a symbiotic relationship between the HSPCs and their niche exists in this pre-leukemic model, demonstrating the relevance of stromal inflammation and metabolism in leukemogenesis.

Another important conclusion of this thesis is mesenchymal S100A8/9 expression at the transcript level independently predicted disease outcome in LR-MDS patients regardless of the mutational status of the MDS clones. Interestingly, S100A8 expression has been shown to correlate with poor outcome in AML where high S100A8 level in leukemic blasts predicted worse clinical outcome.[105] In solid tumors, stromal parameters have been shown to predict clinical outcome and resistance to chemotherapy in a broad range of cancer types including breast cancer, lung cancer and liver tumors.[106-109] In a recent report studying microenvironmental remodeling as a prognostic factor in AML, the distinct pattern of stromal composition in the leukemic bone marrow at diagnosis is associated with the heterogeneous post-treatment clinical course of AML. Specifically, higher number of immunophenotypically defined primitive mesenchymal stromal cells (CD146$^+$ enriched) in the BM is strongly associated with early relapse, whereas higher number of osteoblasts is significantly associated with late relapse.[110] Considering the precedents, our data shows inflammatory BM niche factors may be used as prognostic markers in LR-MDS. Nonetheless, future investigations are required to confirm our finding in larger patient cohorts of other independent studies, paving the way to incorporate molecular cues in the inflammatory BM niche as novel prognostic parameters and hopefully as new therapeutic avenues for leukemia predispositions.

## REFERENCES


1. Raaijmakers MH, Mukherjee S, Guo S, et al. Bone progenitor dysfunction induces myelodysplasia and secondary leukaemia. *Nature*. 2010;464(7290):852-857.
2. Medyouf H, Mossner M, Jann JC, et al. Myelodysplastic cells in patients reprogram mesenchymal stromal cells to establish a transplantable stem cell niche disease unit. *Cell Stem Cell*. 2014;14(6):824-837.
3. G anan-Gomez I, Wei Y, Starczynowski DT, et al. Deregulation of innate immune and inflammatory signaling in myelodysplastic syndromes. *Leukemia*. 2015;29(7):1458-1469.
4. Kode A, Manavalan JS, Mosialou I, et al. Leukaemogenesis induced by an activating beta-catenin mutation in osteoblasts. *Nature*. 2014;506(7487):240-244.
5. Zambetti NA, Bindels EM, Van Strien PM, et al. Deficiency of the ribosome biogenesis gene Sbds in hematopoietic stem and progenitor cells causes neutropenia in mice by attenuating lineage progression in myelocytes. *Haematologica*. 2015;100(10):1285-1293.
6. Li C, Chen H, Ding F, et al. A novel p53 target gene, S100A9, induces p53-dependent cellular apoptosis and mediates the p53 apoptosis pathway. *Biochem J*. 2009;422(2):363-372.
7. Basiorka AA, McGraw KL, Eksioglu EA, et al. The NLRP3 inflammasome functions as a driver of the myelodysplastic syndrome phenotype. *Blood*. 2016;128(25):2960-2975.
8. Schneider RK, Schenone M, Ferreira MV, et al. Rps14 haploinsufficiency causes a block in erythroid differentiation mediated by S100A8 and S100A9. *Nature Medicine*. 2016;22(3):288-297.
9. Wei Y, Chen R, Dimicoli S, et al. Global H3K4me3 genome mapping reveals alterations of innate immunity signaling and overexpression of JMJD3 in human myelodysplastic syndrome CD34+ cells. *Leukemia*. 2013;27(11):2177-2186.
10. Choi CW, Chung YJ, Slape C, Aplan PD. Impaired differentiation and apoptosis of hematopoietic precursors in a mouse model of myelodysplastic syndrome. *Haematologica*. 2008;93(9):1394-1397.
11. Chung YJ, Robert C, Gough SM, Rassool FV, Aplan PD. Oxidative stress leads to increased mutation frequency in a murine model of myelodysplastic syndrome. *Leuk Res*. 2014;38(1):95-102.
12. Mantovani A, Allavena P, Sica A, Balkwill F. Cancer-related inflammation. *Nature*. 2008;454(7203):436-444.
13. Grivennikov SI, Greten FR, Karin M. Immunity, inflammation, and cancer. *Cell*. 2010;140(6):883-899.
14. Hanahan D, Weinberg RA. The hallmarks of cancer. *Cell*. 2000;100(1):57-70.
15. Hanahan D, Weinberg RA. Hallmarks of cancer: the next generation. *Cell*. 2011;144(5):646-674.
16. Hanahan D, Coussens LM. Accessories to the crime: functions of cells recruited to the tumor microenvironment. *Cancer Cell*. 2012;21(3):309-322.
17. Dong L, Yu WM, Zheng H, et al. Leukaemogenic effects of Ptpn11 activating mutations in the stem cell microenvironment. *Nature*. 2016.
18. Murdoch C, Giannoudis A, Lewis CE. Mechanisms regulating the recruitment of macrophages into hypoxic areas of tumors and other ischemic tissues. *Blood*. 2004;104(8):2224-2234.
19. Condeelis J, Pollard JW. Macrophages: obligate partners for tumor cell migration, invasion, and metastasis. *Cell*. 2006;124(2):263-266.
20. Schepers K, Pietras EM, Reynaud D, et al. Myeloproliferative neoplasia remodels the endosteal bone marrow niche into a self-reinforcing leukemic niche. *Cell Stem Cell*. 2013;13(3):285-299.

21. Arranz L, Sanchez-Aguilera A, Martin-Perez D, et al. Neuropathy of haematopoietic stem cell niche is essential for myeloproliferative neoplasms. *Nature*. 2014;512(7512):78-81.

22. Lewis AM, Varghese S, Xu H, Alexander HR. Interleukin-1 and cancer progression: the emerging role of interleukin-1 receptor antagonist as a novel therapeutic agent in cancer treatment. *J Transl Med*. 2006;4:48.

23. Widmer U, Manogue KR, Cerami A, Sherry B. Genomic cloning and promoter analysis of macrophage inflammatory protein (MIP)-2, MIP-1 alpha, and MIP-1 beta, members of the chemokine superfamily of proinflammatory cytokines. *J Immunol*. 1993;150(11):4996-5012.

24. Coffelt SB, Hughes R, Lewis CE. Tumor-associated macrophages: Effectors of angiogenesis and tumor progression. *Biochimica Et Biophysica Acta-Reviews on Cancer*. 2009;1796(1):11-18.

25. Hiratsuka S, Watanabe A, Aburatani H, Maru Y. Tumour-mediated upregulation of chemoattractants and recruitment of myeloid cells predetermines lung metastasis. *Nature Cell Biology*. 2006;8(12):1369-U1331.

26. Chen XH, Eksioglu EA, Zhou JM, et al. Induction of myelodysplasia by myeloid-derived suppressor cells. *Journal of Clinical Investigation*. 2013;123(11):4595-4611.

27. Camacho V, McClearn V, Patel S, Welner RS. Regulation of normal and leukemic stem cells through cytokine signaling and the microenvironment. *Int J Hematol*. 2017.

28. Moudra A, Hubackova S, Machalova V, et al. Dynamic alterations of bone marrow cytokine landscape of myelodysplastic syndromes patients treated with 5-azacytidine. *Oncoimmunology*. 2016;5(10):e1183860.

29. Takeuchi O, Akira S. Pattern recognition receptors and inflammation. *Cell*. 2010;140(6):805-820.

30. Kitagawa M, Saito I, Kuwata T, et al. Overexpression of tumor necrosis factor (TNF)-alpha and interferon (IFN)-gamma by bone marrow cells from patients with myelodysplastic syndromes. *Leukemia*. 1997;11(12):2049-2054.

31. Sawanobori M, Yamaguchi S, Hasegawa M, et al. Expression of TNF receptors and related signaling molecules in the bone marrow from patients with myelodysplastic syndromes. *Leuk Res*. 2003;27(7):583-591.

32. Wei Y, Dimicoli S, Bueso-Ramos C, et al. Toll-like receptor alterations in myelodysplastic syndrome. *Leukemia*. 2013;27(9):1832-1840.

33. Kuninaka N, Kurata M, Yamamoto K, et al. Expression of Toll-like receptor 9 in bone marrow cells of myelodysplastic syndromes is down-regulated during transformation to overt leukemia. *Exp Mol Pathol*. 2010;88(2):293-298.

34. Kinzler KW, Vogelstein B. Landscaping the cancer terrain. *Science*. 1998;280(5366):1036-1037.

35. Cunha GR, Hayward SW, Wang YZ, Ricke WA. Role of the stromal microenvironment in carcinogenesis of the prostate. *Int J Cancer*. 2003;107(1):1-10.

36. Bhowmick NA, Chytil A, Plieth D, et al. TGF-beta signaling in fibroblasts modulates the oncogenic potential of adjacent epithelia. *Science*. 2004;303(5659):848-851.

37. Achyut BR, Bader DA, Robles AI, et al. Inflammation-Mediated Genetic and Epigenetic Alterations Drive Cancer Development in the Neighboring Epithelium upon Stromal Abrogation of TGF-beta Signaling. *Plos Genetics*. 2013;9(2).

38. Hu B, Castillo E, Harewood L, et al. Multifocal epithelial tumors and field cancerization from loss of mesenchymal CSL signaling. *Cell*. 2012;149(6):1207-1220.

39. Slaughter DP, Southwick HW, Smejkal W. Field cancerization in oral stratified squamous epithelium; clinical implications of multicentric origin. *Cancer*. 1953;6(5):963-968.

40. Dotto GP. Multifocal epithelial tumors and field cancerization: stroma as a primary determinant. *J Clin Invest*. 2014;124(4):1446-1453.

41. Dakubo GD, Jakupciak JP, Birch-Machin MA, Parr RL. Clinical implications and utility of field cancerization. *Cancer Cell Int*. 2007;7:2.

42. Tu S, Bhagat G, Cui G, et al. Overexpression of interleukin-1beta induces gastric inflammation and cancer and mobilizes myeloid-derived suppressor cells in mice. *Cancer Cell*. 2008;14(5):408-419.

43. Bachelor MA, Bowden GT. UVA-mediated activation of signaling pathways involved in skin tumor promotion and progression. *Seminars in Cancer Biology*. 2004;14(2):131-138.

44. Campisi J, Demaria M. Cellular senescence links inflammation and aging. *Febs Journal*. 2011;278:45-46.

45. Kuilman T, Peeper DS. Senescence-messaging secretome: SMS-ing cellular stress. *Nature Reviews Cancer*. 2009;9(2):81-94.

46. Kuilman T, Michaloglou C, Vredeveld LCW, et al. Oncogene-induced senescence relayed by an interleukin-dependent inflammatory network. *Cell*. 2008;133(6):1019-1031.

47. Erez N, Truitt M, Olson P, Arron ST, Hanahan D. Cancer-Associated Fibroblasts Are Activated in Incipient Neoplasia to Orchestrate Tumor-Promoting Inflammation in an NF-kappaB-Dependent Manner. *Cancer Cell*. 2010;17(2):135-147.

48. Scadden DT. Rethinking stroma: lessons from the blood. *Cell Stem Cell*. 2012;10(6):648-649.

49. Nemeth J, Stein I, Haag D, et al. S100A8 and S100A9 are novel nuclear factor kappa B target genes during malignant progression of murine and human liver carcinogenesis. *Hepatology*. 2009;50(4):1251-1262.

50. Wang YY, Cen JN, He J, et al. Accelerated cellular senescence in myelodysplastic syndrome. *Exp Hematol*. 2009;37(11):1310-1317.

51. Xiao Y, Wang J, Song H, Zou P, Zhou D, Liu L. CD34+ cells from patients with myelodysplastic syndrome present different p21 dependent premature senescence. *Leuk Res*. 2013;37(3):333-340.

52. Hoare M, Narita M. Transmitting senescence to the cell neighbourhood. *Nat Cell Biol*. 2013;15(8):887-889.

53. Krtolica A, Parrinello S, Lockett S, Desprez PY, Campisi J. Senescent fibroblasts promote epithelial cell growth and tumorigenesis: a link between cancer and aging. *Proc Natl Acad Sci U S A*. 2001;98(21):12072-12077.

54. Bavik C, Coleman I, Dean JP, Knudsen B, Plymate S, Nelson PS. The gene expression program of prostate fibroblast senescence modulates neoplastic epithelial cell proliferation through paracrine mechanisms. *Cancer Res*. 2006;66(2):794-802.

55. Coppe JP, Boysen M, Sun CH, et al. A role for fibroblasts in mediating the effects of tobacco-induced epithelial cell growth and invasion. *Mol Cancer Res*. 2008;6(7):1085-1098.

56. Parrinello S, Coppe JP, Krtolica A, Campisi J. Stromal-epithelial interactions in aging and cancer: senescent fibroblasts alter epithelial cell differentiation. *J Cell Sci*. 2005;118(Pt 3):485-496.

57. Liu D, Hornsby PJ. Senescent human fibroblasts increase the early growth of xenograft tumors via matrix metalloproteinase secretion. *Cancer Res*. 2007;67(7):3117-3126.

58. Odink K, Cerletti N, Bruggen J, et al. Two calcium-binding proteins in infiltrate macrophages of rheumatoid arthritis. *Nature*. 1987;330(6143):80-82.

59. Wilkinson MM, Busuttil A, Hayward C, Brock DJ, Dorin JR, Van Heyningen V. Expression pattern of two related cystic fibrosis-associated calcium-binding proteins in normal and abnormal tissues. *J Cell Sci*. 1988;91 ( Pt 2):221-230.

60. Kelly SE, Jones DB, Fleming S. Calgranulin expression in inflammatory dermatoses. *J Pathol*. 1989;159(1):17-21.

61. Vogl T, Eisenblatter M, Voller T, et al. Alarmin S100A8/S100A9 as a biomarker for molecular imaging of local inflammatory activity. *Nat Commun*. 2014;5:4593.

62. Miao L, Grebhardt S, Shi J, Peipe I, Zhang J, Mayer D. Prostaglandin E2 stimulates S100A8 expression by activating protein kinase A and CCAAT/enhancer-binding-protein-beta in prostate cancer cells. *Int J Biochem Cell Biol*. 2012;44(11):1919-1928.

63. Rahimi F, Hsu K, Endoh Y, Geczy CL. FGF-2, IL-1beta and TGF-beta regulate fibroblast expression of S100A8. *FEBS J*. 2005;272(11):2811-2827.

64. Grimbaldeston MA, Geczy CL, Tedla N, Finlay-Jones JJ, Hart PH. S100A8 induction in keratinocytes by ultraviolet A irradiation is dependent on reactive oxygen intermediates. *J Invest Dermatol*. 2003;121(5):1168-1174.

65. Lee YM, Kim YK, Eun HC, Chung JH. Changes in S100A8 expression in UV-irradiated and aged human skin in vivo. *Arch Dermatol Res*. 2009;301(7):523-529.

66. Kraus S, Arber N. Inflammation and colorectal cancer. *Curr Opin Pharmacol*. 2009;9(4):405-410.

67. Hussain SP, Hofseth LJ, Harris CC. Radical causes of cancer. *Nat Rev Cancer*. 2003;3(4):276-285.

68. Sternlicht MD, Lochter A, Sympson CJ, et al. The stromal proteinase MMP3/stromelysin-1 promotes mammary carcinogenesis. *Cell*. 1999;98(2):137-146.

69. Radisky DC, Levy DD, Littlepage LE, et al. Rac1b and reactive oxygen species mediate MMP-3-induced EMT and genomic instability. *Nature*. 2005;436(7047):123-127.

70. Takizawa H, Saito Y, Kovtonyuk LV, Frisch K, Manz MG. Direct Sensing of Lipopolysaccharide Limits Hematopoietic Stem Cell Selfrenewal Via TLR4-TRIF-ROS-p38 Pathway. *Blood*. 2014;124(21).

71. Vogl T, Tenbrock K, Ludwig S, et al. Mrp8 and Mrp14 are endogenous activators of Toll- like receptor 4, promoting lethal, endotoxin-induced shock. *Nature Medicine*. 2007;13(9):1042-1049.

72. van Lent PLEM, Grevers L, Blom AB, et al. Myeloid-related proteins S100A8/S100A9 regulate joint inflammation and cartilage destruction during antigen-induced arthritis. *Annals of the Rheumatic Diseases*. 2008;67(12):1750-1758.

73. Ehrchen JM, Sunderkotter C, Foell D, Vogl T, Roth J. The endogenous Toll-like receptor 4 agonist S100A8/S100A9 (calprotectin) as innate amplifier of infection, autoimmunity, and cancer. *Journal of Leukocyte Biology*. 2009;86(3):557-566.

74. Ichikawa M, Williams R, Wang L, Vogl T, Srikrishna G. S100A8/A9 Activate Key Genes and Pathways in Colon Tumor Progression (vol 9, pg 133, 2011). *Molecular Cancer Research*. 2011;9(9):1266-1266.

75. Kagoya Y, Yoshimi A, Tsuruta-Kishino T, et al. JAK2V617F(+) myeloproliferative neoplasm clones evoke paracrine DNA damage to adjacent normal cells through secretion of lipocalin-2. *Blood*. 2014;124(19):2996-3006.

76. Lu M, Xia LJ, Liu YC, et al. Lipocalin produced by myelofibrosis cells affects the fate of both hematopoietic and marrow microenvironmental cells. *Blood*. 2015;126(8):972-982.

77. Zhao JL, Ma C, O'Connell RM, et al. Conversion of danger signals into cytokine signals by hematopoietic stem and progenitor cells for regulation of stress-induced hematopoiesis. *Cell Stem Cell*. 2014;14(4):445-459.

78. Challen GA, Boles NC, Chambers SM, Goodell MA. Distinct hematopoietic stem cell subtypes are differentially regulated by TGF-beta1. *Cell Stem Cell*. 2010;6(3):265-278.

79. Maeda K, Malykhin A, Teague-Weber BN, Sun XH, Farris AD, Coggeshall KM. Interleukin-6 aborts lymphopoiesis and elevates production of myeloid cells in systemic lupus erythematosus-prone B6.Sle1.Yaa animals. *Blood*. 2009;113(19):4534-4540.

80. Mossadegh-Keller N, Sarrazin S, Kandalla PK, et al. M-CSF instructs myeloid lineage fate in single haematopoietic stem cells. *Nature*. 2013;497(7448):239-243.

81. Schuettpelz LG, Link DC. Regulation of hematopoietic stem cell activity by inflammation. *Front Immunol*. 2013;4:204.

82. Walter D, Lier A, Geiselhart A, et al. Exit from dormancy provokes DNA-damage-induced attrition in haematopoietic stem cells. *Nature*. 2015;520(7548):549-552.

83. Maeda S, Kamata H, Luo JL, Leffert H, Karin M. IKKbeta couples hepatocyte death to cytokine-driven compensatory proliferation that promotes chemical hepatocarcinogenesis. *Cell*. 2005;121(7):977-990.

84. Sakurai T, He G, Matsuzawa A, et al. Hepatocyte necrosis induced by oxidative stress and IL-1 alpha release mediate carcinogen-induced compensatory proliferation and liver tumorigenesis. *Cancer Cell*. 2008;14(2):156-165.

85. Zheng L, Dai H, Zhou M, et al. Fen1 mutations result in autoimmunity, chronic inflammation and cancers. *Nat Med*. 2007;13(7):812-819.

86. De Santa F, Totaro MG, Prosperini E, Notarbartolo S, Testa G, Natoli G. The histone H3 lysine-27 demethylase Jmjd3 links inflammation to inhibition of polycomb-mediated gene silencing. *Cell*. 2007;130(6):1083-1094.

87. Hahn MA, Hahn T, Lee DH, et al. Methylation of Polycomb Target Genes in Intestinal Cancer Is Mediated by Inflammation. *Cancer Research*. 2008;68(24):10280-10289.

88. Genovese G, Kahler AK, Handsaker RE, et al. Clonal hematopoiesis and blood-cancer risk inferred from blood DNA sequence. *N Engl J Med*. 2014;371(26):2477-2487.

89. Jaiswal S, Fontanillas P, Flannick J, et al. Age-related clonal hematopoiesis associated with adverse outcomes. *N Engl J Med*. 2014;371(26):2488-2498.

90. Yoshizato T, Dumitriu B, Hosokawa K, et al. Somatic Mutations and Clonal Hematopoiesis in Aplastic Anemia. *N Engl J Med*. 2015;373(1):35-47.

91. Swindell WR, Johnston A, Xing X, et al. Robust shifts in S100a9 expression with aging: a novel mechanism for chronic inflammation. *Sci Rep*. 2013;3:1215.

92. Wang J, Li Z, He Y, et al. Loss of Asxl1 leads to myelodysplastic syndrome-like disease in mice. *Blood*. 2014;123(4):541-553.

93. Abdel-Wahab O, Gao J, Adli M, et al. Deletion of Asxl1 results in myelodysplasia and severe developmental defects in vivo. *J Exp Med*. 2013;210(12):2641-2659.

94. Bejar R, Stevenson K, Abdel-Wahab O, et al. Clinical effect of point mutations in myelodysplastic syndromes. *N Engl J Med*. 2011;364(26):2496-2506.

95. Thol F, Friesen I, Damm F, et al. Prognostic significance of ASXL1 mutations in patients with myelodysplastic syndromes. *J Clin Oncol*. 2011;29(18):2499-2506.

96. Guryanova OA, Shank K, Spitzer B, et al. DNMT3A mutations promote anthracycline resistance in acute myeloid leukemia via impaired nucleosome remodeling. *Nat Med*. 2016;22(12):1488-1495.

97. Armstrong AJ, Haggman M, Stadler WM, et al. Long-term survival and biomarker correlates of tasquinimod efficacy in a multicenter randomized study of men with minimally symptomatic metastatic castration-resistant prostate cancer. *Clin Cancer Res*. 2013;19(24):6891-6901.

98. Yan L, Bjork P, Butuc R, et al. Beneficial effects of quinoline-3-carboxamide (ABR-215757) on atherosclerotic plaque morphology in S100A12 transgenic ApoE null mice. *Atherosclerosis*. 2013;228(1):69-79.

99. Helmersson S, Sundstedt A, Deronic A, Leanderson T, Ivars F. Amelioration of experimental autoimmune encephalomyelitis by the quinoline-3-carboxamide paquinimod: reduced priming of proinflammatory effector CD4(+) T cells. *Am J Pathol*. 2013;182(5):1671-1680.

100. Valencia T, Kim JY, Abu-Baker S, et al. Metabolic reprogramming of stromal fibroblasts through p62-mTORC1 signaling promotes inflammation and tumorigenesis. *Cancer Cell*. 2014;26(1):121-135.

101. Martinez-Outschoorn UE, Sotgia F, Lisanti MP. Power surge: supporting cells "fuel" cancer cell mitochondria. *Cell Metab*. 2012;15(1):4-5.

102. Nieman KM, Kenny HA, Penicka CV, et al. Adipocytes promote ovarian cancer metastasis and provide energy for rapid tumor growth. *Nat Med*. 2011;17(11):1498-1503.

103. Rattigan YI, Patel BB, Ackerstaff E, et al. Lactate is a mediator of metabolic cooperation between stromal carcinoma associated fibroblasts and glycolytic tumor cells in the tumor microenvironment. *Exp Cell Res*. 2012;318(4):326-335.

104. Sotgia F, Martinez-Outschoorn UE, Howell A, Pestell RG, Pavlides S, Lisanti MP. Caveolin-1 and cancer metabolism in the tumor microenvironment: markers, models, and mechanisms. *Annu Rev Pathol*. 2012;7:423-467.

105. Nicolas E, Ramus C, Berthier S, et al. Expression of S100A8 in leukemic cells predicts poor survival in de novo AML patients. *Leukemia*. 2011;25(1):57-65.

106. Finak G, Bertos N, Pepin F, et al. Stromal gene expression predicts clinical outcome in breast cancer. *Nat Med*. 2008;14(5):518-527.

107. Farmer P, Bonnefoi H, Anderle P, et al. A stroma-related gene signature predicts resistance to neoadjuvant chemotherapy in breast cancer. *Nature Medicine*. 2009;15(1):68-74.

108. Edlund K, Lindskog C, Saito A, et al. CD99 is a novel prognostic stromal marker in non-small cell lung cancer. *International Journal of Cancer*. 2012;131(10):2264-2273.

109. Sulpice L, Rayar M, Desille M, et al. Molecular Profiling of Stroma Identifies Osteopontin as an Independent Predictor of Poor Prognosis in Intrahepatic Cholangiocarcinoma. *Hepatology*. 2013;58(6):1992-2000.

110. Kim JA, Shim JS, Lee GY, et al. Microenvironmental Remodeling as a Parameter and Prognostic Factor of Heterogeneous Leukemogenesis in Acute Myelogenous Leukemia. *Cancer Research*. 2015;75(11):2222-2231.

# A

# ADDENDUM

## LIST OF ABBREVIATIONS

| | |
|---|---|
| AML | Acute myeloid leukemia |
| ASXL1 | Additional sex combs like 1 |
| BCR-ABL1 | Breakpoint cluster region - Abelson murine leukemia viral oncogene homolog 1 |
| CD48 | Cluster of Differentiation 48 / signaling lymphocytic activation molecule family member 2 |
| CD150 | Cluster of Differentiation 150 / Signaling Lymphocytic Activation Molecule Family Member 1 |
| CXCR4 | C-X-C Motif Chemokine Receptor 4 |
| CXCL4 | Chemokine (C-X-C Motif) Ligand 4 / Platelet Factor 4 |
| c-kit | Mast/stem cell growth factor receptor / CD117 |
| CCL3 | C-C Motif Chemokine Ligand 3 |
| DHE | Dihydroethidium |
| EZH2 | Enhancer Of Zeste 2 Polycomb Repressive Complex 2 Subunit |
| EIF6 | Eukaryotic Translation Initiation Factor 6 |
| FGF1 | Fibroblast Growth Factor 1 |
| HSC | Hematopoietic stem cell |
| HSPC | Hematopoietic stem progenitor cell |
| IDH1 | Isocitrate Dehydrogenase 1 |
| IDH2 | Isocitrate Dehydrogenase 2 |
| IL-1ß | Interleukin 1 Beta |
| IGFBP2 | Insulin Like Growth Factor Binding Protein 2 |
| JAK | Janus Kinase |
| KITL | Proto-Oncogene receptor tyrosine kinase (KIT) ligand |
| LIF: | Leukemia Inhibitory Factor |
| MPL | Thrombopoietin Receptor |
| MPP | Multipotent progenitors |
| MPN | Myeloproliferative neoplasms |
| MDS | Myelodysplastic syndromes |
| LR-MDS | Low-risk myelodysplastic syndromes |
| MAPK | Mitogen-Activated Protein Kinase |
| RPS | small subunit ribosomal protein |
| ROS | Reactive oxygen species |
| SF3B1 | Splicing Factor 3b Subunit 1 |
| Sca-1 | stem cell antigen 1 |
| STAT | Signal Transducer And Activator Of Transcription |
| TMRM | Tetramethylrhodamine, methyl ester |

| | |
|---|---|
| TET2 | Tet Methylcytosine Dioxygenase 2 |
| TGF-ß | Transforming Growth Factor Beta |
| VEGFR2 | Vascular Endothelial Growth Factor Receptor 2 |
| VEGFA | Vascular Endothelial Growth Factor A |
| ASXL1 | Additional Sex Combs Like 1 |
| CML | Chronic myeloid leukaemia |
| DAMP | Danger associated molecular pattern |
| DNMT3A | DNA Methyltransferase 3 Alpha |
| JMJD3 | Lysine-Specific Demethylase 6B |
| LPS | Lipopolysaccharide |
| Lcn-2 | Lipocalin 2 |
| MMP-3 | Matrix Metallopeptidase 3 |
| PTPN11 | Protein Tyrosine Phosphatase, Non-Receptor Type 11 |
| PGE2 | prostaglandin E2 |
| RAGE | receptor for advanced glycation endproducts |
| S100A8 | S100 Calcium Binding Protein A8 |
| S100A9 | S100 Calcium Binding Protein A9 |
| TLR | Toll-like receptor |

## ENGLISH SUMMARY

In the adult hematopoietic system, the mature blood cells including red blood cells, white blood cells and platelets are short-lived and must be continuously replenished by the differentiation of rare hematopoietic stem cells (HSCs) residing in the adult bone marrow. Under homeostatic conditions, the HSCs must be able to renew themselves (termed as self-renewal) via proliferation while differentiating into mature blood cells. Dysregulation of this process may lead to the malignant transformation of HSCs, giving rise to hematopoietic malignancies. The diverse functions of HSCs including self-renewal, differentiation, and proliferation must therefore be tightly regulated and delicately maintained, depending on both cell intrinsic programs and extrinsic molecular cues coming from non-hematopoietic cells in the bone marrow microenvironment. These non-hematopoietic cells are collectively known as the HSC niche, of which the cellular composition is rather complex comprising a wide range of cell types. One of the essential components of the HSC niche is the mesenchymal progenitor cell (MPC).

It is increasingly evident that hematopoietic disorders are the result of an altered tissue homeostasis, rather than disrupted function of hematopoietic cells alone. Although researchers have primarily focused on hematopoietic cell-autonomous contributions, the role of the HSC niche in disease pathogenesis is increasingly appreciated. Data derived from genetic mouse modeling have revealed that primary disruption of specific components of the HSC niche can initiate hematopoietic alterations and even leukemogenesis. However, the underlying molecular mechanisms and the relevance of these findings from mouse models to human disease remain understudied. The work described in this thesis aims to provide new insights addressing these key issues, trying to answer the following questions:

1. Can niche cells critically contribute to leukemogenesis?
2. What is the molecular mechanisms underlying the concept of “niche-induced leukemogenesis” and what is the relevance of such mechanisms to human disease?
3. What’s the effect of diseased hematopoietic cells on their niche?

To answer these questions, the pre-leukemic disorders: Shwachman-Diamond Syndrome (SDS) and myelodysplastic syndromes (MDS) were investigated. We analyzed SDS and MDS mouse models as well as bone marrow samples from human SDS/MDS patients. SDS is particularly relevant in the context of this thesis because it is an inherited, monogenic, disease with a mutation in both hematopoietic and niche cells and characterized by skeletal defects ( osteoporosis), bone marrow failure (neutropenia) and a strong predisposition to develop acute myeloid leukemia (AML). Previous work, including our own, has shown that hematopoietic cell intrinsic loss of the disease-causing gene *Sbds* in mice did not

result in leukemia, suggesting that *Sbds* deficiency in the hematopoietic cells alone is not sufficient to drive leukemogenesis and ancillary (niche) cells may be implicated. While, SDS is a rare disease, it can be modelled because of its monogenic origin and findings in SDS may be of broader significance to more prevalent hematopoietic diseases characterized by bone marrow failure and leukemogenesis such as MDS. Therefore, we also studied the contribution of the HSC niche in MDS pathogenesis in mouse models and human patients.
**Chapter 2** describes the first transcriptomic analysis of purified mesenchymal cells from low-risk MDS (LR-MDS) patients. The data address a key issue in the field where the current knowledge about mesenchymal elements in pre-leukemic patients is derived from observations in *ex vivo* expanded stromal cells, with uncertain relevance to their *in vivo* counterparts. Findings from this chapter revealed that purified LR-MDS mesenchymal cells are transcriptionally distinct from their normal counterparts, characterized by inflammatory signaling, cellular stress and the upregulation of negative regulators of hematopoiesis. In comparison to expanded stromal cells, purified MDS mesenchyme is enriched in signatures indicative of response to external stimuli, chemokine activity and immune regulation, stressing the relevance of tissue context and active cross-talk of mesenchymal cells with other cellular elements in the MDS bone marrow that is lacking in the culture dish.

**Chapter 3** of this thesis aims to define the molecular mechanism(s) underlying the recently described concept of "niche-induced leukemogenesis" by modeling SDS in a model where *Sbds* is specifically deleted in MPCs in the bone marrow microenvironment. As a result of this mesenchymal *Sbds* deletion, mice developed osteoporosis and myelodysplasia recapitulating clinical symptoms in SDS patients. Molecularly, *Sbds* deficiency in the MPCs caused genotoxic stress in hematopoietic stem/progenitor cells (HSPCs), characterized by mitochondrial dysfunction, oxidative stress and DNA damage, along with cell cycle checkpoint activation. To define the molecular mechanisms driving this genotoxic stress in HSPCs, we performed transcriptomic analysis of *Sbds*-deficient MPCs in comparison to control MPCs. This analysis revealed activation of the p53 pathway, a molecular mechanism commonly associated with ribosomopathies. Interestingly, genetic rescue studies revealed that both the bone and hematopoietic phenotypes described above are p53 dependent, raising the important question what molecules downstream of p53 could drive genotoxic stress in the HSPCs. By comparing the gene expression data of purified mesenchymal cells from the SDS mouse model to human SDS patients, we demonstrated that *Sbds* deficient MPCs in both mice and human display overexpression of many inflammatory molecules, including the alarmins *S100a8* and *S100a9*, which are *bona fide* p53 downstream targets. Next, via *in vivo* transplantation analysis and *in vitro* recombinant S100A8/9 studies, we observed that niche-derived S100A8 and S100A9 (S100A8/9) are sufficient to induce genotoxic stress in HSPCs, partially via their canonical receptor toll-like-receptor 4 (TLR4).

Seeking the broader relevance of the abovementioned findings to human pre-leukemic

disorders, we performed transcriptional analyses in MPCs purified from a homogeneous cohort of 45 LR-MDS patients. Mesenchymal S100A8/9 overexpression identified a subset of LR-MDS patients with activated niche p53 and TLR signaling. These patients are clinically undiscernible from the patients with low niche-S100A8/9 expression based on current risk scores, which are largely based on hematopoietic cell autonomous parameters. Interestingly, patients with a high level of mesenchymal S100A8/9 expression have worse clinical outcome, characterized by higher frequency of leukemic evolution and a shorter time to leukemia progression, reflected a shorter event-free survival. Together, the data in chapter 3 establish a novel concept of an inflammatory niche-induced genotoxic stress in HSPCs. It is conceivable that this pathophysiologic mechanism induces a higher rate of genetic aberrancies in HSPC and/or the selection of certain genetic aberrancies that confer a competitive advantage of aberrant cells to their normal counterparts, thus contributing to the bone marrow failure and leukemogenesis. Ongoing experiments in the lab are testing this notion and offer the perspective of niche-instructed prognostic and therapeutic strategies in human leukemia predisposition syndromes.

**Chapter 4** aims to further investigate the potential molecular mechanism(s) driving the inflammatory signatures in the MPCs from LR-MDS patients. By comparing the transcriptional data obtained from LR-MDS patients to their counterparts, we observed activation of the NF-κB mediated inflammatory signaling as a biological commonality in LR-MDS mesenchymal cells. Testing the functional relevance of this molecular program, we took an *ex vivo* genetic approach in combination with co-culture studies demonstrating that mesenchymal NF-κB activation attenuated the number and function of normal HSPCs. These data complement a recent finding of NF-κB activation in the HSPCs in MDS patients suggesting NF-κB-mediated inflammatory feedback loop can be an important pathophysiological factor in MDS.

The previous chapters indicate that inflammatory alterations in the mesenchymal niche can play an important role in the pathophysiology of bone marrow failure and leukemogenesis. An important remaining question is what drives these inflammatory alterations in niche cells. In the SDS model it is clear that loss of *Sbds* is the cause of a series of (p53-driven) events leading to inflammation, but in the case of MDS this is much less apparent. **Chapter 5** studies whether primary alterations in hematopoietic cells can affect their niche using a transgenic mouse model of MDS: *vav1-NUP98-HOXD13* (NHD13). In this mouse model, the expression of the disease-causing transgene NHD13 (which infrequently occurs in human MDS) is restricted to the hematopoietic cells, making it a suitable model to study the effect of MDS cells on their niche. NHD13 mice dysplay reduced numbers of HSPCs, but transplantation of normal HSPCs in NHD13 recipients did not result in altered differentiation suggesting the loss of HSPCs in NHD13 mice is likely due to hematopoietic-cell intrinsic factors. A series of primary and secondary transplantation experiments revealed normal

numbers and function of wildtype donor HSPCs after exposure to the NHD13+ bone marrow microenvironment (BMME). Together, the findings in this particular mouse model of MDS do not support the notion that hematopoietic cells in MDS induce long-term effects on niche cells attenuating normal hematopoiesis. Future investigations, including those using different genetic abnormalities in HSPC (more common in human MDS), are warranted to shed further light on this important topic.

To conclude, the work described in this thesis provides novel mechanistic insights into the contribution of the HSC niche to leukemogenesis, establishing the relevance of concepts and mechanisms revealed in mouse models to human disease states. These insights further stress the importance of incorporating niche contributions in our thinking about the pathophysiology of bone marrow failure and leukemogenesis. They set the stage for future investigations aiming to better understand niche contributions to leukemogenesis and integrate niche-derived molecular clues into the current prognostic and treatment regimens for human leukemia predisposition syndromes.

## NEDERLANDSE SAMENVATTING (DUTCH SUMMARY)

Rode bloedcellen, witte bloedcellen en bloedplaatjes hebben bij volwassenen een korte levensduur en worden voortdurend aangemaakt door differentiatie vanuit zeldzame hematopoëtische stamcellen (HSCs) in het beenmerg. HSCs moeten tijdens fysiologische omstandigheden in staat zijn om zichzelf te delen in zowel een andere HSC als een meer uitgerijpte cel met de capaciteit om zich te ontwikkelen naar verschillende soorten volwassen bloedcellen. Een verstoring in dit proces kan leiden tot kwaadaardige transformatie van gezonde HSCs naar bloedkanker stamcellen, wat leidt tot de ontwikkeling van hematopoëtische maligniteiten. Daarom worden de diverse functies van HSCs streng bewaakt en in balans gehouden door zowel cel-intrinsieke factoren als cel-extrinsieke moleculaire signalen van cellen in de beenmerg micro-omgeving. Deze niet-hematopoëtische cellen staan bekend als de zogenaamde HSC niche. De HSC niche bestaat uit verschillende celtypes, waaronder mesenchymale voorloper/progenitor cellen (MPCs).

Het wordt steeds duidelijker dat, net als solide maligniteiten, hematopoëtische maligniteiten waarschijnlijk ontstaan door een verstoorde orgaan/weefsel homeostase in plaats van een ontregeling in één enkele cel. Hoewel een groot deel van het wetenschappelijke onderzoek zich richt op cel-intrinsieke bijdragen aan bloedkanker, zoals veel voorkomende mutaties in leukemiecellen, is de rol van de HSC niche in de pathogenese van bloedkanker in zekere mate ondergewaardeerd gebleven. Data verkregen uit genetische muizenmodellen hebben aangetoond dat primaire veranderingen in de HSC niche voldoende kunnen zijn om veranderingen in bloedcellen te induceren waaronder een aanleg voor het ontstaan van acute myeloide leukemie (AML). Echter, de onderliggende moleculaire mechanismen voor deze 'niche-geinduceerde leukemogenese' en hun relevantie voor humane ziekte is nog onbekend. Het werk beschreven in dit proefschrift heeft als doel om nieuwe inzichten over deze cruciale onderwerpen te verschaffen, en probeert de volgende vragen te beantwoorden:

1. Wat is de bijdrage van niche cellen aan het ontstaan van leukemie?
2. Welke moleculaire mechanismen zijn verantwoordelijk voor deze bijdrage en wat is de relevantie van deze bevindingen voor humane ziekten?
3. Wat is het effect van de genetisch veranderde hematopoëtische cellen op hun niche?

Hiertoe werden in dit proefschrift twee beenmergzieken met een verhoogd risico op het ontwikkelen van leukemie bestudeerd: Shwachman-Diamond Syndroom (SDS) en myelodysplastische syndromen (MDS). Door het combineren van muizenmodellen van deze ziekten en weefselmonsters van SDS/MDS patiënten hebben we getracht onze vraagstellingen te adresseren. SDS is bijzonder geschikt voor dit onderzoek, omdat een zeldzaam optredende, aangeboren mutatie in één enkel gen (*Sbds*) in alle cellen van het

lichaam (waaronder zowel niche als bloedcellen) neutropenie (lage aantal neutrofielen), leukemie predispositie, skeletafwijkingen en osteoporose veroorzaakt. Onderzoek in muizen heeft eerder aangetoond dat verlies van *Sbds* in bloedcellen alleen niet leidt naar het ontwikkelen van leukemie, wat impliceert dat een bijdrage van verstoorde niche cellen mogelijk nodig is. In tegenstelling tot SDS is MDS een relatief veel voorkomende pre-leukemische aandoening, wat het belang van het ontrafelen van de bijdrage van de HSC niche aan de pathogenese van deze ziekte onderstreept. Het is voorstelbaar dat mechanistische inzichten in een zeldzame, goed te modelleren ziekte als SDS, van belang zijn voor andere, vakere voorkomende ziekten met gedeelde klinische aspecten zoals beenmergfalen en een verhoogde kans op het ontstaan van AML.

**Hoofdstuk 2** beschrijft voor het eerst het transcriptoom (genexpressie profiel) van, niet-gemanipuleerde, mesenchymale cellen gezuiverd uit laag-risico MDS-patiënten en pakt hiermee een belangrijke vraag in het onderzoeksveld aan. De huidige kennis over mesenchymale cellen in patienten met een verhoogde kans op het onstaan van AML is beperkt tot bevindingen in *ex vivo* geëxpandeerde stromale cellen. Een belangrijke vraag is of deze, buiten het lichaam in een kweekschaal ge-expandeerde en gemanipuleerde, cellen vergelijkbaar zijn met hun tegenhangers in het zieke beenmerg. De bevindingen in dit hoofdstuk laten zien dat MDS mesenchymale cellen transcriptioneel fundamenteel verschillen met hun normale tegenhangers. Deze verschillen worden gekenmerkt door inflammatoire signalering, cellulaire stress, en opregulatie van hematopoëtische factoren die een negatieve invloed hebben op de ontwikkeling van bloedvormende stamcellen. Bovendien bleken de mesenchymale cellen die direct uit het beenmerg gewonnen werden meer verschillen dan overeenkomsten te vertonen met deze cellen na *ex vivo* expansie. Deze transcriptionele verschillen betroffen onder andere reactie op externe stimuli, chemokine-activiteit en immuunsysteem-regulatie. De data suggereren dat de activiteit van mesenchymale cellen in het beenmerg van MDS patienten beinvloedt wordt door hun omgeving (waaronder afwijkende bloedvormende cellen) en benadrukken het belang van actieve cross-talk van de mesenchymale cellen met andere cellulaire elementen in het MDS beenmerg dat in een kweekschaal ontbreekt.

**Hoofdstuk 3** van dit proefschrift heeft als doelstelling om de onderliggende moleculaire mechanisme(n) van het recent beschreven concept “niche-geïnduceerde leukemie” te ontrafelen. Hiervoor werd gebruikt gemaakt van een SDS muizenmodel waarbij het gemuteerde gen (*Sbds)* specifiek in MPCs van de beenmerg micro-omgeving werd verwijderd. Als gevolg van deze gen-deletie ontwikkelden muizen botontkalking (osteoporose) en myelodysplasie, wat ook voorkomt bij SDS patiënten. Moleculair gezien, veroorzaakte het tekort aan *Sbds* in MPCs genotoxische stress in hematopoëtische stam / progenitorcellen (HSPC), gekenmerkt door mitochondriale dysfunctie, ophoping van vrije

zuurstofradicalen, en DNA schade, evenals activatie van celcyclus barrières. Transcriptoom (genexpressieprofiel) analyse van *Sbds*-deficiënte mesenchymale cellen wees op activatie van het p53 signaalpad, een moleculaire signalerings-cascade geassocieerd met ribosomale aandoeningen. Uitschakeling van p53 in het SDS muizenmodel liet zien dat zowel de bot - als bloed veranderingenhierboven beschreven afhankelijk van p53 activatiezijn. Deze bevinding riep de belangrijke vraag op welke moleculen, geinduceerd door p53, de genotoxische stress in HSPC veroorzaken. Hiervoor werd de genexpressie van mesenchymale cellen uit het muizenmodel met de genexpressie van mesenchymale cellen gezuiverd uit SDS patiënten met elkaar vergeleken. Uit deze vergelijking bleken de ontstekings-gerelateerde moleculen S100A8 en S100A9, welke geactiveerd kunnen worden door p53, verhoogd te zijn in de *Sbds*-deficiënte mesenchymale cellen van zowel muizen als SDS patiënten. Vervolgens werd het duidelijk uit *in vivo* transplantatie analyses en *in vitro* recombinante S100A8/A9 behandelingen, dat S100A8/S100A9, uitgescheiden door de niche, voldoende is om genotoxische stress in HSPC te induceren. Dit effect werd deels veroorzaakt door binding aan de toll-like-receptor 4 (TLR4). Om uit te zoeken in hoeverre deze bevinding relevant is voor andere pre-leukemische aandoeningen, werden MPCs gezuiverd uit een homogene cohort van 45 laag-risico MDS-patiënten en werd hun genexpressieprofiel geanalyseerd. Hieruit bleek dat mesenchymale S100A8/A9 expressie een subgroep van laag-risico MDS patiënten kon identificeren waarin p53 en TLR signalering geactiveerd is. De patiënten met een hoge mesenchymale expressie van S100A8/9 waren op klinische gronden (gebruik makend van risico-classificaties die gebruik maken van kenmerken van bloedvormende cellen) niet te onderscheiden van de rest van de patienten. De MDS patiënten met een hoge S100A8/9 expressie hadden echter een slechtere klinische uitkomst een hogere incidentie van AML met een significant kortere tijd tot het ontstaan daarvan, wat tot een kortere “event-vrije” overleving leidde. Samengevat postuleert het onderzoek in hoofdstuk 3 een nieuw concept waarin inflammatoire veranderingen in een stamcelniche kunnen leiden tot genotoxische stress in stam en progenitorcellen. Het is voorstelbaar dat dit pathofysiologische mechanisme kan leiden tot een verhoogde kans op het ontstaan van genetische afwijkingen in HSPC en/of een competatief voordeel van cellen met genetische afwijkingen ten opzichte van normale bloedcellen, en daarmee een belangrijke rol speelt in het onstaan van beenmergfalen en AML. Dit opent het perspectief dat niche-verstoringen in patiënten met pre-leukemische aandoeningen in de toekomst wellicht gericht aangepakt kunnen worden om de ontwikkeling van leukemie te vertragen of zelfs te voorkomen.

**Hoofdstuk 4** richt zich verder op onderzoek naar de mogelijke moleculaire mechanismen die de inflammatoire niche veranderingen in laag-risico MDS veroorzaken. We hebben dit gedaan door transcriptionele data verkregen uit laag-risico MDS-patiënten te vergelijken met cellen verkregen uit mensen zonder hematologische aandoeningen. Opvallend is dat de activatie van NF-κB gemedieerde-inflammatoire signalering een biologische overeenkomst lijkt te

zijn in laag-risico MDS mesenchymale cellen. De functionele relevantie van dit moleculaire programma werd getoetst door *ex vivo* genetische activatie van NF-κB in mesenchymale cellen. Het kweken van normale HSPC op deze genetisch veranderde mesenchymale cellen leiide tot vermindering van het aantal en de functie van normale HSPCs. Deze resultaten sluiten aan bij de recente bevinding dat NF-κB signalering ook actief is in HSPC van MDS patienten wat mogelijk duidt op het feit dat NF-κB gemedieerde-inflammatoire samenspraak tussen mesenchymale cellen en HSPC een belangrijke pathofysiologische factor in MDS is.

De voorafgaande hoofdstukken toonden aan dat inflammatoire veranderingen in mesenchymale niche cellen een belangrijke rol kunnen spelen in de pathofysiologie van beenmergfalen en leukemische evolutie. Een belangrijke vraag blijft hoe deze inflammatoire veranderingen in niche cellen ontstaan. In het SDS model is dit het gevolg van het verlies van Sbds in deze cellen maar wat deze veranderingen veroorzaakt in MDS is veel minder duidelijk. **Hoofdstuk 5** onderzoekt of primaire veranderingen in hematopoëtische cellen (zoals gevonden in MDS) hun niche kunnen beinvloeden in een transgeen muizenmodel van MDS: het *vav1-NUP98-HOXD13* (NHD13) model. In dit muismodel, is de expressie van de ziekte-veroorzakende transgen NHD13 beperkt tot hematopoëtische cellen, waardoor het een geschikt model is om het effect van MDS cellen op hun niche te bestuderen. NHD13 muizen hebben tekenen van beenmergfalen (lage celaantallen in het bloed) en een verhoogde kans op leukemie maar transplantatie van normale HSPC in NHD13 ontvangers (na het verwijderen van de afwijkende bloedcellen middels bestraling) resulteerde niet in een duidelijk en consistent veranderde bloedvorming. Ook verder onderzoek naar de functie van normale HSPC blootgesteld aan de MDS niche (middels secundaire transplantatie-experimenten) bracht geen overtuigend bewijs dat afwijkende bloedcellen in MDS een permanente verandering van de niche veroorzaken die bijdraagt aan het onderdrukken van de normale bloedvorming. Verder onderzoek, onder andere gebruik makend van andere MDS modellen, zal meer inzicht moeten verschaffen in de onderliggende vraag omdat het goed mogelijk is dat niche-effecten afhankelijk zijn van de aard van de genetische afwijking in HSPC in MDS.

Concluderend, verschaft het werk beschreven in dit proefschrift nieuwe conceptionele en mechanistische inzichten in de bijdrage van de niche aan het ontstaan en ontwikkelen van leukemie en verheldert in hoeverre deze inzichten, ontrafelt in muismodellen, relevant zijn voor humane ziekten. Deze inzichten benadrukken het belang veranderingen in de beenmergniche te incorporeren in het denken over de pathofysiologie van beenmergfalen en het onstaan van leukemie. Een abnormale niche en verstoorde hematopoëtische cellen vormen waarschijnlijk samen de drijfkracht achter het ontwikkelen van leukemie in humane pre-leukemische aandoeningen. De bevindingen in dit proefschrift zullen hopelijk de weg effenen naar toekomstig onderzoek naar bijdragen van de niche aan het ontstaan

van hematopoietische ziekten en uiteindelijk leiden tot nieuwe therapeutische strategieen waarin de niche wordt 'getarged' ten einde beenmergfalen te verminderen en ontstaan van leukemie te vertragen of voorkomen.

## CURRICULUM VITAE

Si Chen was born in Chenzhou, China, on 7 March 1988. After receiving her high school diploma awarded by the International Baccalaureate Diploma Program (IBDP) from Arnhem International School (AIS, Arnhem, the Netherlands), she studied Pre-Medicine at the University College Utrecht (UCU, Utrecht, the Netherlands) and gained her Honors Bachelor of Science degree with *magna cum laude* in 2010. Then she continued with her master studies in Pharmaceutical Science and Drug Innovation at Utrecht University (UU, Utrecht, the Netherlands). After completing her first one-year research project studying the treatment effect of probiotics on the inflammatory response in a murine model of chronic allergic asthma, she continued her second project at Harvard Medical School / Dana-Farber Cancer Institute (Boston, USA) in the group of Prof. Thomas Look, where she contributed to the development of a zebrafish model of myelodysplastic syndrome through tet2 genomic editing. From then on, she became very interested in hematopoietic malignancies. After obtaining her Master of Science degree with *cum laude* from Utrecht University, in 2012, she started her PhD in the research group of Dr. Marc Raaijmakers in the Hematology Department at Erasmus University Medical Center (Rotterdam, the Netherlands). During her PhD training, she studied the role of the mesenchymal niche in regulating normal and malignant hematopoiesis, with a focus on niche contributions to pre-leukemic disorders: Shwachman-Diamond Syndrome and Myelodysplastic syndromes.

## AWARDS & TRAVEL GRANTS

- Top Publication Award - Dutch Hematology Congress (Arnhem, the Netherlands, 2017)
- Abstract Achievement Award – 58$^{th}$ Annual American Society of Hematology (ASH) Conference (San Diego, USA, 2016)
- Erasmus Trustfond Travel Grant (Rotterdam, the Netherlands, 2016)
- Recipient of a) KWF Travel grant; b) Studiefonds Ketel 1 scholarship; c) Mgr J. C. van Overbeekstichting funding; d) Nijbakker Morra Stichting (Netherlands, 2011)
- Excellent Student Scholarship (UCU/UU, the Netherlands, 2007-2012)

# LIST OF PUBLICATIONS

**S Chen**, N A Zambetti, E M J Bindels, K Kenswil, A M Mylona, N M Adisty, R M Hoogenboezem, M A Sanders, E M P Cremers, T M Westers, J H Jansen, A A van de Loosdrecht and M H G P Raaijmakers. Massive parallel RNA sequencing of highly purified mesenchymal elements in low-risk MDS reveals tissue-context-dependent activation of inflammatory programs. *Leukemia*. 2016;30(9):1938- 1942

Noemi A. Zambetti*, Zhen Ping*, **Si Chen***, Keane J. G. Kenswil, Maria A. Mylona, Mathijs A. Sanders, Remco M. Hoogenboezem, Eric M. J. Bindels, Maria N. Adisty, Paulina M. H. Van Strien, Cindy S. van der Leije, Theresia M. Westers, Eline M. P. Cremers, Chiara Milanese, Pier G. Mastroberardino, Johannes P. T. M. van Leeuwen, Bram C. J. van der Eerden, Ivo P. Touw, Taco W. Kuijpers, Roland Kanaar, Arjan A. van de Loosdrecht, Thomas Vogl and Marc H. G. P. Raaijmakers. Mesenchymal Inflammation Drives Genotoxic Stress in Hematopoietic Stem Cells and Predicts Disease Evolution in Human Pre-leukemia. *Cell Stem Cell*. 2016;19(5):613-627. ***co-first author**

**Si Chen**, Zhen Ping, Keane Kenswil, Sjoerd J.F. Hermans, Eric M.J. Bindels, Athina M. Mylona, Niken M. Adisty, Remco M. Hoogenboezem, Mathijs A. Sanders, Eline M.P. Cremers, Dicky J. Lindenbergh-Kortleve, Janneke N. Samsom, Arjan A. van de Loosdrecht, and Marc H.G.P Raaijmakers. Activation of NF-kB driven inflammatory programs in mesenchymal elements is a biologic commonality in low-risk myelodysplastic syndromes. *Manuscript Submitted*

Keane Jared Guillaume Kenswil, Christopher Adrian Jaramillo, Zhen Ping, **Si Chen**, Remco M. Hoogenboezem, Maria Athina Mylona, Maria Niken Adisty, Eric M.J. Bindels, Pieter Koen Bos, Tom Cupedo, Marc Hermanus Gerardus Petrus Raaijmakers. Identification and molecular characterization of endothelial cells associated with hematopoietic niche formation in humans**.** *Cell Reports*. 2017; in revision

Tushar D. Bhagat, **Si Chen**, Matthias Bartenstein, A.,Trevor Barlowe, Patrick Tivnan, Elianna Amin, Mario Marcondes, Mathijs A. Sanders, Remco M. Hoogenboezem, Britta Will, Orsolya Giricz, Suman Kambhampati, Nandini Ramachandra, Gaurav Choudhary, Iaonnis Mantzaris, Vineeth Sukrithan, Remi V.M. Laurence, Davendra Sohal, Amittha Wickrema, Cecilia Yeung, Kira Gritsman, Peter Aplan, Konrad Hochedlinger, Yiting Yu, Kith Pradhan, John M. Greally, Siddhartha Mukherjee, Andrea Pellagatti, Jacqueline Boultwood, Ulrich Steidl, Marc H.G.P. Raaijmakers*, H Joachim Deeg*, Michael G. Kharas*, Amit Verma.* Epigenetically Aberrant Stroma In MDS Propagates Disease Via Wnt/**ß**-Catenin Activation. *Cancer Research*. 2017; in revision

Ana Martín-Pardillos*, Anastasia Tsaalbi-Shtylik*, **Si Chen**, Seka Lazare, Ronald P. van Os, Albertina Dethmers-Ausema, Nima Borhan Fakouri, Matthias Bosshard, Rossana Aprigliano, Barbara van Loon, Daniela C. F. Salvatori, Keiji Hashimoto, Celia Dingemanse-van der Spek, Masaaki Moriya, Lene Juel Rasmussen, Gerald de Haan, Marc H.G.P. Raaijmakers,† and Niels de Wind†. Genomic and functional integrity of the hematopoietic system requires tolerance of oxidative DNA lesions. *Blood.* 2017; in revision; *co-first author

Evisa Gjini, Marc R. Mansour, Jeffry D. Sander, Nadine Moritz, Ashley T. Nguyen, Michiel Kesarsing, Emma Gans, Shuning He, **Si Chen**, Myunggon Ko, You-Yi Kuang, Song Yang, Yi Zhou, Scott Rodig, Leonard I. Zon, Keith Joung, Anjana Rao, A. Thomas Look. A Zebrafish Model of Myelodysplastic Syndrome Produced through tet2 Genomic Editing. *Molecular and Cellular Biology*. 2015 Mar; 35(5): 789–804.

Seil Sagar, Mary E Morgan, **Si Chen**, Arjan P Vos, Johan Garssen, Jeroen van Bergenhenegouwen, Louis Boon, Niki A Georgiou, Aletta D Kraneveld and Gert Folkerts. Bifidobacterium breve and Lactobacillus rhamnosus treatment is as effective as budesonide at reducing inflammation in a murine model for chronic asthma. *Respiratory Research* 2014, 15:46

# PHD PORTFOLIO

Name PhD Student: Si Chen
Erasmus MC Department: Hematology
Research School: Molecular Medicine (MolMed)

PhD Period: October 2012 – March 2017
Promoter: Prof. Dr. Ivo P. Touw
Supervisor: Dr. Marc H.G.P. Raaijmakers

| 1. PhD Training | Year | ECTS |
|---|---|---|
| **General Courses** | | |
| Research management for PhDs/Postdocs | 2012 | 1 |
| Photoshop & Illustrator workshop | 2013 | 0.3 |
| PhD day (4x) | 2013-2016 | 1.2 |
| Get-out-of-your-lab days | 2013 | 0.6 |
| Excel advanced course | 2015 | 0.3 |
| Biomedical english writing course | 2016 | 2 |
| Health economics | 2016 | 1.5 |
| Scientific integrity course | 2016 | 0.3 |
| Presentation skills | 2017 | 2 |
| **In-depth Courses and Workshops** | | |
| analysis of microarray and RNA seq expression data using R/BioC and web tools | 2013 | 3 |
| Biostatistics | 2014 | 3 |
| Molecular aspects of hematological disorders (3x) | 2014-2016 | 2.1 |
| A broad spectrum of NGS application in molecular medicine | 2014 | 0.6 |
| Basic course on R | 2015 | 0.7 |
| Survival analysis course | 2016 | 0.7 |
| **Scientific Meetings Department of Hematology** | | |
| Work discussions (Weekly) | 2012-2017 | 8 |
| Erasmus Hematology Lectures (Monthly) | 2012-2017 | 2 |
| PhD lunch with invited speaker (Monthly) | 2012-2017 | 2.5 |
| Journal club / literature discussions (bi-montly) | 2012-2017 | 7 |
| **National/International conferences** | | |
| Dutch Hematology Congress (2x) (Utrecht) | 2014, 2015 | 0.6 |
| Dutch Chinese Life Sciences Association Annual Meeting (Amsterdam) | 2014 | 0.3 |
| Dutch Society for Stem Cell Research Annual Meeting (2x) (Groningen, Utrecht) | 2015, 2016 | 0.6 |
| Molecular Medicine Day (3x) (Rotterdam) | 2014-2016 | 0.9 |
| Daniel Den Hoed Day (Rotterdam) | 2016 | 1 |
| Tumor Microenvironment in the Hematological Malignancies and its Therapeutic targeting (Lisbon, Portugal) | 2015 | 1 |
| Cancer Metabolism and the Tumor Microenvironment Conference (Paphos, Cyprus) | 2016 | 1 |
| Annual Conference of American Society of Hematology (San Diego, USA) | 2016 | 1 |
| Karolinska Insitute Tumor Microenvironment Annual Conference (Stockholm, Sweden) | 2017 | 1 |
| **Presentations** | | |
| Departmental work discussions (Oral, 8x) (Rotterdam) | 2013-2016 | 4 |
| Journal clubs (Oral, 3x) (Rotterdam) | 2013-2016 | 1.5 |
| Molecular Medicine Day (Poster, 2x) (Rotterdam) | 2014-2016 | 2 |
| Daniel Den Hoed Day (Oral, 1x) (Rotterdam) | 2016 | 1 |
| Dutch Society for Stem Cell Research Annual Meeting (Oral, 1x) (Utrecht) | 2016 | 1 |
| Molecular aspects of hematological disorders (Oral, 1x) (Rotterdam) | 2016 | 1 |
| Cancer Metabolism and the Tumor Microenvironment Conference (Oral 1x) (Paphos, Cyprus) | 2016 | 1 |
| Annual Conference of American Society of Hematology (Oral 1x) (San Diego, USA) | 2016 | 1 |
| Karolinska Insitute Tumor Microenvironment Annual Conference (Oral 1x) (Stockholm, Sweden) | 2017 | 1 |
| **2. Teaching, Supervision & Organization Activities** | | |
| Organization and supervision PhD lunch with invited speakers | 2014-2015 | 0.2 |
| Organization of PhD Day | 2015 | 0.2 |
| Supervising Bachelor Internship (9 months) | 2016 | 3 |
| Supervising Master Internship (6 months) | 2016 | 2 |
| **Total** | | 65.1 |

## WORD OF THANKS

It feels surreal that this day has actually arrived: writing the last “chapter” of my PhD thesis. Personally, this is the most precious chapter to me. Reaching the finish line of the PhD is certainly a milestone in my life, which would not have been possible without the help and support from many people. With great joy and gratitude, I want to express my sincere appreciation to you all, who have made this ride a special and memorable one.

The first person I would like to thank is my supervisor **Marc**, who brought me into the group and the department five years ago. When I first joined, I didn’t know much. Now, I know a little more and for much of it I have you to thank. Dear Marc, I sincerely appreciate and treasure everything you have taught me, both scientifically and personally. You showed me how to be a scientist. From you, I learned that doing research is like playing chess, there are many ways to go, we just have to find the smartest way. You have endless passion and curiosity for science; to me, you are the example of “Do what you love and love what you do”. From you, I learned and am still learning how to look ahead and beyond, what it is like to have a scientific strategy and a great vision. Being visionary is my goal as well, learning from you, I hope to excel in that one day. Your never-ending positivism always gave me strength. Countless times I thought I was defeated by failed experiments, and felt discouraged and stuck, but each time you helped find a way to continue. The past 5 years have not always been smooth, at times I was so frustrated and acted emotionally, those moments happened mostly because I cared so much about the project You never took it personally, and we always figured out a solution to achieve our final goal. Thank you for all the patience and understanding! Having worked with you and having witnessed your inspiring aptitude for science, I am sure you will lead the group to continue establishing many more milestones in the field. I wish you all the best and I am looking forward to hearing more scientific breakthroughs from the team!

I would then like to express my deepest gratitude to my promoter **Ivo**. Dear Ivo, thank you for all the support, guidance and advice. You are not only a great scientist, but also a very supportive mentor. During these years, I appreciated all the valuable input you have given me regarding my work and the many critical points you have raised that stimulated me to think about the “why” question of my work. You taught me how to be a critical scientist and I learned to challenge the experiments even in the publications of the "big shots". It is not about the impact factor, but about the science. Thank you for helping me prepare my ASH presentation and supporting me during every step of my PhD development.

Next, I wish to thank all the members of my doctoral reading committee, who have spent the time and effort in helping me improve my thesis. I appreciate all the comments and feedback. Dear **Ruud**, I really appreciate all your efforts in promoting collaborations of our department with other institutes. Thank you for organizing the annual "Molecular Aspects of Hematology Research" seminars, which give us the unique opportunity to discuss our work with hematology researchers from within the country and worldwide. Thank you for being the secretary of the committee and for all your feedback on my thesis, which was most helpful. Dear **Joop**, it was a great pleasure to collaborate with you on the MDS project. Thank you for sharing the genetic abnormality data with us, allowing us to start looking into whether niche signals are correlated with the mutational status of patients. This was an exciting direction to take for us and the field. Thank you for your consistent responsiveness and helpful comments on my thesis! Dear **Sjaak**, thank you for being in my reading committee! Although I didn't have the opportunity to work with you, I appreciate your responsiveness and thoughtful comments/feedback on my thesis.

I would like to extend my appreciation to the members of the big committee for their time and commitment to my defense ceremony. Dear **Prof. Huls**, thank you for accepting the invitation and coming all the way from Groningen! I look forward to our discussions on my defense day. Dear **Rebekka**, as a young female PI, you are a true role model to me. Thank you for all the input during our Thursday morning discussions and thank you for your advice on ASH in December. I wish you and your new group all the best! Dear **Arjan**, your collaboration was essential to my PhD work. Thank you for organizing the HOVON89 clinical trial, which laid the foundation of my work and gave me the access to all the patient samples and clinical information. I also appreciated all the positive feedback you have given me on the manuscripts. Dear **Thomas**, your help was instrumental to the successful publication of our *cell stem cell* paper. With your help and input, we made new discoveries from our S100A8/9 work. You have always been very approachable and willing to share mouse models, materials and reagents. Thank you very much for being a wonderful collaborator!

My heartfelt thanks to Prof. **Bob Löwenberg**! Dear Bob, our first encounter was 5 years ago when you interviewed me. Since then, you have been very supportive of my work and me. Thank you for all your valuables insights! I also want to thank you for taking the time to speak with me about my future career opportunities. Your wisdom and guidance are inspiring and I will keep them at heart. I would like to thank all the other PIs in the department (present and past), including **Eric, Jan, Peter, Stefan, Anita, Tom, Mojca, Frank, Moniek, Dick, Pieter** and **Emma**. Thank you all for your feedback and comments on my work during the departmental discussions. Those criticisms helped me to improve my experiments and grow as a scientist. Specifically, I want to thank Eric for helping me with the cord blood materials; Stefan for sharing your experience with me regarding how to stay positive during

revision time; Mojca for the discussions on the survival analysis of the MDS patients; Emma for all the input during our Thursday morning discussions and for sharing your experiences with me on how to continue after my PhD; Peter for helping us with the mutational analysis. Thank you all!

My warmest thanks go to my dearest team! We have always supported, helped and learned from each other; we have also had many fun memories outside the lab together, I feel very lucky to have been in a team with you guys. Dear **Ping**, you have such a beautiful heart! You are a genuine, honest and very thoughtful colleague and friend; and one of the most hard-working people I have ever met! I admire your perseverance and dedication. You are a true example of "a man with honor", as Keane would call you. No matter how many experiments you have on a day, if you promised to help someone, you always would. Even if it meant you may need to work until 3am, you would still keep to your promise sacrificing your own sleeping and resting time. Thank you for giving me a hand throughout these years! I had a great time working closely with you during the revision period, we are an efficient team together! With your devotion, I am sure you will finish your PhD soon with a wonderful thesis. Good luck! Dear **Keane**, I often forget that you joined us as a Master's student. You are very smart, independent and confident. You actively participated in our discussions right from the beginning, so it felt like you have always been part of the PhD crew. I was so happy to hear that you stayed in the group for your PhD. You helped me with a lot of experiments along the way, thank you! I will never forget the time you took over my experiments without any hesitation when I had to attend my oma's funeral. All these contributions are probably quite obvious as you are a co-author in three out of the four experimental chapters in my thesis. All the best with finishing up your PhD! I will miss all our KFC times together with **Ping**. Please come with Ping to visit me in San Francisco, I will certainly miss all the moments we have shared together. Dear **Claire**, you recently joined the group as our technician. Although you are young by age, you are driven, determined and a quick-learner. You learned the whole workflow of RNA sequencing very quickly and took over the difficult project of sequencing the hematopoietic cells of 45 MDS patients. You did a wonderful job! I enjoyed every moment working with you. You are always eager to learn new techniques and help us with our experiments. You are a great asset to the group, all the best in your future projects. Thank you **Sjoerd** and **Jacqueline** for being wonderful students. You are both very motivated and independent. I hope you guys have enjoyed and will continue to enjoy working in the group. I wish you all the best of luck in your future career goals and scientific endeavors.

Here is to all the past members of the group. Dear **Noemi**, being the first PhD student in the group has not been easy, but you have set a great example for all of us. Thank you for being a wonderful office-mate and all the little talks we have had. All those little chats helped me see things more clearly in difficult situations. Thank you for all your support during ASH in San

Diego, you being there calmed me down and gave me a lot of confidence. See you soon in SF! Who would have thought we would end up in the same city after our PhDs? I am excited to join you in the beautiful SF and continue the crazy Hema13 legacy. Dear **Niken**, this thesis would not have seen the light of the day without your help. We worked so closely together on every project. Among others, performing RNA sequencing of the purified niche cells from 55 MDS patients, was a milestone in my PhD, to the group and in the field. In addition to work, I have many fond memories of our fun times together going shopping and enjoying all kinds of cuisines. I hope to visit you soon in Indonesia to relive some of those memories. Dear **Adrian**, you are probably one of the warmest people I know. Your presence brings happiness into the room. Thank you for having been a caring and thoughtful friend. Things have not been easy for you, but you are very optimistic and walked out of it with a positive attitude. Good luck with finishing up your PhD! I am sure you will do great! I also want to thank **Athina**, for establishing the low-input RNA sequencing; **Yongyi** for establishing the NHD13 MDS mouse model; **Uttara** for helping with the co-culture work and **Niels** for setting up the whole IHC facility. Wherever you are today, I wish you all the best in your professional and personal life.

I would like to acknowledge all the other people who have made great contributions to the delivery and analysis of the data described in this thesis. First, I want to thank **Eric**. Dear Eric, we like to call you Sensei, it is for fun, but it definitely is a reflection of who you are to us. You are a wealth of knowledge when it comes to experimental techniques, which you selflessly shared with us. I will never forget you teaching me every single step of the experiments required during the revision time of the NFkB work. Not to mention the important role you played in our RNA sequencing experiments. You sacrifice your own time to teach and help other people, so you have to use the weekends for your own experiments. I admire your love for science and wish you all the best in your project and scientific pursuits. Regarding the RNA sequencing data, which is a big part of my thesis, I want to give my sincere thanks to **Mathijs** and **Remco** for all your support with the bioinformatical and statistical analysis. From helping us to troubleshoot the data quality produced by low-input sequencing method, to provide us with processed sequencing data that's easy for us to analyze, to help us with survival analysis of patients, you were there with us every step of the way and are always willing to help. I could not thank you both enough for all the time, effort and patience you have invested in our project. I extend many thanks also to **Elodie**, who curated all our RNA sequencing data for the online platform that made finding and working with our data super easy. Dear **Elwin**, **Peter** and **Michael**, thank you for your help and support regarding all the flow cytometry analysis and cell sorting experiments. You have been very flexible and understanding of us with our many "5 minute" delays. Dear Elwin, I also appreciated all the advice you have given me regarding how to set up a co-culture experiment and how you are always willing to answer all kinds of "quick" questions from me. I want to acknowledge

all the members of the **BMT lab** for your help with the bone marrow samples from normal donors and patients. Speaking of patient samples, I cannot forget to thank **Eline** and **Theresia** for your help with collecting the MDS patient samples from the HOVN89 study. It was very easy to work out the logistics with you, thank you for being so communicative and responsive! Concerning the MDS project, I would like to extend my acknowledgement to **Dana**, for providing us with the clinical information of all the patients. Thank you for all the help! In addition, I want to thank **King** Lam for preparing and providing the bone marrow slides and reviewing them with me. Dear **Pier** and **Chiara**, with your great help and guidance, we managed to perform mitochondrial functional analysis and different ROS experiments, which are important parts of my thesis. Thank you for sharing reagents and your knowledge with us. Dear **Dicky**, thank you for introducing me to the entire IHC and IF procedures. You were very kind, patient and well organized. Many thanks for sharing your reagents with us and helping us establish our own IHC facility. Dear **Janneke**, thank you for your helpful insights on the analysis of our IHC data and your kind support on the IHC-related experiments. I appreciated the efficient collaboration with your group! Dear **François**, with your help, we managed to perform mutational studies from 300 cells. We were excited about this new breakthrough, which allows us to check for mutations in rare cell populations. Thank you for all your help and patience!

A big part of this thesis involves animal experiments. I would like to acknowledge the members of **EDC** and the **article 14** team for managing our mice and ensuring our animal experiments were performed according to the requirements of animal welfare & ethics criteria. Dear **Mathieu**, **Amélie**, **Henk**, **Sabine** and **Thea**, thank you for all the feedback on the DEC protocols! Thank you for always willing to work out a solution with us in complicated situations. Dear **Jessica**, **Vincent**, **Ingeborg**, **Eva**, **Charlotte**, and the other staff of EDC: thank you for taking great care of our mice and working with us when there were big experiments. Thank you for being communicative and flexible, adapting to our requests in those days. I truly appreciate all your help!

Being a member of the Lab Day Committee (LDC) together with **Claudia**, **Larissa** and **Shiraz** was a fun episode in my PhD journey. Thank you for all the fun we had together organizing the Halloween party, Sinterklaas games, Christmas Dinch and the escape room events for the lab day out. Additionally, I want to thank Claudia for the fun conversations we have had and for sharing contacts with me regarding thesis printing. You are a caring and thoughtful colleague.

I would like to express my sincere gratitude to **Egied**. Dear Egied, I appreciate all the time and effort you have invested in turning my thesis into this beautiful piece of art. Thank you for helping me with the figures, cover design and layout. Because of your generous help, I could

focus on the writing part, so I managed to finish my thesis in a strict timeline. Dear **Annelies**, you helped me with so many administration matters in these years. You are always kind, patient and helpful. With your help, all the arrangements of my defense ceremony went very smoothly. Thank you so much! Good luck with your new position! I want to extend this gratitude to **Eudia**, always having a big smile and being extremely friendly. Thank you for helping me finish the rest of the arrangements! I wish you all the best in our department. I would also like to thank **Leenke**, I really appreciate your responsiveness and willingness to help in any way you can.

In these 5 years, I am very lucky to have worked with many amazing colleagues who have become my dearest friends. In addition to the some of you who I have mentioned earlier, I want to acknowledge my awesome paranymph **Paulette**. Dear Paulette, we have worked side by side on every transplantation experiment. I will never forget my first transplant experience, you stayed with me until late in the evenings and remained supportive. When Niken left, you have been a great help to my sequencing project. We always say you have a magic touch, whenever we have problems, you always managed to solve it and make the experiments work. Not only are you a countable colleague, but also you are a loving friend. Outside the lab, we have shared many great memories together, which I will miss very dearly. Your delicious bakeries, our gym-times, dinners, brunches and girl-talks, we must continue all these when you come to visit me in the US. Thank you for being a helpful colleague and a supportive and loving friend. Sometimes you guys would call me the adopted Asian kid of the Touw group as a joke, there is certainly some truth in it, as the next person I want to thank is **Onno**. Dear Onno, you are one of the kindest people I know! You are patient, caring and genuine. Thank you for helping me with all the confocal experiments. You had to stay behind the confocal for hours for some of the experiments, yet you were always there to help. You are a great listener and counselor, thank you for all the coffee chats during my difficult moments! I am counting on you coming to visit me and Noemi in SF, so I can repay you all the coffee. Take care and see you soon! I want to extend my acknowledgement to the other members (present and past) of the Touw group. Dear **Patricia**, I admire how you organized the tremendous amount of culturing work of the IPS cells together with Paulette. Thank you for all the little hallway conversations and your support during my DSSCR talk and preparation for ASH. Good luck with finishing up your PhD, I am sure you will do a great job! Dear **Emanuele**, you are a very warm-hearted person! Thank you for all the tips about Rome and helping me with the arrangements. You are a great addition to the Asian office! Actually, it was more that we crashed your office, haha! I had a lot of fun being your officemate; there are always snacks, fresh coffee and Italian liquor. Thank you for that! All the best with your PhD as well! Dear **Michiyo**, thank you for bringing us amazing local snacks wherever you travel. Hearing the stories from you about your family, I admire your passion for research. Wish you all the best in the rest of the time you are here. Dear **Szaby** and **Hans**, thank you

for your input on my work during our Thursday morning meetings. Good luck with your own projects. Dear **Julia**, or Germie, thank you for being a wonderful roommate! I will bring the minion socks wherever I go. I will never forget that you taught me to make my first pie. I hope to see you soon. Dear **Piotr**, thank you for all the little chats we have had, I hope you are doing well and enjoying your new position.

Certainly, there are other members of the "crazy Hema13 crew" I shall not forget to thank for their support and fun times together. The first person on the list is **Jana**. Dear Jana, my long-lost sister, ex-roommate and partner-in-crime, I appreciate our honest and genuine friendship. We feel completely comfortable with telling each other the utmost truth. To me, this is the definition of a true friendship. No matter under what circumstances, we know we can count on one another. Thank you for being in my life and being an amazing friend. Finish your PhD soon and join me on the west coast! Dear **Kasia**, thank you for giving me the honor to be your paranymph. I am so happy to have met you and become good friends with you. I have learned a lot from you. Thank you for sharing your life experiences with me, and giving me so much good advice. You are strong, caring and determined, and I am sure you will succeed in your life adventures. I look forward to welcoming you in SF when you visit Noemi and me. Dear **Roberto**, you have given me so much mental support I don't even know where to begin. I truly appreciate all the talks we have had and the experiences you have shared with me, they were very helpful. Thank you for cheering me up during my paper-rejection period, encouraging me for my ASH talk, and supporting me in the difficult times. I admire your brilliance and dedication to science and wish you all the best in your scientific journey. Dear **Ferry**, or I should call you "Jan", I really enjoyed our little hall-way conversations on life outside/after a PhD. From the many talks we have had, I started to see post-PhD career opportunities from a different angle, thank you for that. Dear **Monica** and **Julien**, thank you both for the fun times we have had together, the bbqs, wipeouts, halloween parties, etc! Monica, good luck with finishing up your PhD! And Julien, all the best in Sanquin! Dear **Tim** and **Sophie**, I wish I have spent more time with you two, you brought a fun and fresh energy to the department. I wish you both all the best in your PhD and am sure you both will do a great job! Dear **Adil**, thank you for helping me with the Qubit system! I am definitely coming to visit you one day in beautiful Oman. Good luck with your PhD! I also want to thank **Roger**, **Leonie**, **Davine**, **Amiet**, **Inge**, **Marije**, **Eric**, **Aniko**, **Ruth**, **Johan**, **Avinash**, **Kazem**, **Jasper**, **Joyce** and the rest of the people in the department for all the little conversations we have had, for your support and help.

There are several past Hema13 members that I would like to acknowledge. Dear **Marshall**, I miss the super fun costume parties and game nights you organized. You are our barbeque captain. I am looking forward to joining you and Noemi in SF to continue the fun moments we have had in Rotterdam. Dear **Jurre**, your travel stories make me very excited, it is still on

my bucket list to do what you have done. Thank you for all the fun times together! I cannot wait to hear your adventures after you PhD, whether it will be about a non-profit in Africa or back to the wonderland of Australia. I want to thank the group of Chinese friends at EMC, dear **Diya**, **Arwen**, **Wu Bin**, **Ruoyu**, **Zhanmin**, **Yingying**, **Huang Ling**, **Tong Wei**, **Qiushi**, **Bei Bei**, **Liu Fan**, **Lu Tao**, **Kui Kui**, **Danli**, **Xiaolei**, **Zhouqiao**, **Changbin**, **Haibo**, and the others in the group, thank you for the delicious dinners and very fun Werewolf nights we have had. I wish you all the best of luck in your PhD or post-PhD careers. I hope to stay in touch.

From here, I would like to shift my acknowledgements to my dear friends outside the ErasmusMC. The first one on the list is **Greg**. Dear Greg, starting from Boston, we have become friends for life. To me, you are a good friend, but also a great life mentor. I appreciate every suggestion you have given me on how to handle difficult situations during my PhD. Your wisdom and advice have greatly fostered my personal growth during these years. You have taught me so much including the best way to handle conflicts, public speaking, dealing with failures, etc. there is not enough space here to list them all. Thank you for being a wonderful true friend, who is always there to listen, willing to help, and cares about my well-being. Thank you for all the prayers! I look forward to joining you in the US! I extend this sincere gratitude to your parents **Rosemary** and **Miron**, and your beautiful family! I appreciate their love and care! My wholehearted thanks to the girls from UC, **Neda**, **MJ** and **Souki**, you girls are not only friends, but also family to me. I am so lucky to have you girls in my life, we are lifetime friends no matter where we are. Thank you girls for all the moral support during my PhD! I will spare the cheesy words here, you girls know how much each of you means to me. From UC, to China, to Amsterdam, we have been each other's best friends for 10 years. We experienced life and grew up together. No matter where life will bring us, we are there with one another. This gratitude obviously goes to the other members of our UC crew, - Dear **Neha**, we had so much fun together as the crazy Asians in the group, we became very close friends as we were in the same pre-medicine classes back in college. We went through midterms and finals with sleepless nights and partied the next day. From Utrecht, to Boston, to London, distance was never an issue. I cannot wait to visit you in Singapore this summer and look forward to having you over in SF. Thank you for all the support and career counseling! You helped me build a lot of confidence for my next career move. Dear **Timor**, thank you for agreeing on being my other awesome paranymph! I appreciate all your help and support with organizing everything! You have been an amazing and true friend. You always tell me the truth! Even though it might be something unpleasant, you tell me what I need to hear at that moment. I really appreciate your honesty and our genuine friendship. I was so happy to hear you will start your PhD at Erasmus. Good luck with finishing up! No matter what you decide to do afterwards, I know you will have an amazing time because you bring happiness to wherever you go. Dear **Bob**, I love how we can always joke around, but

never take it personal because we both know we care a lot about each other deep down. We can laugh about everything. Spending time with you is a good way to distress. Thank you for being there for me! I look forward to continuing our crazy friendship wherever life takes us. Dear **Layla**, **Marleen**, **Jocelyn**, **Nafi**, and **Mischa**, thank you guys for being amazing friends from UC to now. Although most of us are all in different cities and/or countries now, our fun times together will always remain a precious part of my memory. I am looking forward to our visits. I also want to thank **Saskia** - Souki's mum, **Han** and **Lisbeth** - MJ's parents. Dear Saskia, thank you for having us over in Koudum, and encourage us young girls to go out and enjoy life. Dear Han and Lisbeth, thank you for having me over in Barcelona, and helping me with my life and financial planning. Dear **Vicky** and **Jay**, you are such a beautiful couple! I am so lucky to have met you two and become good friends with both of you. Thank you both for always being there for me, from back to Boston until now. I cannot wait to finally join you in SF, I am so excited!.

I would like to thank my Salsa families from Boston and here in Rotterdam. Salsa is more than a hobby to me. It has brought me many lifetime true friends. Let's start with my salsa buddies in Boston first. Dear **Nikki** and **Mat**, the wonderful Mattikki! You two are a match made in heaven. I will never forget the crazy fun times we have had together! Thank you for supporting my PhD thesis, I really appreciate it! I am so excited to join you two in the US. Dear **Matilda**, my Swedish princess! Thank you for supporting my thesis! I am so happy to have known you and become close friends with you - a talented dancer with a beautiful heart. Cheers to many more crazy stories we will continue to write together. Dear **Bryn**, **Cordula**, **Talia** and **Meghan**, thank you girls for your friendship, love and fun times together! See you girls very soon in the US. My salsa family in Rotterdam is one big reason this city feels like home to me. Poetic motion is one of the places I cannot say goodbye to. Dear **Johnny** and **Gina**, thank you both for creating this family! I am so happy to have joined this big family run by you two - beautiful, talented and genuine artist couple. I have no doubt that your vision will succeed and your dream will grow big. Dear **Willem** and **Ruth**, I appreciate all your support throughout these two years! I am very lucky to have known your beautiful family and become your xiao mei mei, I hope to welcome you two together with the kids in SF one day! Dear **Razia**, we became close friends since fragilidad. I will always remember your super delicious dinners and bakeries. Thank you for being a genuine and supportive friend. I appreciate all the conversations and fun moments we have had. Enjoy your world travel! I will for sure come back to Rotterdam to visit you. I hope to see you soon in SF! Dear **Rene**, thank you for supporting my thesis! I appreciate all the LV salsa nights you organized and every conversation we have had. I look forward to seeing you in SF one day. I want to thank **Raymond**, **Lily**, **Clara**, **Krisia** and the rest of the PM family for the wonderful dances and times together.

My heartfelt thanks go to my dearest parents, **Mama** and **Eric**! Words cannot describe how grateful I am for all your unconditional love and support that you have generously given me! I wouldn't have been where I am today without you. I am sorry that I haven't spent much time by your side, thank you for always being so understanding and supportive of what I do. Because of you, I dare to fly high as I know you have got my back. Thank you for being the amazing parents and my best friends! 亲爱的奶奶，感谢你跟爷爷从小把我抚养长大， 无论走到哪里，我都会铭记你们对我的养育之恩和无条件的宠爱。亲爱的爸爸，从小你就相信我的能力，这一份信任一直伴随着我走到今天。从小就出国的我没有很多时间陪伴你，但是你从来都支持我的决定，感谢你从小到大对我的信任和支持。亲爱的舅舅，也感谢你一直以来的支持和宠爱，这一份关爱我会一直铭记在心。

Dear **Bowen**, I don't think I would have made it through my PhD without you being by my side. Starting from Boston, you supported me to finish my Master's; then you supported me for five years to finish my PhD. Because of you, all the very difficult moments seemed lighter and easier. Who would have thought we could succeed a 5-year cross-continent long-distance relationship, but we made it. We share the same attitude and value in our relationship, but also in our career and life: once we set our goal, we don't give up, we keep trying; we don't settle, we keep looking. Thank you for being my safe haven, for having faith in me, for encouraging me to follow my heart and chase my dream. Life is unpredictable, but I am excited to take the adventure together with you. Just as we always have been, supporting each other, learning from each other and loving each other.